Wintertime Infiltration and the Thermal Dynamics of Black Spruce Peatlands within the Boreal Plains

A Thesis Submitted to the

College of Graduate and Postdoctoral Studies

In Partial Fulfillment of the Requirements

For the Degree of Doctor of Philosophy

In the Department of Civil, Geological and Environmental Engineering

University of Saskatchewan

Saskatoon

By

Toomas Matthew Parratt

PERMISSION TO USE

In presenting this thesis/dissertation in partial fulfillment of the requirements for a Postgraduate degree from the University of Saskatchewan, I agree that the Libraries of this University may make it freely available for inspection. I further agree that permission for copying of this thesis/dissertation in any manner, in whole or in part, for scholarly purposes may be granted by the professor or professors who supervised my thesis/dissertation work or, in their absence, by the Head of the Department or the Dean of the College in which my thesis work was done. It is understood that any copying or publication or use of this thesis/dissertation or parts thereof for financial gain shall not be allowed without my written permission. It is also understood that due recognition shall be given to me and to the University of Saskatchewan in any scholarly use which may be made of any material in my thesis/dissertation.

Requests for permission to copy or to make other uses of materials in this thesis/dissertation in whole or part should be addressed to:

Head of the Department of Civil, Geological and Environmental Engineering
3B48 Engineering Building
57 Campus Drive
University of Saskatchewan
Saskatoon, Saskatchewan S7N 5A9 Canada

OR

Dean
College of Graduate and Postdoctoral Studies
University of Saskatchewan
116 Thorvaldson Building, 110 Science Place
Saskatoon, Saskatchewan S7N 5C9 Canada

ABSTRACT

Preliminary investigations (2005-2008) of subsurface temperatures at various ecosites at a Central Alberta research station within the Boreal Plains revealed a tendency for numerical models to predict lower than observed soil temperatures during the wintertime. In addition, black spruce peatlands were observed to have above freezing temperatures throughout most of the winter in the shallow subsurface, while other ecosites would be frozen at similar depths. The focus of this thesis was to determine why black spruce peatlands were warmer during the winter through field observations and numerical simulations, and any impact that may have on the hydrological cycle.

In subsequent investigations the depth of monitoring was increased from 50 cm to 300 cm allowing for a comprehensive thermal profile over a three-year period (2009 to 2011) to be observed at several ecosites. There was a total of eighteen ecological sites, three of each of six types, which included coniferous, deciduous, harvested, burnt, shallow peatlands, and deep peatlands. Observed wintertime temperatures during the three-year period confirmed the preliminary results that the subsurface of deep peatlands would be frozen for significantly less time than both shallow peatlands and upland sites. It was unclear why the shallow subsurface of the deep peatlands barely ever experienced sub-zero temperatures, especially considering that the thermal conductivities of the wet peat should have resulted in a frost depth deeper than observed, even when considering latent heat losses.

From December 2014 to May 2016 an additional field study was conducted at the deep peatlands, with a focus on the winter months and the possible physical and biological effects of black spruce trees and sphagnum moss on winter infiltration and subsurface temperatures. The objective of the additional study was to develop a conceptual model for the thermal dynamics of a black spruce peatland which could explain the warmer subsurface temperatures and the shallower than expected depth of frost. In addition, an algorithm was developed to allow for more accurate simulation of observed subsurface temperatures. The biological effects were quantified by monitoring adjacent living and dead black spruce trunk temperatures, along with the sphagnum moss layer temperatures overlying the peat.

During the 2015 deployment of additional temperature probes at the black spruce peatland sites large amounts of snowmelt from the tree crown were observed to pool around the base of the

spruce trees. Snow captured by the black spruce crown completely melted away after a few sunny days. The snowmelt from the crown then dripped and drained towards the base of the black spruce trees, where often a deep "cavity" would exist to the depth of the water table. The installation of moisture content probes within the cavity, loosely filled with peat, revealed increased moisture content following sunny days. Throughout the winter there were also minor increases in observed groundwater elevation following the sunny days as a result of the infiltration of crown drip through the cavity. There was also a very large increase in observed groundwater elevation at the end of March, likely due to the infiltration of upland snowmelt through the unfrozen black spruce cavity. The existence of wintertime infiltration within black spruce peatlands was confirmed through field observations and groundwater measurements.

Data from the additional temperature probes facilitated the development of a conceptual model that could explain why the subsurface did not freeze, and accounting for wintertime infiltration through the tree cavity. Sphagnum moss was observed to be a strong insulator, with temperatures never decreasing below freezing in the underlying peat, even under the tree crown where there was a minimal snowpack. Black spruce trees were also observed to warm the subsurface beginning in April resulting in colder than expected tree trunk temperatures. The conduction of longwave radiation to the root zone from the crown through sap circulation is also a plausible explanation for the circular patterns of snowmelt around the black spruce tree root mats amid a prolonged snowpack observed until at least early May beyond the extent of the black spruce tree's roots.

Physically based numerical models utilizing the Simultaneous Heat and Water (SHAW) model were then constructed for six of the eighteen ecological sites from the 2009 to 2011 field study. Models were constructed for: two of the deep peatland sites, with black spruce; two of the shallow peatland sites, with lodgepole pine and black spruce; and two of the burnt sites, with lodgepole pine. The burnt sites were subsequently referred to as upland. The numerical models were constructed and calibrated in increasing complexity, beginning with the upland sites, followed by the shallow peatland sites and then the deep peatland sites. The numerical model was able to accurately simulate subsurface temperatures and the observed depth of frost at the pine upland sites without any alteration to the code, and to a lesser degree the shallow, drier, peatland sites. However, the numerical model, as with the previous attempts from the initial

investigation, failed to identify a set of parameters that resulted in the successful simulation of the observed subsurface thermal profile at the deep peatland sites. The numerical model also erroneously predicted frost to the groundwater table.

The SHAW numerical model was then updated to calculate the thermal conductivity of the sphagnum moss layer in series instead of parallel. By representing sphagnum moss in series, along with estimating new snowpack thermal conductivity coefficients, the Root Mean Square Error (RMSE) of the wintertime simulated temperatures were substantially reduced for deep peatland vadose zones and were better than those achieved for the upland sites. Using this approach, the wintertime temperatures of the deep peatlands were accurately simulated for the first time at the site, supporting the conceptual model that the insulation provided by sphagnum moss prevents the vadose zone from freezing. The unfrozen vadose zone, along with draining of the crown snowmelt to black spruce tree cavities allowed for wintertime infiltration to occur. The model simulations demonstrate the importance of having a healthy sphagnum moss layer overlying the peat to prevent the subsurface from freezing and inhibiting the infiltration of snowmelt from the black spruce tree cavity. It further highlights the need to better understand and incorporate biologically mediated effects, such as the insulating capacity of live versus dead moss and peat, into physically based models.

ACKNOWLEDGEMENTS

If it had not been for the help of numerous people and establishments, I would never been able to complete this thesis. I am especially thankful for Dr. Gordon Putz, my thesis advisor, who would keep me focused and on track to meet any quickly approaching deadlines. I am also thankful to my other committee members, Dr. Charles Maule, Dr. Ken Van Rees, and Dr. Andrew Ireson for their important insights and questions which inspired me to delve deeper into the research than I could have ever expected. I am extremely grateful for my external examiner, Dr. Sean Carey, for his review and understanding that a great thesis is one that raises more questions than answers. Also, many thanks and appreciation to my graduate chair Dr. Christopher Hawkes who supported me throughout this endeavour and made it possible for all the accommodations so that I could graduate. I would like to thank Wendy and Chris Gould at Touchstone farm for providing a loving home, and a warm meal during my visits to the research site and to my father for his old pick-up truck to get me there. Finally, to Dr. Charles Andrews who although may have doubted that I would ever graduate always continued to support me and be happy to review my work.

Additionally, this research was made possible through the exhaustive efforts of Dr. Ellie Prepas who was able to organize the funding for this collaborative research through a Natural Sciences and Engineering Research Council of Canada (NSERC) development grant with the contribution of Suncor Energy Inc., Canadian Natural Resources Ltd., Tervita Corporation, Environment Canada, Oil Sands Research and Information Network (OSRIN), Alberta Newsprint Company, Alberta-Pacific Forest Industries, Hinton Pulp, Millar Western Forest Products Ltd., Slave Lake Pulp, and KBM Resources Group. Without their financial support this research would not have been possible and am forever thankful for the opportunity they provided to conduct my research.

DEDICATION

This thesis is dedicated to my grandfather, Mihkel Salusoo (1926-2018), who often shared stories of his youthful adventures in the forests of Estonia igniting a passion in me as a child to be an explorer of nature. One of his favourite stories was swimming under the islands of the treed (Salu) wetlands (Soo), for which his surname was derived, and was a constant source of inspiration to study the treed wetlands (black spruce peatlands) of Canada.

TABLE OF CONTENTS

LIST OF TABLES

LIST OF FIGURES

LIST OF ABRREVIATIONS

AOSR	Alberta Oil Sands Region
ForHym	Forest Hydrology Model
FORWARD	Forest Watershed and Riparian Disturbance Project
DPA, DPB	Deep Peatland (A/B)
PEST	Parameter Estimation Software Tool
SHAW	Simultaneous Heat and Water
SPA, SPB	Shallow Peatland (A/B)
UPA, UPB	Upland Pine (A/B)

1 INTRODUCTION

The reclamation of tailing ponds to resemble natural landscapes has been an issue of considerable research and investigation over several decades (Cooke and Johnson 2002). The main objective of tailings pond reclamation is the restoration of a massively disturbed ground surface to a stable terrestrial system that is sustainable from both an ecologic and hydrologic standpoint. Over the last few decades, the extraction of oil sand ore has been the main contributor to the generation of tailing ponds worldwide (Woynillowicz et al. 2005). A major centre of oil sands mining has been in the Athabasca Oil Sands deposits north of Fort McMurray in Alberta, Canada. By 2023, it is expected that oil sands extraction activities will cover an area of 1400 km^2 (Alberta Environment 2010). Due to the unprecedented magnitude of the Alberta Oil Sands Region's (AOSR) mining operations, there has been significant pressure on industry to develop plans for tailing pond reclamation that are appropriate for the climatic conditions of northern Alberta (Alberta Environment 2008).

The Athabasca Oil Sand deposits are located within the relatively dry climate of the Western Boreal Plains, where the landscape is comprised of over 65% peatlands, mostly as fens (Chee and Vitt 1989). Current regulatory requirements specify that tailing ponds be reclaimed to a landscape of 'equivalent capability' which existed prior to disturbance (Alberta Environment 2006). Thus, reclaimed tailing ponds are required to have vegetation species characteristic of native peatland communities (Alberta Environment 2010). Re-establishment of an equivalent plant community can be a considerable challenge since peatland ecosystems are considered to take thousands of years to develop (Moore 1989).

Several research projects are attempting to create peatland fens by placing acquired peat materials within hydrogeological settings that sustain specified wetness conditions (Price and Whitehead 2001). Numerous studies have successfully restored damaged fens (Cobbaert et al. 2004; Cooper and MacDonald 2000), but the reclamation of fen systems has been difficult with the Oil Sands industry replacing 1000's of hectares with marshes, lakes and riparian shrubland (Rooney et al. 2012). The fundamental problem is maintaining a stable groundwater table within a reclaimed landscape that will sustain the ecosystem of a naturally occurring fen peatland during drought years and not flood during wet periods.

Numerical model studies have been used to evaluate the possibility of engineering reclaimed tailing ponds to provide the required hydrological conditions for fen peatlands through the combined use of conceptual and mathematical models of the critical flow processes (Carrera-Hernández et al. 2012; Price et al. 2010). These numerical models were used to determine the optimum system geometry, including the ratio of upland to fen area, thickness and slope of sand materials, and the thickness of peat and liner that would sustain a peatland ecosystem. It is believed that by modelling soil conductivity, layer thickness, and the terrain of the landscape a representative hydrogeological model can be implemented for use in reclamation design (Keshta et al. 2010).

Numerical simulations suggest that an upland area of at least twice that of the fen could sustain adequate wetness when simulating the climate of 1998, one of the driest summers recorded in Northern Alberta (Price et al. 2010). However, the reversal is true within the Western Boreal Plains landscape with the area of peatlands being up to twice the area of the uplands (Vitt and Chee 1990). It has been suggested that naturally occurring Boreal Plains fens are sustained through significant subsurface water input (LaRose et al. 1997); but the source of the recharge is unknown. Some fens within the Athabasca Oil Sands region occur even when completely bordered by uplands with highly transient and deep groundwater tables (Smerdon et al. 2005), yet the fen ecosystem remains viable all year long (Ferone and Devito 2004). The hydrological budget and cycle of peatlands within the Western Boreal Plains is poorly understood and it is likely that key hydrological processes are currently missing from reclamation models.

Important Canadian hydrological processes such as snowmelt within coniferous forests and infiltration into frozen ground (Carey and Pomeroy 2009) are absent from both our present conceptual and numerical models of reclaimed sites. It is well known that forest cover is the most significant factor in decreasing snow accumulation and increasing snow ablation (Varhola et al. 2010). Numerous Russian experiments within the Russian Boreal forest have found the accumulation of snow in clearings to be up to 60% greater than the accumulated snow in spruce forests with less of a difference observed in pine forests (Kuz'min 1963). It has been assumed that this difference is solely accounted for by sublimation or by being transported from the canopy to a clearing by wind (Gelfan et al. 2004). Hypothetically, it is possible that wintertime snowmelt and infiltration may be occurring since most snowpack observations are made in late

winter to early spring. Studies within the Finnish Boreal forest have demonstrated that moisture is up taken by coniferous trees in the winter, along with unexplained increases in soil moisture (Sevanto et al. 2006). Differences in long wave radiation to forest snowpacks have also been observed between varying coniferous species (pine and spruce), yet the variations were attributed to elevation difference and not to species (Ellis et al. 2011). However, the effect of black spruce trees and sphagnum moss on wintertime subsurface temperatures has yet to be incorporated into reclamation models for the Athabasca Oil Sand's tailing ponds, along with the associated impacts on snowmelt and wintertime infiltration.

To provide the petroleum industry, specifically the oil sands, with the tools needed to support reclamation plans and to manage cumulative effects the knowledge gained from previous forestry studies was to be built upon. The original purpose of the Boreal Plains research site was to collect a comprehensive suite of field data to address fundamental questions regarding linkages between natural disturbances such as wildfire and man-made disturbances such as forest harvest. By expanding the understanding of ecosystem functioning within the Boreal Plains in an increasingly disturbed landscape, hydrological models could be calibrated and validated for direct application to forest management plans. Thus, it was determined that the data and information collected at this research site would also be informative in mitigating the negative effects of man-made disturbances within the oil sands and how to best return the landscape to a similar hydrological function as a native watershed.

The research goal of this thesis is to study the thermal effects of black spruce trees and sphagnum moss on wintertime subsurface temperatures to provide a better understanding the observed shallower than expected depth of frost and to improve the numerical simulation of the subsurface temperature profiles.

Chapter 2 provides a literature review of the relevant topics associated with the research goal including: 1) the climate, geology; and vegetation of the Boreal Plains; 2) peatlands; 3) peatland hydrology; 4) thermal properties of peat; 5) freezing of sphagnum moss; 6) forest snowpacks; 7) coniferous trees in winter; 8) recirculation of tree sap via vascular flow; 9) reclaiming wetlands in the Boreal Plains; and 10) numerical simulation of black spruce peatlands.

Chapter 3 provides a description of the six ecological sites, along with the subsurface temperature and moisture content data collected over a three-year period (2009-2011). The collection of this data occurred prior to the commencement of this thesis by the FORWARD II research group, and is subsequently referred to as Phase 1 (Prepas et al. 2008). A comparison of the ecological site's temperatures and moisture contents is made through a series of box plots. Finally, the hypothesis that the shallower depths of frost observed at the black spruce peatlands are due to the increase in latent heat released during the freezing process is tested by using Stefan's equation.

Chapter 4 provides a summary of the field study of the two deep peatland ecological sites from mid-December to the end of April for the winters of 2015, and 2016. This data was solely collected by the author during the thesis field work as part of the FORWARD III research group and is subsequently referred to as Phase 2. It has been hypothesised that black spruce trees possibly conduct sensible energy down their trunks in the permafrost zone of the Northwest Territories, yet no data has been collected to date (Chasmer et al. 2011). To test this hypothesis additional measurements were taken from the black spruce tree's trunks and the sphagnum moss layer to determine if warming the root zone was occurring during the wintertime (Objective 1). Additional measurements were obtained from the trunks of adjacent living and dead black spruce trees, along with temperatures in the root zone and sphagnum moss layer. Observed moisture content measurements, along with groundwater elevations from the field study were also used to determine if wintertime infiltration was occurring (Objective 2).

Chapter 5 provides the details of the construction and calibration of the SHAW numerical models for each of the six ecological sites (Objective 3). The SHAW model was then updated with a new algorithm to estimate the thermal conductivity of the sphagnum moss layer in the two deep peatland sites and recalibrated (Objective 4). The updated SHAW model was then used to test the hypothesis that the shallower than expected depth of frost is due to the insulating effect of the sphagnum moss layer.

Chapter 6 provides a summary, conclusions and recommendations based on the findings of the previous three chapters. The importance of improved understanding and representation of the effects of black spruce tree peatlands on subsurface temperatures and infiltration in hydrological models and in future reclamation designs for wetlands is emphasized (Objective 5). Without

improved understanding and representation, the frost depths and infiltration of snowmelt and upslope runoff that would occur in a designed reclaimed peatland may substantially differ from a natural black spruce peatland.

1.1 Objectives

A summary and list of the research program objectives is as follows:

1. Monitor black spruce trunks and sphagnum moss temperatures in addition to subsurface temperatures for the development of a conceptual model of the thermal dynamics of Boreal Plains' peatlands;
2. Confirm the existence of wintertime infiltration of both black spruce crown snowmelt and upland snowpack runoff through tree root cavities in peatlands on the Boreal Plains based upon field observations and measurements;
3. Estimate Soil Heat and Water (SHAW) model parameters for six ecological sites: two deep peatlands, with black spruce; two shallow peatlands, with black spruce and pine; and two upland sites with pine from observed temperature and moisture profiles;
4. Update the Soil Heat and Water (SHAW) model with an algorithm for sphagnum moss thermal conductivity to reduce wintertime modeling residuals, the observed temperature minus the simulated; and
5. Determine if the effects of black spruce trees and sphagnum moss should be represented in hydrological models and be included in tailings pond closure plans.

2 LITERATURE REVIEW

2.1 Boreal Plains

The Canadian Boreal Forest contains a western sub-region known as the Boreal Plains eco-zone. The Boreal Plains extends across the Canadian provinces of Manitoba, Saskatchewan, and Alberta with minor extensions into British Columbia and the Northwest Territories (Ecological Stratification Working Group 1996). The Boreal Plains has unique climatic, geological, and vegetative characteristics that make it difficult to implement hydrological models developed outside of the eco-zone for the purposes of land management and reclamation design (Ireson et al. 2015; Price et al. 2010).

2.1.1 Climate

The ecosystems of different eco-zones are often mainly a function of the regional climate (Ecological Stratification Working Group 1996). Climate plays a role in defining the ecology of a site by impacting the hydrology, vegetation, and soils. Climate in the Boreal Plains eco-zone is continental, with long cold winters and short warm summers, and is considered sub-humid (Zoltai et al. 1998). The western Alberta foothills are a few degrees warmer than the rest of the eco-zone with an annual average daily temperature of 2.6°C (1971-2015, Whitecourt, Alberta) with 201 days of below freezing temperatures (Environment Canada 2015).

Precipitation greatly varies within the Boreal Plains ranging from 300 mm in northern Alberta to 625 mm in southwestern Manitoba (Ecological Stratification Working Group 1996). In Whitecourt, Alberta the average annual precipitation is 578 mm, of which a quarter accumulates as snow (Environment Canada 2015). Within the Boreal Plains eco-zone it is possible for lake evaporation to exceed precipitation by up to 100 mm $year^{-1}$, which can result in an order of magnitude change in surface runoff between adjacent years with only a normal variation in precipitation (Prepas et al. 2001).

Historic climate trends in Alberta show an increase in air temperature, and a decrease in precipitation with decreased winter and spring snowfalls (Li et al. 2000). These climatic trends, if they continue, will result in less spring and early-summer runoff coming from snowmelt. Typically snowfall begins in October or early November with the region remaining snow-covered for six to seven months of the year (Environment Canada 2015).

2.1.2 Geology

The Boreal Plains is underlain with soft sedimentary bedrock, which subsequent glaciations formed into the rolling moraines of the uplands and lacustrine deposits of the lowlands (Finkelstein 1990). The dominant soils are Luvisolic which are phosphorus-rich with high clay content and are derived from eluvial (*in situ* weathering) and illuvial (movement of soil particles to deeper soil horizons by water percolating downward) processes (Canada Agriculture et al. 1998). Watersheds on soft sedimentary bedrock typically export more phosphorus (P), an important nutrient in stream water quality (Prepas et al. 2001).

The high concentration of P in the Boreal Plains reflects the marine origin of the sedimentary rock over much of the region. The dominance of forest vegetation has also resulted in downward clay leaching which is the dominant process forming Luvisolic soils (Ecological Stratification Working Group 1996). The majority of the soils have formed on alkaline parent materials that are fine-grained and calcium-rich which retain nutrients as calcium and magnesium phosphates as opposed to iron and aluminum phosphates that form in more acidic environments (Reddy et al. 1999). Acidic soils, such as the Brunisolic soils, are generally found in regions of sand and gravel glacial outwash and have a scattered distribution throughout the boreal forests of Alberta and Saskatchewan (Smith et al. 2011).

Areas of low relief within the Boreal Plains are typically situated upon fine-grained soils that are often poorly drained and are ideal for peatland formation, referred to as organic soils. Ponds would have originally formed on the lacustrine deposits of the lowlands following glaciation, but thousands of years of peatland formation has erased them from the landscape. In the well-drained high slope upland areas the organic layers are often thin, while in low-lying peatlands the thickness can exceed several meters (Ecological Stratification Working Group 1996). The formation of substantial peatlands across the Boreal Plains has allowed for double the area of wetlands when compared to the significantly wetter Boreal Shield (National Wetlands Working Group 1988). Consequently, the Boreal Plains has substantially fewer open water bodies as an eco-zone due to peatland formation.

2.1.3 Vegetation

The topographic relief is a dominate factor that influences the vegetation characteristics of the Boreal Plains eco-zone. Wetland areas are typically dominated by black spruce (*Picea mariana* [Mill.] BSP) with some larch (*Larix laricina* [Du Roi] K. Koch), and an understory of peat mosses (*Sphagnum* spp), common Labrador tea (*Ledum groenlandicum*), bog cranberry (*Vaccinium vitis-idaea*), cloudberry (*Rubus chamaemorus*), three-leaved false Solomon's seal (*Smilacina trifolia*), and sedges (*Carex* spp.) (Couling et al. 2007) . The uplands have a mixture of trees including trembling aspen (*Populus tremuloides* Michx.), balsam poplar (*P. balsamifera* L.), white spruce (*Picea glauca* (Moench)Voss), lodgepole pine (*Pinus contorta* Dougl. ex Loud. var. *latifolia* Engelm.), and jack pine (*P. banksiana* Lamb.)(Smith et al. 2003). Differences in the forest composition or bio-diversity have been shown to impact post-disturbance recovery rates and successional pathways (Arseneault 2001; Stocks et al. 1998). Even the bio-mass of forested catchments varies drastically spatially and temporally due to the diversity of trees, shrubs and lower vegetation, unlike agriculture with cultivated monocultures (Ollinger et al. 2002).

Hydrological models often simulate forests with algorithms developed for farmed crops, failing to capture the true spatial variability and complexity that exists not only horizontally, but also vertically. A forest contains an understory, which includes lower vegetation and litter that insulates the soils by reducing sunlight and trapping long wave radiation emitted from the ground. Stand height, structure and leaf-area index (LAI) can also affect soil temperature regimes by insulating the ground from the atmosphere (Bond-Lamberty et al. 2005). During the summer months, especially on south- or west-facing slopes, the insulation is the greatest since biomass is most abundant, but the amount of insulation or biomass varies both temporally and spatially on the Boreal Plains.

Typically canopy cover begins to increase for most plant species after snowmelt (May to June), peaks in the summer (July to August) and then loses biomass in the fall (September to October) (Barr et al. 2004). During the winter months (November to April), the canopy cover is appreciably reduced after leaf-off, especially in the mixed wood forests, but not within the coniferous stands. The understory also experiences similar changes in biomass, with increases in the summer months, a decline during the autumn and relatively low biomass in winter (Barr et al. 2004). Other factors affecting differences in vegetation biomass throughout the Boreal Plains

include slope, aspect, type of disturbance (e.g., wildfire, forest harvest, disease and insect outbreaks), time since disturbance (age of stand) and type of treatment applied after disturbance (Fowler and Helvey 1981).

2.2 Peatlands

Northern peatlands are a massive sink of carbon, accounting for approximately 30% of the planet's terrestrial sources or about 450 Pg of carbon, yet they only cover 3% of the earth's land surface or 3.5 million km^2 (Gorham 1995; Tolonen and Turunen 1996). Within the Boreal Plains of Canada peatland-pond complexes can cover over 50% of a watershed (Kuhry et al. 1993; Vitt et al. 1995). Thus, peatlands are an important component of the global carbon budget and their removal from the Boreal Plains could significantly influence the atmospheric carbon cycle. The importance and use of peatlands has been known for centuries and includes mining of peatlands for fuel, various uses in horticulture and medicine, and more recently the value of peatlands in palaeoecology, where macro- and microfossils are used in strati-graphic reconstructions of palaeoclimates (Foster and Wright Jr 1990). Therefore, an understanding of the general dynamics of peatland growth is crucial to evaluate the implications of direct human activities, such as draining and mining, on long-term sustainability of peatlands and their effectiveness as a terrestrial carbon sink.

Peatland ecosystems accumulate carbon because annual net primary productivity (NPP) of the peatland vegetation generally exceeds the annual decomposition of litter and peat. Boreal Plains peatlands though have low rates of NPP, decomposition and net carbon dioxide (CO_2) exchange compared to other ecosystems (Belyea 1996; Frolking et al. 1998; Thormann and Bayley 1997). However northern peatlands have been a consistent sink for CO_2 over the last couple of millennia with NPP being greater than decomposition.

Northern peatlands experience much slower decomposition rates than most ecosystems due to a combination of effects. Typically a large portion of the peat profile is saturated which limits oxygen diffusion and creates anoxic conditions (Clymo 1992). Secondly, Sphagna and some other peatland vegetation tissues are naturally resistive to decomposition which is amplified by the cool temperatures found in northern climates (Hogg 1993; Johnson and Damman 1993; Puranen et al. 1999). It has been hypothesized that the accumulation of peat has a theoretical limit because even very low decomposition rates applied to an ever-increasing mass of peat will

eventually approach and equal NPP, thus reaching a state of equilibrium (Clymo 1984). Therefore, the long-term NPP and the rate of decomposition in the anoxic zone are the major factors effecting peatland growth rates and the total carbon accumulation in the peatland.

A few simple peatland growth models exist and conceptually can be divided into two separate approaches. Typically, a peatland growth model can be allogenic, i.e., controlled by external factors such as climate and local basin hydrology, or autogenic, i.e. controlled by internal factors such as production and decomposition rates (Frolking et al. 2001). Most of the mathematical models have stressed autogenic mechanisms in simulating peatland dynamics concentrating on peat production and decomposition without considering the effects of hydrology on these rates (Clymo 1992). The difficulties of integrating the dynamics of external climate and internal hydrology into mixed models have been discussed conceptually for decades (Hilbert et al. 2000). Only recently have mixed models been successfully implemented for modelling peatland dynamics as function of both external temperature and wind, and also with an internal water table (Deng et al. 2015).

In Clymo's peat models (Clymo 1984, 1992), a constant water table depth divides the peat profile into the acrotelm, the surface oxic zone where faster aerobic decomposition pathways dominate, and the catotelm, the deeper anoxic zone where slower, anaerobic decomposition occurs. The anoxic catotelm layer decomposes very slowly, at roughly 0.1% of the rate in the acrotelm layer (Belyea and Clymo 2001). The peat growth model can also be simplified by not simulating the mass balance of the acrotelm, but instead focusing on the accumulation of peat in the catotelm. The simplified peat growth model assumes that the acrotelm is a constant mass that "floats" on top of the accumulating catotelm since litter mass loss passing through the oxic acrotelm layer is typically 80%–90% (Clymo 1992). In a typical northern bog, the top 0.2– 0.4m will be oxic and above the water table for much of the year, whereas the peat below about 0.4–0.6 m will be anoxic due to being submerged.

Thus the position of the water table averaged over a few years is the key to understanding and predicting peatland growth (Shurpali et al. 1995). The groundwater table is significant both locally within a peatland and within the entire watershed. The depth to groundwater table influences both plant species composition and rates of net ecosystem production (Silvola et al. 1996). The relationship between water table position and peatland growth is a non-linear

relationship since growth may be inhibited by either very wet or very dry conditions. Water table depth also strongly influences rates of decomposition, as the unsaturated zone is primarily oxic while, below the water table, anoxic conditions prevail (Waddington and Roulet 1996). Finally, the position of the water table is critical because, being influenced by both climate and internal peatland hydrology, it integrates external and internal factors. The mathematical representation of the water table allows for the representation of mixed allogenic and autogenic peat growth within a model.

2.3 Peatland Hydrology

Knowledge about the hydrology of peatland systems and the factors influencing them is very limited with very few studies having been conducted within the Boreal Plains. This understanding is necessary, though, to accurately predict the impacts of disturbances on groundwater tables and to aid in the reclamation of tailing ponds which attempt to incorporate a functioning peatland ecosystem. The hydrologic connections of a peatland to a landscape disturbance can greatly influence its ecology due to anthropogenic influences on either raising or lowering the water table (Bedford et al. 1999; Devito and Hill 1997; Winter and LaBaugh 2003). Especially in the low-relief landscapes of the Boreal Plains, where minor variation in topography can drive complex local and regional groundwater flow systems with spatial patterns of groundwater recharge and discharge that can be difficult to predict (Winter and Woo 1990). Therefore the position of a peatland within a watershed can strongly influence the hydrogeological flow regime, and result in different responses to catchment disturbance or reclamation designs than what was predicted (Petrone et al. 2008; Winter et al. 2001).

Even though the geomorphology of the Boreal Plains is similar to the adjacent Prairies ecozone, the climate is cooler and wetter which has allowed for peat development at the riparian edges of many wetlands and ponds, forming pond–peatland complexes (Klassen 1989; National Wetlands Working Group 1988). These riparian peatlands often serve as a hydrological connection and buffer between surface waters and surrounding uplands. In humid locations, drought seems to be the key factor controlling the timing, extent, and direction of groundwater flow through the peatland (Devito et al. 1997; Fraser et al. 2001; Siegel and Glaser 1987). However in the sub-humid landscape of the Boreal Plains the interactions of surface water and shallow groundwater flow in pond–peatland complexes seems to be tightly linked to precipitation events and is

described as a “piston” flow, a process in which water from a precipitation event is only released to the stream when a subsequent precipitation event occurs (McEachern et al. 2006).

Although there are differences in climate between the Boreal Plains and Prairies, the magnitude and timing of precipitation does not differ greatly. The main difference between the two eco-zones is the agricultural land use of the Prairies which has increased drifting snow accumulation in depressions with increased snowmelt runoff over frozen soils (Hayashi et al. 2003). In comparison, the undisturbed forested catchments of the Boreal Plains have very little snow drift with relatively small springtime snowpacks on the peatlands that are insufficient to contribute to runoff during snowmelt (Ferone and Devito 2004). The probability of a surface runoff event occurring in a Boreal Plains peatland system is further reduced as most precipitation events occur during the late spring to summer when soils have thawed, and plant transpiration is high.

Some functioning peatlands within the Boreal Plains have also been observed to have no contribution of groundwater flow from the uplands, even when large hydraulic gradients were present (Ferone and Devito 2004). It was found that although large hydraulic gradients can exist between uplands and adjacent peatlands, that the actual groundwater fluxes from hillslopes were negligible due to the low horizontal permeability of the clay rich substrate (Hendry 1982; Winter and Rosenberry 1995), and the presence of hydraulic depressions at the base of hillslopes.

In most cases the largest non-atmospheric flux observed in Boreal Plains peatlands were with open water bodies such as ponds and streams. The importance and sensitivity of these short flow-path connections between open water and peatlands have yet to be studied, especially with respect to susceptibility to landscape disturbance. However even though the trend in seasonal groundwater fluctuations differs between peatland systems, it appears to be driven by differences in peatland storage and basin/catchment morphometry. Thus, the importance of topography in both disturbed landscapes and in reclaimed tailing ponds may be a crucial factor since both peatland storage and basin morphometry are closely linked to topography.

Dynamic groundwater flow patterns indicate that pond–peatland hydrologic connectivity must be understood to predict water quality and ecological function of peatlands, and to evaluate the ability to reclaim peatlands on the Boreal Plains. The key to understanding the dynamic groundwater flow regime of the Boreal Plains peatlands may be tightly linked to wintertime

forest hydrological processes The main difference between Prairie wetlands and Boreal Plains peatlands has been identified as snowpack accumulation and snowmelt runoff since both eco-zones have similar geology and summertime precipitation events.

2.4 Thermal Properties of Peatlands

The organic soil horizons, and especially mosses, play an important role on soil temperature and frost depths in high-latitude ecosystems (Bonan and Shugart 1989; Dyrness 1982; Nicolsky et al. 2009; Yoshikawa and Hinzman 2003; Yoshikawa et al. 2002). Typically, organic materials have much lower thermal conductivity values than mineral soils (Farouki 1981) which reduces vertical heat fluxes and insulates the subsurface from air temperatures. The thermal conductivity of peat is influenced by moisture content, the phase of moisture (liquid or ice), the bulk density, and if the peat is living or decomposing (Farouki 1981; Yoshikawa et al. 2002). The large heterogeneity in the surface of the peatland with a variety of moss colonies can result in very large differences in surface temperatures by over 25 ºC during the summer (Leonard et al. 2017; Leonard et al. 2021). However this is mainly due to the subsurface heterogeneity of uneven ice thawing, resulting in the presence of frozen peat along side frost-free patches of peat well into the growing season (Leonard et al. 2021; Petrone et al. 2008).

Peat has very high porosity (Yi et al. 2009) which can result in great variability in thermal conductivity with changes in moisture content. Studies have shown that as peat becomes saturated the thermal conductivity will increase to that of water (Andersland and Anderson 1978; Farouki 1981; Johansen 1977). Even under unsaturated conditions the thermal conductivity of live sphagnum moss in Alaska was observed to have significant variability, ranging from less than 0.05 to 0.3 $Wm^{-1}K^{-1}$ (O'Donnell et al. 2009). Further it was discovered in Finland that thermal conductivity of frozen saturated surface peats can be three times higher than unsaturated peats with only a 9% difference in water content (Kujala et al. 2008).

Predicting thermal conductivity in organic soils with respect to moisture content is far more difficult than in mineral soils which can be accurately estimated using volumetric ratios in parallel (McGaw 1969). Andersland and Anderson (1978) observed a nonlinear relationship between the thermal conductivity of peat and moisture content, while Johansen (1977) reported a linear relationship between the square root of thermal conductivity and the degree of saturation. The thermal conductivity of organic matter, as with mineral soils, increases with bulk density

(Andersland and Anderson 1978), and bulk density typically increases with decomposition of soil organic matter (Manies et al. 2004). Thus, to accurately predict the depth and timing of frost within the Boreal Plains peatlands it is important that models incorporate an algorithm to estimate reliably the thermal properties of moss and peat with respect to moisture content.

Most soil thermal models and ecosystem process-based models typically prescribe a constant average thermal conductivity value for thawed and frozen peat (Romanovsky and Osterkamp 2000; Zhuang et al. 2001). This simple approach to represent the thermal conductivity of peats fails to recognize the importance of the interannual and seasonal variability of moisture content, even though the effect is well known (Romanovsky and Osterkamp 1997). The variability in the thermal conductivity due to moisture content in surface organic horizons has been shown to have a profound effect on simulated soil temperatures at depth (Bonan 1991). Several recent studies have tried to calculate the thermal conductivity of organic materials using moisture dependent weighting factors, know as a Kersten number (Farouki 1981; Kersten 1949) and apply them to the thermal conductivities with a dry and saturated moisture content (Lawrence and Slater 2008; Yi et al. 2009).

The thermal conductivity of an individual peat particle is approximately 0.25 $Wm^{-1}K^{-1}$ (Campbell et al. 2002), however the thermal conductivity of completely dry peat soil samples ranged from 0.083 to 0.1 $Wm^{-1}K^{-1}$ due to air (0.025 $Wm^{-1}K^{-1}$) occupying 70% of the total volume (Zhao and Si 2019). It was also found that an increase in moisture content had a very sharp effect on thermal conductivity values in mineral soils, while only a gradual increase was observed in peat soils (Zhao and Si 2019). It has been suggested that the difference in effect of moisture content on thermal conductivities is due to the importance of water creating “bridges” between mineral particles, while as peat is fibrous and interconnected the “bridges” created by increased water content do not greatly increase their interconnection (Lu et al. 2007; Tarnawski and Leong 2012).

The thermal conductivities in frozen soils can be double the unfrozen conductivity with identical moisture contents due to the difference in thermal conductivities between water (0.58 $Wm^{-1}K^{-1}$) and ice (2.18 $Wm^{-1}K^{-1}$) (Côté and Konrad 2005; De Vries 1963; Sturm et al. 2002). Similarly, the thermal conductivities in frozen peat samples were found to be higher than unfrozen samples, with a greater difference found with increased moisture contents (Zhao and Si 2019). Thus, the

moisture content of the surface peat layers at time of freezing has a major impact on the thermal conductivities throughout the winter and into the spring.

Soils with higher moisture contents tend to have higher thermal conductivities than drier material, however Zhao and Si (2019) observed the opposite with the thermal conductivities of peat soils (0.5 $Wm^{-1}K^{-1}$) being half of sandy soils (1.2 $Wm^{-1}K^{-1}$), yet the sandy soil had a moisture content of 0.05 m^3m^{-3} compared to the peat of 0.4 m^3m^{-3}. The reduced thermal conductivity of the peat soil at reclaimed sites in Fort McMurray, Alberta resulted in the date for root growth (>6 ºC) to occur 20 days after the sandy soil. The delayed temperature rise within the reclaimed peat soils is consistent with the observed poor growth of aspen and jack pine seedlings, and as a result a peat-mineral soil mix has been recommended for warmer spring soils (Zhao and Si 2019).

However, in-situ measurements of thermal conductivity of black spruce peatlands, which include a living layer of moss overlying the peat, were found to much lower than that expected of peat. The thermal conductivity of a black spruce peatland moss layer (0 to 0.10 m) in Alaska was found to range from 0.03 to 0.09 W m^{-1} ºC^{-1}, which is less than completely dry peat samples, yet moisture content ranged from 0.85 to 5.7 g g^{-1} (Sharratt 1997). These lower than expected estimates for the thermal conductivity of moss when compared to peat is supported by similar finding in Sweden which determined that the thermal conductivity of the bryophyte layer varied from an average of 0.08 W m^{-1} ºC^{-1} for the summer to a reduced conductivity of 0.03 W m^{-1} ºC^{-1} in winter time to match observed temperatures (Porada et al. 2016). Both of these studies suggest methodologies for estimating thermal conductivities for non-living materials may not be applicable to living moss layers.

2.5 Freezing of Sphagnum Moss

The leaf tissue of sphagnum mosses consists of a single layer of two types of cells, living chlorophyllous cells which are surrounded by dead hyaline cells. It is these dead hyaline cells, which have special pores to absorb water, that give sphagnum moss the ability to hold up to twenty times its own weight in water (Maseyk et al. 1999). It was observed from laboratory experiments that distinct cytological changes started to occur at -1.1 ºC, with the formation of ice within the hyaline cells and surrounding the leaf (Buchner and Neuner 2010). Within 2 seconds of ice nucleation the chlorophyllous cells shrink in volume by approximately 80%, with the

cellular water rapidly draining towards the surrounding ice. When the same experiment was repeated after the leaflets were heat killed, exposed to 60 ºC for 5 minutes, there was no observed reduction in volume of the chlorophyllous cells. The remaining cellular water does not freeze due to isolated proteins, phospholipids, nucleic acids, and intact cells which are present in all living system and typically account for 20-40% of the dry weight (Crowe et al. 1990). Further mosses are non-vascular, lacking the vessel cells present in higher order plants, which easily spreads the ice throughout a vascular plant once nucleation begins within a leaf (Hacker and Neuner 2007).

Additionally, mosses are known to have evolved to capture atmospheric moisture by inducing ice nucleation on the cell surface though specialized proteins (Moffett 2015). Due to the differences in vapour pressure over ice and water, the formation of ice on the cell surface would result in increased sorption of water from the atmosphere through the Bergeron-Findeisen mechanism (Pruppacher and Klett 2012). The Bergeron-Findeisen mechanism is the process by which ice crystal growth occurs through sublimation when the ambient vapor pressure falls between the saturation vapor pressure over water and the lower saturation vapor pressure over ice (Pruppacher and Klett 2012). While the formation of ice crystals on the cell surface is beneficial for mosses as an additional source of water, the encasement in ice may result in considerable stress factors due to reduced fluxes of oxygen and CO_2 leading to the accumulation of ethanol and other toxic metabolites (Andrews 1996).

2.6 Forest Snowpacks

The effects of forest cover on snow accumulation and snow melt or ablation have been a topic of substantial research over the last century. Peak snow water equivalent (SWE), the maximum amount of liquid water within the snowpack, is typically used to represent snow accumulation; with the snow melt or ablation rate calculated from the peak SWE divided by the time for the snowpack to melt from its peak. Numerous studies have demonstrated that as forest cover increases both snow accumulation and snow ablation rates decrease with a strong linear relationship (Varhola et al. 2010). Almost identical linear relationships have been developed relating forest cover to snow accumulation in both Canada (Pomeroy et al. 2002) and Russia (Kuz'min 1963). Although the difference in snow accumulation between forested and nearby

open fields varies according to site specific conditions, reductions of peak SWE of up to 60% have been recorded under forest canopies (Varhola et al. 2010).

Several attempts have been made to develop a model for snow accumulation and ablation rates within forests. Forest snowpack models have been developed using a variety of techniques from local-scale empirical studies comparing forested to open areas (Boon 2009; Jost et al. 2007; Winkler et al. 2005), to temperature-index methods (Watson and Putz 2014), to physically-based algorithms (Essery et al. 2008; Hedstrom and Pomeroy 1998; Hendrick et al. 1971). Local-scale empirical models have been developed from a wide range of studies to provide first-order estimates of snow accumulation in forests. However, since empirical models do not explicitly express the governing processes, they are of little use in the design of engineered landscapes and offer little predictive capability in reclaimed watersheds.

Although temperature-index or degree-day models are based on an empirical relationship between air temperature and melt rate, they have been preferred over the physically based energy balance models which require atmospheric data that is often not available (Hock 2003). Operational hydrological models often implement a temperature-index model because air temperature data are the only available input, and it is relatively easy to interpolate and extrapolate for climate change scenarios. Even though temperature-index models fail to explicitly consider solar radiation, air temperature has been shown to implicitly incorporate its effect in computationally simple snow melt models that still perform reasonably well (Hock 2003; Watson and Putz 2014).

It is well known that the primary driver of snow ablation or melt is the net available energy, which can be explicitly expressed with an energy balance model that includes incoming and reflected shortwave radiation, incoming and outgoing longwave radiation, sensible and latent heat fluxes and ground heat conduction as independent variables (Ellis et al. 2011; Walter et al. 2005). The forest canopy can have numerous effects on the energy dynamics of a snowpack including reducing incoming shortwave radiation via canopy extinction through reflection and absorption (Ellis and Pomeroy 2007; Link and Marks 1999). Although longwave radiation has been shown to increase from foliage thermal emissions (Black et al. 1991; Reifsnyder and Lull 1965), typically the net effect results in a loss of energy for snow melt (Essery et al. 2008). Wind speeds are also reduced by forest canopies which can have orders of magnitude impacts on

sensible and latent heat fluxes. Numerous studies have shown that open areas have higher snow ablation rates than a forest (Boon 2007; Hendrick et al. 1971; Teti 2008), yet still accumulate more snow than a forest.

One possible explanation of this 'radiative paradox' of why snow accumulation within forested areas are up to 40% less than open areas has been canopy interception and sublimation (Essery and Etchevers 2004). It has been suggested that under certain conditions that 60% of snowfall can be intercepted by the forest canopy, with almost 70% of the intercepted snow being sublimated back to the atmosphere (Hedstrom and Pomeroy 1998; Pomeroy et al. 1998). Another possible explanation for the 'radiative paradox' is that increased canopy density actually begins to increase net radiation to the snowpack (Sicart et al. 2004). This is due to "enhanced" longwave radiation being emitted from the forest canopy to the snowpack, and is more likely to occur during clear skies, at higher altitude, with low solar angle when the snowpack has a high albedo.

It is also possible that water is lost from the snowpack due to internal sublimation, which is referred to as depth hoar. When there is a significant enough temperature gradient, $> 20\ ^{o}C\ m^{-1}$, then a water vapour pressure gradient will be induced with a flux of water from the warm base of the snowpack to the top of the snowpack in contact with the cold air (Domine et al. 2018). As the water vapour is transported to the top of the snowpack large faceted striated hollow crystals form at the bottom of the snowpack causing the depth hoar. If the forest floor is warmer than an open field there would be a larger temperature gradient, resulting in a greater amount of depth hoar.

Even though the 'radiative paradox' is implicitly expressed in hydrological models through empirical relationships, an accurate simulation of snowpack dynamics within coniferous forests has eluded hydrologists (Ellis et al. 2010). This is likely not a concern when simulations are solely concerned with peak stream flows from snowmelt and their timing but may lead to substantial errors in recharge rates and the prediction of groundwater elevations.

If loss of snowpack to the atmosphere through sublimation is the explanation for less peak snowpack in forested areas, it is implicitly assumed that; 1) no infiltration occurs during the winter since the ground is frozen and melted snow will simply refreeze within the snowpack; and 2) coniferous trees are dormant during the winter and have no biological effect on warming the soil to allow infiltration. Since canopy snow interception and ablation losses are often measured

using a hanging tree experiment (a tree is severed at the trunk and suspended with a collar to a weighing scale) these assumptions have never been fully tested in various stands (Pomeroy et al. 2005). However, this would suggest that coniferous trees have evolved to increase water losses to the atmosphere, which creates another paradox of why coniferous trees have a competitive advantage over deciduous trees in cold climate semi-arid regions like the Boreal Plains of Alberta.

2.7 Coniferous Trees in Winter

Coniferous trees of the Boreal forest restrict their photosynthetic capacity before the winter stresses of freezing temperatures and lack of available water begins (Ensminger et al. 2004; Öquist and Huner 2003; Parker 1963). The wintertime inhibition of photosynthetic capacity is triggered by both reduced sun light and lower temperatures. However despite restricted photosynthetic activity, warm wintertime weather can cause relatively high rates of respiration in an attempt to replenish carbohydrate reserves (Cowling and Kedrowski 1980; Schulze et al. 1967)). Within a matter of days coniferous trees can up regulate their photosynthetic capacity (Mäkelä et al. 2004; Ottander and Öquist 1991) and may experience continuous photosynthesis year round during milder winters (Berbigier et al. 2001; Hansen et al. 1996; Schaberg et al. 1995) Within the Boreal forests of Finland photosynthesis was observed in a Scots pine forest in all months except January (Sevanto et al. 2006).

Wintertime photosynthesis is mainly controlled by air temperature (Lundmark et al. 1988; Suni et al. 2003) and soil temperature (Jarvis and Linder 2000; Schwarz et al. 1997) The ability to uptake water is critical for coniferous trees, for any photosynthetic activity would involve water losses due to transpiration, which if not recovered could result in lethal desiccation (Boyce et al. 1991). Coniferous trees exhibit some of the smallest xylem diameters for conducting water between the crown and roots of any temperate tree (Ewers 1985). Coniferous trees can even maintain 25% liquid water content within their xylem and phloem of the tree trunk at air temperatures as low as –20°C (Sparks et al. 2001). However during freezing temperatures the xylem in coniferous trees experiences a 20–50% loss in conductivity, or ability to transport water from the roots to the crown, further increasing their ability to conserve water during the wintertime (Sparks and Black 2000; Sperry and Sullivan 1992; Sperry et al. 1994). It has been suggested that coniferous tree attributes of small diameter conduits to prevent freeze-induced

cavitation, high liquid water content at below freezing temperatures, and reduced xylem hydraulic conductivities allows them to dominate the Boreal forest (Sakai and Larcher 1987; Sparks et al. 2001).

A major implication of coniferous wintertime photosynthesis is that once storage is exhausted, a source of water uptake is required to prevent lethal embolisms from forming (Jarvis and Linder 2000). Coniferous trees have been shown to use either unfrozen soil water or crown snow meltwater extracted through their needles or shoot bark (Boyce et al. 1991; Cowling and Kedrowski 1980) for wintertime photosynthesis. Stem water content varied by greater than 20% in lodgepole pine located in Idaho among winter-thaw periods, but always remained greater than summer water contents (Sparks et al. 2001). Wintertime decreases in coniferous stem water content probably resulted from foliar evaporation occurring with limited uptake of water from frozen soils (Katz et al. 1989; Sperry 1993).

The increases in coniferous tree water content during the winter would indicate the availability and uptake of liquid water. Uptake of water through the root system is not always possible because soil temperatures below freezing severely limit soil to root hydraulic conductivity (Coleman et al. 1992; Owston et al. 1972; Teskey and Hinckley 1981). Alternatively coniferous trees can uptake water by their stems or needles to replenish photosynthetic moisture losses. Mid-winter thaws have exhibited increased stem water contents when preceded by a large amounts of snowfall, while a decrease in mid-winter stem water content occurred when preceded by little or no snowfall (Sevanto et al. 2006; Sparks et al. 2001). Finally, the largest stem water contents have been observed during the winter at temperatures between 0 and 3°C (Sparks et al. 2001). Thus, when snow sublimates from the crown of coniferous trees, a portion of this water may be directly absorbed by the stems and needles instead of being evaporated to the atmosphere.

Uptake of water from melting crown snow was first hypothesized over half a century ago to be an important wintertime process for maintaining water balance in conifers (Stone 1963). It wasn't until a few decades later that observation of a coniferous tree, *Picea abies,* indicated the direct uptake of melting water by stems or needles may be an important mechanism to reduce winter desiccation (Katz et al. 1989). The remarkably complex anatomy of conifer needles (Liesche et al. 2011) and the numerous well-documented cases of needle water uptake (Breshears

et al. 2008; Burgess and Dawson 2004; Limm et al. 2009) present a strong case for foliar uptake and potential implications for wintertime xylem refilling. The needles from a white spruce, *P. glauca*, a common species in the Boreal forest of North America was also found capable of foliar uptake and xylem refilling (Laur and Hacke 2014). Foliar water uptake and subsequent refilling was also observed in Austrian timberline trees in late winter while the ground was still frozen and the trees disconnected from the soil water (Mayr et al. 2014).

Numerous studies have also observed vascular sap flow in the opposite direction, with moisture being absorbed by the leaf/needles and discharged to the soil through the roots, and is referred to as foliar uptake (Eller et al. 2013; Goldsmith 2013; Nadezhdina et al. 2010). It remains to be tested whether foliar uptake occurs in coniferous trees during the wintertime under natural conditions in the Boreal Forest and could be an important hydrological process in determining the fate of sublimating snow from canopies. With a quarter of precipitation occurring as snowfall, it is important to determine the end fate of snowfall losses within the tree crown, whether it is to the atmosphere as sublimation, to the tree as foliar uptake, or to the ground as infiltration. Thus, our current assumption that the biological effects of foliar uptake and vascular flow are inconsequential to snowmelt processes should be reviewed, as new wintertime algorithms may be required in hydrological and reclamation models.

2.8 Recirculation of Sap Flow

The heights to which trees grow was made possible by the evolution of vascular tissues that overcame the limitations of diffusion of nutrients and sugars between cells by internally redistributing nutrient resources through bulk vascular flow. Trees have evolved two main types of vascular tissues, the xylem, which transports water and dissolved minerals upward through the tree, and the phloem which carries the products of photosynthesis to non-photosynthetic structures, such as roots. Sap is the fluid that circulates through the vascular system of a plant, via both xylem and phloem, and is mainly water with dissolved sugars and minerals. Hypotheses for mechanisms controlling phloem transport date back to the 1930s when Ernst Münch proposed that osmotically generated pressure differences between the sources (e.g. leaves) and sinks (e.g. roots) was the main driver (Munch 1930).

Testing these hypotheses has proven to be extremely difficult since detaching the source tissues from the sink prevents the circulation of sap. Therefore, entire functioning plant is required for

experiments. However in recent years due to advances in technology successful experiments have been conducted and demonstrated that plants can alter the shape of phloem cells and the pressures within phloem cells to transport resources (sap) over long distances within a plant (Knoblauch et al. 2016).

Typically, it is assumed that the phloem flow is very low or negligible in comparison to xylem flow, and it is often neglected. However, this assumption may not always be true, especially at night, where experiments have demonstrated that phloem return flows play a significant role in the circulation of minerals through the xylem (Tanner and Beevers 2001; Windt et al. 2006). A mathematical model for trees has been developed that couples xylem and phloem flows and the model was verified using both young oak trees in a controlled setting, and adult beech trees in a natural forest (De Schepper and Steppe 2010). The simulations confirmed that during periods of high transpiration rate that the phloem to xylem flow ratio was approximately 5% but during the night the ratio increased up to 80%, with the two flows being almost equivalent. Another study on walnut trees showed evidence that the continuous recirculation of sap allowed for adequate transport of sugars to develop spring buds during low evaporative demand which would not possible without phloem return flow (Tixier et al. 2017).

While no studies on phloem flow in black spruce trees have been conducted, it has been observed that black spruce trees can have very high xylem sap velocities of up to 60 cm day^{-1}, often double that of balsam firs, especially on the shaded side (Oogathoo et al. 2020). The same study also discovered that the water content of the soil had little effect on sap flows, with solar radiation and vapour pressure deficit being the most important variables, with barely any observable decrease during drought conditions. Similarly, a study within the permafrost of the Northwest territories recorded high average daily sap flows for black spruce trees that exceeded 1000 cm^3 (Patankar et al. 2015).

2.9 Reclaiming Wetlands in the Boreal Plains

Within the Boreal Plains in Northern Alberta, Canada there is increased recognition of the importance of peatland wetlands in returning the landscape to a functioning ecosystem following surface mining of oil sands deposits and mine closure. The area impacted by open-pit oil sands mining reached 895 km^2 by 2017 and is continuing to expand in area (Volik et al. 2020). However, the vast majority of the peatlands destroyed by open-pit mining will not be reclaimed,

but instead converted into upland forest, end pit lakes, riparian shrubland and marshes with a loss of over 295 km^2 of peatlands (Rooney et al. 2012). Since 2015 the Government of Alberta has required the mitigation of wetland losses, with mitigation practices including avoidance of wetland disturbance, minimization of negative effects to wetlands, and wetland replacement (Alberta Environment and Parks 2017).

Oil companies are required by Alberta guidelines to replace the wetlands impacted by oil sands mining, with approximately one-third of disturbed area to be reclaimed as wetlands (Alberta Environment 2014). The first attempts at reclaiming wetlands in the AOSR focused on small, shallow, open-water wetlands and marshes with opportunistic wetlands spontaneously forming in poorly drained areas (Little-Devito et al. 2019; Pouliot et al. 2012). However, the first assessments of these opportunistic wetlands revealed they were not equivalent to native wetlands of the region. within comparison they had reduced vegetation diversity and diminished ecological health resulting in lower peat accumulation and organic soil content (Roy et al. 2016). Subsequently the focus has been on attempts to create a peatland similar to those observed throughout the Boreal Plains (Vitt et al. 2016).

Peatland creation is a relatively new concept, and only has been attempted twice on post-mined oil sands leases at Suncor's Nikanotee Fen and Syncrude's Sandhill Fen (Ketcheson and Price 2016). The Nikanotee Fen was designed based on a landscape optimization approach through numerical modelling of an isolated upland-fen system, while the Sandhill Fen was designed to mimic the landscape of a natural fen systems with the aid of numerical groundwater modelling of adjacent landscapes. The Nikanotee Fen was constructed on an overburden dump (Pouliot et al. 2012), whereas the Sandhill Fen was constructed on a sand-capped, composite tailings (a slurry of tailings sand and fine tailings with gypsum) deposit (Pollard et al. 2012).

Reclamation efforts at the Nikanotee Fen were able to produce a peatland plant community that began to accumulate peat (Borkenhagen and Cooper 2019). However, the plant community had more resemblance to a regional saline fen, with an abundance of vascular plants being dominated by water sedge (*Carex aquatilis*), than to the desired moss dominated rich fen (Borkenhagen and Cooper 2019; Chee and Vitt 1989). It was discovered that in order to increase the establishment of mosses that ponded water or at surface water tables should be limited and nurse plants like Baltic rush (*Juncus balticus*) should be introduced to provide shade (Borkenhagen and Cooper

2019). Furthermore, more than half of Alberta's natural fens are treed, with roughly only 25% of fens being dominated by shrubs and graminoids and there is an even greater disparity in bogs with more than 80% being treed (Alberta Environment and Parks 2018). To date there have been no studies on reclaimed peatlands on the Boreal Plains which introduced native trees, such as black spruces (*Picea mariana*), as a nurse species for bryophytes even though the peatlands are typically treed.

A major challenge facing peatland reclamation in a post-mining landscape is the inclusion of end-pit lakes which result in a surplus volume of tailings sand and overburden materials. The surplus of material tends to create complex hilly topography within a closure landscape instead of the relatively flat pre-mining landscape (Rooney et al. 2012). Numerical modeling of the Nikanotee Fen suggested a minimum upslope to peatland ratio of 2:1 was required with a more conservative 3:1 ratio being implemented in construction (Price et al. 2010). However, in pre-disturbance watersheds the proportion of wetland ecosystems can be over 60%, with less than 25% supporting upland vegetation (Rooney et al. 2012). Thus despite the subhumid climate of the AOSR, wetlands are a dominate landform and cover more than 50,500 km^2 of the region (Alberta Environment and Parks 2018). Healthy fen peatlands are also often observed within the sub-humid climate of the Boreal Plains without any water contributions from groundwater and adjacent hillslopes (Riddell 2008; Smerdon et al. 2008). It was recently discovered that the dominant hydraulic gradient is from peatlands to the adjacent forestlands, opposite of the topographic gradient, and thus the Boreal Plains peatlands are more often a source of groundwater recharge and not a sink as conceptualized in reclamation designs (Hokanson et al. 2020). Thus, the study of these perched peatlands which form in highland areas would be of vital importance in understanding how the hydrological cycle is able to maintain a wetland in a subhumid climate.

One major difference between natural landscapes and reclaimed watersheds within the Boreal Plains is the amount of surface run-off, especially during snowmelt periods (Devito et al. 2005; Redding and Devito 2011). No surface run-off was observed from the natural slopes within the Nikanotee Fen while large volumes of water and sediment would run-off the reclaimed slopes (Ketcheson and Price 2016). Frozen soils on the reclaimed slopes restricted the amount of snowmelt water that would infiltrate into the subsurface with snowmelt run-off ratios ranging

between of 0.7 to 0.9 for reclaimed slopes. With the surface of the peatlands also frozen the snowmelt from the reclaimed slopes began to pond over the fen. By the beginning of April 50% of the Nikanotee Fen was covered in ponded snowmelt water and a peak ponded cover of 80% was reached by mid-April. It was not until enough thermal erosion occurred within the frozen peat creating a localized recharge pipe allowing for percolation to occur before the ponded area began decreasing (Ketcheson and Price 2016). However, this requires that wetlands can only be at the lowest elevation within a reconstructed watershed, otherwise the ponded snowmelt waters would continue to runoff downgradient due to the surface being frozen.

Therefore, understanding the differences between snowmelt run-off and recharge between natural and reclaimed peatlands is important in developing efficient water management strategies. Especially considering the possible major contribution that upland snowmelt could have to the annual water budget of reclaimed wetlands. Findings from the experimental reclaimed peatlands in the Boreal Plains have identified the opportunity for new integrated landscape designs that maximize the detention and redistribution of snowmelt from upland areas (Ketcheson and Price 2016).

2.10 Numerical Simulation of Black Spruce Peatlands

Over the years there have been very few attempts to simulate the subsurface temperatures of black spruce forests, and especially peatlands. The reasons for simulating subsurface temperatures vary, from being boundary condition inputs for complex 3-dimenional groundwater flow models to evaluating the effectiveness of mulching cutlines through black spruce stands. The Simultaneous Heat and Water (SHAW) model (Flerchinger and Saxton 1989), a complex groundwater flow model, was used to estimate the upper thermal conditions and recharge of a permafrost plateau and the surrounding wetlands in the Northwest Territories (Langford et al. 2020). While the SHAW model was able to be reasonably calibrated throughout most of the year, it predicted a frost depth of 1 m within the wetlands yet measured temperatures at -10 cm were never below -1 ºC suggesting a much shallower depth of frost. The poor calibration and simulation of temperatures throughout the winter was attributed to the 1-dimensional nature of the SHAW model and its inability to simulate the spatial redistribution of the snowpack.

The SHAW model was also used to simulate the efficacy of mulching cutlines from seismic surveys within sub-arctic peatlands of the Northwest Territories (Mohammed et al. 2017). It is

well documented that the removal of the black spruce crown, and the subsequent ground compaction from machinery, will result in the thawing of the permafrost in regions with a mean annual air temperature greater than 0 ºC (Wright et al. 2008). The SHAW model was able to accurately simulate peat temperatures in chamber experiments and evaluate the effectiveness of black spruce mulch in insulating the subsurface and preventing the thawing of permafrost (Mohammed et al. 2017).

Additionally, a forest hydrology model (ForHyM) was developed to simulate soil temperatures within a jack pine, black spruce, and aspen forest located in central Saskatchewan (Jagtar Bhatti et al. 2006). While it was possible to simulate the subsurface temperatures at both the jack pine and aspen forest stands using the on-site air temperatures, the black spruce stand simulation required a reduction of 1.6 ºC applied to observed near-ground air temperatures that were used as input to the model. The only explanation given for the year-round reduction in inputted air temperatures for the ForHyM simulations was that moist-to-wet ground surface conditions cooled the air temperatures, yet the aspen forest had higher observed moisture contents due to a higher clay content (Jagtar Bhatti et al. 2006).

3 FIELD STUDY PHASE 1 (2009-2011)

The Forest Watershed and Riparian Disturbance (FORWARD) project was a research program that integrated aquatic and soil sciences, hydrology, and forestry into water quality and quantity models to aid in the management of forested watersheds within the Boreal Plains of western Canada after disturbances (Smith et al. 2003). The FORWARD project also attempted to integrate data from ecosystem analysis into landscape management models to develop best management practices linking hydrological function with detailed forest management plans (Prepas et al. 2008).

There was a total of 18 automated ecological sites in the FORWARD project which continuously monitored subsurface temperatures and water content at various depths up to 300 cm. The 18 automated sites consisted of six types; harvested, wildfire, deciduous, conifer, shallow peatland, and deep peatland, with three sites of each type. Phase 1 refers to all the data collected by the FORWARD research project prior to the commencement of this thesis at each of the 18 ecological sites, whereas Phase 2 (Chapter 4) was the data collected solely from the deep peatland sites during the field study of this thesis project.

Initially an empirical model was developed to simulate the observed subsurface temperatures as a function of the previous day's soil temperature, average annual temperature, and the current day's air temperature with the influence of snow and plant-canopy cover being incorporated as a weighting factor (Bélanger 2009). It was found that by adjusting the lag coefficient that the empirical model could reproduce the seasonal trends of soil temperatures for the spring, summer, and autumn periods, but predicted colder than observed temperatures during the winter at the FORWARD ecological sites.

It was suggested by Bélanger that the simulated wintertime temperatures were colder than observed subsurface temperatures because of the inadequate representation of the insulation from the snowpack and the lack of consideration for latent heat (Bélanger 2009). By using physically based equations to estimate frost depth and subsurface temperatures a greater understanding of the thermal properties of the ecological sites can be achieved. Further, if the physically based model improved winter subsurface temperature simulation, the results would indicate the model structure and underlying assumptions are correct.

After an initial review of all the data from the 18 ecological sites, six sites were selected for further in-depth analysis and comparison. All the deciduous and coniferous ecological sites were not used in the analysis due to complete canopy closure and stand heights greater than 15 m, which violated an assumption in the physical model that observed air temperature was above stand height. The shallow peatland, deep peatland, and wildfire sites were selected due to the lack of canopy closure and stand heights of less than 5 m. One of the wildfire sites had little to no growth on it, and was essentially bare soil, so was omitted from the analysis along with a deep and shallow peatland site due to the degradation of the peat surface at the location of the probes.

The field results of observed subsurface temperatures and moisture contents for the six selected FORWARD ecological sites over a three-year period are presented in this chapter along with frost depth estimates based upon ground surface temperatures. It is hypothesised that the shallower depths of frost observed at the black spruce peatland sites are due to the increase in latent heat released during the freezing process and can be reasonably predicted from Stefan's equation.

3.1 Field Methodology Phase 1

The following section provides details on each of the six selected ecological sites, the data collected, and the statistical analysis performed. Phase 1 refers to the data collected prior to the commencement of the thesis during the years of 2009 to 2011 by the FORWARD research group, while Phase 2 refers to the data collected by the author during the field study for the thesis in the years 2015 and 2016 at the deep peatland sites.

3.1.1 Site Description

The FORWARD project study area is located approximately 225 km northwest of Edmonton, Alberta, Canada in the Boreal Plains eco-zone and is shown with other sites of significant field research in Figure 3-1 (Ireson et al. 2015) . The six study sites are located within five first- to third-order watersheds (Scheidegger 1965; Strahler 1957) which are a subset of the FORWARD research watersheds (Figure 3-2). The Boreal Plains has a sub-humid climate (Zoltai et al. 1998) with long-term averages for precipitation and annual air temperature of 578 mm and 2.6 ºC, respectively, with 24% of the total precipitation falling as snow (Environment Canada 2015). Generally, the study area is snow- covered for six to seven months of the year, beginning in October or November (Environment Canada 2015).

The six study sites include two upland soils sites, two shallow peatlands sites, and two deep peatlands sites with lodgepole pine (*Pinus cortorta* Dougl. ex Loud.var. latifolia Engelm) or black spruce trees (*Picea mariana* (Mill.) BSP) as shown in Figure 3-3. The upland study sites have fine-grained Orthic Gray Luvisolic soils overlaying deep glacial tills (Smith et al. 2003), while the peatlands consist mainly of organic material (Table 3-1) (Ecological Stratification Working Group 1996). Soil classification profiles for each of the sites is also provided using the Canadian system of soil classification (Canada Agriculture et al. 1998). In the shallow peatlands the average thickness of the organic layer was 0.4 m while in the deep peatlands the thickness ranged from 2.0 to 2.9 m.

Figure 3-1 Location of the FORWARD Research Station within the extent of the Boreal Plains Ecozone

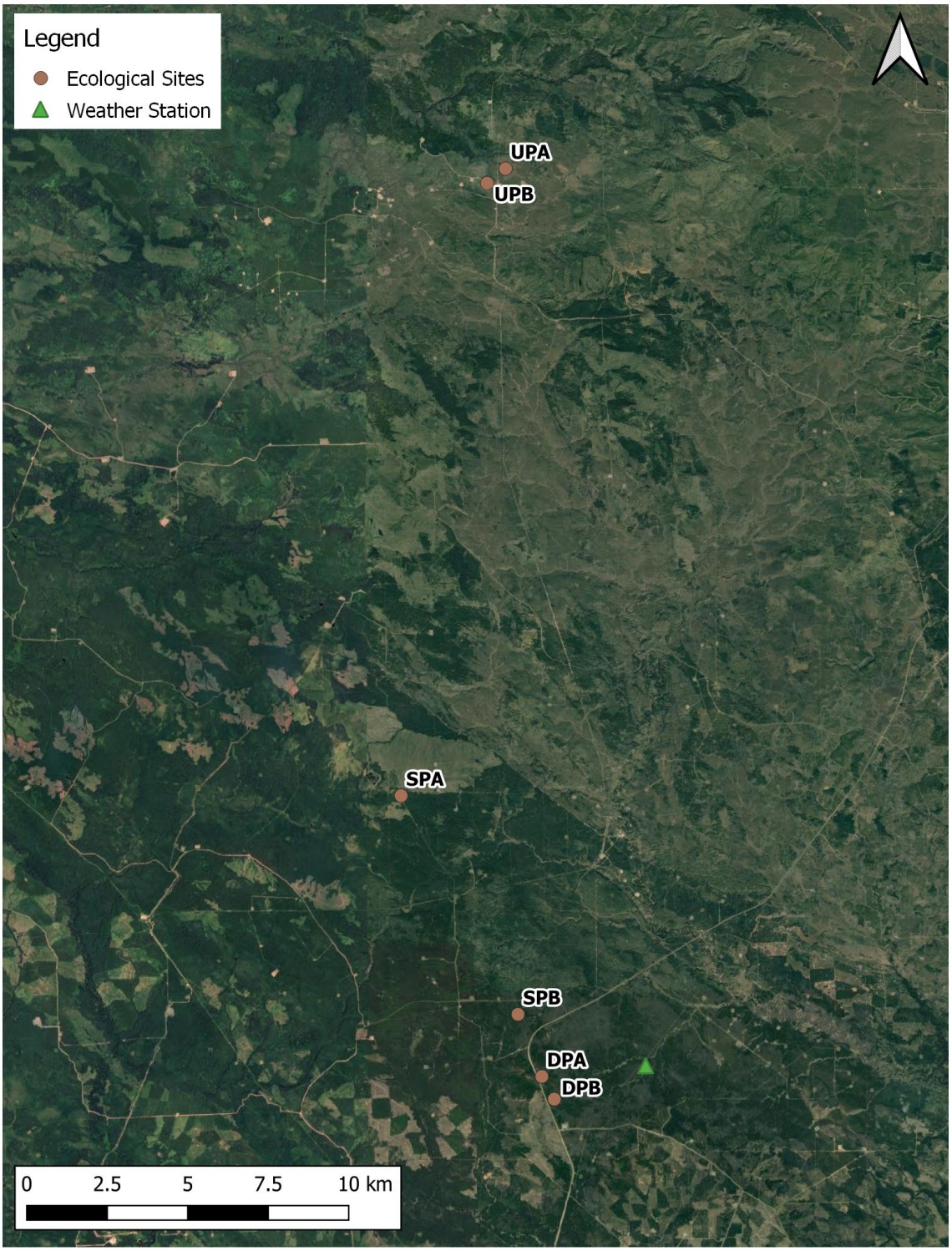

Figure 3-2 Location of the Six Ecological Sites, Deep Peatland A/B (DPA/DPB), Shallow Peatland A/B (SPA/SPB), Upland Pine A/B (UPA/UPB), and the weather station

Table 3-1 Description of Six Study Sites with Soil Profiles

Site Name	Deep Peatland A	Deep Peatland B	Shallow Peatland A	Shallow Peatland B	Upland A	Upland B
Site ID	DPA	DPB	SPA	SPB	UPA	UPB
Vegetation	Black Spruce	Black Spruce	Black Spruce	Lodgepole Pine	Lodgepole Pine	Lodgepole Pine
Elevation (m)	1026	1028	1032	1010	985	991
Type	Plateau Muskeg	Plateau Muskeg	Plateau Muskeg	Plateau Muskeg	Pediment Upland	Pediment Upland
Order	Organic	Organic	Gleysolic	Gleysolic	Luvisolic	Luvisolic
Subgroup	Typic Mesisol	Typic Mesisol	Orthic Humic Gleysol	Humic Luvic Gleysol	Orthic Gray Luvisol	Orthic Gray Luvisol
Depth (cm)	Canadian Soil Classification System					

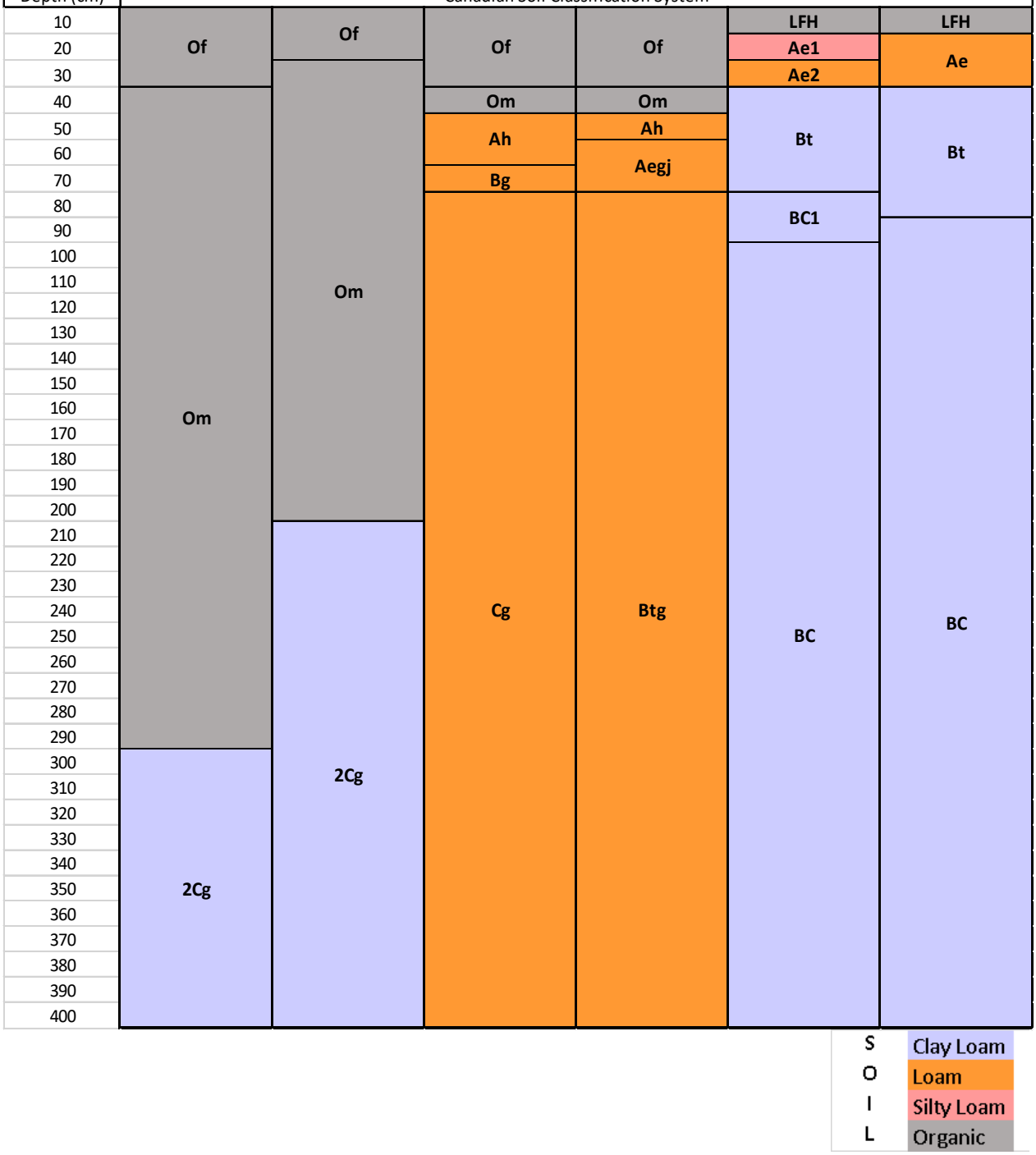

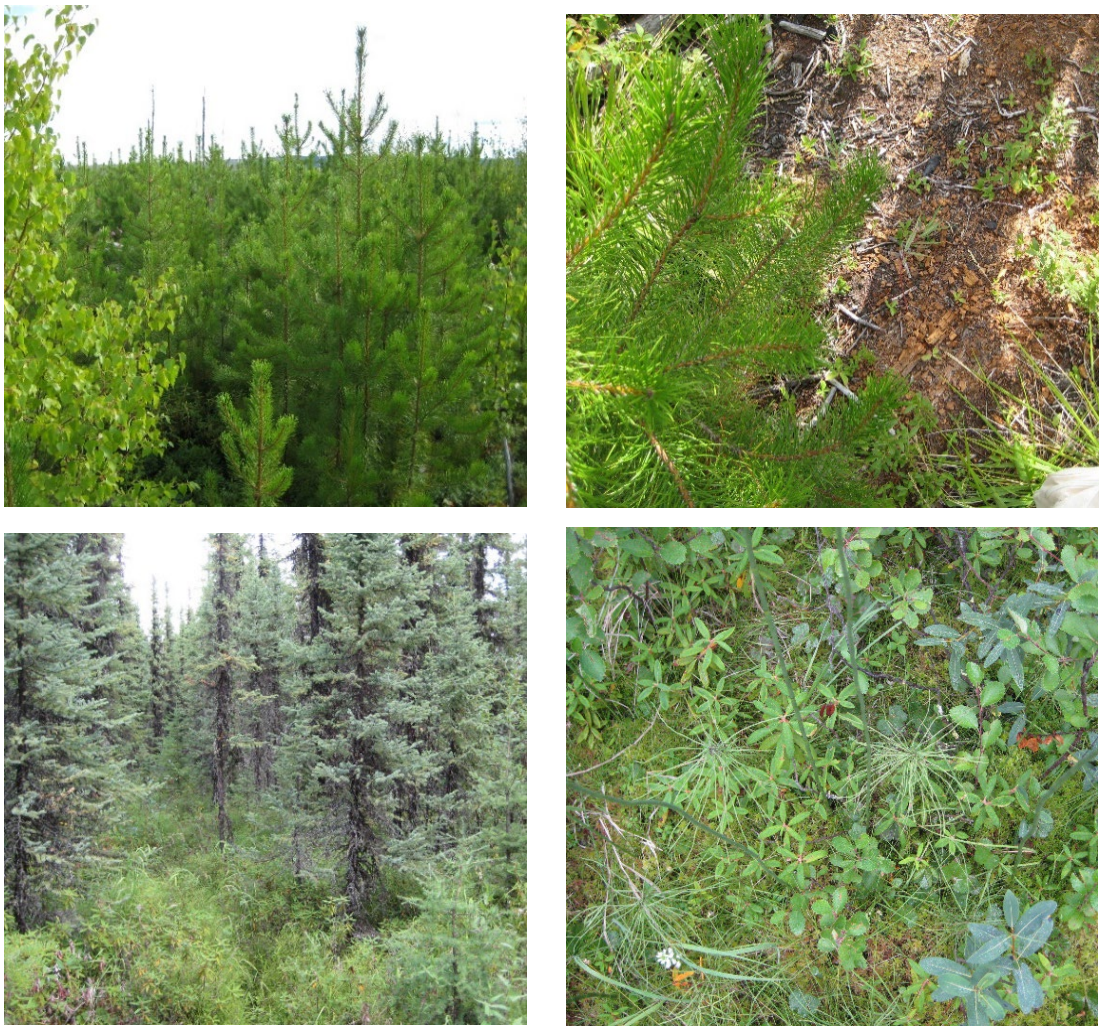

Figure 3-3 Example Photos of Vegetation and Ground Cover at Study Sites, Top Upland Pine (UPA) Bottom Shallow Peatland (SPA)

Soil texture analysis and bulk density measurements were taken throughout the FORWARD research study area, but prior to the installation and monitoring of the automated ecological sites (Chanasyk et al. 2003; Smith et al. 2003). Thus, there were no measurements taken directly at each of the automated sites but were obtained from other similarly classified locations within the same watersheds as the automated sites. The average percentages of sand, silt, and clay, along with dry bulk densities for the same Canadian soil classes as found at the ecological sites are provided in Table 3-2.

Table 3-2 Average Soil Texture and Dry Bulk Density for Canadian Soil Classes at FORWARD Site

Canadian Soil Classification System	Soil Type	Texture			Bulk Density
		Clay%	Sand%	Silt%	kg/m^3
2Cg	Clay Loam	31	33	36	NA
Cg	Loam	25	32	43	1202
Ah	Loam	16	36	47	775
Ae	Loam	22	35	43	1322
Ae1	Silty Loam	11	35	53	1159
Ae2	Loam	21	39	40	1484
Aegj	Loam	19	35	46	1117
AB	Loam	23	33	44	NA
Bg	Loam	21	34	46	NA
Bt	Clay Loam	33	30	37	1504
Btg	Loam	27	33	41	1452
BC	Clay Loam	31	33	36	NA
BC1	Clay Loam	35	30	35	NA
Of	Organic	NA	NA	NA	131
Om	Organic	NA	NA	NA	253

3.1.2 Data Collection

The six study sites were monitored from the fall of 2008 to the summer of 2011 for soil moisture and temperature at varying depths. Soil temperature was measured and recorded either by YSI thermistors (YSI Incorporated, Yellow Springs, OH, USA) or Data Dolphin dataloggers (Optimum Instruments Inc., Edmonton, AB, Canada). Measurements were taken hourly at 0.1, 0.3, 0.5, 1.0, 2.0, and 3.0 m depths within the soil and at the ground surface and 2.0 m above for air temperature. Soil moisture content was measured with theta probes (Delta-T Devices Ltd., Burwell, Cambridge, UK) and recorded by a Data Dolphin datalogger at 0.1, 0.5 and 1.0 m depths. The configuration of the temperature and moisture content probes are presented in Table 3-3. Snow surveys were also completed whenever an ecological site was visited during the winter to download data, which occurred once or twice a season with 3 snow core measurements per visit. In addition, a FORWARD weather station was operated within the Willow watershed which recorded temperature, humidity, wind speed, and solar radiation on an hourly basis.

Table 3-3 Phase 1 Configuration of Probes

Probe	Medium	Elevation (cm)
Temperature	Air	200
Temperature	Air	0
Temperature	Peat/Soil	-10
Temperature	Peat/Soil	-30
Temperature	Peat/Soil	-50
Temperature	Peat/Soil	-100
Temperature	Peat/Soil	-200
Temperature	Peat/Soil	-300
Moisture	Peat/Soil	-50
Moisture	Peat/Soil	-100
Moisture	Peat/Soil	-150

3.1.3 Estimated Depth of Frost

The depth of frost can be estimated from the total latent heat released, which is the energy lost when water freezes, and is dependent upon the moisture content (Equation 3-1) (Hayashi et al. 2007).

Equation 3-1 Latent Heat Released from Freezing the Subsurface (Hayashi et al. 2007)

$$Q_L = L\theta\rho\frac{dx}{dt} \quad \text{.....(3-1)}$$

Where:

Q_L is the latent heat released (kJ m^{-2} s^{-1})
L is the specific latent heat of water (334 kJ kg^{-1})
θ is the volumetric ice content (m^3 m^{-3})
ρ is the density of ice (1000 kg m^{-3})
x is the depth of frost (m)
t is the time (s)

Additionally, the heat conducted through the frozen layer can be estimated from the difference in temperature between the surface and the frost line, assumed to be 0 ºC, and the thermal resistance, which is the thickness divided by the thermal conductivity (Equation 3-2) (Hayashi et al. 2007).

Equation 3-2 Heat Conducted through the Frozen Layer (Hayashi et al. 2007)

$$Q_{FLUX} = \frac{\Delta T}{R} = \frac{\Delta T}{x/k} \quad \text{.....(3-2)}$$

Where:

Q_{FLUX} is the heat conducted through the frozen layer (kJ m^{-2} s^{-1})
ΔT is the difference in temperature between surface and frostline (ºC)
R is the thermal resistance (ºC W^{-1})
k is the thermal conductivity (W ºC^{-1} m^{-1})
x is the depth of frost (m)

In 1889 Josef Stefan was the first to assume that the heat conducted through the frozen layer was equal to the latent heat released and could be solved for to estimate the depth of frost (Equation 3-3) (Hayashi et al. 2007). Stefan's equation is still commonly applied and was used to estimate the depth of frost at each of the six study sites for 2009, 2010, and 2011.

Equation 3-3 Stefan's (1889) Equation for Estimating Depth of Frost (Hayashi et al. 2007)

$$x = \sqrt{\frac{2k}{L\theta\rho}\int \Delta T dt} \quad \text{.....(3-3)}$$

Where:

x is the depth of frost (m)
k is the soil thermal conductivity (W ºC^{-1} m^{-1})
ΔT is the temperature gradient (ºC)
L is the specific latent heat of water (334 kJ kg^{-1})
θ is the volumetric ice content (m^3m^{-3})
ρ is the density of ice (kg m^{-3})
t is the time (s)

The integral of the temperature gradient with time is also referred to as the freezing index and is the summation of average daily ground surface temperatures assuming a temperature of 0 ºC at the frost line Equation 3-4.

Equation 3-4 Calculation of Freezing Index

$$\sum_{i=1}^{n}(TS_i - TF_i) \quad \text{.....(3-4)}$$

Where:

TS_i is average daily temperature at the surface on day i (ºC)
TF_i is average daily temperature at the frost line on day i (0 ºC)
n is the number of days to the minimum freezing index and maximum depth of frost (days)
i is the number of days since the first continuous frost occurred

The summation starts with the first day in the fall with an average daily temperature of less than 0 ºC, and the summation resets at zero if there is a series of warms days resulting in a positive value. The day with the minimum value for the summation of the freezing index is considered the day when the maximum frost depth occurs and is used for subsequent calculations. A time unit conversion is also required to convert the thermal conductivity from seconds to days.

3.2 Field Results Phase 1

A description of the results and frost depth analysis from the three years of monitoring data at each of the six ecological sites is presented in this section.

3.2.1 Observed Temperatures

Box plots were created for each set of observed winter temperatures illustrating the differences between each ecological site by year. Winter temperatures include all hourly observations made in January, February, and March for 2009, 2010, and 2011. The naming convention for the ecological sites is the first two letters indicating the soil type (Deep Peatland (DP), Shallow Peatland (SP), Upland (UP)) with the third letter distinguishing between the duplicate sites (A or B). For each of the box plots the median is plotted with the first and third quartile, which is 25% of the data above and below the median, as the top and bottom of the box. The whiskers are plotted at the 5 and 95 percentiles of the data with outliers included. All the hourly raw data was used to generate the box plots, with no averaging.

3.2.1.1 Air Temperature at +200 cm

There was very little difference of air temperature at 200 cm above ground surface between ecological sites (Figure 3-4), which is expected due to the proximity of all the sites and the lack of canopy closure. The median and quantile temperatures of UPB were slightly warmer than the rest of sites, but not statistically significant. The median winter temperature in 2010 was slightly warmer than 2009 and 2011, however the minimum winter temperature was roughly 10 ºC warmer at all sites. With consistent air temperatures at all sites, any variations in subsurface temperatures between sites would be a result of the properties of soil, vegetation cover and snowpack.

3.2.1.2 Ground Surface Temperature

The winter observed ground surface temperature was highly dependent upon whether the probe was buried within the snowpack or not. The presence of a snowpack would prevent air temperatures from exceeding 0 ºC during warmer winter days and insulate it from extreme cold temperatures at night. Further the presence and thickness of the snowpack around the air temperature data collection post was influenced by the canopy cover. The collection posts at DPB and SPB were partially shaded, while the ground surface temperature probe at DPA, UPA, and UPB were fully exposed. There were unknown issues with SPA's ground surface probe, with it often having a very poor correlation with the 200 cm air probe during the summer, and the data was omitted from analysis. The ground surface temperatures were coldest in 2010, even though 2010 had the warmest 200 cm air temperatures because there was less of a snowpack (Figure 3-5). The distribution of winter ground surface temperatures over the three years of observations only varied slightly between sites, with peatlands being slightly warmer.

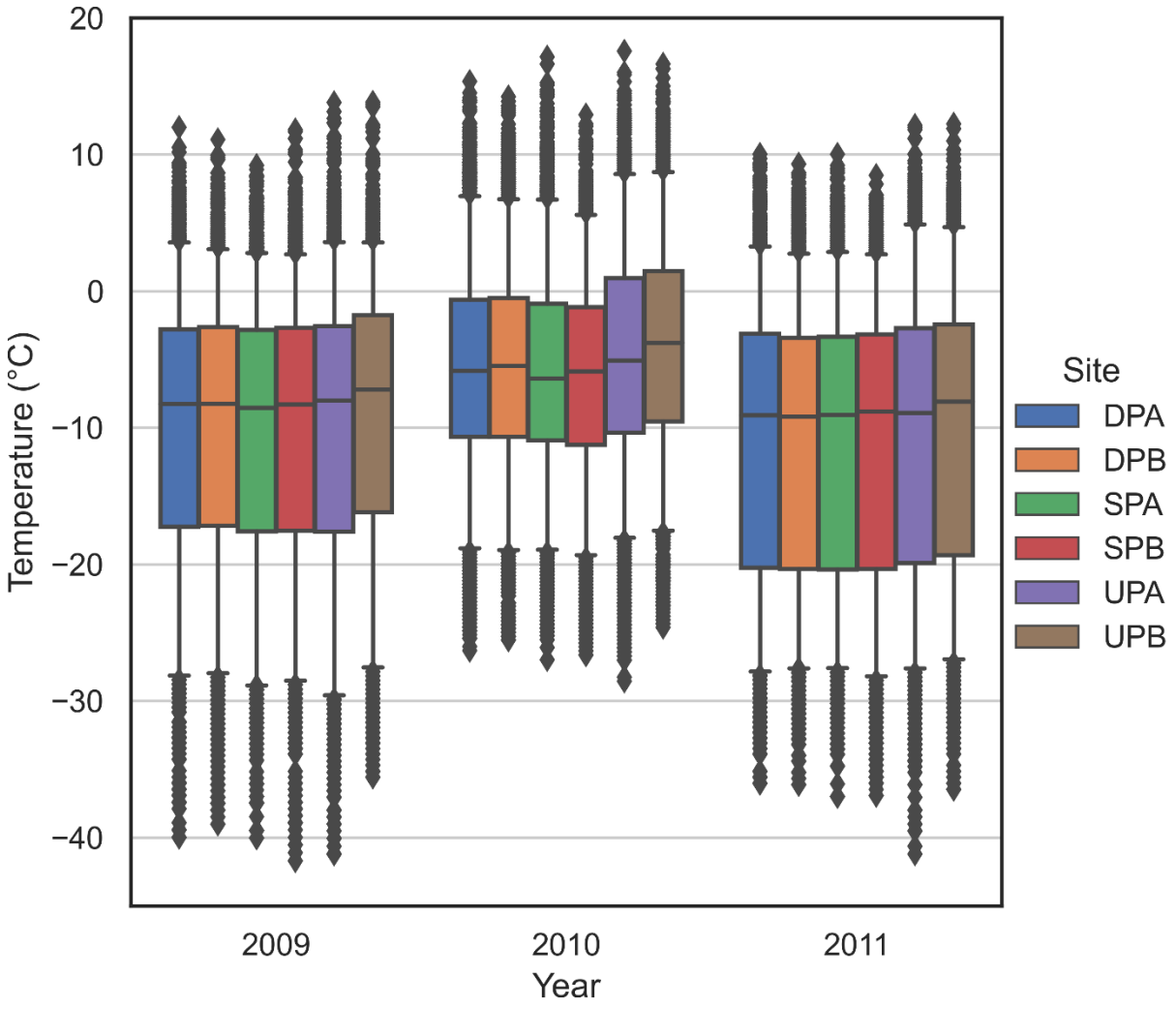

Figure 3-4 Box Plots of Air Temperatures at +200 cm for Ecological Sites by Year for the Winter Months of January, February, and March of Hourly Data

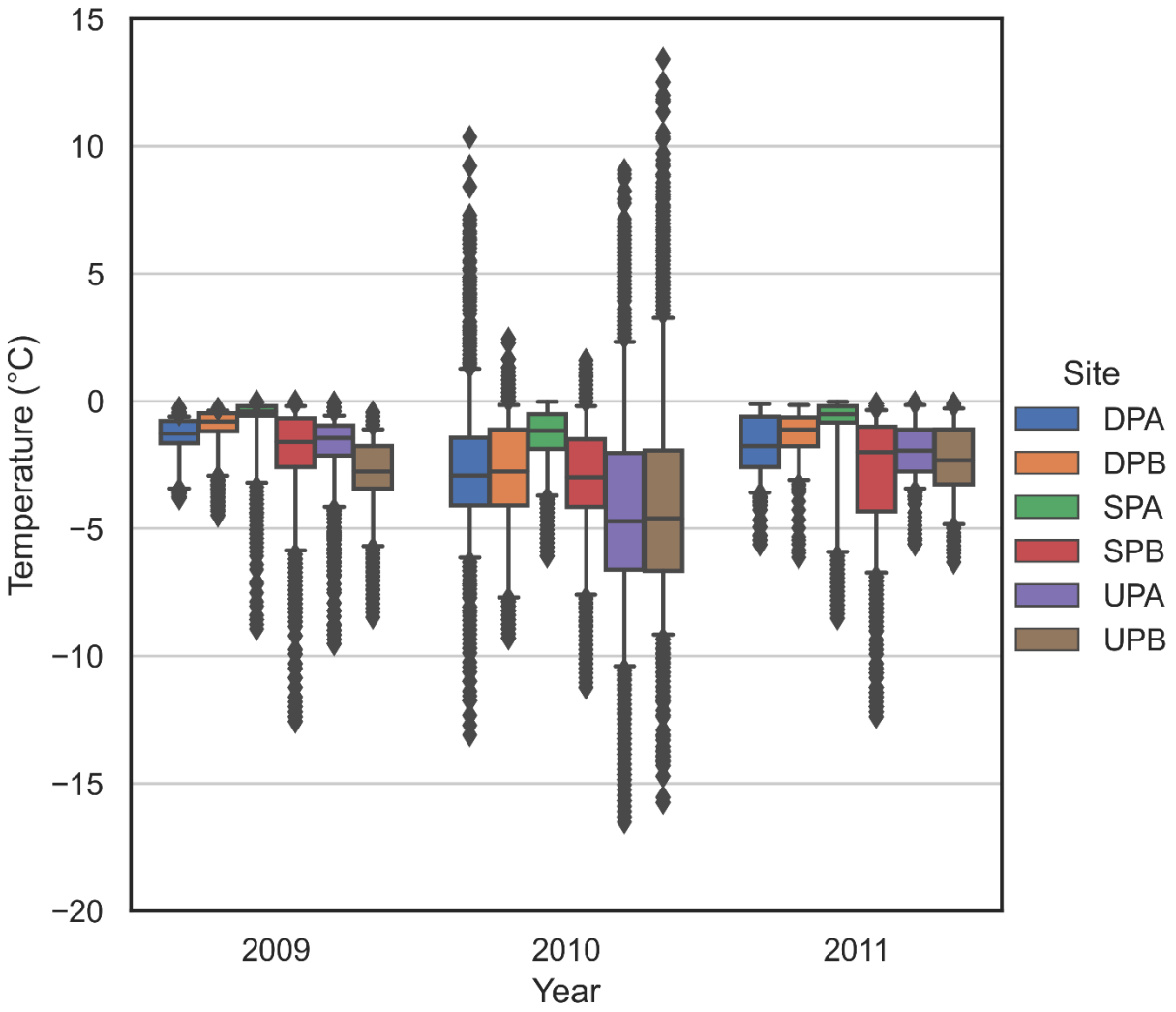

Figure 3-5 Box Plots of Ground Surface Temperature by Ecological Sites for the Winter Months of January, February, and March of Hourly Data

3.2.1.3 Soil Temperature at -10 cm

The magnitude of range in winter soil temperatures at a depth of 10 cm varied greatly between ecological sites, with the deep peatlands (DPA, DPB) having the least amount of variability, especially in 2009 (Figure 3-6). The pine upland sites (UPA, UPB) along with the black spruce dominated shallow peatlands (SPA) had similar variability in their range of temperatures, however the upland sites were on average colder in 2010 and 2011. The pine dominated shallow peatland (SPB) had both the greatest range in observed temperatures and was the coldest out of all six sites. DPA and DPB sites were below 0 ºC for approximately 12-17% of the winter period whereas the SPA site was below 0 ºC over half of the observed period. The pine dominated sites (SPB, UPA, UPB) were below 0 ºC over 90% of the time. It should also be noted that while the

winter observed air temperatures in 2010 were the warmest, the soil temperatures at SPB, UPA, and UPB sites were the coldest, similar to the ground surface temperatures.

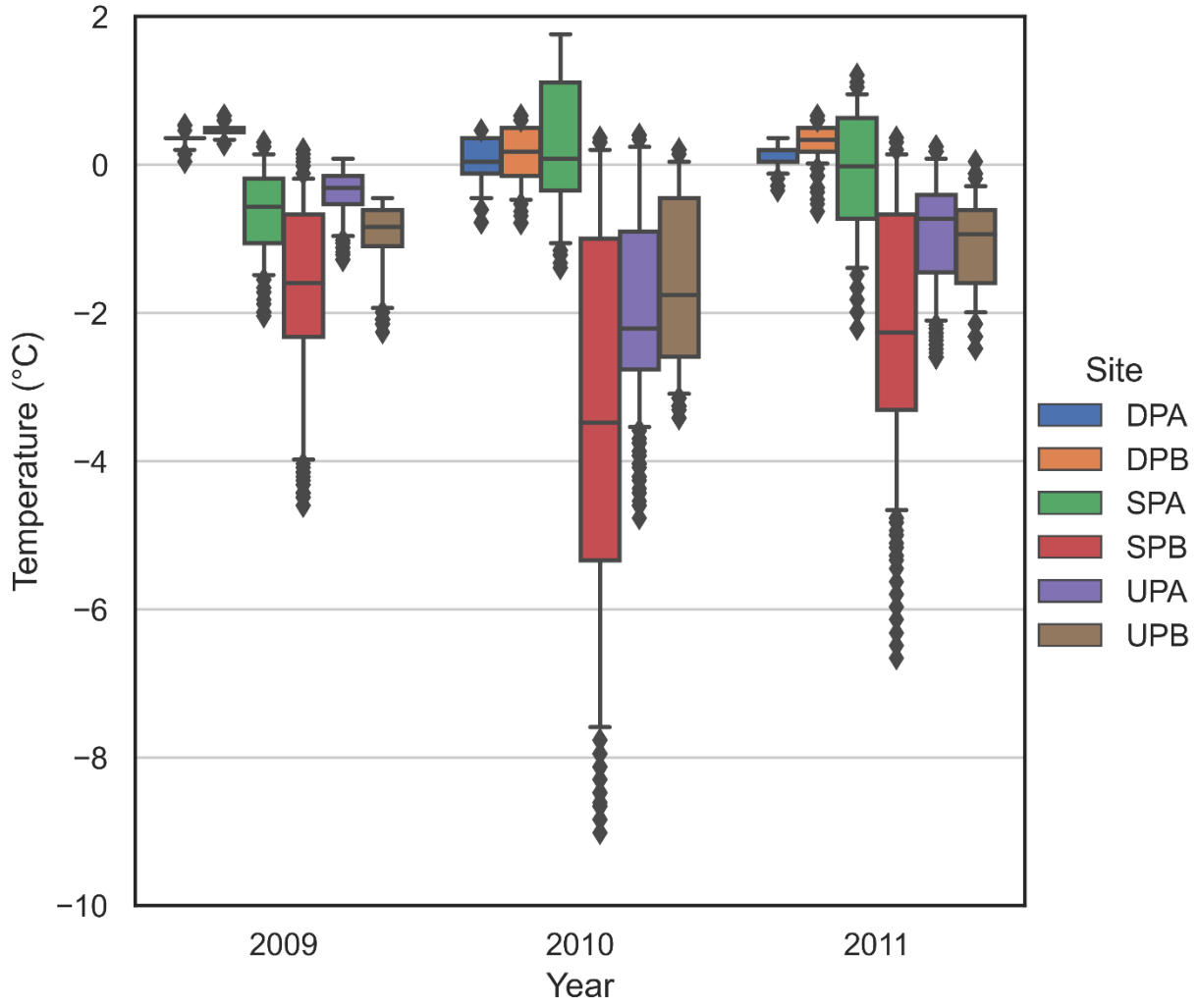

Figure 3-6 Box Plots of Soil Temperatures at -10 cm for Ecological Sites by Year for the Winter Months of January, February, and March of Hourly Data

3.2.1.4 Soil Temperature at -30 cm

The magnitude of the range in winter soil temperatures at a depth of 30 cm were near consistent between the three black spruce dominated ecological sites (DPA, DPB, SPA), and only changed slightly by year (Figure 3-7). In comparison the pine dominated upland sites (UPA, UPB) had similar magnitude in ranges in temperature, but varied greatly from year to year. The pine dominated shallow peatland (SPB) was the coldest ecological site and had the greatest variability, especially during 2010 which had 10 ºC warmer minimum temperatures suggesting factors other than air temperature were having an effect. At -30 cm the two deep peatland sites

never experienced frost while the black spruce shallow peatland was below 0 ºC approximately 70% of the time. All the pine dominated ecological sites were below 0 ºC over 99% of the time during the three winters. As with the -10 cm observed subsurface temperatures SPB, UPA, and UPB were the coldest in 2010 even through the air temperatures were warmer than in 2009 and 2011.

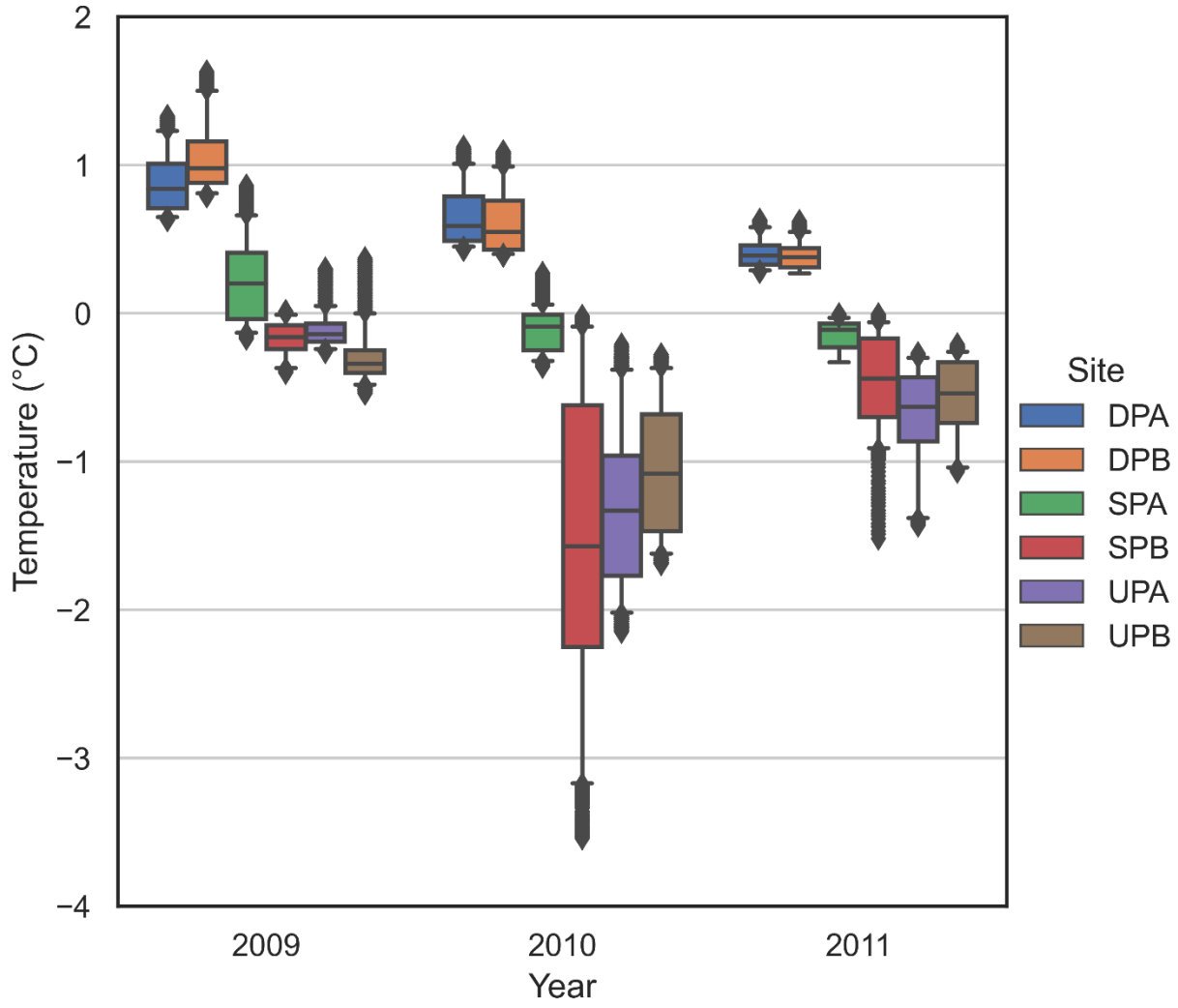

Figure 3-7 Box Plots of Soil Temperatures at -30 cm for Ecological Sites by Year for the Winter Months of January, February, and March of Hourly Data

3.2.1.5 Soil Temperature at -50 cm

The magnitude of range and median winter temperatures at a depth of 50 cm were near consistent between all the peatland ecological sites (DPA, DPB, SPA, SPB), with the DPA site being the coldest of the peatland sites except for in 2010 when SPB was colder (Figure 3-8). The peatland sites never were below 0 ºC at a depth of 50 cm and had near consistent responses in temperature due to the presence of the groundwater table as indicated by the complete saturation of the moisture content probes at this elevation (Section 3.2.2). The normalizing effect on temperature due to saturated conditions at this depth demonstrates that the difference in shallower soil temperatures is due to the thermal characteristics of the vadose zone and not because of the presence of shallow groundwater. In the two pine upland sites (UPA, UPB) the unsaturated soils 50 cm below ground surface were below 0 ºC over 60% of the time.

3.2.1.6 Soil Temperature at -100 cm

The magnitude of range in winter temperatures at a depth of 100 cm were similar in all ecological sites with little variation from year to year (Figure 3-9). The median temperatures vary between sites, with the deep peatlands being slightly warmer than the shallow peatlands and a lot warmer than the upland sites. Again, none of the peatland sites were ever below 0 ºC at -100 cm while UPA was below 0 ºC most of the time in 2010 and partially in 2011. No measurements were obtained at UPA in 2009 due to instrument error.

3.2.1.7 Soil Temperature at -200 cm

The magnitude of range in winter temperatures at a depth of 200 cm were similar in all ecological sites with a slightly greater range in UPB (Figure 3-10). The median temperatures varied between sites but differed from the measurements made at 100 cm depth since the shallow peatland probes are now situated within the mineral soils, like the upland sites. At this depth, the deep peatland sites are much warmer than both the shallow peatland sites and upland sites, with the shallow peatland sites being slightly warmer than the uplands sites in 2009 and 2010. At a depth of 200 cm none of the sites ever were below 0 ºC. No measurements were obtained at UPB in 2009 due to instrument error.

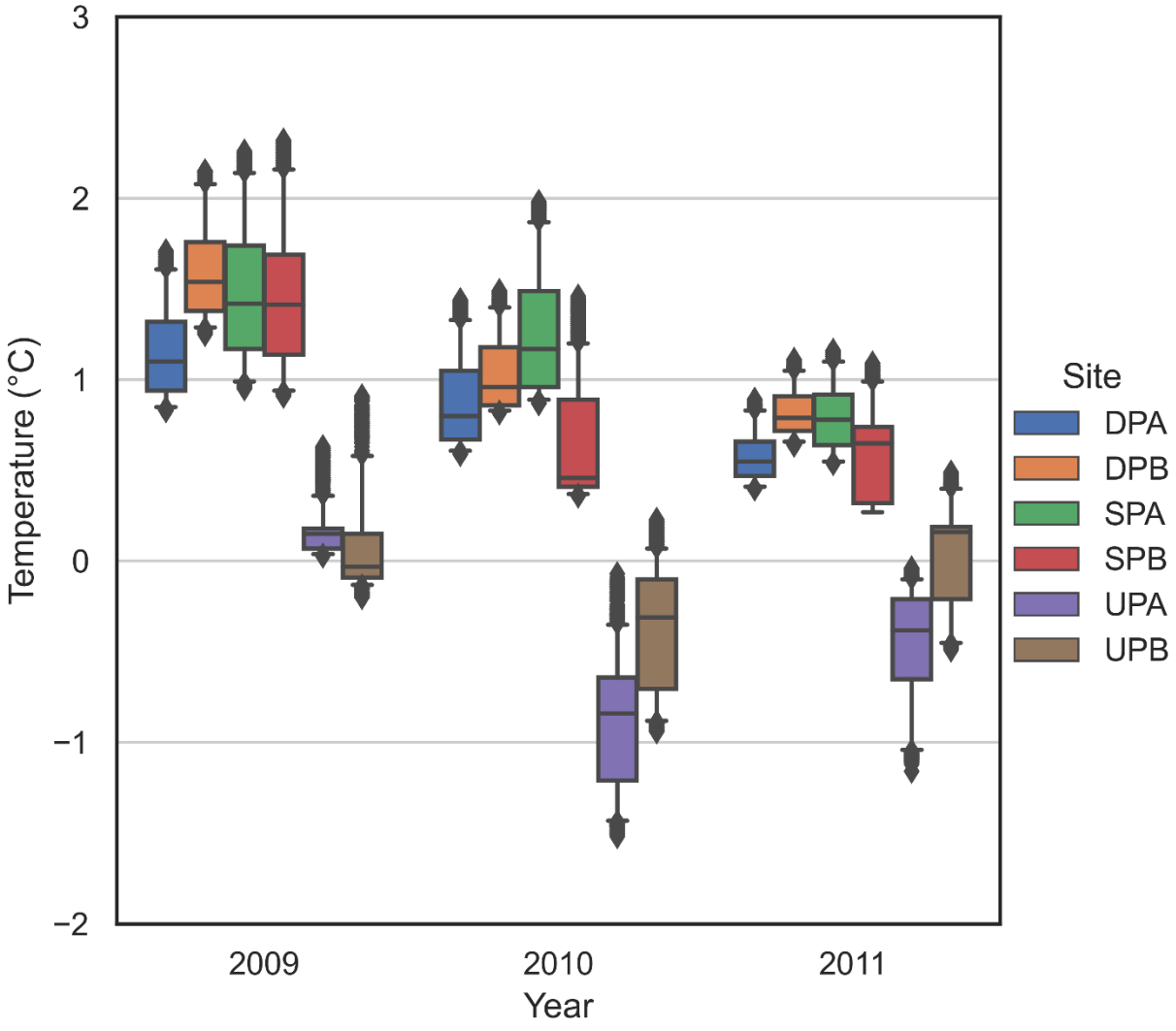

Figure 3-8 Box Plots of Soil Temperatures at -50 cm for Ecological Sites by Year for the Winter Months of January, February, and March of Hourly Data

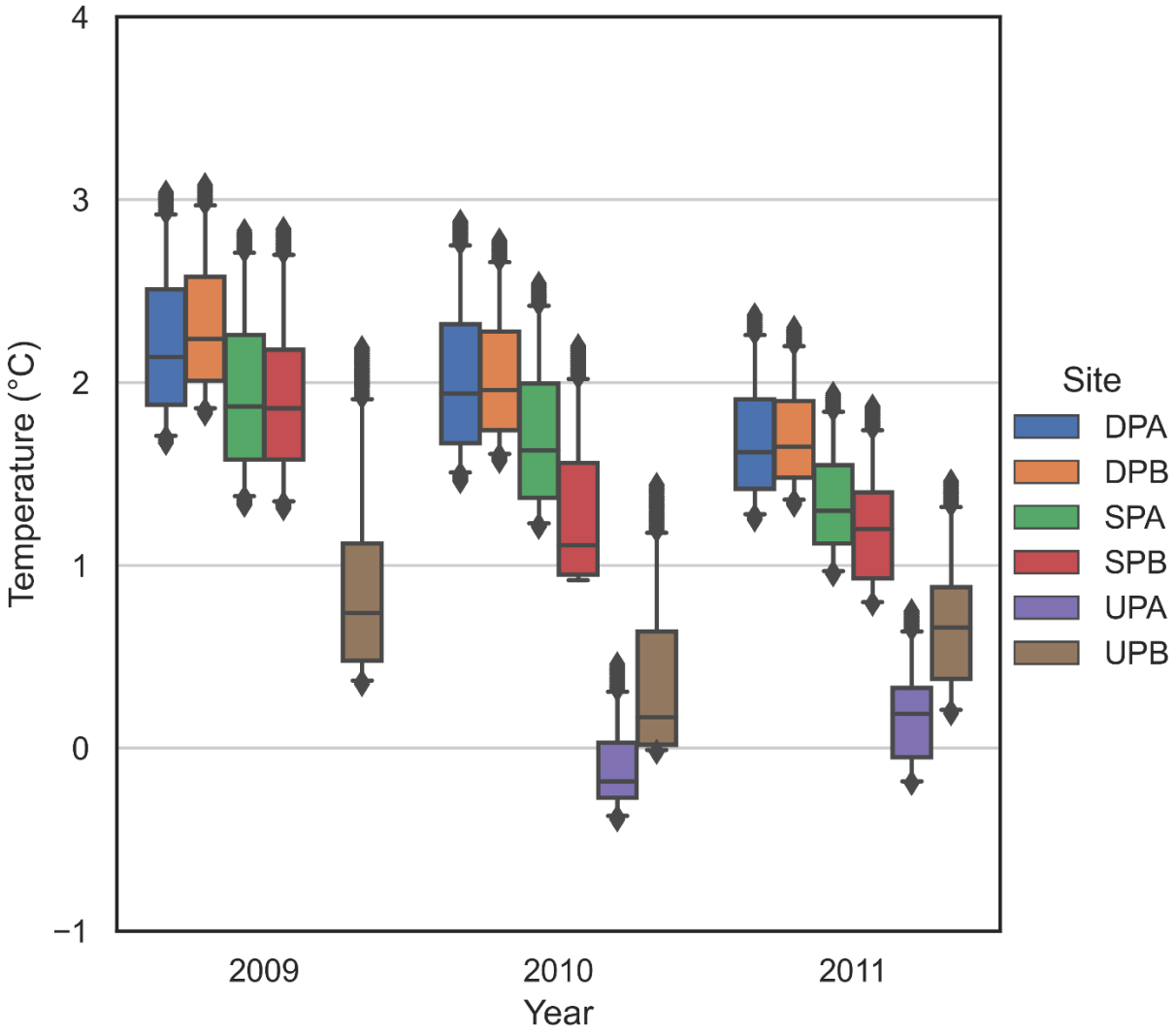

Figure 3-9 Box Plots of Soil Temperatures at -100 cm for Ecological Sites by Year for the Winter Months of January, February, and March of Hourly Data

3.2.1.8 Soil Temperature at -300 cm

The magnitude of range in wintertime temperatures at a depth of 300 cm differed dependent on soil type, with the deep peatland having the least variability, followed by the shallow peatland, and with the upland sites having the greatest variability (Figure 3-11). The median temperatures varied between sites with the deep peatlands being the warmest, but now with the upland sites having a median temperature warmer than the shallow peatlands. In 2009 the median temperature for UPB was comparable to the DPA, and even warmer than the observed temperature in 2011. No measurements were obtained at UPB in 2010 due to instrument error.

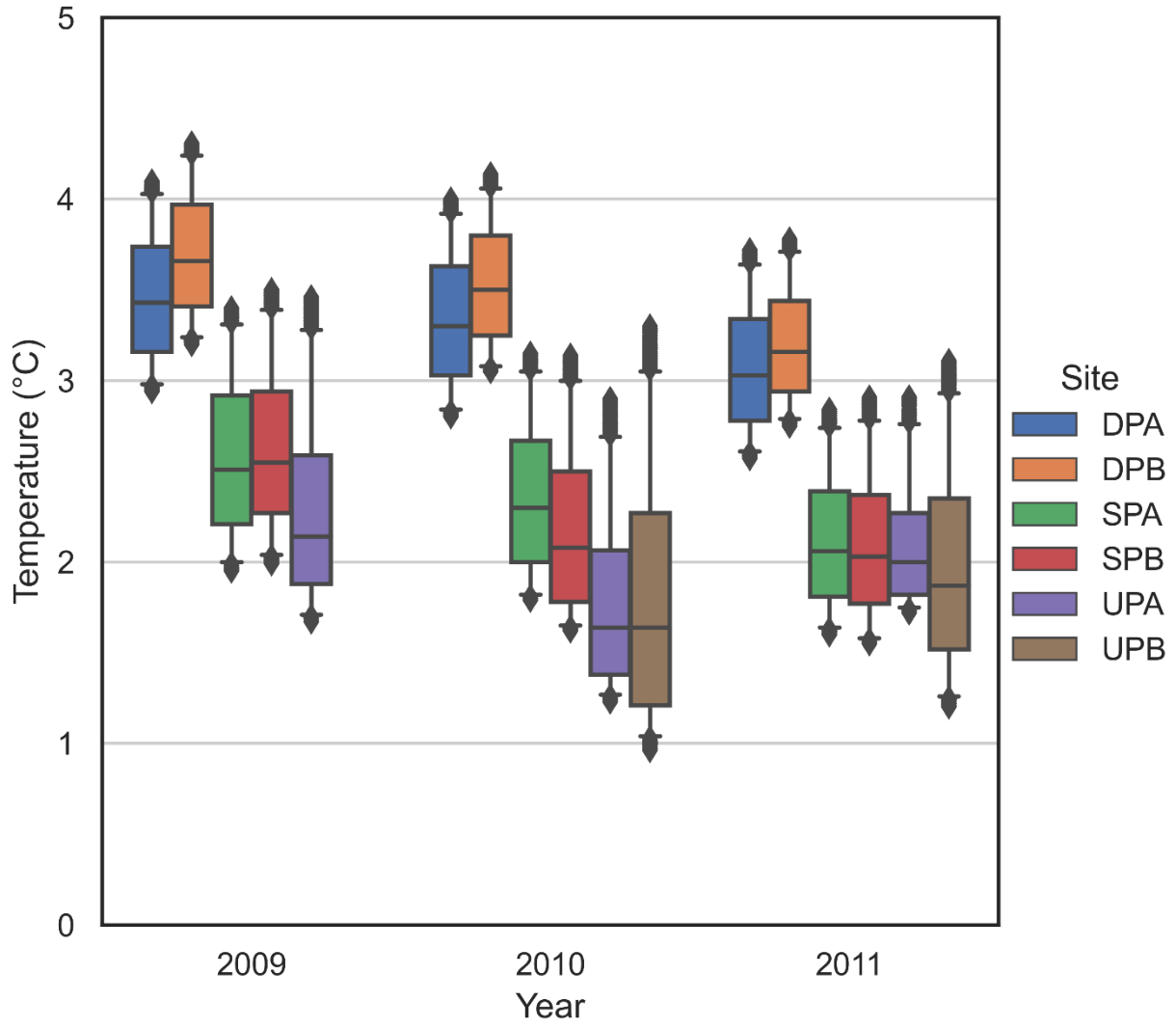

Figure 3-10 Box Plots of Soil Temperatures at -200 cm for Ecological Sites by Year for the Winter Months of January, February, and March of Hourly Data

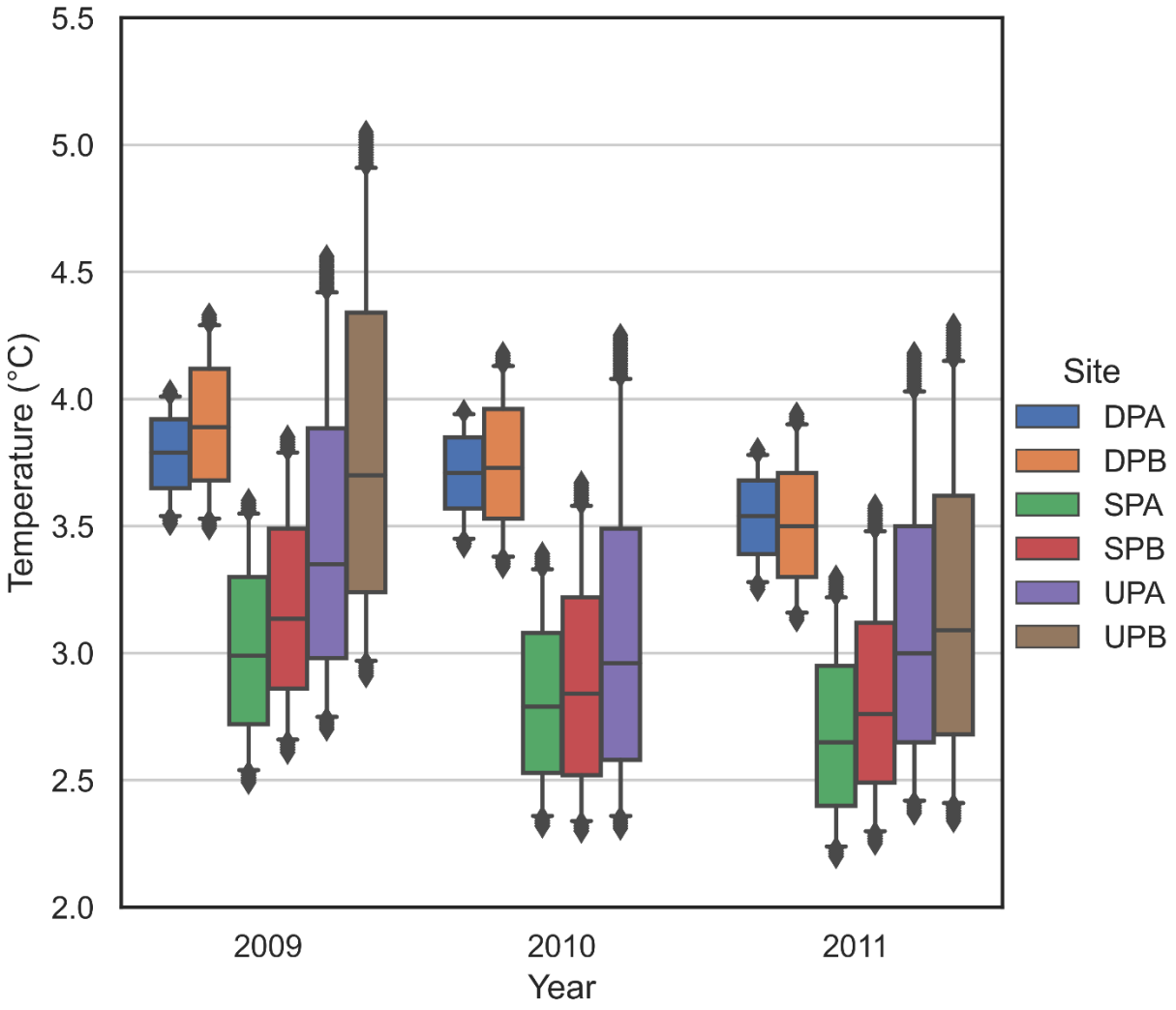

Figure 3-11 Box Plots of Soil Temperatures at -300 cm for Ecological Sites by Year for the Winter Months of January, February, and March of Hourly Data

3.2.2 Observed Moisture Contents

Box plots were created for each set of observed wintertime moisture contents illustrating the differences between ecological sites. Wintertime moisture contents include observations made on an hourly basis for January, February, and March, of 2009, 2010, and 2011. The naming convention for the ecological sites follows that described for the temperature probes. For each of the box plots the median is plotted with the first and third quartile, which is 25% of the data above and below the median, as the top and bottom of the box. The whiskers are plotted at the 5 and 95 percentiles of the data with outliers included. All the hourly raw data was used to

generate the box plots, with no averaging. Box plots were plotted by site instead of by year because there was often little variation of moisture contents within the year, and even when combining all years of data resulted in little variation, especially at depth.

Because the soil moisture probes can only detect liquid water the observed variability in moisture contents at -10 cm was likely due to changes in the percent ice content within the soil or peat and not from any changes in the actual water content. Further all the liquid water does not freeze at sub-zero temperatures, resulting in observable moisture contents of less than 0.15 m^3 m^{-3}, even when temperatures are below 0 ºC during the months of January, February, and March (Figure 3-6, Figure 3-12). The amount of ice content can be roughly estimated as the difference in moisture content observed during the winter from that observed in October when the subsurface is completely thawed. Both DPA and DPB had a higher-than-expected observable ice content, which was estimated from the difference in measured moisture contents from that in October. The longer than expected period of frost was due to the soil moisture probes being installed at the top of hummocks and not located at the same absolute elevation as the -10 cm temperature probes. During the winter month of January, February, and March from 2009 to 2011 the soil moisture probes indicated that ice had formed in the subsurface and was not hydrologically active except during one warm day at UPA when the ice partially thawed resulting in the moisture content exceeding 0.3 m^3 m^{-3} before refreezing that night.

There was very little variability in the observed moisture contents at -50 cm for the deep peatland (DPA and DPB) sites and at the black spruce shallow peatland (SPA) site due to the peat always being saturated since the water table was above the probe (Figure 3-13). During the same period the pine shallow peatland (SPB) was saturated approximately 50% of the time, while neither of the upland sites were ever saturated at -50 cm. Both the deep peatland sites had moisture contents > 0.8 m^3 m^{-3} indicating they were still organic materials, while the shallow black spruce peatland (SPA) was beginning to transition from an organic to a mineral soil and the pine shallow peatland (SPB) probe was in the mineral soil.

All the -100 cm moisture content probes at the peatland sites (DPA, DPB, SPA, SPB) were saturated the entire time with both the deep peatland soil moisture probes still in organic material (Figure 3-14). The soil moisture probes at both the shallow peatland sites were in mineral soils at a depth of 100 cm. Both the upland pine sites were saturated approximately half of the time,

which is demonstrated when the medians, the upper quartile of 75%, and the upper whisker of 95% of the data are all equal to what would likely be the total porosity of the soil.

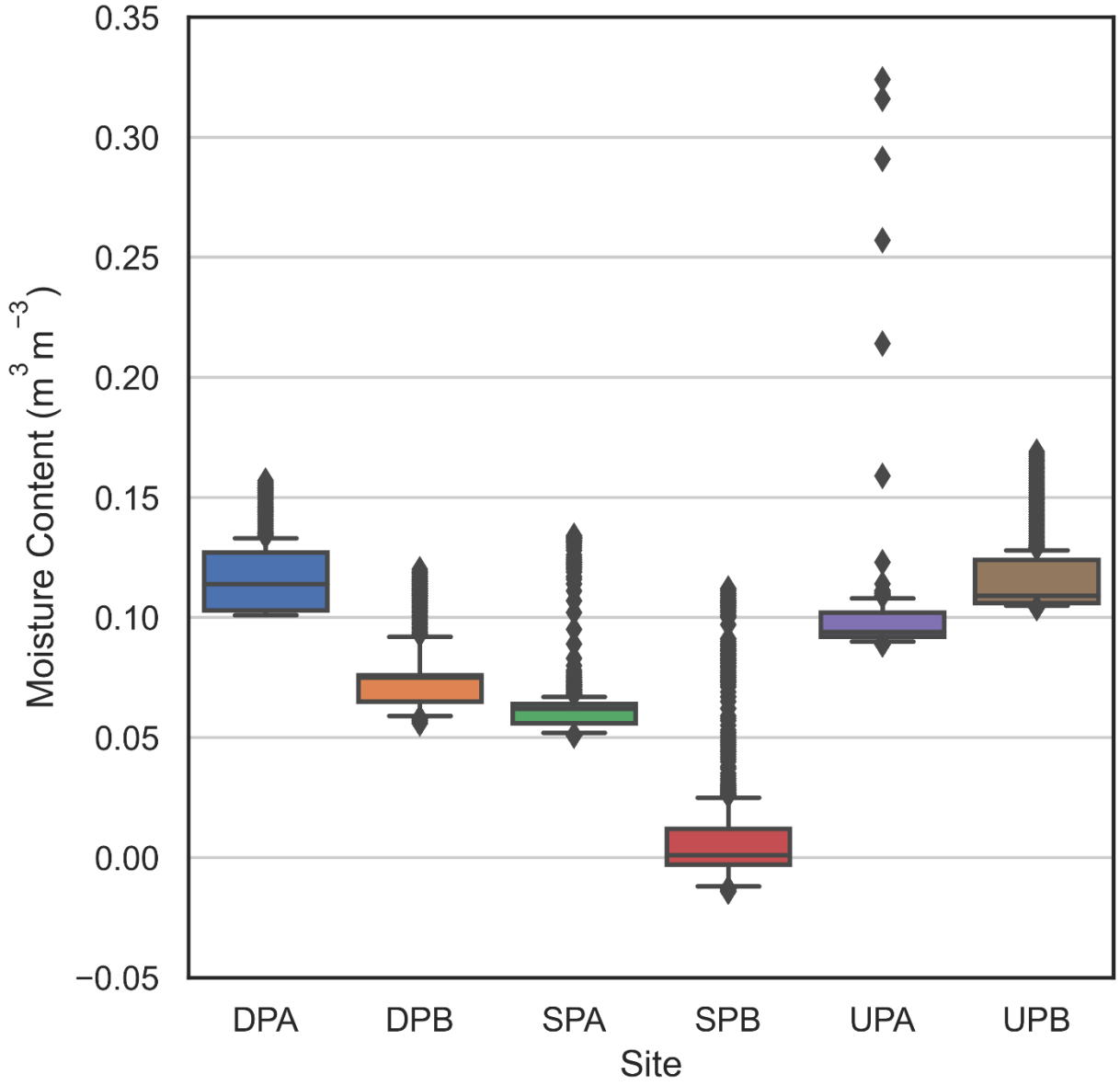

Figure 3-12 Box Plots of Moisture Contents at -10 cm for Ecological Sites for the Winter Months of January, February, and March of Hourly Data for 2009, 2010, and 2011.

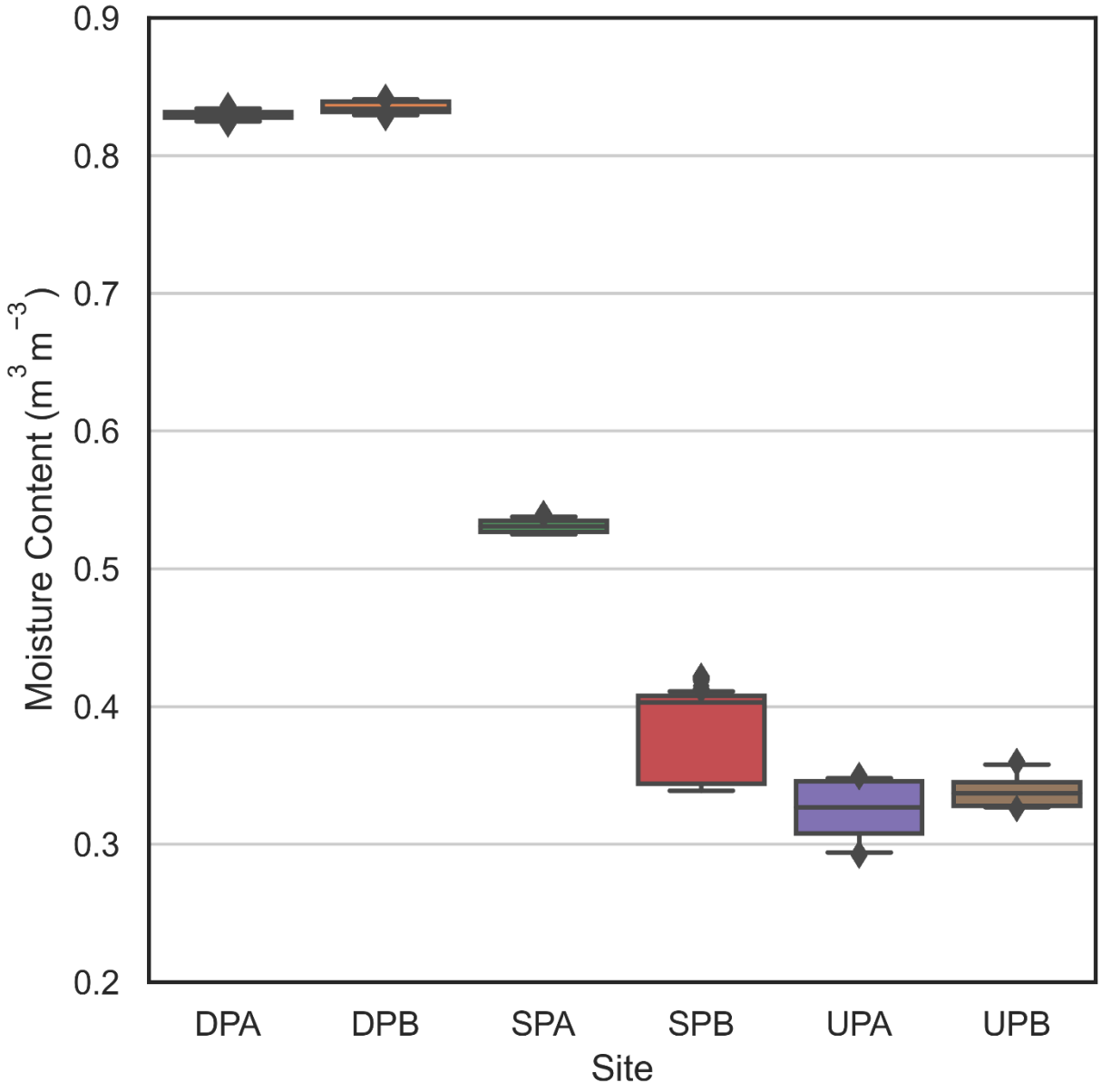

Figure 3-13 Box Plots of Moisture Contents at -50 cm for Ecological Sites for the Winter Months of January, February, and March of Hourly Data for 2009, 2010, and 2011

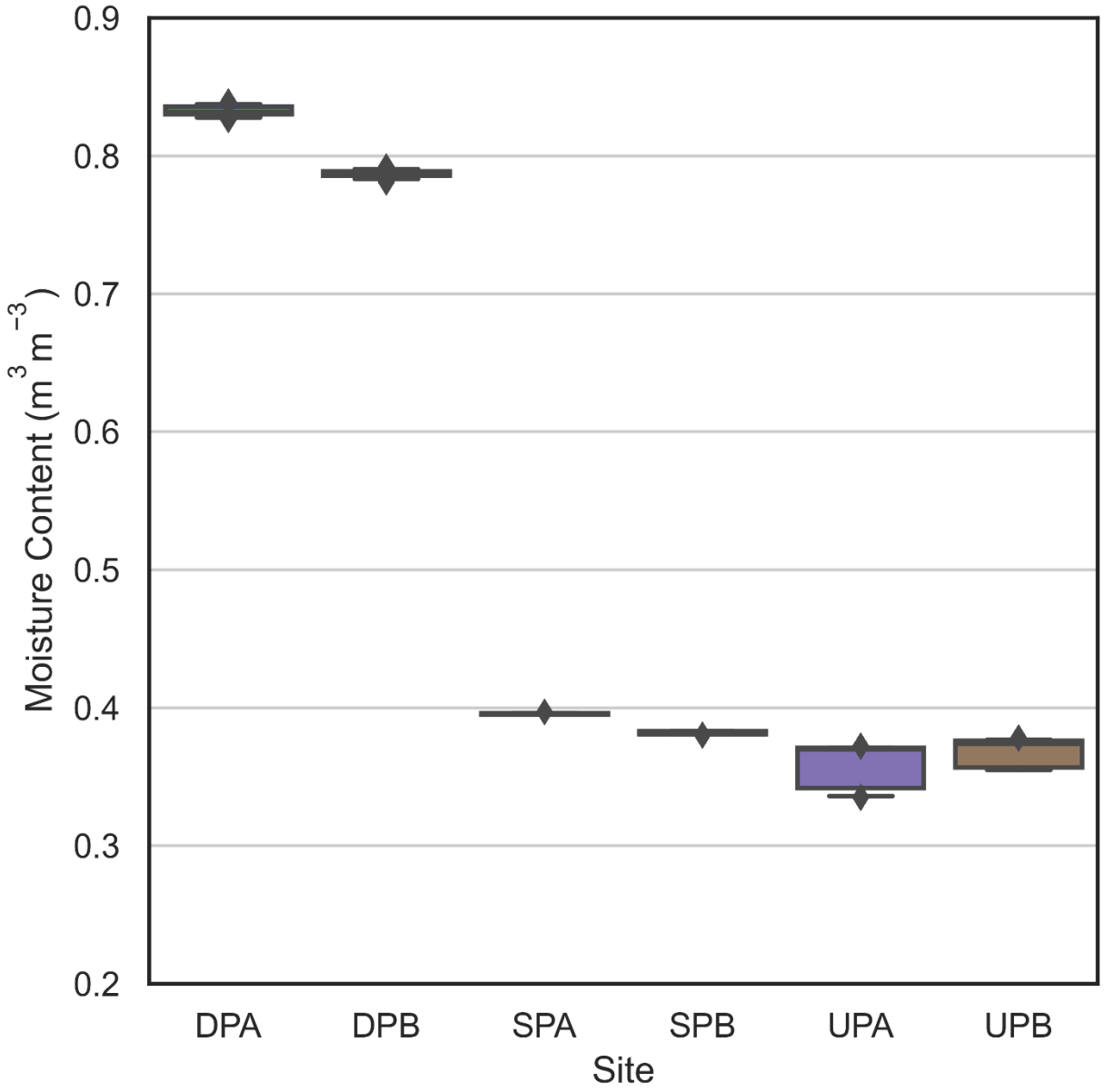

Figure 3-14 Box Plots of Moisture Contents at -100 cm for Ecological Sites for the Winter Months of January, February, and March of Hourly Data for 2009, 2010, and 2011

3.2.3 Snowpack Survey

The snowpack surveys at each of the ecological sites were often completed a few weeks apart. Therefore, it was difficult to make any direct comparisons between sites. Further the snowpack surveys at a particular ecological site were typically performed in different months year to year, thus only allowing for very generalized comparison. The average snowpack depth (cm) and the average snow water equivalent (SWE), the amount of water if all the snow melted, for each of

the snowpack surveys at the ecological sites for 2009, 2010 and 2011 are presented in Table 3-4. The averages were determined from the sampled three snow cores taken at each site. It did appear that the 2010 winter had approximately half the observed snowpack compared to the 2009 and 2011 winter.

In general, there did not seem to be a substantial difference in snowpack depths between ecological sites with the upland pine sites (UPA & UPB) maybe having a slightly greater snowpack than the deep peatland sites (DPA & DPB). This would be expected due to the proximity of the ecological sites and the similar stand characteristics, as none of the sites had complete canopy closure. Thus, there was no evidence from the limited snowpack surveys that would support the idea that the shallower depth of frost observed at the deep peatland sites was due to a substantially deeper snowpack. This was also supported by the observed ground surface temperatures, which are below the snowpack, having similar ranges in temperature (Figure 3-5)

Table 3-4 Average Snowpack Depths and Snow Water Equivalents (SWE) for 2009-2011

Site	Date	Depth (cm)	SWE (ml)
DPA	1/15/2009	70.3	7.5
DPB	1/15/2009	77.3	9.5
UPA	1/28/2009	79.0	14.8
UPB	1/28/2009	84.3	9.0
SPB	2/12/2009	75.3	19.9
DPA	3/3/2009	71.0	16.4
DPB	3/3/2009	71.0	16.5
UPA	4/1/2009	73.3	19.2
UPB	4/1/2009	79.0	16.2
UPA	2/15/2010	43.0	6.2
UPB	2/15/2010	48.0	9.4
SPB	2/23/2010	38.3	6.5
DPA	3/1/2010	40.0	6.8
DPB	3/1/2010	33.0	6.8
UPA	12/1/2010	10.8	1.4
UPB	12/1/2010	11.3	1.3
SPB	12/1/2010	11.7	1.0
DPB	2/22/2011	71.3	15.6
DPA	2/22/2011	71.7	14.8
UPB	4/12/2011	56.7	18.3
UPA	4/12/2011	59.0	17.4

3.3 Estimated Depth of Frost

The depth of frost can be estimated at each of the six ecological sites by calculating the freezing index from ground surface temperatures (Equation 3-4), which is the summation of daily mean temperatures starting from the first day with a daily average temperature of less than 0 ºC until the minimum freezing index is obtained. The date of the minimum freezing index is assumed to be the date of maximum frost depth, since after this date thawing of the subsurface begins to occur. The freezing index was calculated for all six ecological sites for both air (200 cm) and ground surface temperatures (Table 3-5). The effect of the snowpack on the freezing index is apparent with a drastic reduction in ºC ·days calculated at 200 cm compared to the ground surface, The largest difference was in 2009 and the smallest in 2010. In 2010 the upland sites (UPA and UPB) had only a minor reduction in the freezing index due to the snowpack. As noted earlier the calculated freezing index for SPA at the ground surface is erroneous due to issues with the probe and is only shown for demonstrative purposes of estimated frost depth with a very low freezing index.

Table 3-5 Freezing Index for Air (200 cm) and Ground Surface Temperatures by Year for Each of the Ecological Sites

Site	Freezing Index (ºC · days)					
	Air 200 cm			Ground Surface 0 cm		
	2009	2010	2011	2009	2010	2011
DPA	1529	1193	1739	289	618	590
DPB	1520	1180	1738	215	553	496
SPA	1583	1172	1751	136	183	217
SPB	1561	1198	1780	297	525	537
UPA	1507	1064	1657	341	747	555
UPB	1361	930	1569	426	761	639

The calculated freezing index for each of the sites was then used to estimate the depth of frost using Stefan's formula (Equation 3-3) for each year (Table 3-6). Design tables (Kersten 1949; US Army and US Air Force 1988) were used to obtain thermal conductivity values for frozen peat at low (160 kg m^{-3}) and high (320 kg m^{-3}) densities at varying moisture contents and for frozen silt and clay soils at low (1120 kg m^{-3}), medium (1440 kg m^{-3}) and high (1760 kg m^{-3}) densities. The thermal conductivity values obtained from the design tables ranged from 0.05 to

1.04 W $^{o}C^{-1}$ m^{-1} for peat and 0.31 to 1.8 W $^{o}C^{-1}$ m^{-1} for silty clay soils with varying moisture contents (Figure 3-15).

Table 3-6 Observed and Estimated Frost Depth at the Ecological Sites using Stefan's Equation (Equation 3-3)

Site	Observed Depth of Frost (cm)			Estimated Depth of Frost (cm)		
	2009	2010	2011	2009	2010	2011
DPA	<10	10-30	10-30	32-49	46-72	45-70
DPB	<10	10-30	10-30	27-42	44-68	41-65
SPA	30-50	30-50	30-50	22-34	25-39	27-43
SPB	30-50	30-50	30-50	32-50	42-66	43-67
UPA	30-50	>100	>100	84-112	124-166	107-144
UPB	30-50	>100	50-100	94-126	125-168	115-154

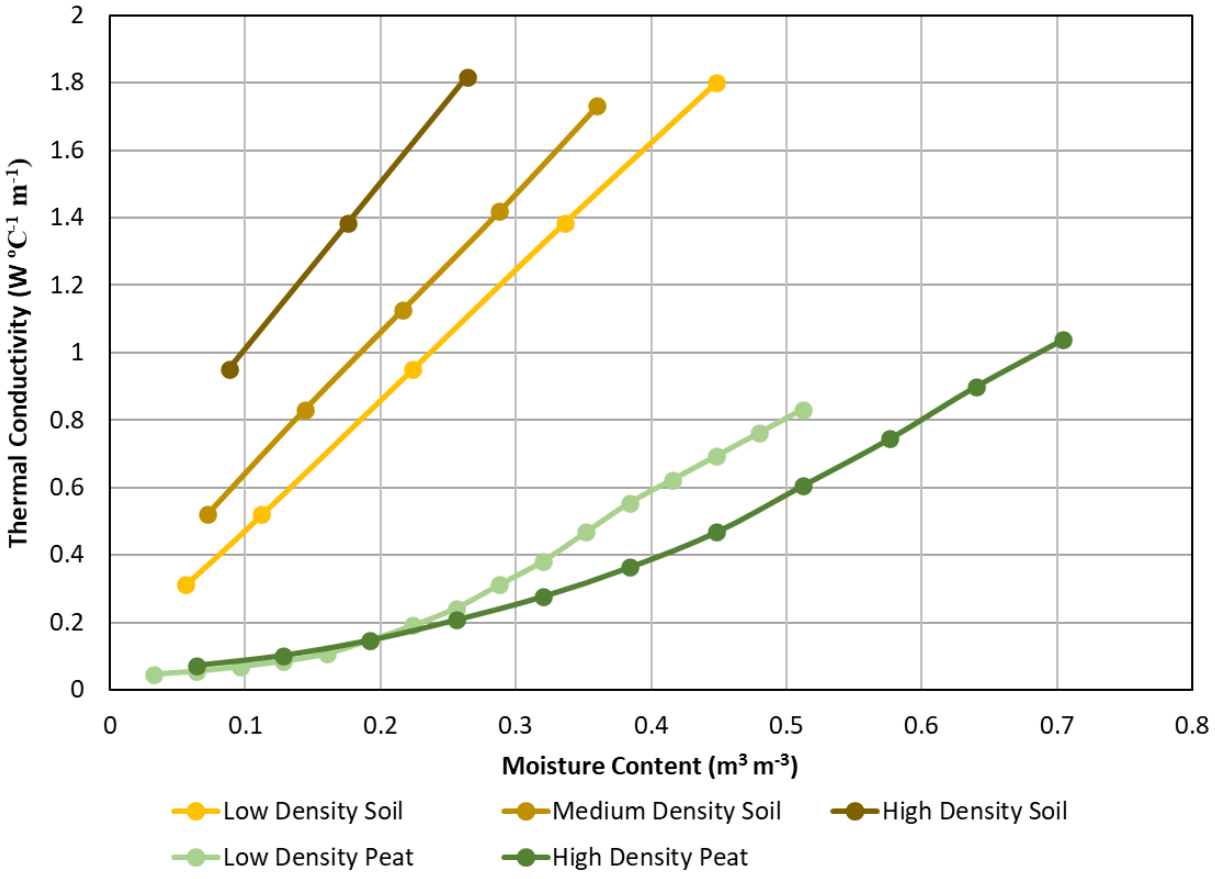

Figure 3-15 Thermal Conductivities Obtained from Design Tables (Kersten 1949; US Army and US Air Force 1988) for Low (160 kg m^{-3}) and High (320 kg m^{-3}) Density Peat and Low (1120 kg m^{-3}), Medium (1440 kg m^{-3}) and High Density Soil (1760 kg m^{-3}) (Silt & Clay) under Varying Moisture Contents

It is well known that Stefan's equation will overestimate the depth of frost because it ignores volumetric heat losses when subsurface temperatures drop below 0 ºC, as was the case with the upland sites. When temperature drops below 0 ºC there is additional heat loss due to changes in sensible heat, which is a function of the thermal capacity of the soil and water and would need to be accounted for if temperatures dropped substantially in the subsurface. However, neglecting volumetric heat losses can not explain the differences between the estimated and observed frost depths at the deep peatland sites because the subsurface temperatures never drop below -1 ºC, resulting in negligible changes in volumetric heat.

3.4 Discussion

From the observed 2009-2011 temperatures it was apparent that the deep peatland sites (DPA, DPB) have a shallower depth of frost than the shallow peatlands (SPA, SPB), which have a shallower depth of frost than upland sites (UPA, UPB). The differences in latent heat and thermal conductivity between the moist organic peat and the drier mineral soils of the uplands can reasonably explain the shallower depth of frost observed at the shallow peatlands. However, it can not explain the depth of frost observed at the deep peatlands that had similar or greater freezing index than SPB, which should have resulted in a slighter deeper depth of frost if thermal conductivity and moisture contents were equal.

It could be argued that the deep peatlands are wetter, thus resulting in a greater release of latent heat and a shallower depth of frost, but this fails to consider the change in thermal conductivity due the increased ice content. Stefan's equation can also be used to illustrate the effect of moisture content on the depth of frost using the freezing index calculated at deep peatland site DPA from the observed ground surface temperatures in 2009, 2010, 2011 (Figure 3-16).

The thermal conductivities were obtained from the design tables for frozen peat (Figure 3-15) and were the same values used to develop Table 3-6. Frozen thermal conductivities for the low-density peat, 160 kg m^{-3}, ranged from 0.05 to 0.83 W $ºC^{-1}$ m^{-1} and for the high density peat, 320 kg m^{-3}, ranged from 0.07 to 1.04 W $ºC^{-1}$ m^{-1}. The thermal conductivity of unfrozen peat was not considered as only freezing was considered and not depth of thawing under permafrost conditions.

Unlike mineral soils where frost depth decreases with increased moisture, a minimum depth of frost was estimated to occur at a moisture content of 0.15 to 0.20 m^3 m^{-3}, with any change in moisture content increasing frost depth. Although Stefan's equation was able to reasonably predict the depth of frost at the pine shallow peatland site SPB which had an annual frost depth of at least -30 cm (Table 3-6), it could not predict the very shallow frost line observed at the deep peatland sites. Further the maximum estimated frost depth for peat occurs at saturated conditions, which might explain why localized flooding at SPB in 2010 could result in the colder subsurface temperatures compared to 2011 which had a higher freezing index (Figure 3-6, Figure 3-7).

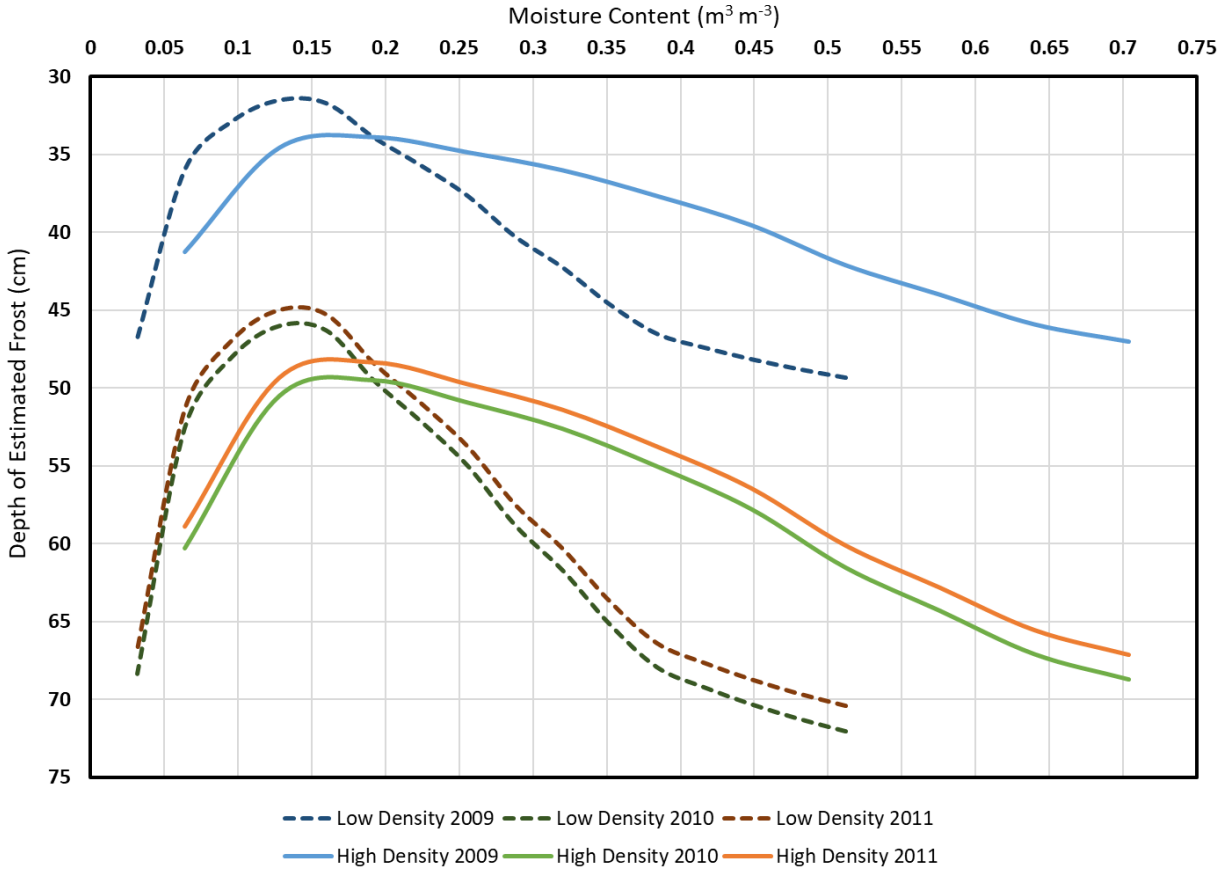

Figure 3-16 The Sensitivity of Moisture Content on Estimated Depth of Frost using Stefan's Equation for DPA's Freezing Index (2009, 2010, 2011) for Low (160 kg m^{-3}) and High (320 kg m^{-3}) Density Peat

Application of Stefan's equation to the ecological sites rejects the hypothesis that the shallower depth of frost observed at the black spruce peatlands (DPA, DPB) compared to the other sites was due to the increase in latent heat released during the freezing process. Further, the

assumption that a wetter subsurface results in warmer subsurface temperatures is not supported when comparing the subsurface temperatures of the upland pine sites (UPA, UPB) with the shallow peatland pine site (SPB), which was wetter yet had colder observed temperatures at -10 and -30 cm (Figure 3-6, Figure 3-7). Similar results were also observed at a reclamation site in Northern Alberta, with the moist peat temperatures approximately 10 to 20 ºC colder than the drier sand temperatures for the month of December and required an additional 20 days to thaw (Zhao and Si 2019).

Utilizing the Stefan equation to account for the release of available latent heat has shown there is insufficient energy available to prevent freezing of the subsurface of the deep peatlands to 30 cm. Hence latent heat alone can not explain why there was only very shallow observed frost depth (<10 cm in 2010, 2011) at the deep peatland sites (Figure 3-6). In contrast utilizing the Stefan equation to account for the release of latent heat did reasonably predict the depth of frost at the upland pine sites (UPA, UPB) and the pine shallow peatland site (SPB). Because the pine shallow peatland (SPB), which does not have a surface layer of sphagnum moss, does freeze it is thought that the surface vegetation, both the black spruce trees and sphagnum moss combined (DPA, DPB), was having a significant effect in reducing the depth of frost. Further, the differences in observed wintertime temperatures between black spruce peatland sites and lodgepole pine upland sites and the pine shallow peatland site could not be simulated with the current empirical equations implemented in hydrological simulation models such as SWAT (Bélanger 2009).

To create improved hydrological models for the Boreal Plains and the peatlands within them it is vital that subsurface temperature be more accurately simulated to allow for better estimates of infiltration rates of snowmelt. If hydrological models are over predicting the depth of frost within peatlands, then the simulated time for the subsurface to thaw would likely extend beyond time required for the snowpack to fully melt. If the models are simulating an impermeable barrier of solid ice, due to the relative closeness of the groundwater table to the surface within peatlands, the result would be most of the snowmelt becoming runoff with very little recharge occurring. While the depth of frost is not as important a factor as the moisture content of the subsurface in preventing the infiltration of snowmelt, with increased moisture decreasing the permeability, it does determine for how long the barrier to infiltration will remain. Thus, to better understand

how the vegetation, both the black spruce trees and sphagnum moss, are affecting subsurface temperatures additional monitoring and analysis is required so that more complex physically based models, that fully couple heat and moisture transport, can be developed that account for both latent and sensible heat.

4 FIELD STUDY PHASE 2 (2015-2016)

The hypothesis that black spruce trees can conduct sensible energy down their trunks and reduce the depth of frost by warming the root zone through sap recirculation is tested in this chapter. To test this hypothesis additional monitoring was required, with probes being deployed in the black spruce tree trunks and within the living sphagnum moss layer, with the objective of developing a conceptual model of the thermal dynamics of the Boreal Plains' peatlands (Objective 1). In addition, field observations and measurements from the Phase 2 field study will be used to confirm the existence of wintertime infiltration of snowmelt, both crown drip and upslope runoff, occurs through the black spruce tree root cavities (Objective 2).

Since the focus of the Phase 2 study is strictly on the effect of black spruce trees and sphagnum moss no further investigation was required of the pine sites, upland (UPA, UPB) and shallow peatland (SPB), since none of these had black spruce trees or a layer of sphagnum moss (Figure 4-1). Irreparable damage had occurred at the surface of the black spruce shallow peatland (SPA) over the 4-year period between field studies. Therefore, SPA was decommissioned along with most of the original FORWARD ecological sites. Materials from the decommissioned sites were then used to repair and add additional probes at the black spruce deep peatland sites (DPA, DPB).

Figure 4-1 Ground cover at the Pine Shallow Peatland (SPB)

Due to observed degradation of the sphagnum moss layer occurring at the peatland sites in the past (Figure 4-2) it was decided that monitoring and site visits would only occur while a frozen pathway existed. Thus, the temperature and moisture content probes were deployed starting in December and were retrieved at the end of April along with the data. The probes were retrieved from the site at the end of April to minimize animal damage and to ensure that there would be enough probes for the following winter of study, as wintertime was the primary focus. Also due to the limited battery life of certain probes they often required replacement every couple of months, which could not occur during the summer.

Figure 4-2 Degradation of Sphagnum Moss Layer Due to Site Visits at a Shallow Peatland (Top) and a Deep Peatland (Bottom)

4.1 Field Methodology Phase 2

The Phase 2 field study was the measurement data collected by the author at both deep peatland sites (DPA, DPB) in 2015 and 2016. The collected data was needed to test the hypothesis that black spruce trees can conduct sensible heat down their trunk warming the root zone through sap recirculation and to develop a conceptual model for black spruce peatlands that could explain the shallow depth of frost observed in Phase 1. Most of the original probes from Phase 1 were

reinitiated, along with new probes for both moisture content and temperature in a variety of locations including within the living sphagnum moss layer and the tree trunk. The location of these new probes was selected based on observations made in the field and was documented in photographs.

4.1.1 Study Area

The two black spruce deep peatland sites, DPA and DPB, were more closely observed in Phase 2. The characteristics of the two sites were described in Section 3.1.1 Site Descriptions for the Phase 1 field study.

4.1.2 Data Collection

In addition to the temperature and moisture content probes already deployed in Phase 1, new probes were deployed to help better understand the heat fluxes occurring through the system and to help develop a conceptual model. The new Phase 2 probes provided measurements of temperature and moisture content within the sphagnum moss and black spruce trees (live and dead) at various depths/elevations as illustrated in Figure 4-3, and temperatures in the snowpack. A photograph of a site is shown in Figure 4-4 . In addition, a water level logger was installed in Phase 2 within a piezometer at each site to monitor the groundwater elevation of the peatland. However, the geodetic elevation of the piezometer was unknown so only drawdown could be observed.

The temperatures of adjacent live and dead black spruce tree were monitored at the base of the trunk on the north side to identify periods when the sap flow in the living tree would cause a measurable difference of temperature. It was expected that the greatest difference of temperature between living and dead trees would occur at the base of the tree trunk on the shaded side, since there would be minimal warming from incoming solar radiation. Temperatures were also monitored in the trunk at 200 cm above ground within the crown of the same live and dead trees being monitored at the base also on the north side. Temperatures were expected to differ within the crown due to the presence of snow on the living tree, which would insulate the trunk of the tree from the atmosphere. Temperature monitoring in the tree trunks was also used to identify periods of snowmelt when temperatures did not increase on warm days due to latent heat absorption.

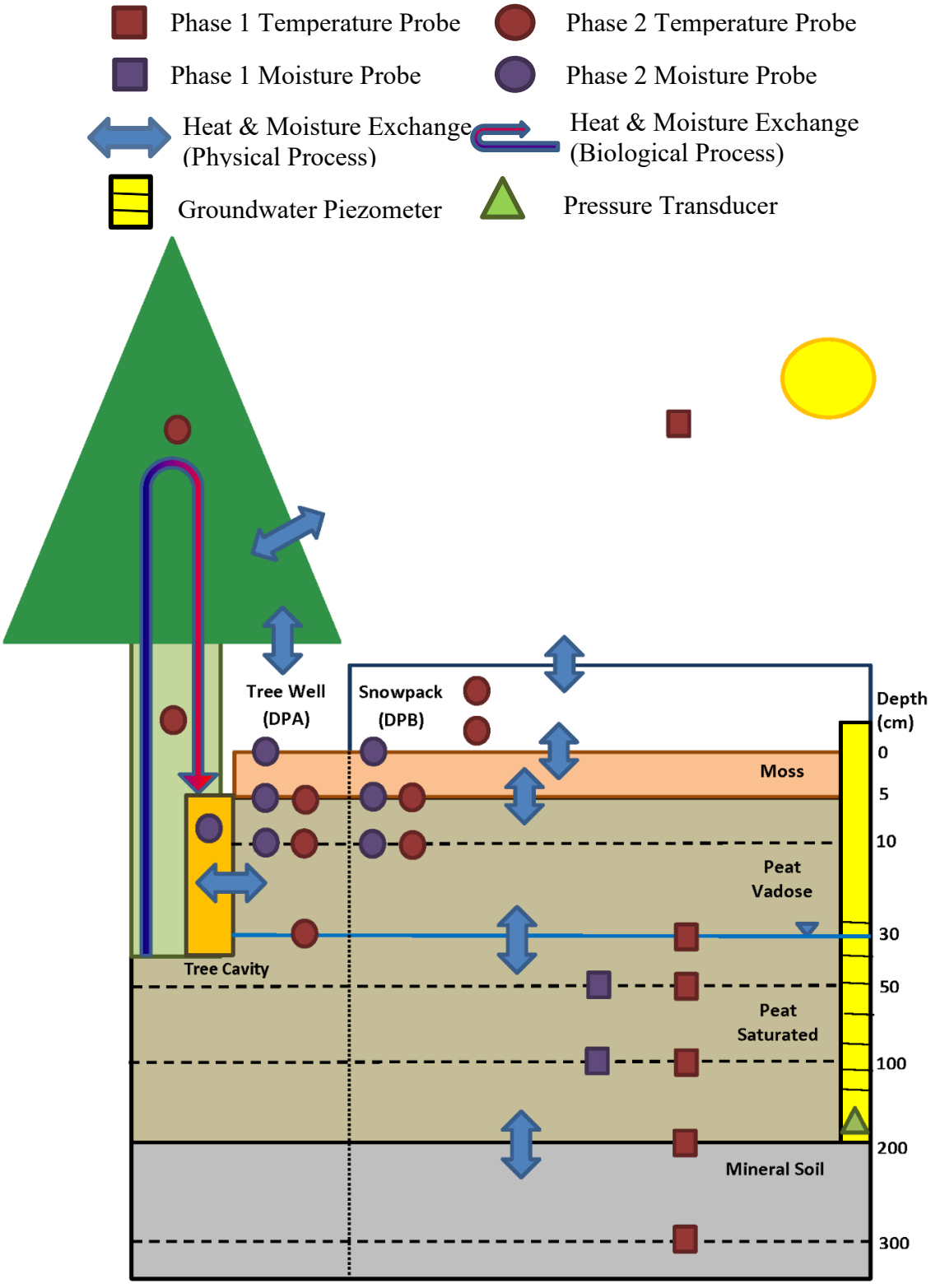

Figure 4-3 Probe Deployment in the Phase 2 Field Study

Figure 4-4 Example of Deep Peatland Monitoring Station (DPA)

To determine if the translocation flow of sap through the phloem from the needles to the roots was warming the subsurface temperature probes were placed within the black spruce root zone (-10 cm, -30 cm) beneath the sphagnum moss, with another probe placed directly above them in the moss layer at (-5 cm). If the subsurface was warming from the ground surface down due to incoming solar radiation, then the moss layer would increase in temperature before the root zone and be at a higher temperature to allow for the downward flux of heat. However, if the temperature in the root zone increases before temperature in the moss layer and is at a higher temperature than the moss and the groundwater beneath it, then the only other possible source of heat would be from the roots themselves.

To determine if the source of heat warming the roots was metabolic or from the translocation flow of sap, the subsurface temperatures were compared to the living trunk sapwood

temperatures, with a strong correlation indicative of sap flow warming the roots and not the metabolism of sugars. Heat is know to dissipate from a cell when organic material (i.e. sugar) is metabolized, regardless if it is a tree root cell or bacteria within the soil, and is a recognized indicator for metabolic activity (Barros et al. 2011; Chakrawal et al. 2021). The heat generated from cellular metabolism would not be dependent on atmospheric temperatures, and thus root zone warming events that occur while air temperatures are below 0 ºC are likely due to metabolic activity and could not be due to the circulation of sap flow.

For the Winter of 2015 DPA was monitored with Phase 1 probes and with additional Phase 2 probes at the beginning of March. DPB probes were installed at the end of March 2015 and were not monitored until Winter of 2016. To prevent the sphagnum moss layer from being damaged during probe installation all field work was completed while a snowpack was present. During Phase 1 it was observed that walking directly on the moss during the summer results in significant degradation of the surface layer and subsequent flooding in badly damaged area.

Decagon GS1 volumetric moisture probes were installed with Data Dolphin loggers (Optimum Instruments Inc., Edmonton, AB, Canada) to monitor moisture content within the peat and snow. GS1 probes determine volumetric water content (VWC) by measuring the dielectric constant of the medium using capacitance and frequency domain technology Figure 4-5). The 70 MHz frequency minimizes salinity and textural effects, making the GS1 accurate in almost any soil or soil-less medium. The two-prong design and high measurement frequency allows the GS1 to measure VWC from 0 to 100% (VWC of saturated soils is generally 40 to 60% depending on the soil type) and allows accurate measurement of all soils and soil-less medias with a wide range of salinities. GS1 probes were deployed at both monitoring sites within the sphagnum moss, the peat, and within a cavity under a black spruce tree.

To install the GS1 probes within the sphagnum moss and peat the snowpack (if present) was first removed intact with a snow shovel. The GS1 moisture content probes that were installed in the sphagnum moss at the surface (0 cm) and at the moss/peat interface (5 cm) were installed horizontally while the peat probe (10 cm) was installed vertically. A 3-inch (7.62cm) wood core hole bit was used to extract the moss/peat as an intact plug which was reinserted back into the hole after the probe was installed. For the GS1 probe within the tree cavity the void was loosely filled in with locally sourced peat to provide a medium for the probe to be installed in.

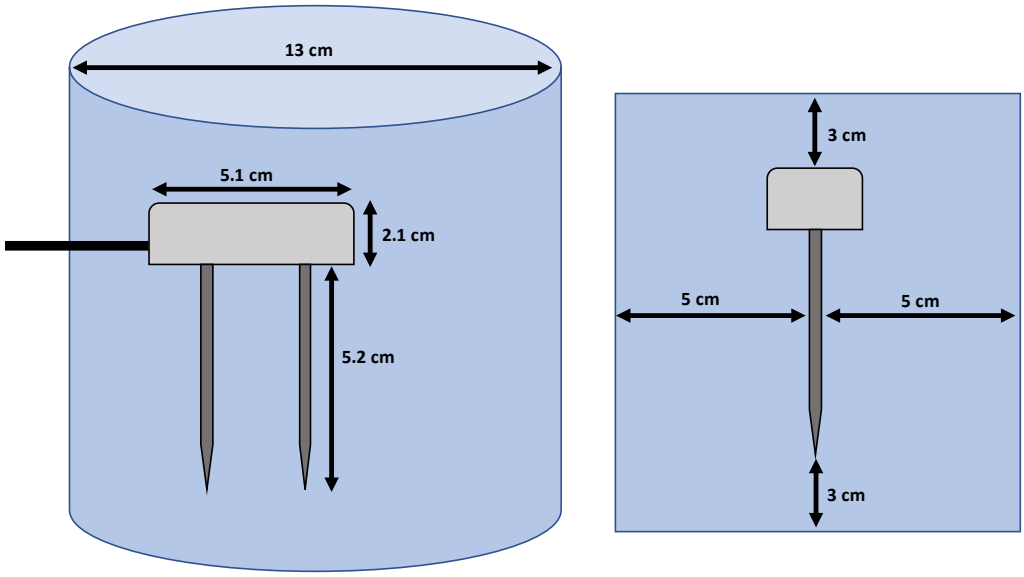

Figure 4-5 Idealized Measurement Volume of Decagon GS1 sensor, Adapted from: (Cobos 2015)

Temperature measurements were recorded either with HOBO U23 temperature sensors (Onset Computer Corporation, Bourne, MA, USA) for the tree, sphagnum moss, vadose zone peat and snowpack (Phase 2) or the YSI thermistors (YSI Incorporated, Yellow Springs, OH, USA) deployed in Phase 1 for the saturated subsurface and air temperatures.

To monitor temperatures within a black spruce tree, holes were drilled at the base of the trunk (+5 cm) and in the trunk in the crown (+200 cm) at a slightly larger diameter (0.5 cm) and depth (4.0 cm) than the HOBO U23 sensor. The HOBO U23 sensor was placed within the sapwood, with the sensor extending from the bark towards the center of tree. The probes were all placed in mature black spruce trees with a diameter of approximately 25 cm, so the end of the temperature sensor would be roughly 8 cm from the center of the tree. The holes were drilled on the north side of the trunk to minimize the influence of solar radiation on observed temperatures. The temperatures probes were then installed into the drilled hole with wood glue to secure the probe in place.

Both living and dead black spruce trees were monitored to determine if there was any biological effect on temperature. One living and one dead tree occupying the same tree well was selected to

be monitored at both DPA and DPB sites for a total of four trees, two living and two dead, all approximately equal diameter (Figure 4-6). It should also be noted that while a black spruce tree was considered dead if it did not have any green needles, thus it was not photosynthesizing, it still had a sap wood consistent with a living tree when drilled.

For the sphagnum moss and peat vadose zone temperatures the HOBO U23 probes were installed into drilled holes to the desired depth using a drill bit extension. The snowpack temperature probes were taped to a wooden stake and pushed into the snowpack.

A complete list of all probes monitored in Phase 2 at DPA and DPB along with medium, elevation, location, year, and probe type are presented in Table 4-1.

Figure 4-6 Example of Living and Dead Black Spruce Trees Monitored for Temperature in Phase 2

Table 4-1 Deployment of Probes in Phase 2

Site	Measurement	Medium	Elevation (cm)	Location	Year	Probe Type
DPA	Temperature	Peat	-5	Under Canopy	Mar 2015/2016	HOBO
DPA	Temperature	Peat	-10	Under Canopy	2016	HOBO
DPA	Temperature	Peat	-30	Under Canopy	2015/2016	YSI
DPA	Temperature	Peat	-50	Under Snowpack	2015/2016	YSI
DPA	Temperature	Peat	-100	Under Snowpack	2015/2016	YSI
DPA	Temperature	Peat	-200	Under Snowpack	2015/2016	YSI
DPA	Temperature	Mineral Soil	-300	Under Snowpack	2015/2016	YSI
DPA	Temperature	Moss	0	Under Canopy	Mar 2015	HOBO
DPA	Temperature	Moss	0	Under Snowpack	Mar 2015	HOBO
DPA	Temperature	Live Tree	+5	Trunk Base	2015/2016	HOBO
DPA	Temperature	Live Tree	+200	Trunk Canopy	2015/2016	HOBO
DPA	Temperature	Dead Tree	+5	Trunk Base	Mar 2015/2016	HOBO
DPA	Temperature	Dead Tree	+200	Trunk Canopy	Mar 2015/2016	HOBO
DPA	Temperature	Snow	+30	Snowpack	Mar 2015	HOBO
DPA	Temperature	Snow	+5	Snowpack	Mar 2015	HOBO
DPA	Moisture	Peat	-10	Under Snowpack	2015	Theta
DPA	Moisture	Peat	-10	Under Canopy	2016	GS1
DPA	Moisture	Peat	-50	Under Snowpack	2015/2016	Theta
DPA	Moisture	Peat	-100	Under Snowpack	2015/2016	Theta
DPA	Moisture	Moss	0	Under Canopy	Mar 2015/2016	GS1
DPA	Moisture	Moss	-5	Under Canopy	Mar 2015/2016	GS1
DPA	Moisture	Peat Fill	-10	Tree Cavity	Mar 2015/2016	GS1
DPA	Pressure	Peat	N/A	Piezometer	2016	Transducer
DPB	Temperature	Peat	-5	Under Snowpack	2016	HOBO
DPB	Temperature	Peat	-10	Under Snowpack	2016	HOBO
DPB	Temperature	Peat	-30	Under Snowpack	2016	YSI
DPB	Temperature	Peat	-50	Under Snowpack	2016	YSI
DPB	Temperature	Peat	-100	Under Snowpack	2016	YSI
DPB	Temperature	Mineral Soil	-200	Under Snowpack	2016	YSI
DPB	Temperature	Mineral Soil	-300	Under Snowpack	2016	YSI
DPB	Temperature	Live Tree	+5	Trunk Base	2016	HOBO
DPB	Temperature	Live Tree	+200	Trunk Canopy	2016	HOBO
DPB	Temperature	Dead Tree	+5	Trunk Base	2016	HOBO
DPB	Temperature	Dead Tree	+200	Trunk Canopy	2016	HOBO
DPB	Moisture	Peat	-10	Under Snowpack	2016	Theta
DPB	Moisture	Peat	-50	Under Snowpack	2016	Theta
DPB	Moisture	Peat	-100	Under Snowpack	2016	Theta
DPB	Moisture	Moss	0	Under Snowpack	2016	GS1
DPB	Moisture	Moss	-5	Under Snowpack	2016	GS1
DPB	Moisture	Peat Fill	-10	Tree Cavity	2016	GS1
DPB	Pressure	Peat	N/A	Piezometer	2016	Transducer

4.2 Field Results Phase 2

This section is a description of the results and analysis of the two winters (2015 and 2016) of field surveys and monitoring of the two deep peatland sites, DPA and DPB.

4.2.1 Field Visual Observations

The first major observation made was the occurrence of large depressions in the snowpack underneath the crown of the black spruce trees; termed a tree well. In comparison, the tree wells around nearby lodgepole pines were significantly smaller in diameter (Figure 4-7). A field visit was conducted immediately following a significant snowfall event to determine if the lack of snow under the black spruce crown was due to interception by the needles and branches. However, the black spruce tree wells were all observed to be full of snow immediately after the event both from throughfall from the crown and blowing across the snowpack (Figure 4-8).

Figure 4-7 Example of Black Spruce (Center) and Lodgepole Pine Tree (Left) wells

Figure 4-8 Black Spruce Tree Well after a Snowfall event at DPA Monitoring Site (see Figure 4-4)

A second major observation was made on the same day following the major snowfall event. A significant amount of drip from the crown was observed occurring due to incoming solar radiation. Daytime air temperatures did not exceed 5 ºC, yet there was virtually no snow in the southern exposed tree crown while the north exposed crown still had an accumulation of the previous day's snowfall (Figure 4-9).

Liquid water was also observed at the base of the black spruce tree trunk, and it appeared that the drip from the crown was further melting the snowpack underneath the branches instead of refreezing, creating a slushie mixture of water and snow (Figure 4-10).

Figure 4-9 Accumulation of Snow in Black Spruce Tree Crown Southern Exposure (Left), Northern Exposure (Right)

Figure 4-10 Accumulation of Snowmelt from the Crown as Liquid Water at the base of a Black Spruce Trunk

As the snow melted and drained from around the tree well a void or cavity was often exposed at the base of the black spruce tree trunk. It appeared that the cavity acts as a preferential pathway to infiltrate snowmelt to the underlying saturated peat (as demonstrated by the soil moisture probes and piezometer), bypassing the surrounding frozen ground surface (Figure 4-11). By the end of April, the radial extent of liquid water around the base of the black spruce trees had increased to encompass the entire extent of the tree well, while the ground between tree root mats remained frozen (Figure 4-12). As the snowpack surrounding a black spruce tree melted it drained to the black spruce cavity and infiltrated into the ground, unlike the cutlines which were void of black spruce trees. Along the cutlines the snowmelt would runoff from the peatland due to the peat being frozen to a depth substantial enough to prevent any penetration of a ¼ inch metal rod (Figure 4-13).

The sites were only visited when the ice along the cutline and in between black spruce tree root mats was thick enough to support a person walking on it, which was determined using a ¼ inch metal rod (Figure 4-14). Although solid ice was present until the end of April along the cutline and in between black spruce tree mats, the steel rod could easily penetrate the subsurface within the tree well.

Figure 4-11 Examples of a Cavity at the Base of Black Spruce Trunks

Figure 4-12 Extent of Liquid Water in Black Spruce Tree Wells at the End of April

Figure 4-13 Snowmelt Runoff from Peatland Cutlines Void of Black Spruce Trees

Figure 4-14 Example of Solid Ice Pathway Between Two Black Spruce Tree Root Mats used to Visit Peatland Sites (April 20, 2015)

The effect of snowmelt infiltration on the sphagnum moss health was evident by late May, with moss colonies around the black spruce tree being green and vibrant while along the cutline they were desiccated, and browning (Figure 4-15).

Figure 4-15 Examples of Sphagnum Moss Colonies Surrounding a Black Spruce Tree (Top) and in a Cutline (Bottom)

4.2.2 Observed Temperatures

Time series graphs of the observed winter subsurface and air temperatures were created to understand the effect black spruce trees and sphagnum moss have on temperature. Winter temperatures were observed every 15 minutes during the winter of 2015 in DPA and for both DPA and DPB during the winter of 2016. All observed time-series graphs are of the raw 15-minute observed data.

4.2.2.1 Peat Temperatures

In December 2014 all the DPA site's Phase 1 temperature probes located below the water table, i.e., greater than 30 cm in depth, were reinitiated. The temperature probes above the water table were all damaged and had to be rewired with an additional temperature probe installed at -5 cm. However, all the DPA vadose zone temperature probes (-5, -10, -30 cm) were deployed under the crown of a black spruce tree within its tree well. The Winter 2015 DPA observed 15-minute subsurface temperatures are plotted in Figure 4-16, except for the -10 cm probe which failed shortly after deployment.

Up until January 23, 2015, the observed subsurface temperatures behaved as expected, with temperatures increasing with depth due to the upward gradient of heat to the snowpack. Then for the next three days daily maximum air temperatures ranged from 5.7 to 9.8 ºC and resulted in the -30 and -50 cm peat probes reaching an equilibrium of approximately 1.5 ºC, while the -100 cm probe dropped slightly in temperature. After February 10, 2015, the peat under the black spruce crown at -30 cm became warmer than the -50 cm probe outside of the tree well underneath the snowpack and had a slight increase in daily variability. The large difference in temperature between the -200 and -300 cm probes is due to the change in medium from peat to mineral soil, and thus a significant decrease in moisture content and thermal conductivity.

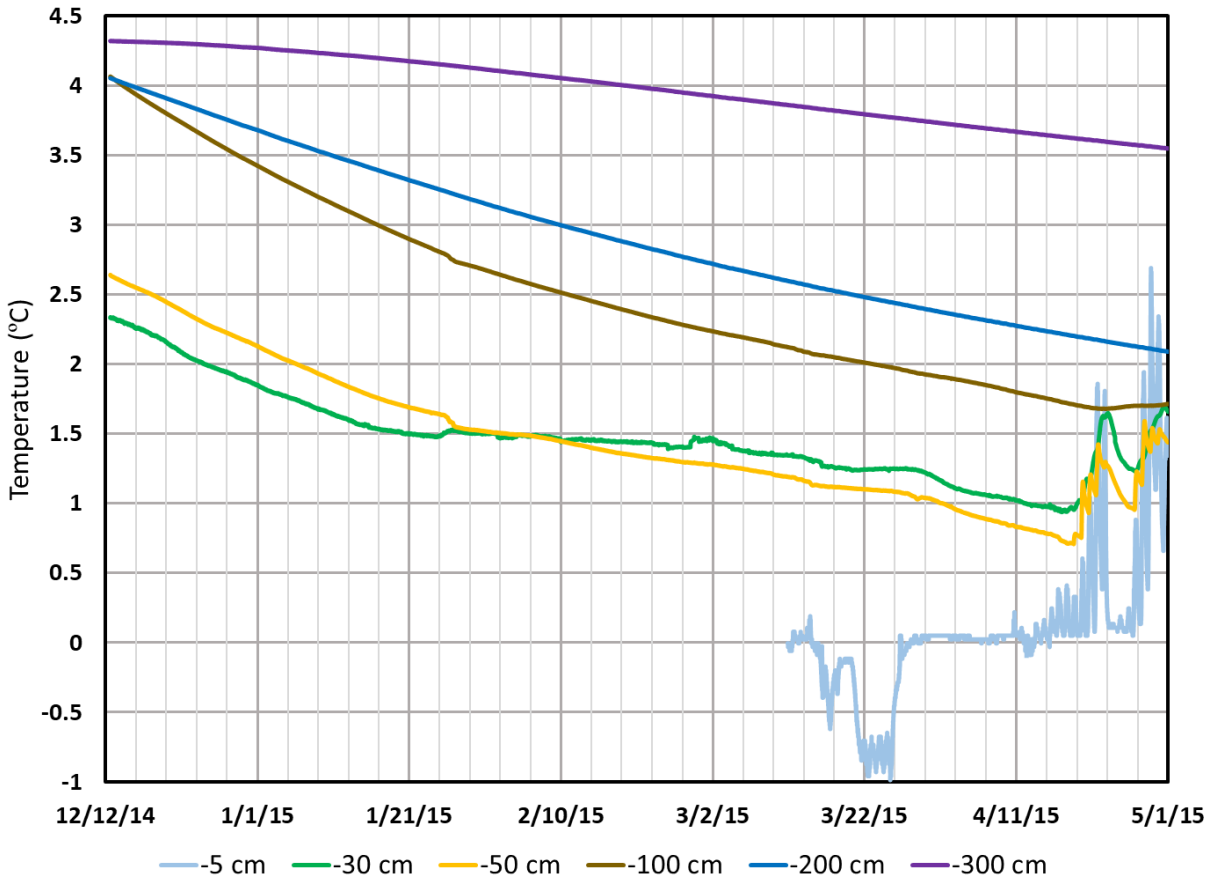

Figure 4-16 Observed 15 Minute Subsurface Temperatures from the Winter 2015 Field Study at Deep Peatland A (DPA)

Sphagnum moss temperatures were also monitored at the ground surface (0 cm) from March 13, 2015 to May 1, 2015 under the tree crown, and under the snowpack outside the tree well beyond the influence of tree crown. The results are illustrated in Figure 4-17 along with air temperatures at +200 cm (on a separate axis). From March 16 to 26, the sphagnum moss under the black spruce crown was frozen with little to no snow pack, resulting in a good correlation between moss and air temperatures which are scaled at about a ratio of 10:1. From March 26 until mid April the moss temperatures under the black spruce crown were dampened compared to air temperatures due to the presence of snow in the tree well, but still showed a greater response to air temperature than the moss temperatures outside of the tree well. After April 21, moss in the tree well and air temperatures were highly correlated, except for air temperatures below 0 ºC as the moss started to lose latent heat due to freezing instead of sensible heat. Observed moss temperatures from outside the tree well barely fluctuated from 0 ºC due to the thickness of the snowpack and its insulating effect.

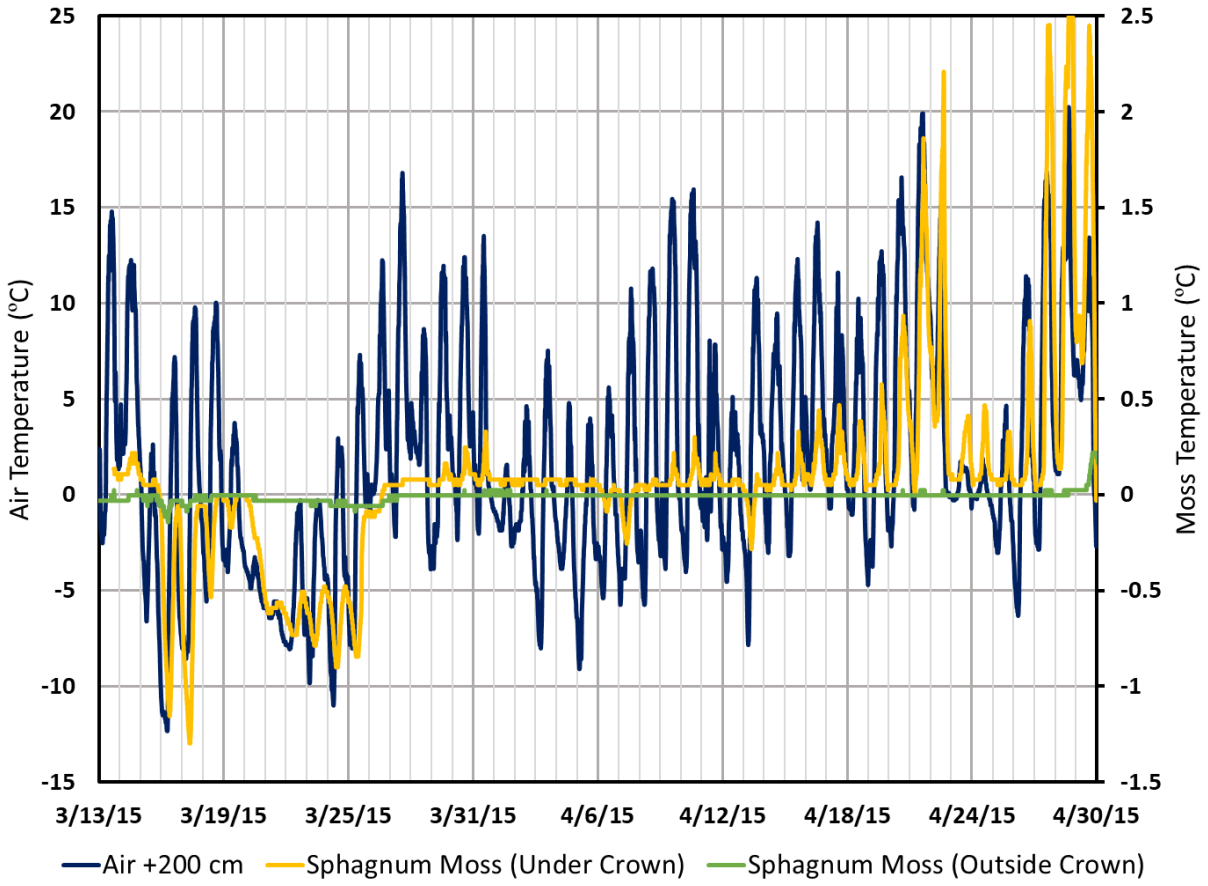

Figure 4-17 Observed 15 Minute Moss Temperatures from Under the Canopy and Outside the Influence of the Canopy for the Winter 2015 Field Study at Deep Peatland A (DPA)

In December 2015, all the DPB Phase 1 temperature probes were reinitiated with only the -10 cm probe having to be replaced. As at the DPA site, an additional temperature probe was installed at -5 cm, but outside of the tree well under the snowpack alongside the -10 cm and -30 cm probe locations. The malfunctioning -10 cm temperature probe at DPA was also replaced.

Unlike the DPA 2015 observed peat temperatures at -30 cm, the 2016 temperatures were already warmer than the peat -50 cm depth and always had increased daily variability compared to the deeper probes (Figure 4-18). This was likely due to a warmer than normal fall, for even the -100 cm probe was warmer than the -200 cm probe until after the first week of January, almost a month later than in 2015. By the middle of March, even the peat at -10 cm was warmer than at the -50 cm depth and warmer than the -30 cm by the beginning of April.

Near the end of March there is an observed drop in temperatures at -30 cm and -50 cm that was not observed at shallower depths. This was likely due to the infiltration of snowmelt cooling the probes located near the water table. The -5 and -10 cm probes had increasing daily variability by the end of March due to the lack of a snowpack and the sphagnum moss layer completely thawing out resulting in changes to sensible heat. However, the peat at -10 cm was warmer and had greater fluctuations than at -5 cm and so the source of heat warming the peat at -10 cm had to be from the location of the black spruce tree root system and not the surface.

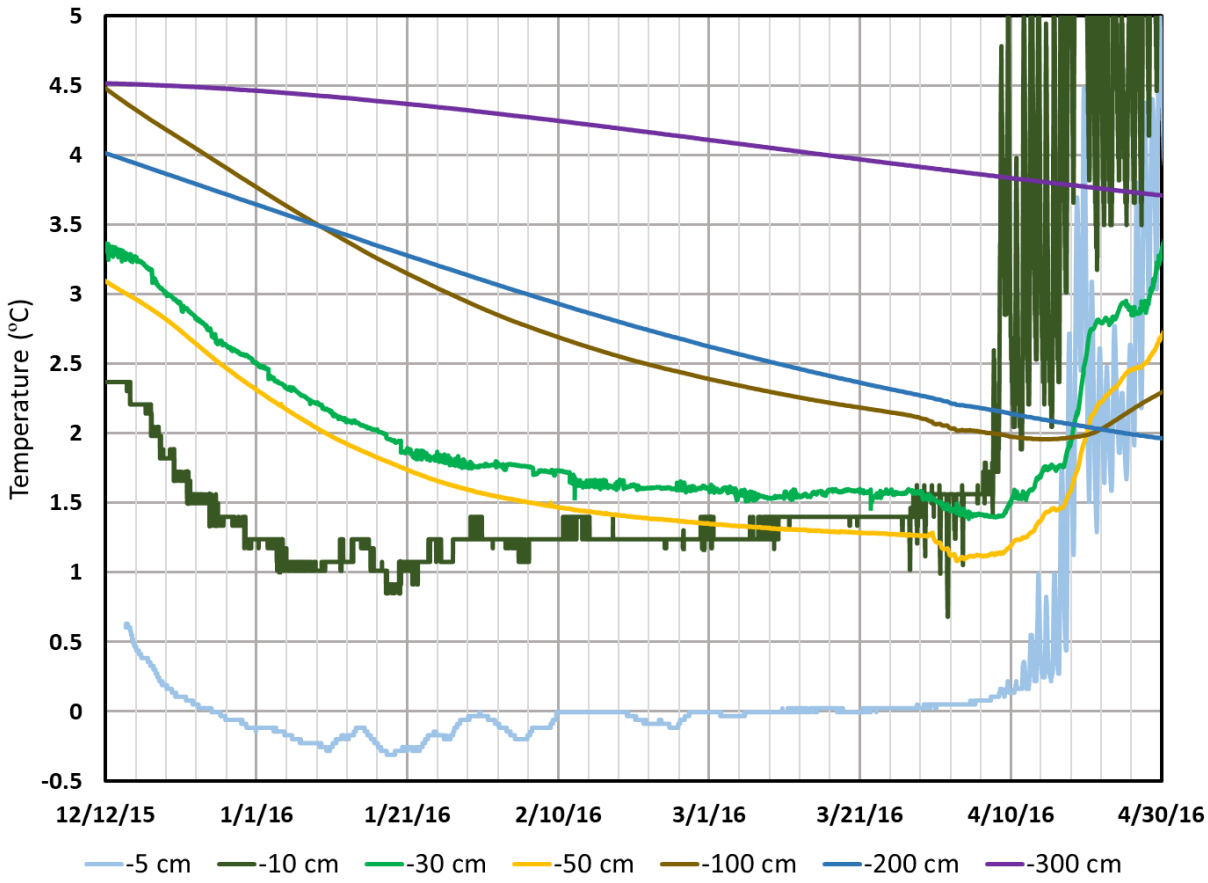

Figure 4-18 Observed 15 Minute Subsurface Temperatures from the Winter 2016 Field Study at Deep Peatland A (DPA) under the Tree Crown

The observed subsurface temperatures at DPB from under the snowpack outside of the tree well are what would be expected with temperatures decreasing with depth from the beginning of January until the end of March (Figure 4-19). Also, the daily variability of the -30 cm probe is equivalent to all the probes deeper than it unlike the -30 cm probe at DPA located under the tree crown. Even the -10 cm probe has hardly any diurnal temperature fluctuations by the end of the

April in comparison to DPA where temperatures fluctuated more than 3 ºC daily. This is likely due to the ground surface still being frozen with a snowpack present, but unfortunately the -5 cm temperature probe failed on April 10. It should also be noted that at DPB both the -200 cm and -300 cm probes are located within a mineral soil which is the reason why they are similar in temperature and are over 1 ºC warmer than the peat at -100 cm. Also, DPB is like DPA in that peat temperatures drop near the end of March at -10 cm, -30 cm, and -50 cm depths likely due to the infiltration of snowmelt. At DPB the clayey loam mineral soil was located at -200 cm resulting in the -200 and -300 cm temperatures being similar. As with DPA, the mineral soil was found to be approximately 1.5 ºC warmer than the peat at -100 cm.

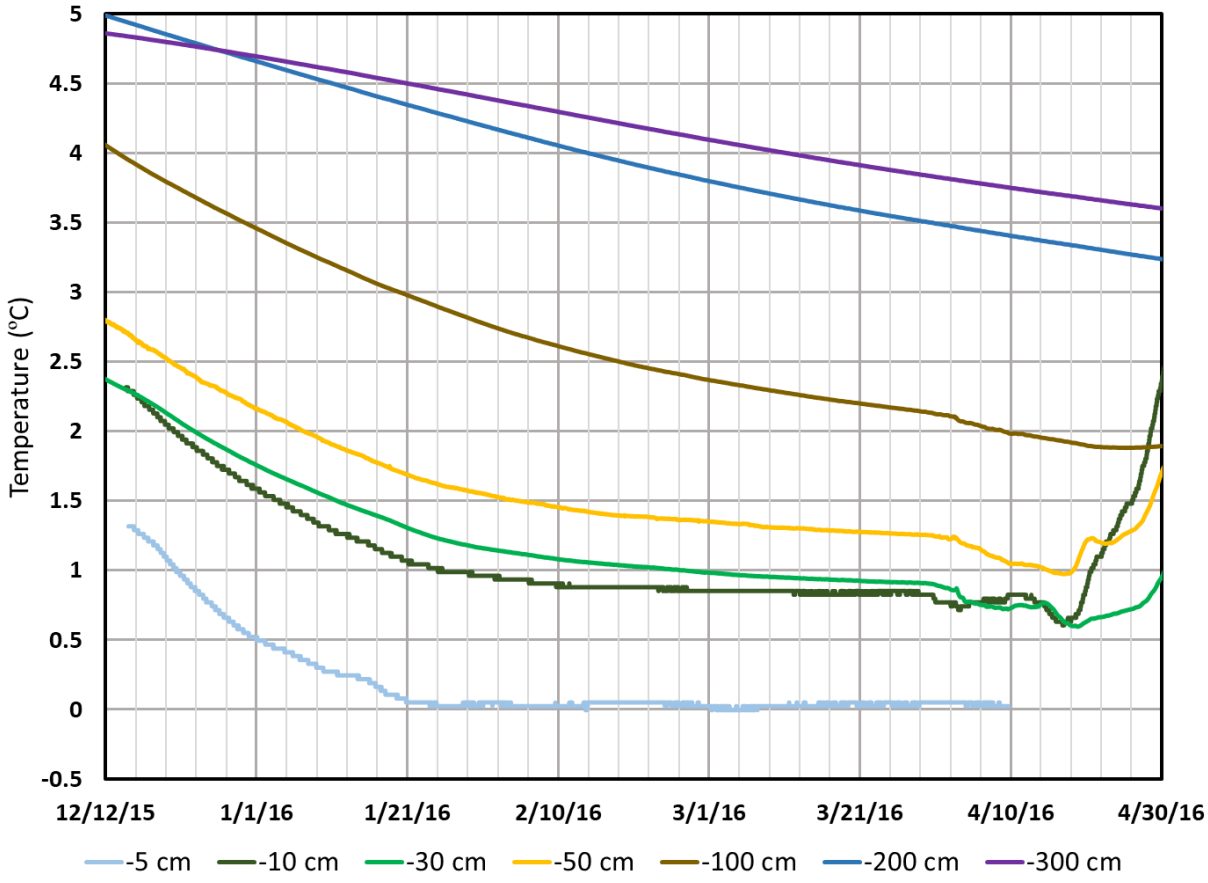

Figure 4-19 Observed 15 Minute Subsurface Temperatures from the Winter 2016 Field Study at Deep Peatland B (DPB) outside the Tree Crown and Well

4.2.2.2 Black Spruce Temperatures

The trunk temperatures of live and dead black spruce trees were monitored at both deep peatland sites within the trunk at the base (+5 cm) and within the trunk in the crown (+200 cm). At DPA temperature probes were installed on December 12, 2014, within a living Black Spruce tree and monitored until May 1, 2015 (Figure 4-20).

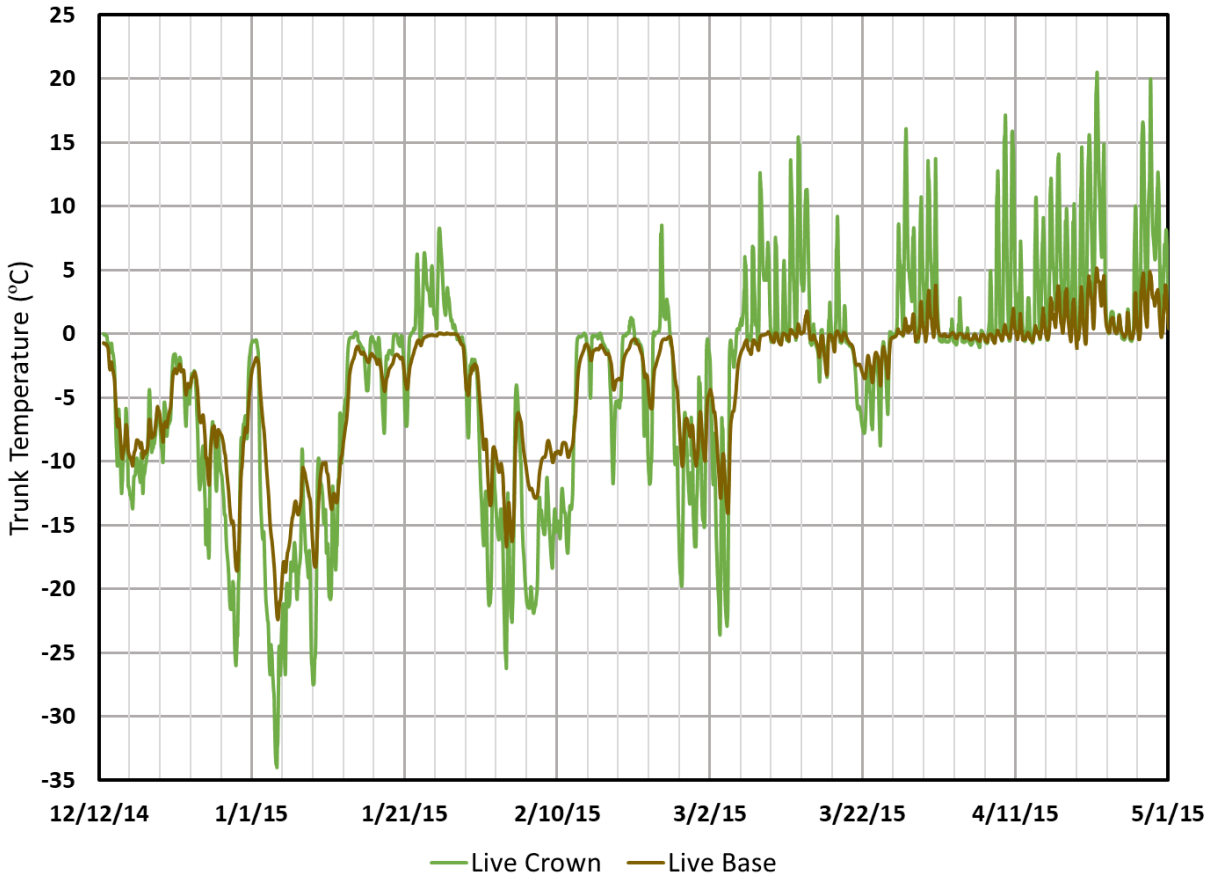

Figure 4-20 Observed 15 Minute Crown and Base Trunk Temperatures in a Living Black Spruce Tree Trunk from the Winter 2015 Field Study at Deep Peatland A (DPA)

Up until the end of March the temperature of the base of the living spruce tree trunk was below freezing and dampened in signal but highly correlated with the trunk temperature in the crown. There was no correlation when crown trunk temperatures exceeded 0 ºC, as the base of the trunk remained below freezing. This was likely due to changes in latent heat occurring at the base of the trunk from melting snow/ice. During the month of April, trunk temperatures in the crown and at the base barely dropped below freezing, and temperatures at the base never exceeded 5 ºC. When the crown trunk temperatures were below 5 ºC in April, the second to last 4 days of the

graph, the crown and base trunk temperatures were nearly the same, suggesting the dampening increased with warmer temperatures.

The monitoring of the dead black spruce tree at DPA didn't begin until March 13, 2015; and is shown with the living trunk measurements for comparison in Figure 4-21. Until the end of March the temperature in the dead and live trunk bases were well correlated with the temperature in the dead base being dampened compared to the dead crown trunk. This supports the concept that the dampening at the base of the trunk was likely due to the insulation of the snowpack and changes in latent heat due to its freezing and thawing. By the first week of April the dead base trunk temperatures were highly correlated with the dead crown trunk temperatures, with a slight amount of dampening. The living base trunk temperatures in comparison never exceeded 5 ºC, while the dead base temperatures often exceeded 10 ºC daily throughout April.

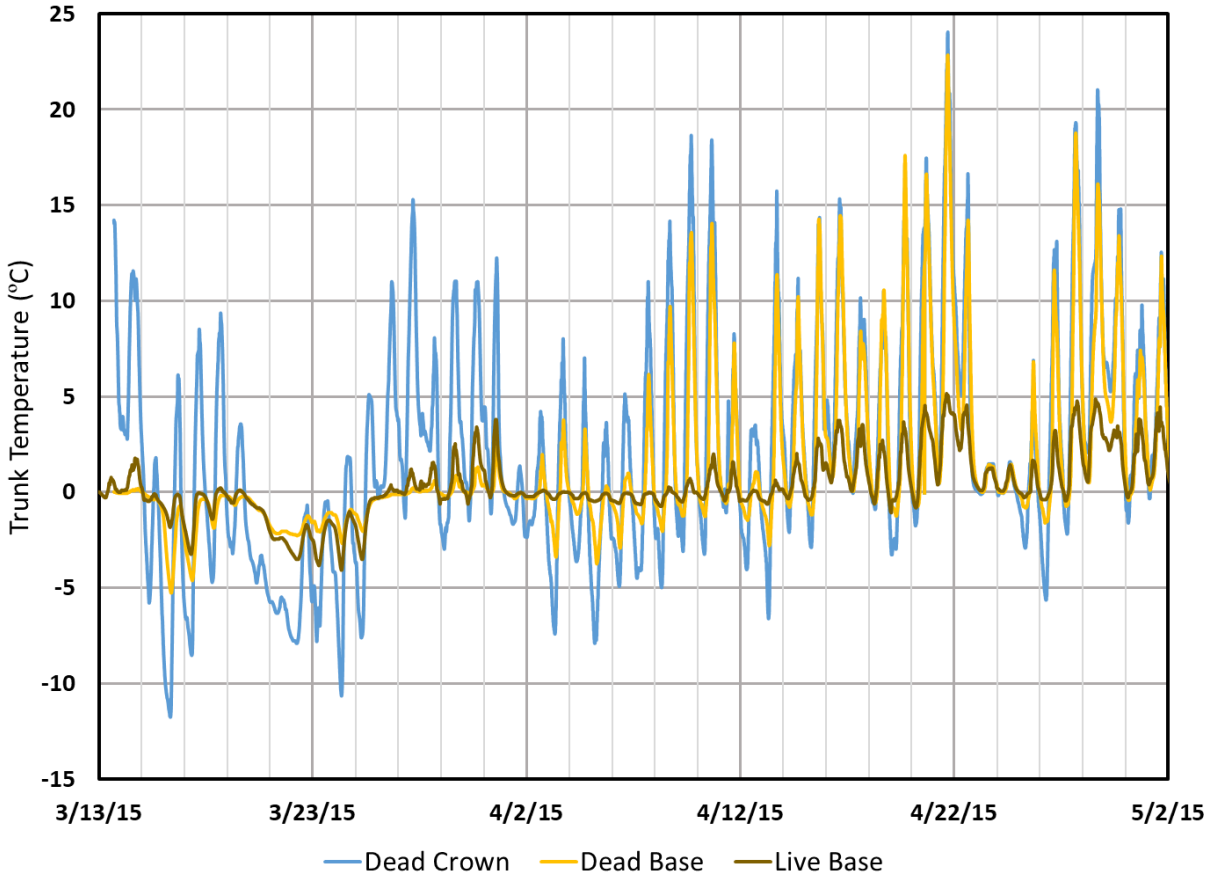

Figure 4-21 Observed 15 Minute Crown and Base Trunk Temperatures in a Dead Black Spruce Tree compared to a Living Trunk Base from the 2015 Field Study at Deep Peatland A (DPA)

In the winter of 2016, black spruce tree temperatures, living and dead, were monitored at both deep peatland sites at the trunk base (+5 cm) and crown's trunk (+200 cm). The living and dead observed 15-minute temperatures for the black spruce crown at DPA are plotted in Figure 4-22 and for DPB in Figure 4-23. Crown trunk temperatures for living and dead trees were highly correlated and were very similar between sites with two exceptions. When temperatures rose above freezing within the dead crown it would take a few days, if at all, for the living crown's trunk to also exceed 0 ºC. For instance, in the beginning of February the dead crown's temperatures exceeded 0 ºC, but it took until February 10, 2016, for the live crown's trunk to warm to a similar temperature (Figure 4-22). Then from February 14, 2016, to February 18, 2016, the dead crown's trunk exceeded 0 ºC, but the living crown's trunk never does (Figure 4-22). For a few days after a warming event the living tree's crown trunk temperatures were highly dampened compared to the dead tree's crown trunk before returning to a high degree of correlation. This was likely due to an increased amount of snow trapped by the living tree crown and changes occurring in latent heat, because although the dead tree still had branches, it was mostly void of needles to capture the snow.

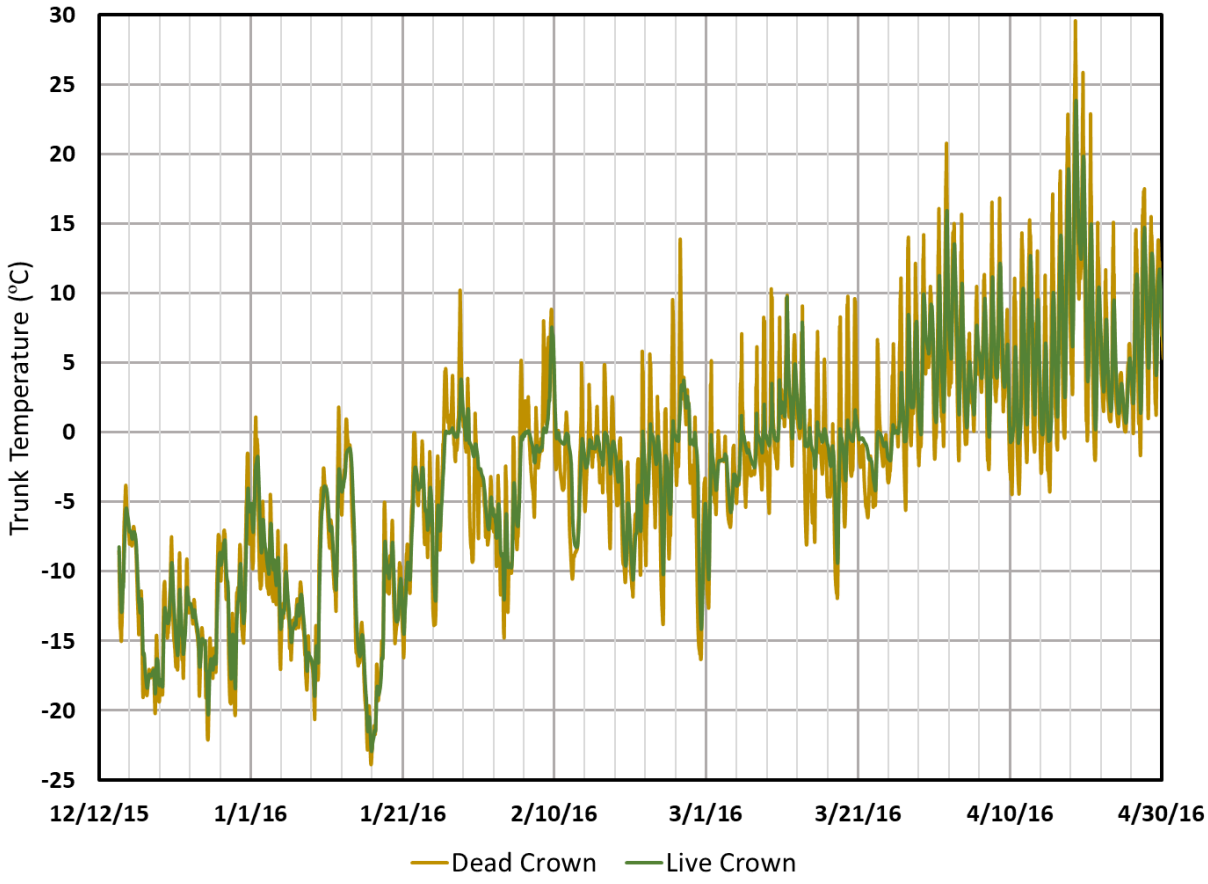

Figure 4-22 Observed 15 Minute Living and Dead Tree Crown Trunk Temperatures in Black Spruce Trees from the Winter 2016 Field Study at Deep Peatland A (DPA)

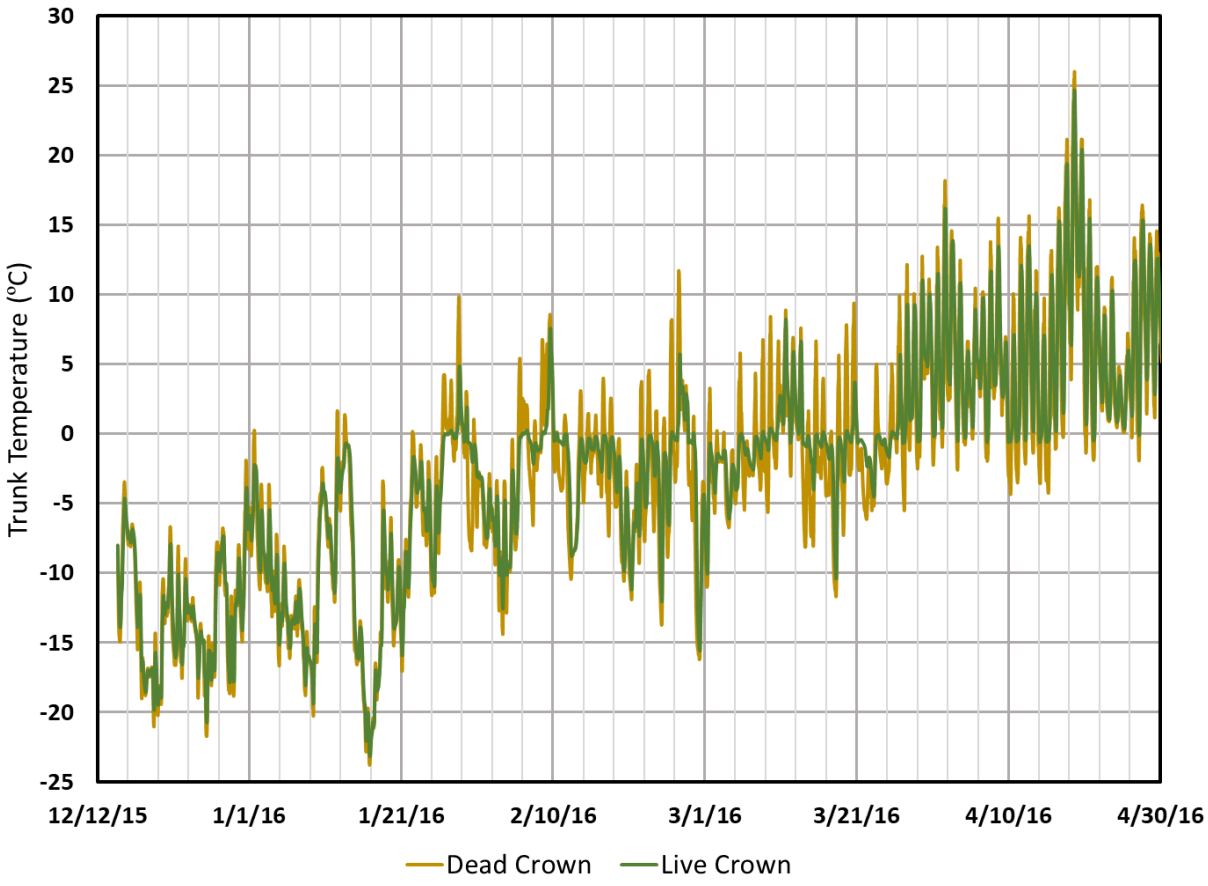

Figure 4-23 Observed 15 Minute Living and Dead Tree Crown Trunk Temperatures in Black Spruce Trees from the Winter 2016 Field Study at Deep Peatland B (DPB)

The observed living and dead trunk temperatures at the base of the black spruce trees are shown in Figure 4-24 for DPA and Figure 4-25 for DPB. As with the crown trunk temperatures there was very little difference in observed temperatures between DPA and DPB. Until the end of March trunk temperatures at the base of living and dead black spruce trees were nearly identical except for a cold period in the middle of January when the living trunk temperatures were approximately 5 ºC colder than the dead trunk base at DPB. This was likely due to the presence of a thicker snowpack at the base of the dead tree. However, by mid-April the temperatures began to diverge when the dead trunk base exceeded 5 ºC at DPB, like at the DPA site in 2015, suggesting a biological process could be cooling the living trunk.

Because there was a very strong correlation between the living and dead tree base trunk temperatures throughout the preceding month of March, it is unlikely they differ in thermal properties or moisture contents (Figure 4-25). It is only during warm days when the tree is

photosynthesizing that the temperatures consistently diverge, suggesting one explanation could be a biological process that effects the thermal properties. Further, if there was a difference in a physically based thermal property the temperature would be dampened at both the maximum and minimums. However, it is only the maximum temperatures that are dampened in the living trunk base with nearly identical daily minimums with the dead trunk base. The temperature probe at the base of the DPA site living tree was damaged by an animal on March 21, 2016. Hence comparisons could not be made after that date.

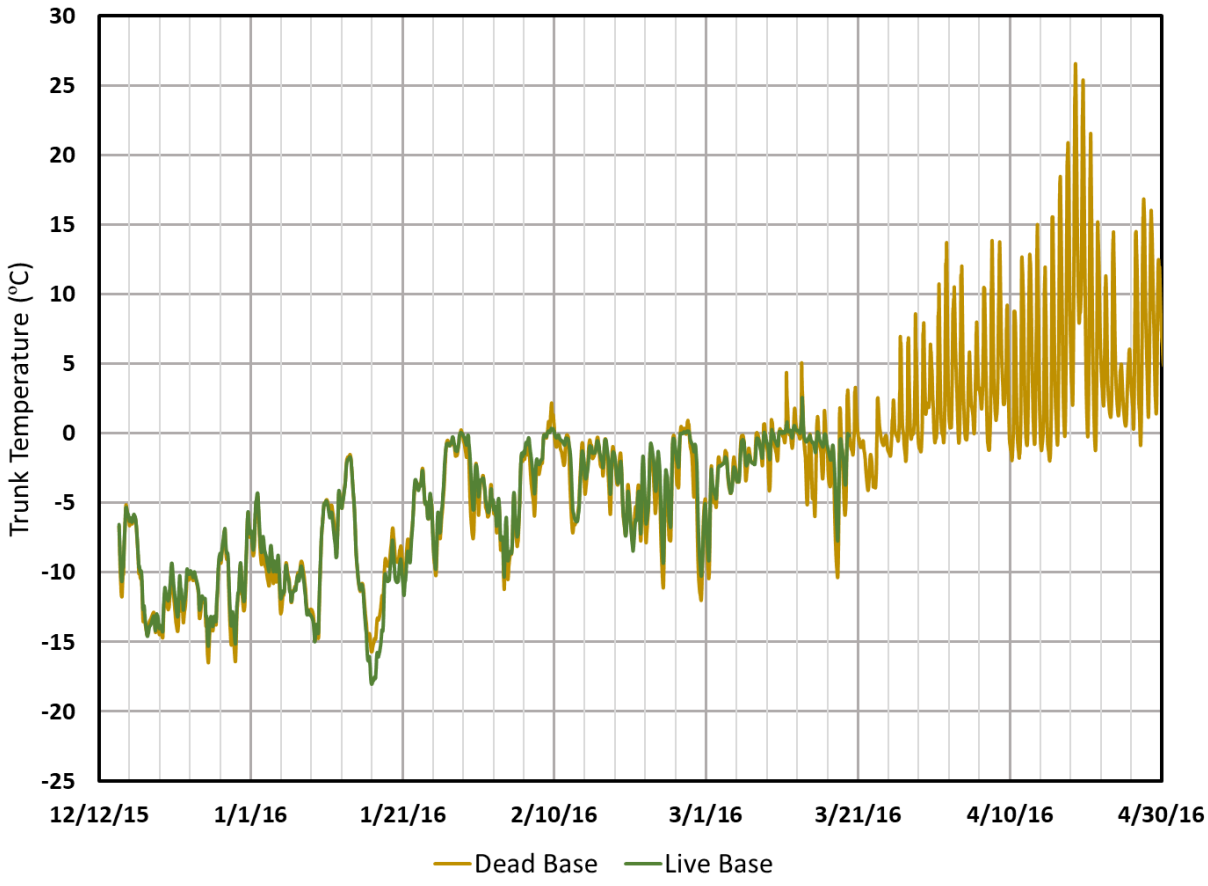

Figure 4-24 Observed 15 Minute Living and Dead Trunk Base Temperatures in Black Spruce Trees from the Winter 2016 Field Study at Deep Peatland A (DPA)

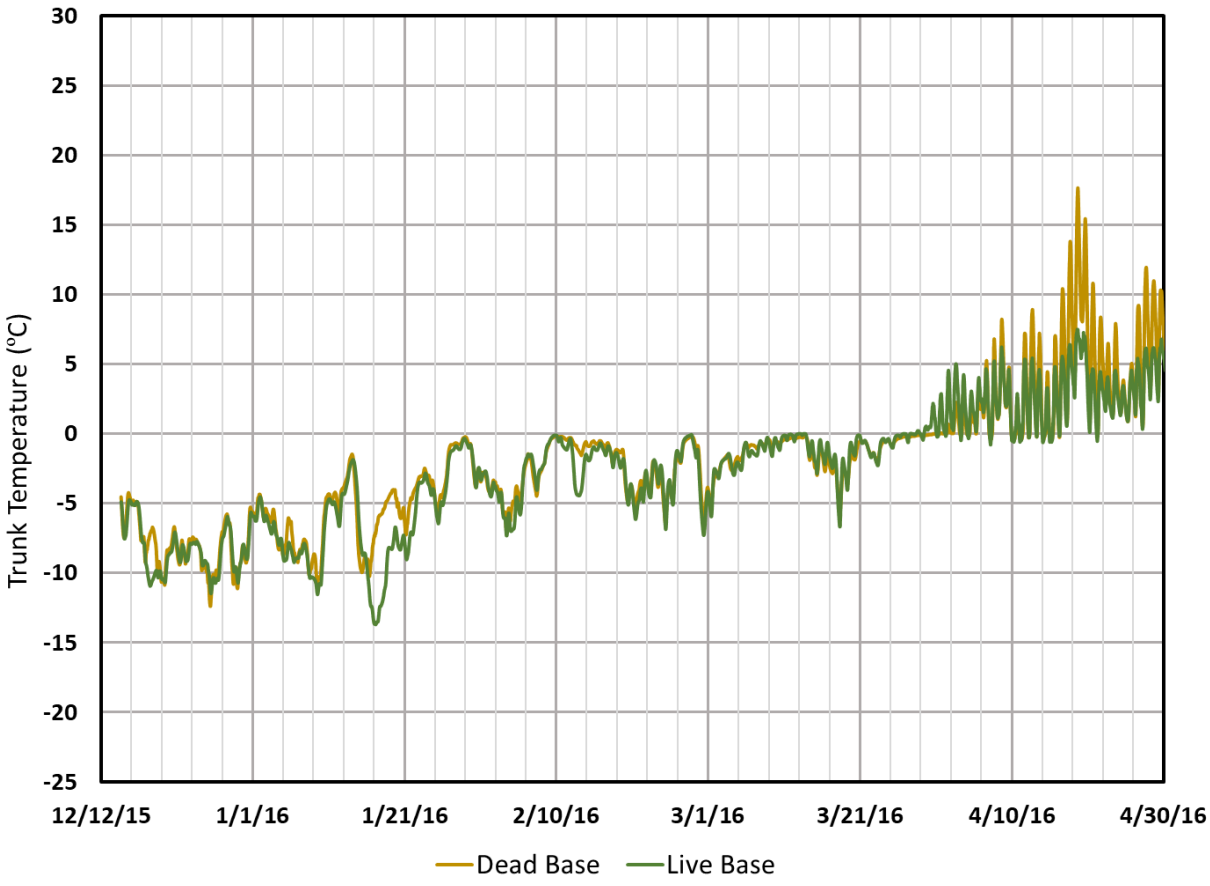

Figure 4-25 Observed 15 Minute Living and Dead Trunk Base Temperatures in Black Spruce Trees from the Winter 2016 Field Study at Deep Peatland B (DPB)

4.2.2.3 Snowpack Temperatures

On March 13, 2015, temperature probes were inserted near the top of the snowpack (+30 cm) and at the base of the snowpack (+5 cm) at DPA to monitor snowpack temperatures just outside of the tree well. However, it soon became apparent that it was difficult to distinguish when the top probe became exposed to the atmosphere, while the base of the snowpack was always 0 ºC until it melted at the end of April (Figure 4-26). Due to the difficulties of monitoring temperature at the top of the snowpack and the lack of any signal or fluctuations of temperature at the base no attempt was made to monitor snow temperatures in 2016 at DPA or DPB.

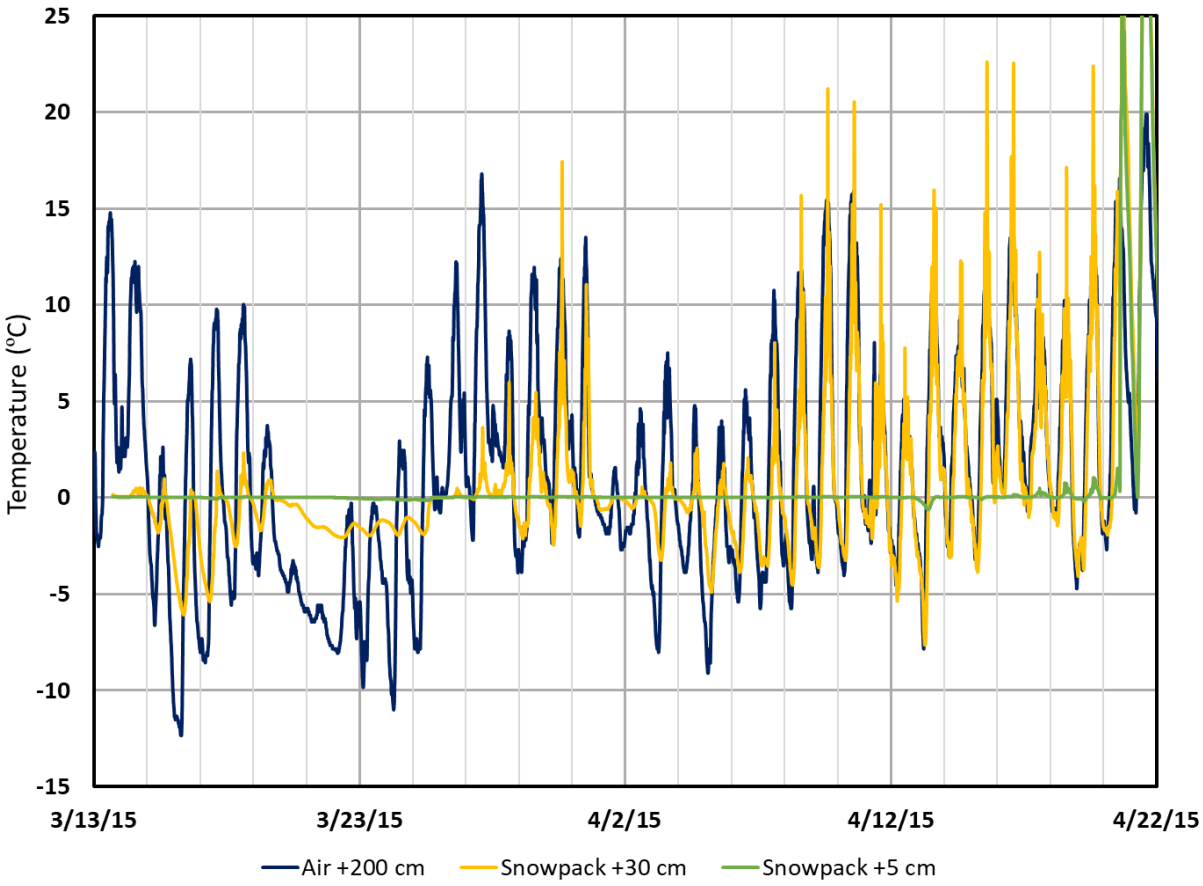

Figure 4-26 Observed 15 Minute Snowpack and Air Temperatures from the Winter2015 Field Study at Deep Peatland A (DPA)

4.2.3 Observed Moisture Contents/Water Levels

Time series graphs were created for the observed sphagnum moss and peat winter moisture contents to better understand the freeze-thaw cycles under a black spruce crown and within a tree cavity. In addition, groundwater surface elevation changes were recorded with a pressure transducer within a piezometer at both DPA and DPB for the 2016 winter.

4.2.3.1 Moisture Contents

The DPA's Phase 1 moisture content probes under the snowpack were reinitiated in March 2015, along with additional moisture content probes under the tree crown. The new GS1 moisture content probes were installed at the surface of the sphagnum moss (0 cm), at the moss/peat interface (-5 cm) and in a loosely filled in tree cavity. The Winter 2015 observed moisture contents at DPA are presented in Figure 4-27. The diurnal changes in moisture contents, especially within the sphagnum moss layer, was due to changes in the physical state of water

held within the moss. GS1 probes are only able to detect liquid water, so as the water freezes or thaws the observable moisture content changes accordingly.

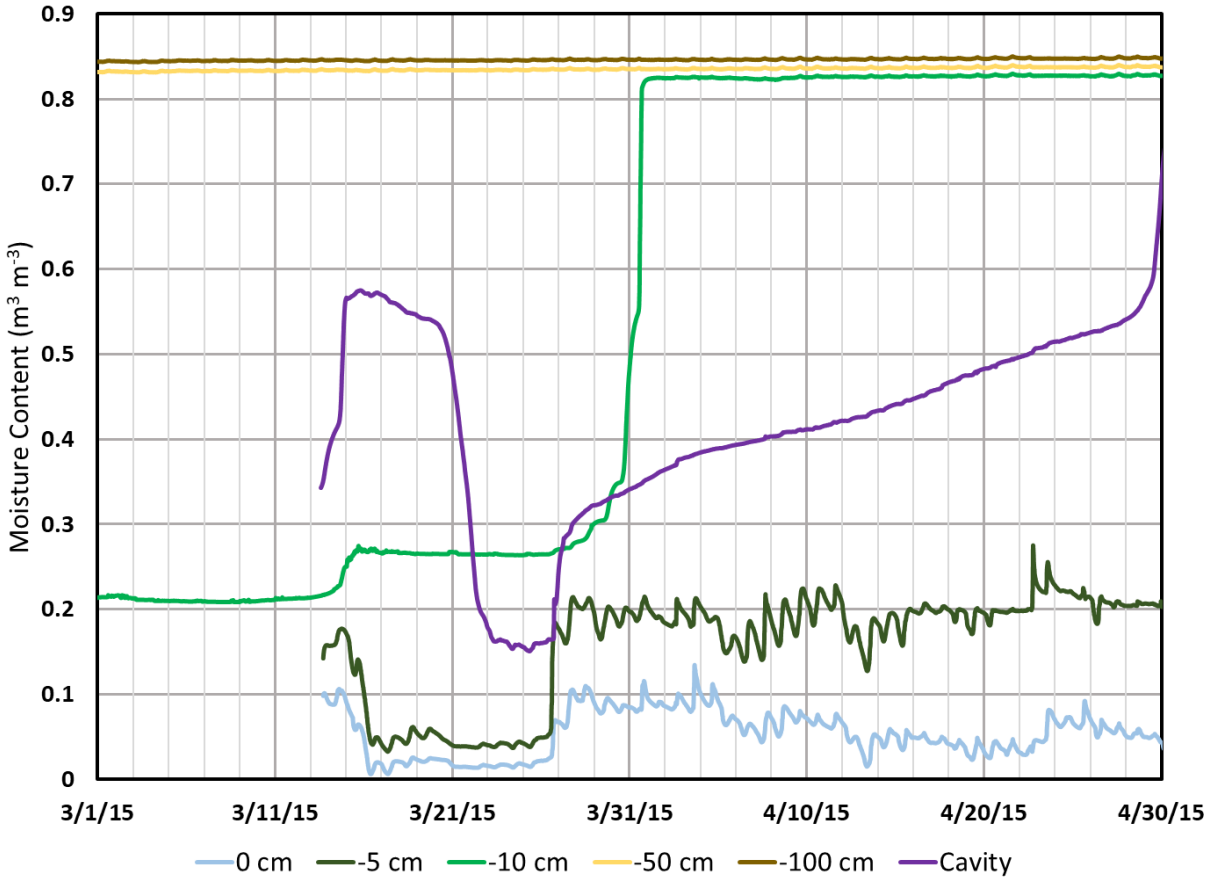

Figure 4-27 Observed 15 Minute Moss (0, -5cm), Peat (-10, -50, -100) and Tree Cavity Moisture Contents from the Winter 2015 Field Study at Deep Peatland A (DPA)

There seemed to be very little change in total moisture content within the sphagnum moss layer in comparison to the tree cavity and the -10 cm probe. The tree cavity probe showed a sudden rapid increase in moisture content on March 15 with only a slight increase observed at -10 cm. Further the moisture contents at 0 and -5 cm had decreasing moisture contents due to them freezing, suggesting the source of water to the tree cavity was snowmelt from the black spruce tree crown branches. The moisture content at -10 cm would have increased at a similar rate as the tree cavity if it was due to a rise in elevation of the groundwater, and the moss layer probes (0, -5 cm) would have increased, not decreased, if it was due to melting of the surrounding snowpack. The drainage of snowmelt from the crown to the tree cavity was also observed during field visits (Figure 4-10).

During April a slower increase in moisture content was observed that was probably due to the rising of the groundwater table as indicated by the saturation of the -10 cm moisture content probe located outside of the tree well. The saturation of the -10 cm probe was more likely due to the groundwater table rising from the infiltration of upslope snowmelt as opposed to a frozen layer blocking infiltration as the subsurface temperatures were above zero.

By December 2015, the Phase 1 moisture content probes located outside of the tree well at -50 and -100 cm had been reactivated in their Phase 1 locations at both DPA and DPB. The -10 cm Theta probes at DPA and DPB were moved and replaced with GS1 probes, with the DPA probes relocated under the black spruce crown and the DPB probes to under the snowpack just outside the tree well. Additional moisture content probes were also installed at DPB at the surface of the moss (0 cm) and at the moss/peat interface (-5cm) alongside the -10 cm probe under the snowpack outside of the tree well. Like DPA, DPB also had a GS1 moisture probe installed within a loosely filled cavity at the base of the tree. The observed winter 2016 moss, peat, and tree cavity moisture contents for DPA are shown in Figure 4-28 and in Figure 4-29 for DPB.

Comparing the moisture contents for the sphagnum moss layer under the tree crown (DPA) and under the snowpack (DPB) it is evident that even though DPA had little to no snowpack it still had higher observed liquid water contents. The diurnal changes in moisture content were much smaller at DPB compared to DPA due to the insulation of the snowpack but DPB was almost completely frozen, with nearly any observable liquid moisture content until the end of February.

There were three multiple day thaw-freeze events that occurred at DPB after maximum daily temperatures exceeded 8 ºC (January 28, February 9, February 26) which caused a spike in moisture contents at -5 and -10 cm with only slight increase at the surface. The same peaks were observed at DPA during the same period following a warm day but were less pronounced due to the daily fluctuations occurring. It is paradoxical that while the moss at DPA had a greater thermal connection with the atmosphere it had a higher liquid moisture content than the moss at DPB. By the end of April, the moisture contents within the moss (0, -5 cm) at DPA exceeded 15% while at DPB they had dropped to below 7%. This is consistent with the observed health conditions of the sphagnum moss from under the black spruce crown compared to the cutline (Figure 4-15).

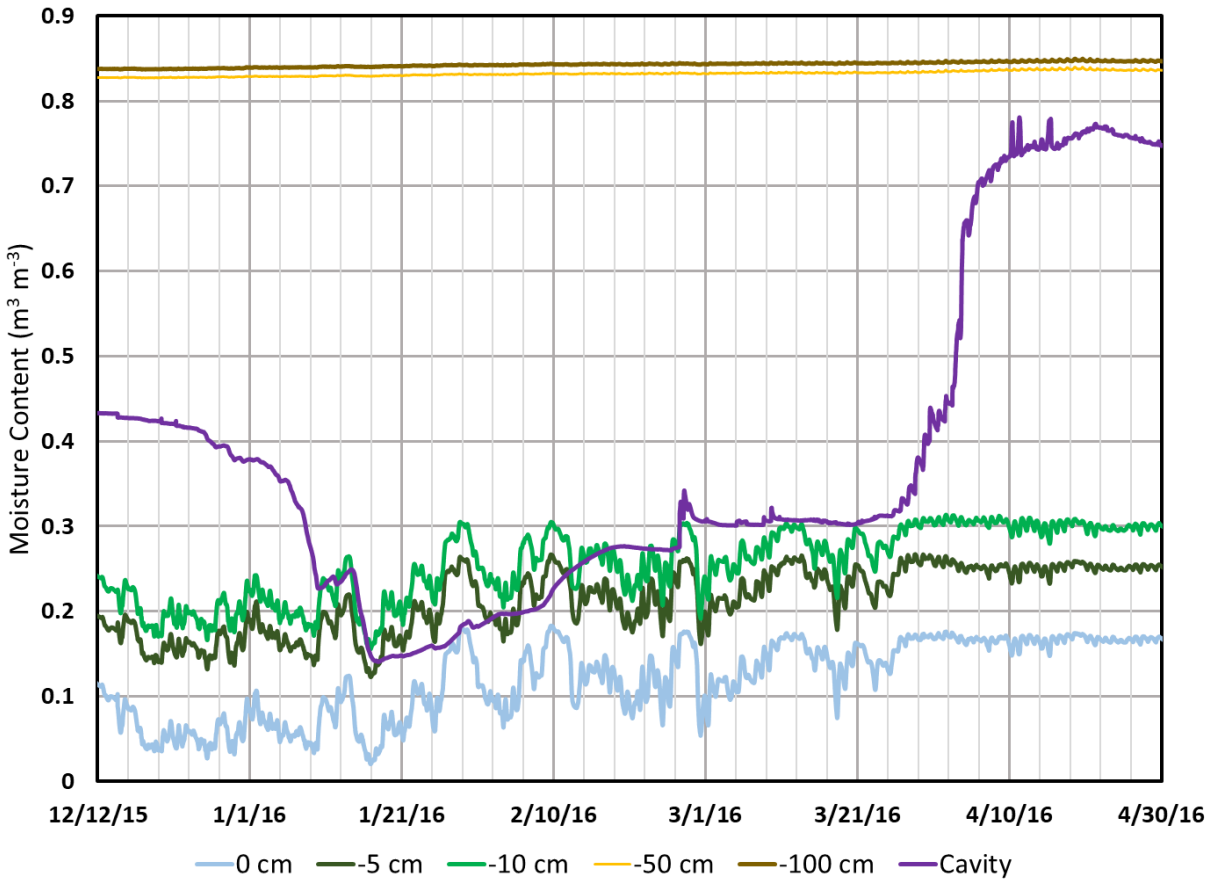

Figure 4-28 Observed 15 Minute Moss (0, -5cm), Peat (-10, -50, -100 cm), and Tree Cavity Moisture Contents from the Winter 2016 Field Study at Deep Peatland A (DPA)

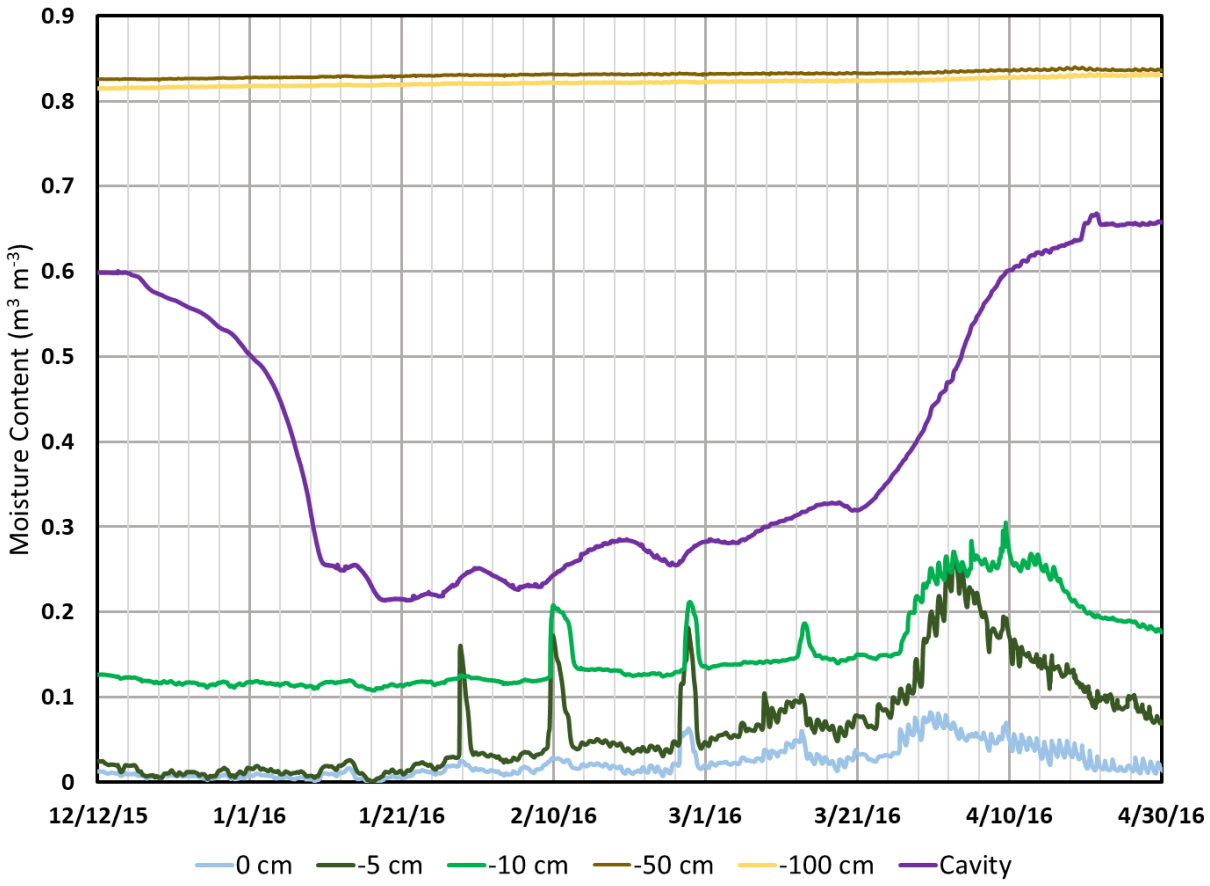

Figure 4-29 Observed 15 Minute Moss (0, -5 cm), Peat (-10, -50, -100 cm) and Tree Cavity Moisture Contents from the Winter 2016 Field Study at Deep Peatland B (DPB)

The tree cavity moisture contents also showed an increase following warm days lasting for approximately a week or more before decreasing again. The pattern was much more pronounced at DPB than at DPA likely due to the infiltration of snowmelt as drip from the black spruce tree's crown. Both DPA and DPB showed a dramatic increase in moisture contents starting on March 21 and becoming saturated by the middle of April due to snowmelt occurring outside the tree well. During this same period moisture contents increase at DPB but began to decrease a few weeks later, while DPA observations showed no increase at all. This was likely because there was often a pathway for snowmelt to drain from outside the tree well toward the black spruce tree trunk, where the tree cavity is located, but at DPA the probes were located outside of the preferential pathway (Figure 4-12). Temperature readings were not obtained from the tree cavity because they needed to be back filled with peat that would alter the temperature. However, it was unlikely that temperatures dropped below zero within the cavity itself but would freeze at the

surface. A thin layer of ice was often observed at the tree cavity in the months of January and February if water had pooled in the cavity but was never observed to be frozen solid.

4.2.3.2 Groundwater Elevations

Groundwater elevations were monitored with pressure transducers during the winter of 2016 in existing piezometers installed to the mineral soil and screened within the peat. The exact elevation of the pressure transducer was unknown, so the groundwater elevation was set to 1 m at both DPA and DPB on the date of installation, November 17, 2015. The change in groundwater elevations from date of installation are shown in Figure 4-30. The piezometer at DPB was located within a small clearing void of any trees while the piezometer at DPA was located close to a mat of black spruce trees and is the likely reason for the minor diurnal fluctuations observed at DPA. Also, since the deep peatland sites are plateau muskegs (Table 3-1), due to their location at the upper boundary of the watershed and overlying fine-grained materials, there is likely very little to no groundwater contribution from upgradient. It is likely that both deep peatland sites are a source of groundwater recharge and not discharge, thus any observed increases in groundwater elevation would be the direct result of local infiltration.

There was also a slight increase in groundwater elevations following the warm days which saw moisture content increases within the tree cavity, demonstrating infiltration occurred during the winter. This was most evident at DPA on February 10, 2016 which had crown trunk temperatures exceeding 5 ºC (Figure 4-22) followed by an increase in tree cavity moisture content over the next week (Figure 4-28) which correlated to the same time period the groundwater elevation rose at DPA (Figure 4-30). It is difficult to estimate the exact amount of recharge as groundwater elevations were decreasing by approximately 0.5 cm day^{-1} until the first warm day (+8 ºC) at the end of January, after which they started increasing by roughly 0.1 cm day^{-1}. Thus, recharge could range anywhere from 0.6 cm day^{-1} assuming drainage out of the peatland remained constant at 0.5 cm day^{-1}, to a recharge of only 0.1 cm day^{-1} if there was zero drainage occurring. This is assuming that the peat mats were floating since minimal change was observed in vadose zone moisture contents. The largest increase in groundwater elevations occurred at the end of March, when infiltration of upslope snowmelt was occurring to the peatland.

The change in the slope of the plot of groundwater elevations that occurs during the month of December in both DPA and DPB was perplexing and could be due changes in the capillary fringe due to the snowpack. It was also interesting that even though there was over a 60 cm change in groundwater levels there was no recorded change of moisture content at the -50 cm probes (Figure 4-28, Figure 4-29). It is possible that the moisture content probes were simply unable to accurately measure the differences in moisture from being below the water table and from within the capillary fringe. Another plausible explanation is that the peat mat is floating and would rise/fall with any changes in groundwater elevation. The piezometers were inserted into the clayey loam and unlikely to move, while the moisture content probes were only in the peat and would remain at a constant depth from the peat surface.

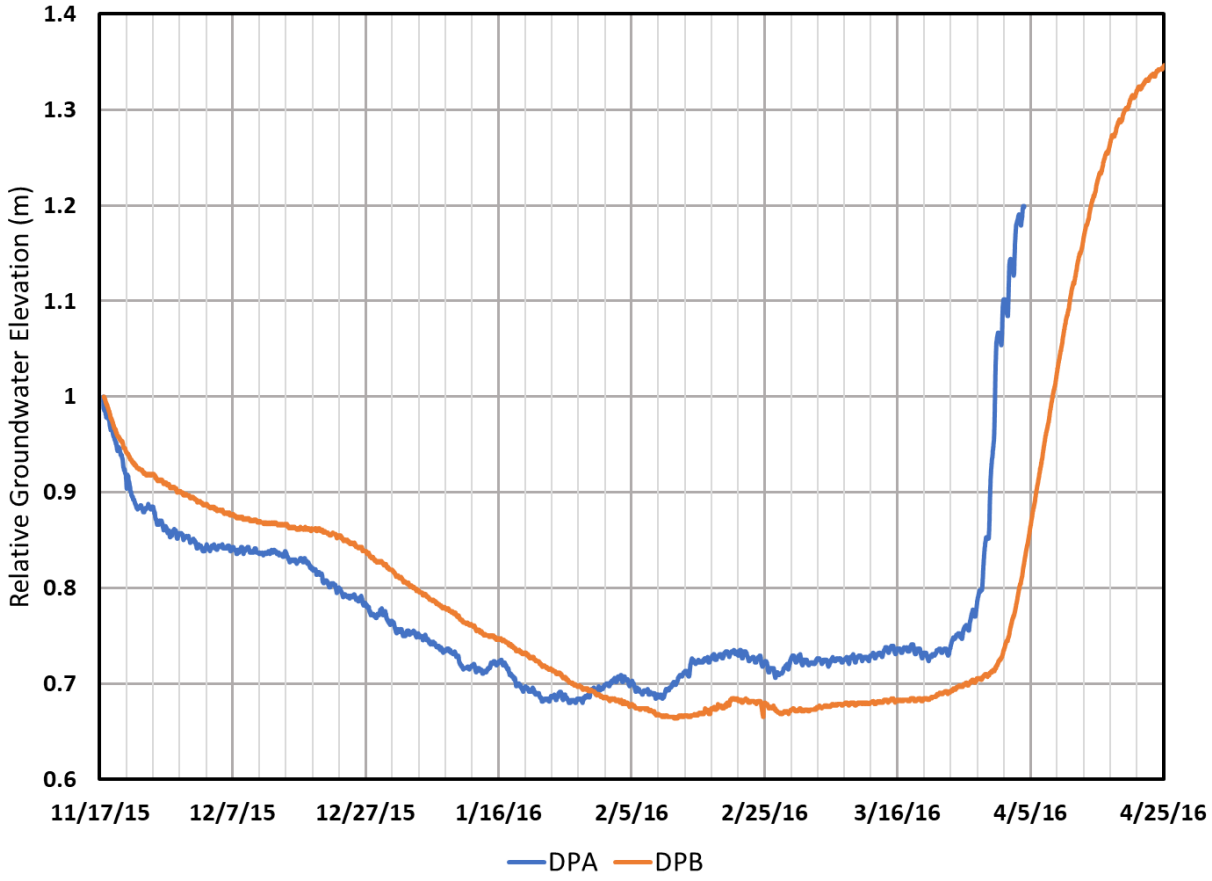

Figure 4-30 Observed 15 Minute Change in Groundwater Elevation from the Winter 2016 Field Study at Deep Peatland A (DPA) and Deep Peatland B (DPB)

4.3 Analysis of Phase 2

An analysis of change in temperatures and temperature gradients for the two deep peatland ecological sites (DPA and DPB) are presented in this section.

4.3.1 Change in 5-Day Moving Average Temperature

For both DPA (2015, 2016) and DPB (2016), the change in the 5-day moving average subsurface temperature was calculated to determine if peat/soil was warming (a + gradient) or cooling (a - gradient) and to compare rates at different depths. Originally the change in daily average subsurface temperature was calculated, however the differences in daily temperature at depth were within the measurement error of the temperature probes resulting in higher than expected variability. To reduce the variability introduced due to the probe's accuracy a multiple day average, using the observed temperatures from the days prior and after, was calculated for each day. It was found that by including the 2 days prior and after in the calculation of the average temperature, for a 5-day moving average temperature, resulted in the elimination of variation due to measurement noise. Thus, the 5-day moving average for each day was calculated and subtracted from the next day's 5-day moving average to generate the change in 5-day moving average temperature. Further, only the YSI probes could be used in this analysis, as the HOBO probes (0, -5, -10 cm) were not sensitive enough, even with a 5-day averaging, to produce meaningful results.

The change in 5-day moving average subsurface temperature at DPA (primary axis) and the maximum daily air temperature (secondary axis) are shown in Figure 4-31. The change in 5-day moving average temperatures at -200 and -300 cm was consistent, with -300 cm slightly decreasing while -200 cm was slightly increasing toward a state of equilibrium with each other. The change in temperature at -100 cm was also consistent except for a few days after the January 24 warming event where it tracked with the -50 cm change in temperature until intercepting the -200 cm change in temperature after which it tracks with the -200 cm. The change in temperature at -30 cm and -50 cm would have very similar lines of "best fit" if all the fluctuations were removed but are inversely correlated until the beginning of April when they become highly correlated.

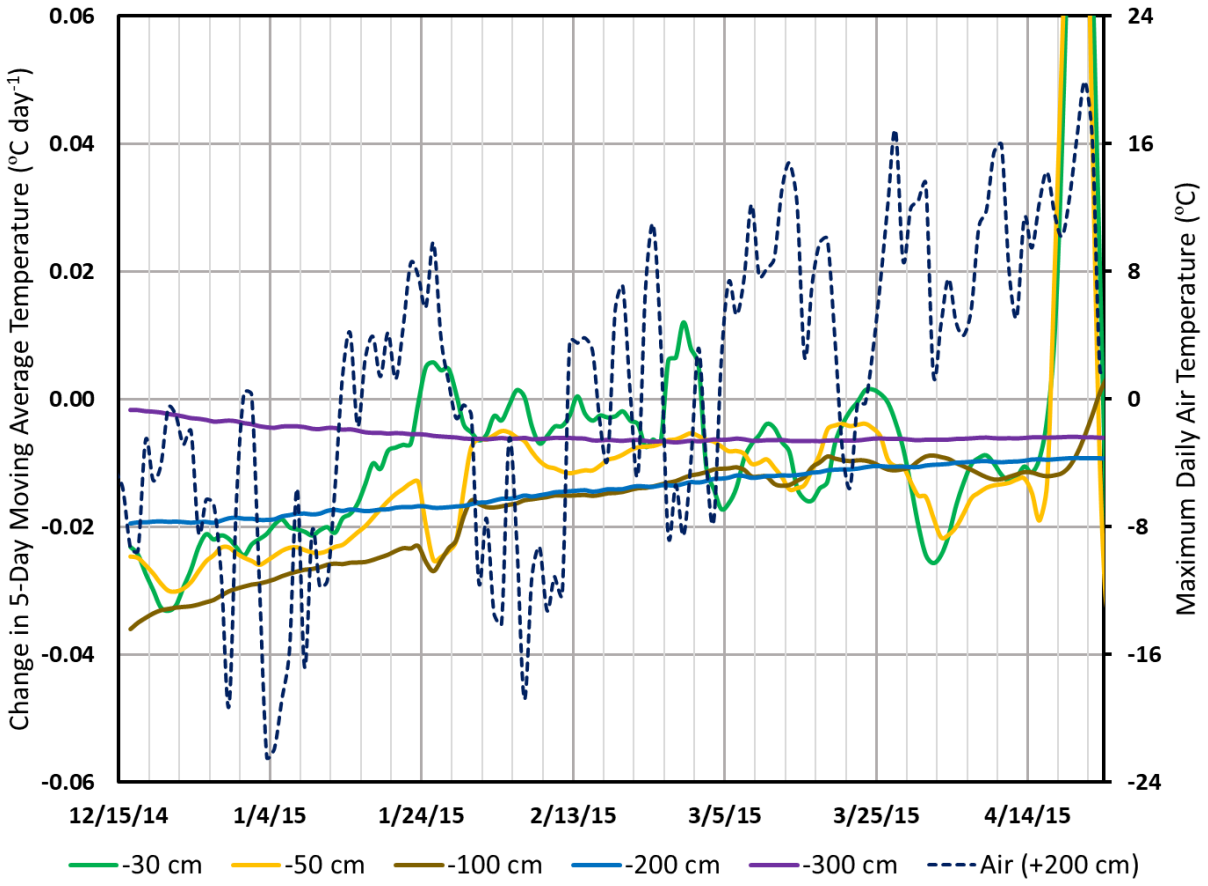

Figure 4-31 Change in 5-Day Moving Average of Subsurface Temperatures and Maximum Daily Air Temperatures at DPA for Winter 2015

There were also periods when the -30 cm change in temperature increased, and it didn't always correspond to warm days, and sometimes it would be the opposite. During the beginning of March there were multiple warm days, yet the -30 cm probe was losing more heat than during times when the maximum daily temperature was less than -8 ºC.

The change in 5-day moving average subsurface temperatures for DPA in 2016 (Figure 4-32) were very similar to 2015 except for the -50 cm probe which had hardly any fluctuations, but still tracked with -30 cm change in temperatures. The 2016 DPA data lacked a multiple day warming event in January that resulted in the mixing event observed in 2015 suggesting that changes in temperature at -50 cm probe can be highly influenced by the infiltration of snowmelt from the crown and the root system of the black spruce tree and not by air temperature. As with 2015, there was also a major cooling event at the end of March that correlated to maximum daily air temperature of 8 ºC and was due to the infiltration of snowmelt.

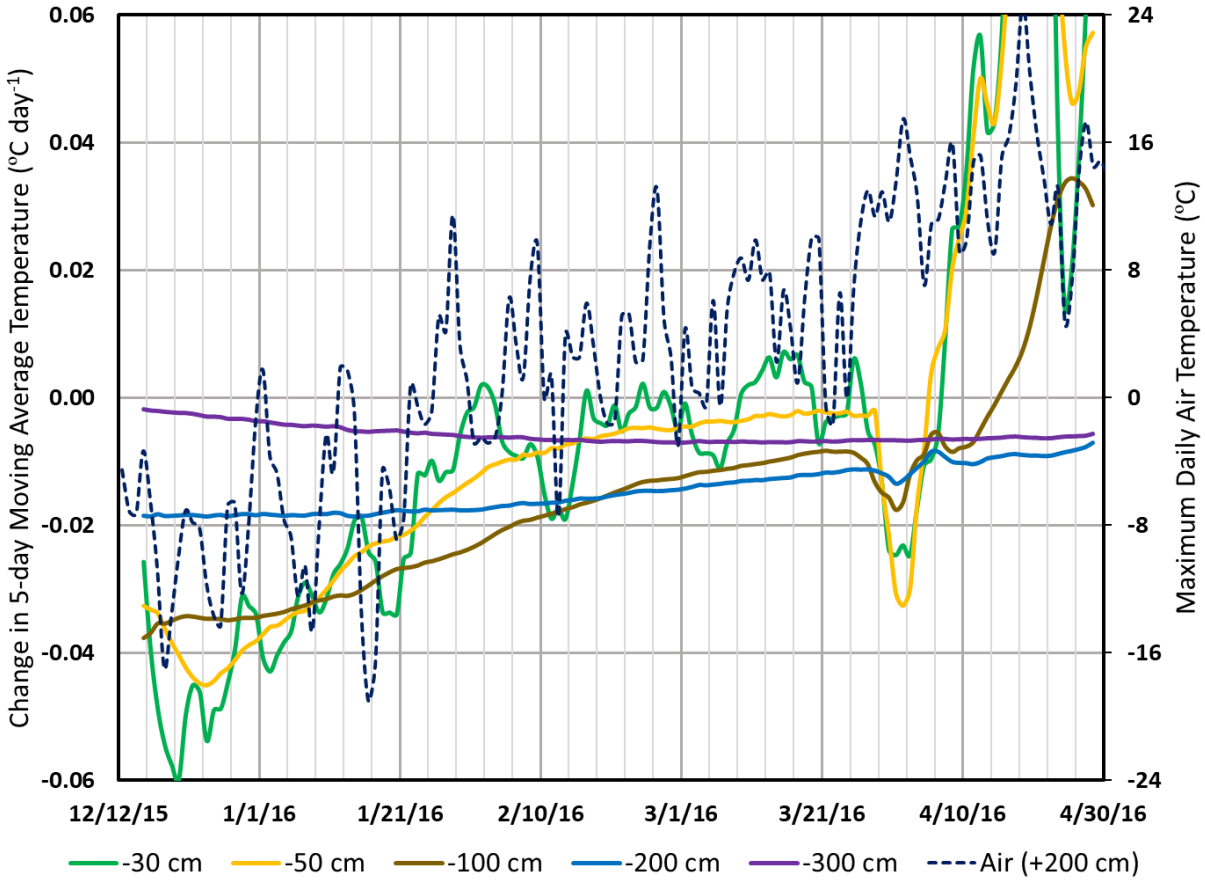

Figure 4-32 Change in 5-Day Moving Average Subsurface Temperatures and Maximum Daily Air Temperatures at DPA for Winter 2016

The change in 5-day moving average subsurface temperatures for DPB in 2016 were consistent with a system in equilibrium with a snowpack at 0 ºC (Figure 4-33). The changes in temperature at -100, -200, and -300 had very little fluctuations and by the end of February were in equilibrium with all three roughly losing the same amount of heat per day. The -30 and -50 cm probes were in equilibrium the entire winter, but unlike DPA there was more fluctuations at the -50 cm probe compared to the -30 cm. This became very evident by the end of April with the -50 cm probe having a much larger increase in temperature versus the -30 cm probe, while at DPA the -30 and -50 cm probes were almost identical with the -50 cm probe being dampened.

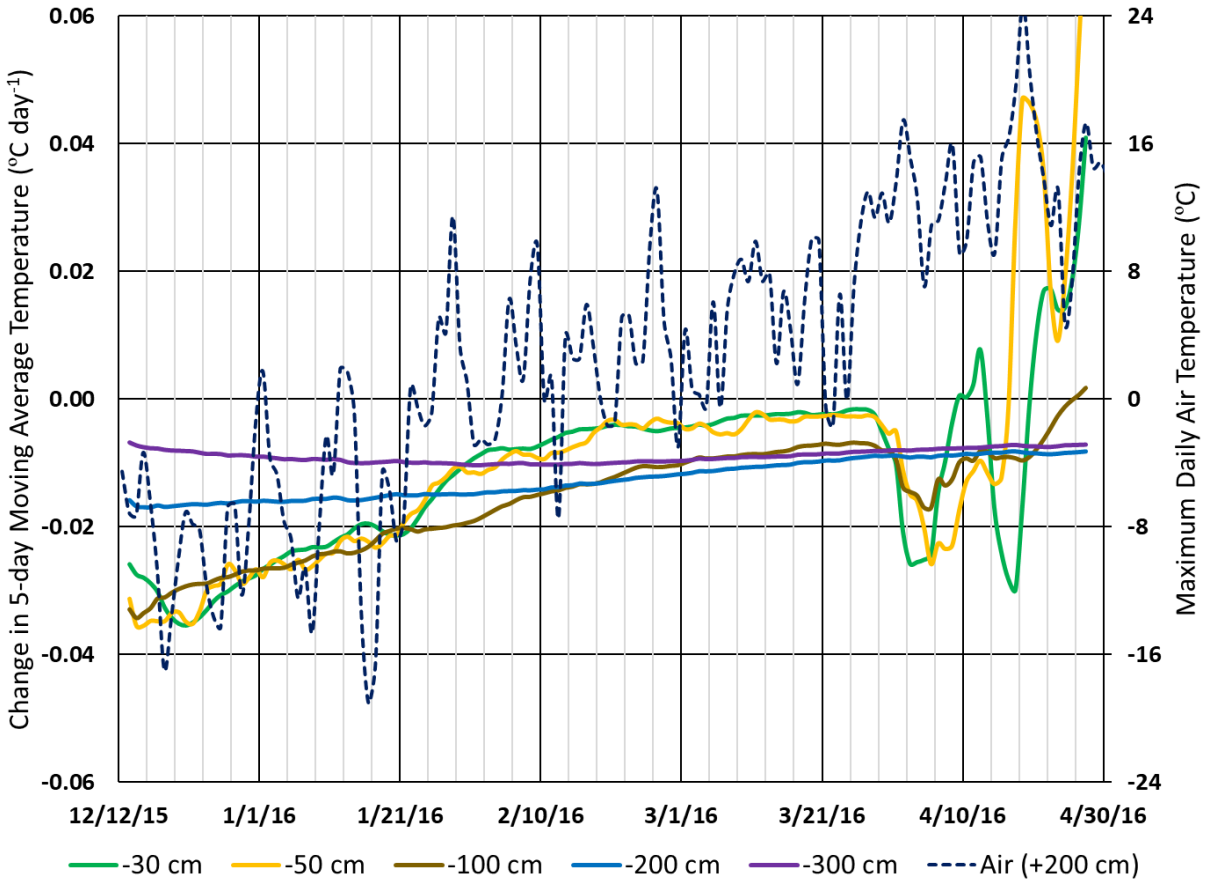

Figure 4-33 Change in 5-Day Moving Average Subsurface Temperatures at DPB for Winter 2016 with Maximum Daily Air Temperatures

4.3.2 Thermal Gradients

Thermal gradients were calculated for DPA and DPB for the 2016 field study from daily averaged data to determine if the flux of heat was upwards or downwards. Daily averaged data was used, as opposed to a 5-day moving average, because there were large enough differences in temperature with elevation that probe signal variation was not an issue. Thermal gradients, difference in temperature divided by difference in elevation, were calculated for the -5 to -30 cm, -30 to -50 cm, -50 to -100 cm, and -100 to -300 cm elevation increments. The temperature at the higher elevation was always subtracted from the temperature at the lower elevation so that a positive thermal gradient indicates a warmer lower elevation and an upwards flux of heat. Conversely a negative thermal gradient, indicates a cooler lower elevation and a downwards flux of heat. The thermal gradient calculation results are plotted in Figure 4-34. The -200 cm probe was not used in this analysis due to the difference in medium between the two sites, with DPA

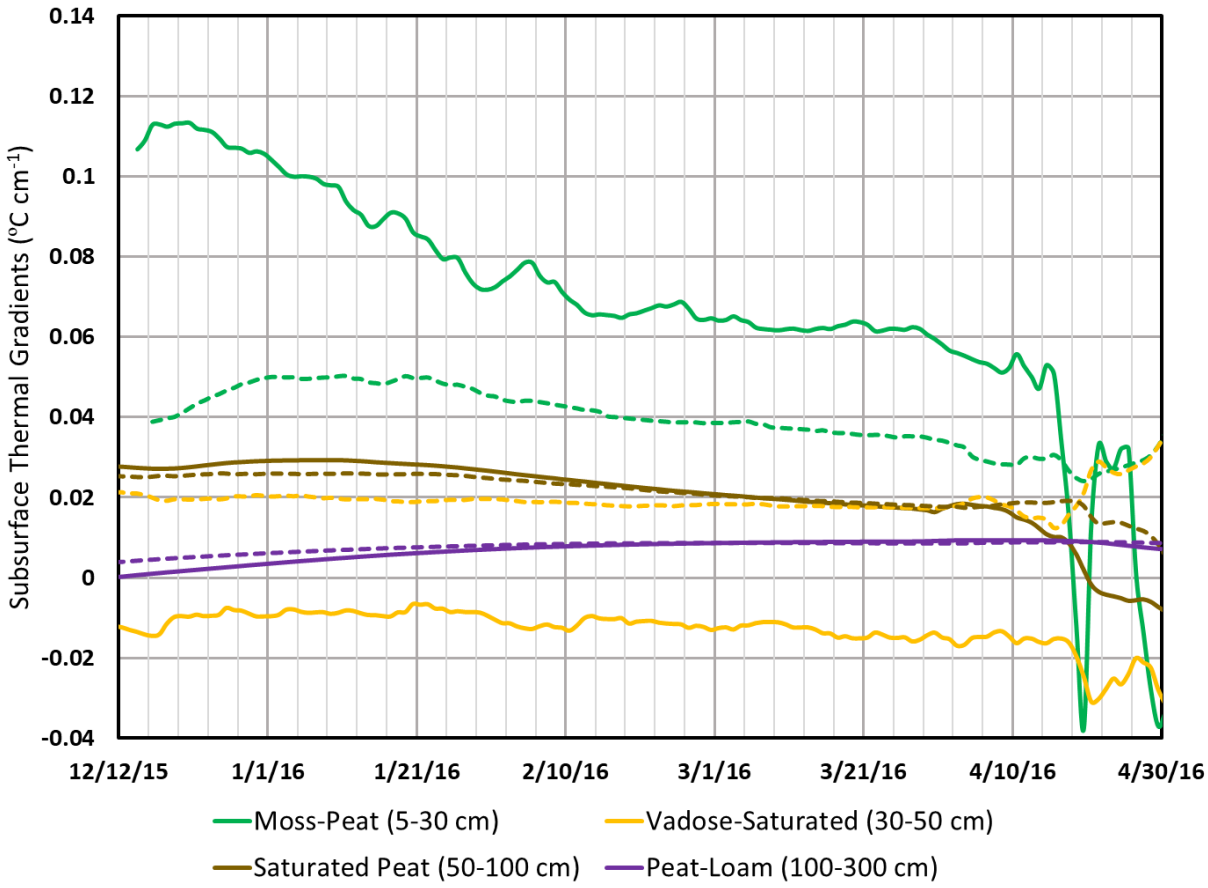

Figure 4-34 Subsurface Thermal Gradients for DPA (Solid) and DPB (Dashed) for Daily Average Temperatures from 2016 Field Study

Note: A positive thermal gradient indicates a warmer lower elevation and an upwards flux of heat. A negative thermal gradient indicates a cooler lower elevation and a downwards flux of heat

located in peat at 200 cm while DPB is within a clayey loam at 200 cm. The -10 cm probe was also not used since it was very close in temperature to the -30 cm and the difference in probe sensitivities became an issue, while the -5 cm probe was consistently around 0 ºC.

The thermal gradients within the saturated peat (-50 to -100 cm) and between the mineral soil and peat (-100 to -300 cm) were nearly identical between DPA and DPB. This is because spatial difference in temperature due to the presence of black spruce trees would diminish at depth, especially below the groundwater table, where there should be little to no variation in temperatures at the same elevation due to the high thermal conductivity of water. The moss to peat (-5 to -30 cm) thermal gradients of probes located within the tree well at DPA were very

different from the observed gradients under the snowpack at DPB. The -5 to -30 cm thermal gradient at DPA was approximately 50 % greater than at DPB by the beginning of September, resulting in a 50% increase in heat losses assuming an equivalent thermal conductivity. It was surprising that the heat loss was not greater due to the minimal depth or lack of snowpack within the tree well, as the insulation provided by the snowpack outside of the tree well should have had a greater effect.

The biggest difference in thermal gradients was from the vadose to saturated zone (30-50 cm) between DPA and DPB, with DPA gradients being negative (indicating cooling downwards) instead of positive (indicating cooling upwards). At DPB the thermal gradient between the vadose and saturated peat reached an equilibrium with the gradient within the saturated peat itself (50-100 cm) with a loss of heat toward the snowpack. However, at DPA the gradient was consistently cooling downwards suggesting that the black spruce root zone at -30 cm is a source of heat both towards the surface moss layer and toward the groundwater table. The drastic changes in thermal gradients at the end of April is likely due to moss completely thawing within the tree well and becoming a source of heat on warm days at DPA, while DPB was likely still thawing so there was very little change in sensible heat.

4.4 Discussion

Due to the spacing of black spruce trees in peatlands and the lack of canopy closure, a large percentage of snowfall can become captured within the branches of their crown, especially when there is any wind. Also, it seemed from visual observation that the shortness of the black spruce branches and the morphology of their needles allowed them to accumulate larger volumes of snow within the crown before throughfall occurred in comparison to the lodgepole pine, but additional investigations would be required to confirm this comment. Thus, large volumes of snow captured by the black spruce's branches can remain until it quickly melts during the next few sunny days due to the very low albedo of the black spruce tree. Further it was documented in the field that when the snow melted within the black spruce's crown it would drip solely as liquid water (Figure 4-10), whereas with the lodgepole pine trees wet snow would fall through as large lumps and not individual droplets. This was likely due to the black spruce branches being shorter and stiffer, allowing them to support a larger snow load, but this perception would need to be tested and verified. Periods of snowmelt from the crown could also be inferred by

comparing the crown trunk temperatures of living and dead black spruce trees, with the dead tree crown trunk having large fluctuations in temperature, while the living tree crown trunk maintains a constant temperature of 0 ºC due to changes in latent heat occurring (Figure 4-22 and Figure 4-23).

It is often assumed that snowmelt dripping from the tree branches will refreeze once it hits the underlying snowpack/ground surface and would not remain as liquid water at the base of the tree. Yet liquid water was often observed at the base of the black spruce tree trunks throughout the winter. After snowmelt drip from the crown occurred, as liquid water drops and not as wet snow, it accumulated at the base of the tree, further melting the snow within the tree well into a slushie mix of snow and water (Figure 4-12). With increasing distance from the base of the trunk the slushie mix transitioned to snow, with liquid water at the cavity located at the base of the tree trunk. It also appeared that the liquid water drained towards the cavity and was most likely the source of water when moisture contents were observed to increase (Figure 4-27).

It is also likely that the stored meltwater within the tree cavity provided a source of water for the sphagnum moss within the tree well, explaining the higher observed moisture contents (Figure 4-28) in comparison to outside the tree well (Figure 4-29). Future research should investigate if the increased moisture from the snowmelt of the black spruce's crown can result in healthier sphagnum moss colonies within the tree well in comparison to the colonies within a cutline (Figure 4-15).

The preliminary field study results suggest that without the presence of black spruce trees, the snowpack overlying the peat would melt from the top down instead from the root zone up, likely resulting in initial snowmelt refreezing at the surface of the moss becoming a partial to complete barrier to the infiltration of future snowmelt (Figure 4-13).

While it was hypothesised that black spruce trees conduct sensible energy down their trunks warming the root zone in the winter through sap recirculation, persistent and significant differences in living and dead base of tree trunk temperatures were not observed until the beginning of April (Figure 4-24, Figure 4-25). Therefore, the hypothesis is rejected. Throughout the month of April, the day-time temperatures at the base of the dead black spruce tree would often exceed 10 ºC, while the living black spruce trees were much cooler, never exceeding 7.5 ºC at DPB in 2016 and 5 ºC at DPA in 2015 (Figure 4-35). During the night, when temperatures

were cooler, there was little difference observed between the living and dead trees, often having the same daily minimum temperature. This would be expected due to the decreased differences in atmospheric and subsurface temperatures and the reduction of sap flow at night.

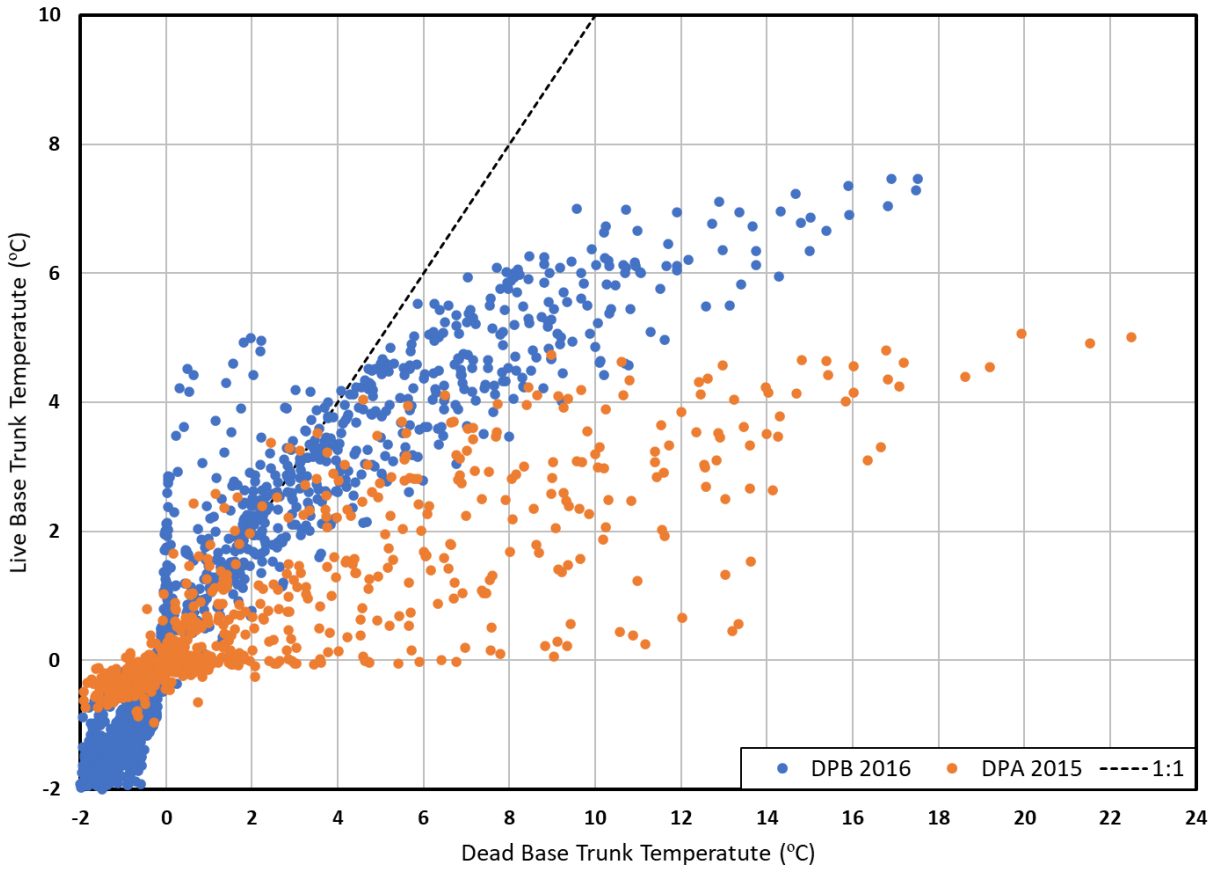

Figure 4-35 Live Versus Dead Hourly Averaged Base Trunk Temperatures for Black Spruce Trees in April for DPA (2015, 1 Living 1 Dead) and DPB (2016, 1 Living 1 Dead)

To investigate if the differences observed between the living and dead tree trunk bases was also having an effect on subsurface temperatures within the root zone, a comparison was made between the -10 cm temperatures, where the black spruce roots are, with the overlying moss layer and base of trunk temperatures for most of April (Figure 4-36). The black spruce root zone was always warmer than the overlying moss layer, and experienced greater diurnal temperature fluctuations, with warming of up to a 5 ºC range in a single day. Thus, the black spruce root zone was warming the subsurface from the bottom up, as opposed to incoming solar radiation warming the subsurface from the surface downwards. Also, unlike the brief periods of warming identified with a positive change in the 5-day moving average at -30 cm that showed no

correlation to atmospheric conditions (Figure 4-31, Figure 4-32), the warming that occurred in April did. The maximum daily temperature observed at -10 cm always equaled or exceeded the maximum daily temperature observed in the living trunk base and was always less than the maximum daily temperature in the dead trunk base. Since tree trunk temperatures were monitored on the north side, it is expected that the south side of the living tree was warmer but still cooler than the temperatures observed in the dead tree trunk base. Thus, it is possible for the root zone temperatures to be warmer than the living tree trunk temperatures, since the root zone was monitored on the south side to maximize the effect of incoming solar radiation, but still much cooler than the temperatures of the dead trunk base. The bounding of daily maximum temperature in the root zone by living and dead tree trunk temperatures, along with the root zone temperatures always exceeding the overlying moss temperatures is supporting evidence for the hypothesis that translocation sap flow is warming the subsurface, at least in April.

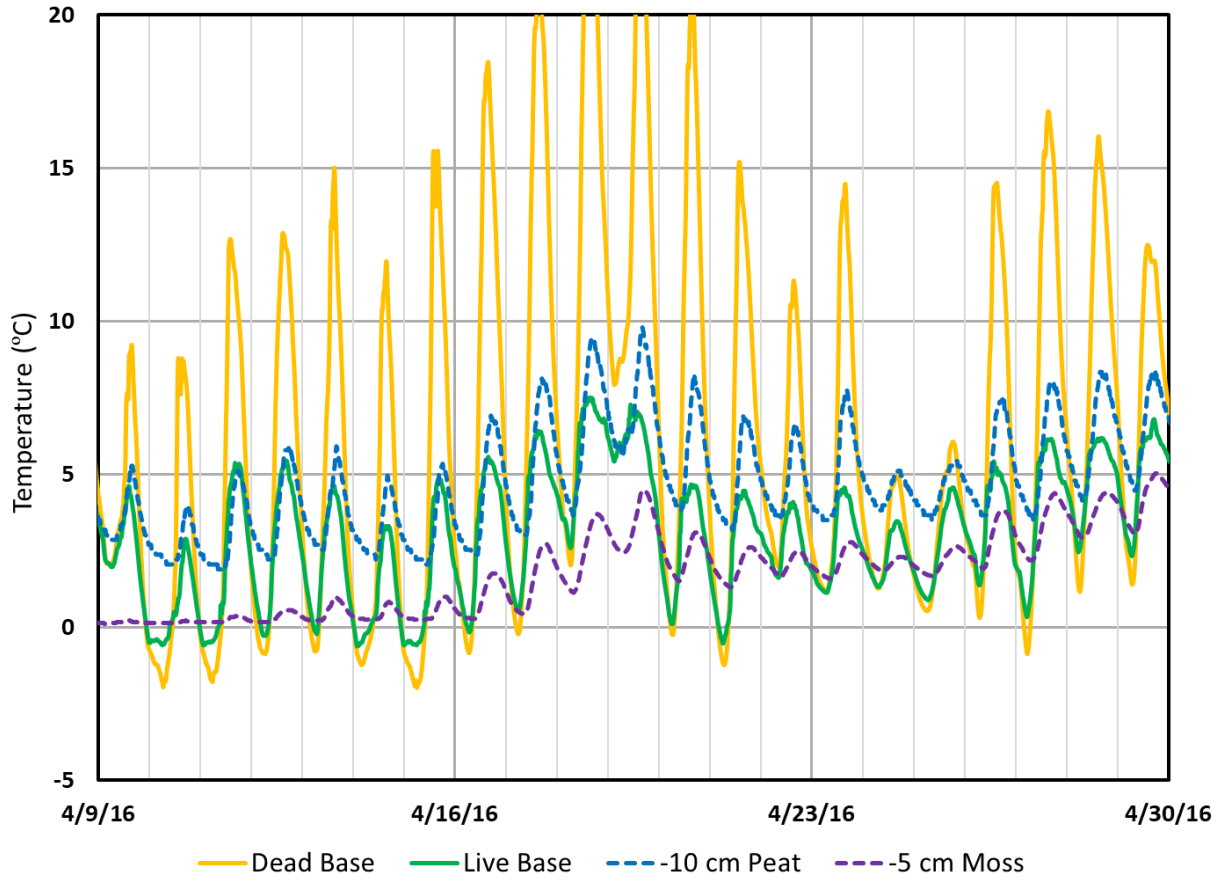

Figure 4-36 Comparison of Black Spruce Root Zone (-10 cm Peat, DPA) with Overlying Moss Layer (-5 cm Moss, DPA) and Black Spruce Living and Dead Base Trunk Temperatures (DPB)

Even though it was determined that the circulation of sap within the black spruce tree was not warming the root zone throughout the winter, there was strong evidence that this process started to occur at the end of March and all throughout April. While the circulation of sap could not explain the shallower than expected depth of frost it is a plausible explanation to the persistence of a snowpack/ice in between the black spruce root mats until at least the end of April and should be further tested (Figure 4-12, Figure 4-37). Throughout April the incoming solar radiation captured by the crown appears to be directly transferred to the root zone via the vascular tissue and not emitted as long-wave radiation to the ground surface.

Figure 4-37 Example of Snow Around Black Spruce Trees at the End of April

Further on a catchment scale, the presence of black spruce trees on peatlands can have a very important role in the hydrological cycle. When snowmelt occurs in the surrounding upland lodgepole pine areas very little infiltration may occur, depending on the texture and frozen conditions, resulting in large amounts of surface runoff. Because Boreal Plains peatlands often

formed over centuries on beaver dammed streams, naturally the upland runoff would flow towards the peatland, the location of the historic stream channel. The presence of black spruce trees on the peatland allows the upland snowmelt runoff to infiltrate through the unfrozen tree cavities and was the likely source of water for the observed substantial rise in groundwater (Figure 4-30). Without black spruce trees it is very possible the entire surface of the peatland would be frozen drastically reducing snowmelt infiltration with increased ponding resulting in runoff, similar to the observed condition within cutlines at the current study deep peatland sites and also reported at reclaimed peatland sites (Ketcheson and Price 2016).

However, it is still unclear why the water within the tree cavity did not completely freeze, or why the sphagnum moss and peat within the tree well were insulated from the atmosphere, with a dampened response in temperature, yet there was little to no snowpack (Figure 4-17). Because the hypothesis that the black spruce tree roots system was warming the subsurface throughout the winter was disproven, as differences in living and dead tree trunk bases only occurred in April, a more detailed analysis of the thermal conductivity of the sphagnum moss layer is required as a possible explanation for the very shallow depth of frost observed at the deep peatland sites.

5 NUMERICAL SIMULATION of PHASE 1

Numerical simulation of observed subsurface temperatures and moisture contents of the six ecological sites from Phase 1 are described in this chapter. Section 5.1 provides details about the numerical model used, the governing equations, and parameterization. A description of the six ecological sites Deep Peatland A/B (DPA/DPB), Shallow Peatland A/B (SPA/SPB), and Upland Pine A/B (UPA/UPB) for Phase 1 was presented in Section 3.1.1 Site Descriptions. The observed temperatures used to calibrate the model were previously presented in Section 3.2.1 and the moisture contents in Section 3.2.2.

The numerical simulations will be used to test the hypothesis that the shallower than expected frost depth in the deep peatland sites is due to the insulating effect of the sphagnum moss layer. To test this hypothesis model parameters for the numerical simulations must be estimated for each of the six ecological sites to simulate the observed temperature and moisture profiles (Objective 3). The numerical simulation then must be updated with a new algorithm for the sphagnum moss thermal conductivity to determine if the wintertime residuals, observed temperature minus simulated, is reduced (Objective 4).

5.1 Numerical Simulation Methodology

To investigate and better understand the observed differences in frost depths at the ecological sites the temperature profiles were simulated using a numerical model and the atmospheric data collected from the weather station (Figure 3-2). Conceptually the simulation of the thermal profile could be viewed as a series of resistors and capacitors, like an electrical flow diagram, with atmospheric conditions at the top of the model and a constant soil temperature at the bottom of the model at an elevation of -450 cm (Figure 5-1). As atmospheric conditions change so do the fluxes of heat in or out of the subsurface depending on the current thermal state of the system and the physical characteristics of the tree's crown and snowpack if present. The thermal resistance of each soil zone can be estimated from the zone thickness and the calculated thermal conductivity in parallel, which is the volumetric average of thermal conductivities for the following mediums, air (a), water (w), ice (i), organics (o), clay and silts (c), and sands (s) as shown in.

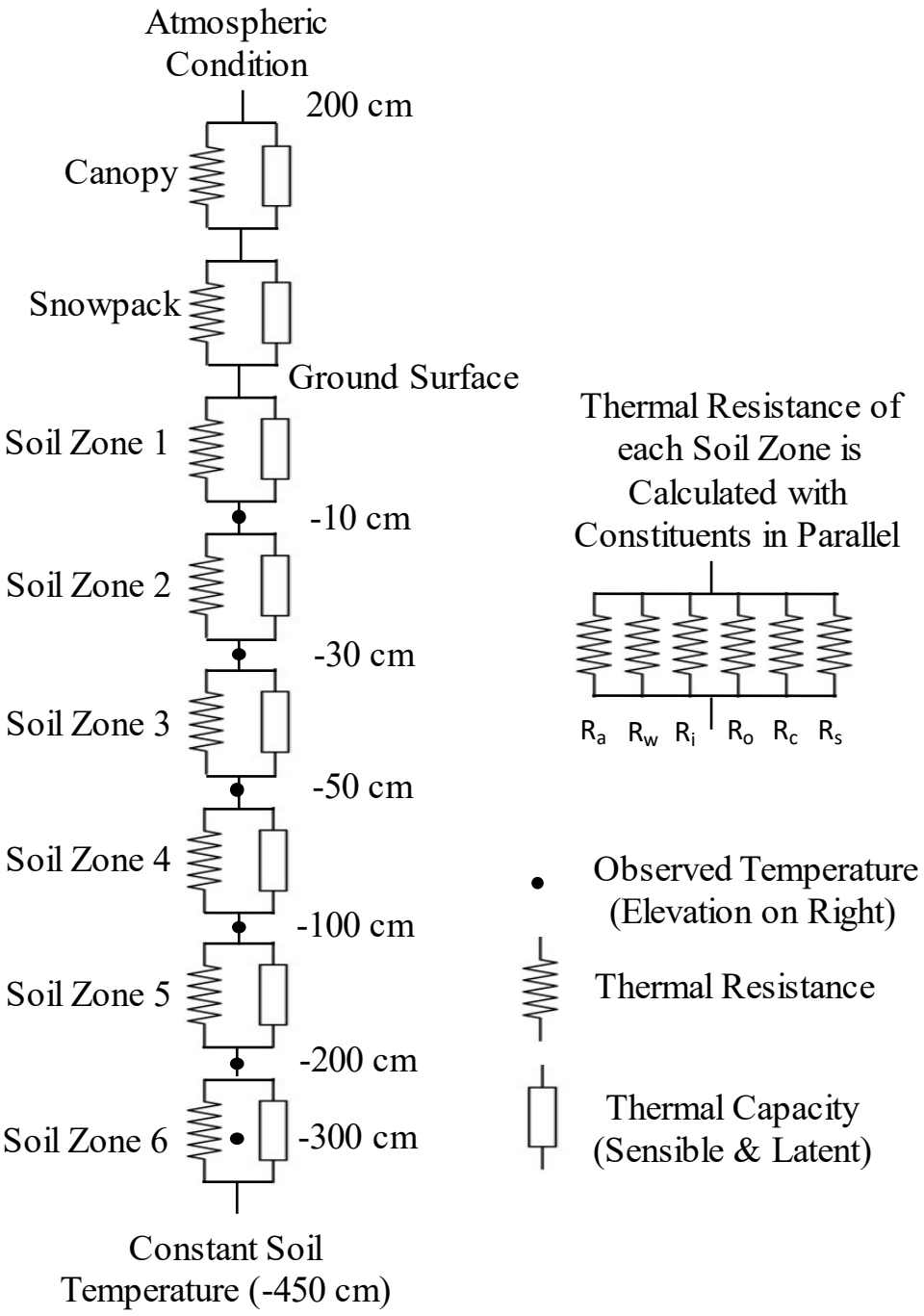

Figure 5-1 Conceptual Schematic of Thermal Simulation of Ecological Sites with Thermal Resistance of each Soil Zone Represented in Parallel and Comprised of Air (a), Water (w), Ice (i), Organic (o), Clays and Silts (c), and Sand (s) Constituents

Equation 5-1 Soil Thermal Conductivity in Parallel heat flow

$$K = x_s K_s + x_c K_c + x_o K_o + x_w K_w + x_i K_i + + x_a K_a \quad \text{.....(5-1)}$$

Where:

K_s is the thermal conductivity of the sand (8.8 W m^{-1} °C^{-1})
K_c is the thermal conductivity of the silt/clay (2.92 W m^{-1} °C^{-1})
K_o is the thermal conductivity of the organic material (0.25 W m^{-1} °C^{-1})
K_w is the thermal conductivity of the liquid soil water (0.57 W m^{-1} °C^{-1})
K_i is the thermal conductivity of the frozen soil water (ice) (2.2 W m^{-1} °C^{-1})
K_a is the thermal conductivity of the air/vapour (0.025 W m^{-1} °C^{-1})
x is the volumetric fraction of the given media (m^3 m^{-3})

It should be possible to adjust the soil zone's thermal resistance, along with volumetric and latent heat capacity, to reasonably reproduce the observed thermal profiles from the observed weather conditions. To test this approach the Simultaneous Heat and Water (SHAW) (Flerchinger 2000) model was used to determine if a set of physical parameters, for both the tree's crown and subsurface, exist in which the observed temperatures can be reasonably simulated. It should be noted that for the most part a soil zone is typically comprised of the soil interval between two probes, except for Soil Zone 6 which is interval from the -200 cm probe down to the bottom of the model at -450 cm. A slight adjustment to the zone elevations was sometimes required to ensure that each soil zone was comprised of similar soil classification types as presented in Table 3-1.

Further the ecological site models were constructed and calibrated in increasing complexity, starting with the upland pine sites, followed by the shallow peatland sites, and finishing with the deep peatland sites. At the upland sites all six soil zones were mineral soils, with a large organic matter content in zone 1. Soil zones 1 and 2 of the shallow peatland model were simulated as peat, while soil zones 1 thru 5 were peat in the deep peatland models, with the remaining zones being mineral soils.

It should be noted that the sole purpose of the SHAW simulations was to determine if there exists a representative set of physical parameters and values, which dictate the thermal conductivity and volumetric and latent heat capacities, that can reasonably reproduce the observed temperatures at each site. Note although the physical parameters and values selected will be representative, they may not provide an optimum estimation of individual properties for

the ecological sites. For instance, due to the uncertainties in soil texture the bulk density estimated during calibration reflects the soil texture specified in the model which may not be the exact conditions at the ecological site. If you were to specify the true soil texture a different bulk density value would be estimated, but both models would have the same thermal properties for the same zone due to non-uniqueness. To ensure the physical parameters being estimated were representative, maximum and minimum bounds were set during the calibration process either based upon field data collected from the FORWARD research site or from the Canadian forest and tundra mineral soils database (Siltanen et al. 1997). Not only is it possible, but highly likely that there exist multiple parameter values which produce equally reasonable results in the simulation of observed temperatures. Thus, the focus of the simulations should be on the temperature residuals and not on the estimated parameters themselves. Further studies would be required to obtain additional field measurements to reduce the uncertainty of estimated parameter values.

5.1.1 The SHAW Numerical Model

The Simultaneous Heat and Water (SHAW) model was initially developed by the United States Department of Agriculture (USDA) (Flerchinger and Saxton 1989) to simulate runoff under frozen soil conditions in northern Idaho and eastern Washington. SHAW utilizes a very detailed approach to simulate the interrelated physical processes of heat and water transfer within a freezing and thawing soil profile. Further the SHAW model was modified to include saturated soil conditions and the simulation of evapotranspiration in a multi-species plant canopy (Flerchinger and Pierson 1991, 1997; Flerchinger 2000).

The SHAW model simulates a one-dimensional vertical profile extending from the top of a plant's crown to a specified depth within the soil. The system is simulated by integrating multiple equations for the plant's vegetation, snowpack, and soil into one simultaneous solution. Interrelated heat and water fluxes are computed throughout the system and include the effects of soil freezing and thawing. Hourly outputs from the SHAW model include evaporation, transpiration, surface energy balance, water balance summary, soil frost depth, snow depth, runoff, and soil profiles of temperature, water, and ice. Detailed descriptions of the equations which represent the physical processes within the model are given in the model technical documentation (Flerchinger 2000).

The SHAW model inputs are initial conditions for snow, soil temperature, and water content profiles; hourly weather conditions (temperature, wind speed, humidity, precipitation, and solar radiation); general site information; and parameters describing the vegetative cover, snow, and soil. General site information includes slope, aspect, latitude, and surface roughness parameters. Vegetation parameters include leaf area index, plant height and biomass, leaf dimension, rooting depth, and plant resistance parameters. Input soil parameters are texture, bulk density, albedo, and coefficients for the soil water potential and water content relationship given by the Van Genuchten equation (Van Genuchten 1980). The SHAW model was used to better understand how the physical properties effecting energy transfer differ between study sites by accurately simulating observed temperatures within the soil profiles, especially during winter conditions.

5.1.1.1 Soil Energy Equations

The SHAW model uses the following state equation for the temperature distribution in the soil matrix, considering both convective heat transfer by liquid and latent heat transfer by vapor for a layer of freezing soil (Equation 5-2).

Equation 5-2 Heat Transport Process Represented by SHAW within the Soil (Flerchinger 2000)

$$C_s \frac{\partial T}{\partial t} - \rho_i L_f \frac{\partial \theta_i}{\partial t} = \frac{\partial}{\partial z}\left(k_s \frac{\partial T}{\partial z}\right) - \rho_l c_l \frac{\partial q_l T}{\partial z} - L_v \left(\frac{\partial q_v}{\partial z} - \frac{\partial \rho_v}{\partial t}\right) \quad \text{.....(5-2)}$$

Where:

C_s is the volumetric heat capacity of the soil (J kg^{-1} °C^{-1})
T is the temperature of the soil (°C)
ρ_i is the density of ice (kg m^{-3})
L_f is the latent heat of fusion (J kg^{-1})
θ_i is the volumetric ice content (m^3 m^{-3})
k_s is the soil thermal conductivity (W m^{-1} °C^{-1})
ρ_l is the density of water (kg m^{-3})
c_l is the specific heat capacity of water (J kg^{-1} °C^{-1})
q_l is the liquid water flux (m s^{-1})
L_v is the latent heat of vaporization (J kg^{-1})
q_v is the water vapour flux (kg m^{-2} s^{-1})
ρ_v is the vapour density (kg m^{-3})
z is the vertical distance (m)
t is the time (s)

Originally the SHAW model was set-up to conduct simulations assuming no-heat-flux at the lower boundary at a depth of 4.5 m. However, it soon became evident that the simulations would not be able to match observed temperatures at a depth of 3.0 m utilizing that set-up and that the lower boundary condition had to be estimated using the Force-Restore Method (FRM) (Hirota et al. 2002). The modified SHAW model used in this study estimates the lower boundary temperature using the FRM equation (Equation 5-3) at the end of each time step.

Equation 5-3 FRM to Estimate Lower Boundary Temperature (Hirota et al. 2002)

$$\left(1 + \frac{2z}{d_d}\right)\frac{\partial T}{\partial t} = \frac{2}{C_s d_d}G - \omega(T - T_{AVG}) \quad \text{.....(5-3)}$$

Where:

z is the depth below the surface of the lower boundary condition(m)
ω is the frequency of fluctuation period (diurnal or annual, s^{-1})
d_d is the dampening depth (m)
G is the vertical conductive heat flux (W m^{-2})
C_s is the volumetric heat capacity of the soil (J m^{-3} °C^{-1})
T_{AVG} is the average soil temperature (°C)
T is the temperature at depth z (°C)
t is time (s)

5.1.1.2 Snowpack Energy Equations

The primary mechanism for energy transfer within a snowpack is thermal conduction between and within ice crystals. Thermal conductivity of snow has been empirically related to density by many researchers, although geometry of the snow crystals is important as well. Equation 5-4 is the empirical equation used in the SHAW model to estimate the thermal conductivity of the snowpack.

Equation 5-4 Thermal Conductivity of the Snowpack (Anderson 1976)

$$k_{sp} = a_{sp} + b_{sp}\left(\rho_{sp}/\rho_{l}\right)^{c_{sp}} \quad \text{.....(5-4)}$$

Where:

k_{sp} is the thermal conductivity of the snow (W m^{-1} °C^{-1})
a_{sp} is the empirical coefficient (a) for the snowpack (W m^{-1} °C^{-1})
b_{sp} is the empirical coefficient (b) for the snowpack (W m^{-1} °C^{-1})
c_{sp} is the empirical coefficient (c) for the snowpack (Unitless)
ρ_{sp} is the density of the simulated snowpack (kg m^{-3})
ρ_{l} is the density of water (kg m^{-3})

5.1.2 Model Calibration

The SHAW model is physically based, therefore most of the input parameters can either be measured in the field or obtained from the literature as demonstrated in numerous studies (Flerchinger and Hanson 1989; Flerchinger and Pierson 1991; Hayhoe 1994). Initially a SHAW model had to be setup for each site with appropriate discretization and assignment of SHAW nodes to the soil and hydraulic zones based on the observed soil profiles. Then each site model was run using literature/default parameter values to ensure the model ran and produced results which could be compared to observed field measurements. Each site model was then calibrated to the observed data, both temperature and moisture content, using the automated parameter estimation software PEST (Doherty 2016).

PEST is a calibration tool that can change the parameter values of model input files and reads model output files for comparison to observed values. PEST first runs the model with the parameters initially specified and calculates the residuals from the output files and observed data. It then changes each parameter, one at a time, and reruns the model to calculate the new residual due to the change in the parameter. PEST does this for every parameter being estimated, with the parameter being set to the initial value after each sensitivity run. After PEST has determined the sensitivity of each parameter it compiles a matrix of this information to estimate the optimal change of parameter values from the initial set. PEST then repeats this entire process using the newly estimated parameters as the initial values for the sensitivity runs, with this process repeated until there is no change in residuals from one iteration to the next (Doherty 2016).

An initial set of exploratory simulations, in which almost all possible SHAW model parameters were adjusted, was performed on the upland pine sites (UPA, UPB) to determine which parameters were the most sensitive. The most sensitive parameters were then used to calibrate each of the six ecological sites, with insensitive or non-unique parameters being held constant throughout the calibration process. For example, since clay and silt have the same thermal conductivity PEST found that the model was insensitive to the ratio of clay to silt, for a soil zone with 20% clay and 80% silt would have the same thermal conductivity as 80% clay and 20% silt. Further, parameters that solely affected plant transpiration were found to have very low sensitivities, typically requiring changes so large that the model became numerically instable before it affected the residuals. The fixed parameters were either held at SHAW default values or set equal to averages of observed field values.

5.1.3 Model Parameters

The SHAW model required very fine spacing of model nodes near the ground surface due to the large daily fluctuation of temperatures and increased spacing with depth to maintain numerical stability. Due to this numerical requirement a total of 21 nodes were used to represent the 6 soil zones at each of the ecological sites. The node elevation and associated soil zone with each node are presented in Table 5-1.

During calibration PEST was set up to estimate a single parameter value for all the nodes within a soil zone and were not allowed to vary node to node but only zone to zone. This reduced the number of estimated values for any given soil parameter from 21 to 6, the same number of temperature probes, to prevent the calibration of an overfitted model. Additionally, since the primary focus of the SHAW model was to simulate temperatures, and there were only three moisture content probes, the hydraulic parameters were grouped into three zones, A, B, and C, instead of 6. As with the soil zones slight adjustments were made to the hydraulic zone's elevations to try to maintain a similar soil classification type within each zone. Thus, there are slight differences in the SHAW nodes associated with the soil and hydraulic zones between ecological sites to best represent the observed soil profiles (Table 3-1).

Table 5-1 SHAW Node Elevations with Typical Associated Soil and Hydraulic Zones

SHAW Node	Node Elevation	Soil Zones	Hydraulic Zones
1	-0.5	Zone 1	Zone A
2	-2		
3	-4		
4	-6		
5	-8		
6	-10		
7	-15	Zone 2	Zone B
8	-20		
9	-25		
10	-30		
11	-40	Zone 3	
12	-50		
13	-75	Zone 4	Zone C
14	-100		
15	-150	Zone 5	
16	-200		
17	-250	Zone 6	
18	-300		
19	-350		
20	-400		
21	-450		

5.1.3.1 Estimated Parameters

Calibration of the SHAW model consisted of three groups of sensitive parameters: 1) tree crown and surface processes; 2) soil properties; and 3) hydraulic properties. Estimated tree crown and surface process parameters that were found to be sensitive included the dry soil albedo, albedo exponent for wet soils, the albedo of the tree crown, clumping and interception. Clumping is the radiation transfer of a plant species varying from 0 to 1, with one being uniform vegetation and zero eliminating radiation interception by plants. Interception is the maximum amount of precipitation that can be intercepted and stored on the plant species per unit of leaf area index. Due to the non-uniqueness of the soil properties only the dry bulk density was estimated for each soil zone, because it is possible to have the same thermal conductivity with different

combinations of soil texture and dry bulk density. Further the dry bulk densities for each soil type were bounded by the minimum and maximum reported densities from the Canadian forest soils database (Table 5-2).

Table 5-2 Average, Maximum, and Minimum Dry Bulk Densities for Soil Types from Canadian Forest Soils Database (Siltanen et al. 1997)

	Dry Bulk Density (kg m^{-3})		
Soil Type	Average	Maximum	Minimum
2Cg	1365	1780	1010
Cg	1547	1840	950
Ah	1062	1560	570
Ae	1239	1650	200
Ae1	1248	1420	580
Ae2	1299	1540	580
Aegj	1232	1460	660
AB	1371	1630	300
Bg	1469	1560	1200
Bt	1458	1730	490
Btg	1530	1900	1390
BC	1424	1710	290
BC1	1343	1530	740
Of	114	178	50
Om	144	340	50
LFH	144	1510	50

For the hydraulic properties the variables of the Van Genuchten equation were estimated, which included the saturated and residual moisture contents, saturated hydraulic conductivity, and the empirical exponents α, and n for each of the three hydraulic zones at each site. Maximum and minimum bounds for the hydraulic properties for the mineral soils were set to prevent numerical instability (Ippisch et al. 2006) and were reasonable for the given soil textures (Ghanbarian-Alavijeh et al. 2010). The hydraulic properties for the peat were bounded at the range of observed values from laboratory experiments and field data (Schwärzel et al. 2006). In addition, the average temperature (°C) at the dampening depth for the lower boundary condition was also included in the crown surface parameter group because it is typically set to the average ground surface temperature but was estimated by PEST during calibration.

5.1.3.2 Fixed Parameters

In the initial exploratory analysis estimation of the percent sand, silt, and clay resulted in non-uniqueness and issues with calibration. While there was no texture analysis specifically performed at any of the six ecological sites, there was numerous results from within the FORWARD research site for similar soil types. The percent mass could then be calculated from the average percent sand, silt, and clay from FORWARD's texture analysis (Table 3-2) using a typical organic matter (OM) content, assumed to be approximately 60% of the average OM content reported in the Canadian forest soils database (Siltanen et al. 1997), with the exception of the peat which was assumed to have no mineral soil content (Table 5-3). These mass averages were held constant in PEST throughout the calibration process and did not vary between ecological sites.

Table 5-3 Average FORWARD Mass Percentages for Sand, Silt, and Clay based upon Typical Organic Matter Content (OM) by Soil Type

Type	Soil	Clay %	Sand %	Silt %	OM %
2Cg	Clay Loam	30.3	32.6	35.9	1.2
Cg	Loam	24.7	32.1	42.4	0.9
Ah	Loam	15.6	34.3	45.1	4.9
Ae	Loam	21.4	34.6	42.6	1.3
Ae1	Silty Loam	11.2	35.0	52.7	1.2
Ae2	Loam	21.0	38.4	40.0	0.5
Aegj	Loam	19.2	34.2	45.4	1.2
AB	Loam	22.5	33.1	43.7	0.7
Bg	Loam	20.2	33.0	45.3	1.6
Bt	Clay Loam	32.7	29.9	36.7	0.7
Btg	Loam	26.3	32.7	40.4	0.6
BC	Clay Loam	30.6	32.7	35.9	0.7
BC1	Clay Loam	34.8	29.8	34.8	0.6
Of	Organic	0.0	0.0	0.0	100
Om	Organic	0.0	0.0	0.0	100
LFH	Organic	13.5	22.3	31.8	32.4

Additionally, as discussed previously the following parameters were found to be either insensitive or often resulted in numerical instability due to empirical equations requiring a very narrow range of values, thus their values were also held constant during the calibration process

(Table 5-4). The SHAW default values for a coniferous tree were used and were not altered during the calibration or differed site to site. While it is expected that there would be differences in values between a black spruce tree and a lodgepole pine, it is highly unlikely it would be large enough to have any affect on simulated temperatures.

Table 5-4 Parameters Held Constant in PEST to SHAW Default Values for Coniferous Trees (Flerchinger 2000)

Parameter Name	Value	Units
Wind-profile surface-roughness for momentum transfer (Soil)	0.66	cm
Wind-profile surface-roughness for momentum transfer (Snow)	0.15	cm
Coefficient for water potential of dead plant material	-53.72	m
Exponent for water potential of dead plant material	1.32	
Stomatal resistance of plant species with no water stress	100	$s\ m^{-1}$
Empirical exponent relating actual stomatal resistance to leaf potential	5	
Critical leaf water potential at which stomatal resistance is double	200	m
Resistance of leaves for plant species	33000	$m^3\ s\ kg^{-1}$
Resistance of roots for plant species	66000	$m^3\ s\ kg^{-1}$
Leaf area index of plant species	2.35	

5.1.4 Model Targets

PEST used both subsurface temperatures and moisture contents as target observations to calibrate the model. Due to differences in the temperature fluctuations, with diurnal changes observed near the surface but with only seasonal changes at depth, different averaging periods were used to develop targets. For the -10 cm, -30 cm, and -50 cm soil temperatures a daily average was used, while a weekly average was used for the -100 cm, -200 cm, and -300 cm elevations. Different target weights were used to accommodate the difference in periods, with a weight of 1 for the shallow daily averaged targets and a weight of 7 for the deeper weekly average targets.

Similarly different averaging periods were used for the moisture content targets, with a daily average implemented for the -10 cm observed moisture contents and a weekly average used for -50 cm and -100 cm. A weekly average value was used for the -50 cm and -100 cm since there seemed to be little variation in moisture contents, even seasonal, due to those depths often being saturated. The weights used for the moisture content targets were 1 for the daily averaged values, and 7 for the weekly averaged values. It should be noted that a moisture content residual

(observed value minus simulated value) of 0.10 m^3 m^{-3} would be equivalent to a temperature residual of 0.1 ºC. Thus, by design the PEST calibration was heavily weighted to match the observed temperatures and would likely result in hydraulic properties being estimated that differ for actual site values. However, the purpose of the SHAW simulations is to determine if there is any plausible parameter set that can reasonable match observed temperatures and not simulate flow. Further, because the SHAW model is a 1-D vadose model, certain hydraulic properties require unrealistic values to simulate saturation at depth.

5.1.5 FORWARD Weather Station Data

A weather station was operated by the FORWARD research group within the same watershed as deep peatland A (DPA), collecting measurements every 10 minutes (Figure 3-2). The SHAW model requires hourly inputs of air temperature, wind speed, relative humidity, precipitation, and incoming solar radiation. For the purposes of plotting, the data were grouped by simulation year, which is October 1 to September 30, thus the weather input data for 2009 would be October 1, 2008 to September 30, 2009.

Observed temperatures ranged from a maximum of 29.3 ºC on July 25, 2009 to a minimum of -41.5 ºC on March 10, 2009. October 1, 2008 was selected as the start date for the SHAW simulations because temperatures at the start should have been below freezing for an extended period (Figure 5-2). September also experienced periods of freezing temperatures but any frost that did form would have thawed within a day or two. Temperatures during the winter of 2010 were not nearly as cold as in 2009 and 2011, especially for February and March, while temperatures were a lot warmer for March of 2010 compared to other years.

A maximum windspeed of 3.6 m s^{-1} was observed on May 15, 2011and there were over 1,000 hours of no detectable windspeed during the model simulation period, October 1, 2008, to June 30, 2011. March, April, and May tended to be windier than the other months with April of 2010 being the windiest (Figure 5-3). December and January of simulation year 2010 had the lowest median wind speeds. Relative humidity tended to be higher in the winter becoming drier in the spring and rising again in the summer (Figure 5-4).

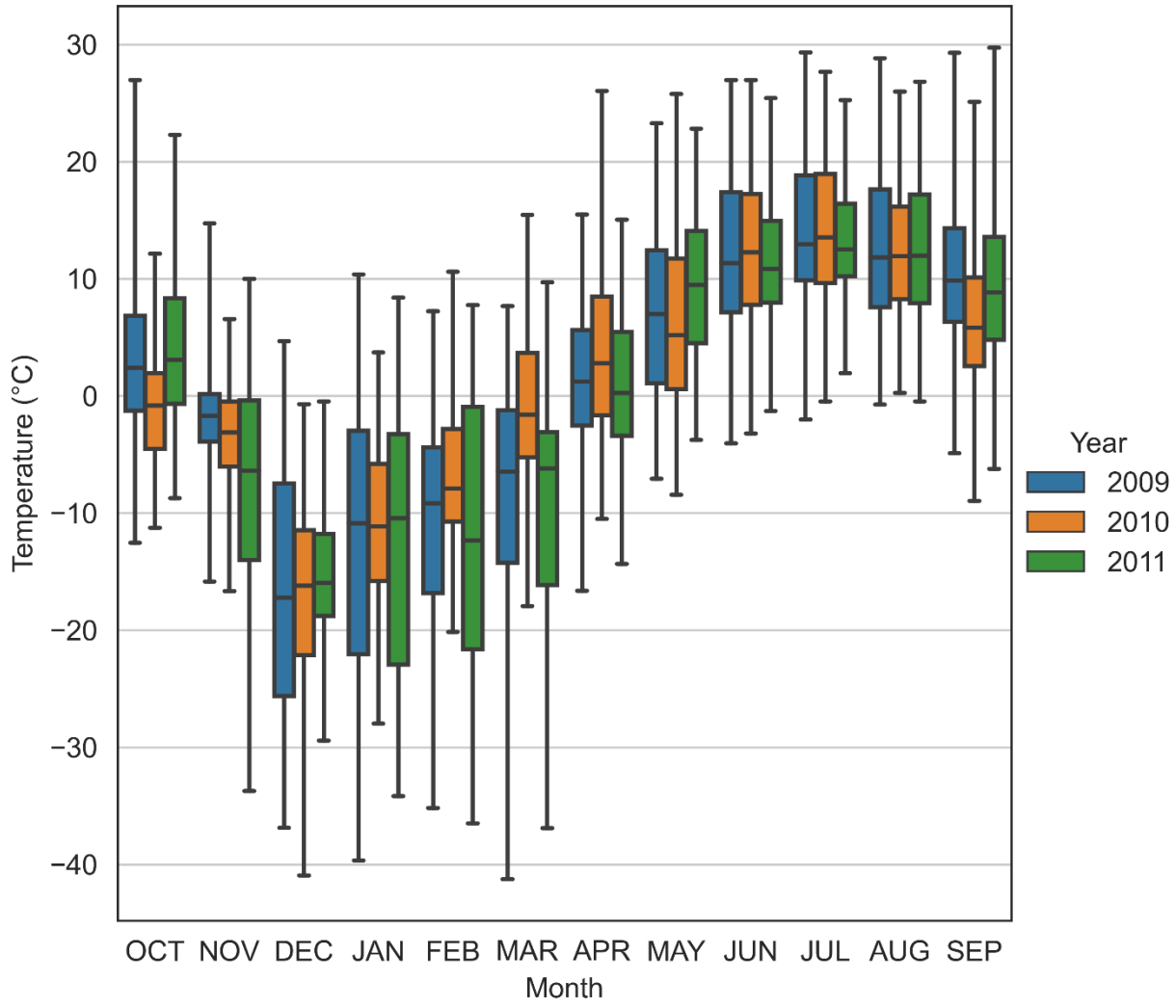

Figure 5-2 Observed Average Hourly Temperatures from the FORWARD Weather Station within DPA's Watershed used for SHAW by Simulation Year (Whiskers Maximum/Minimum)

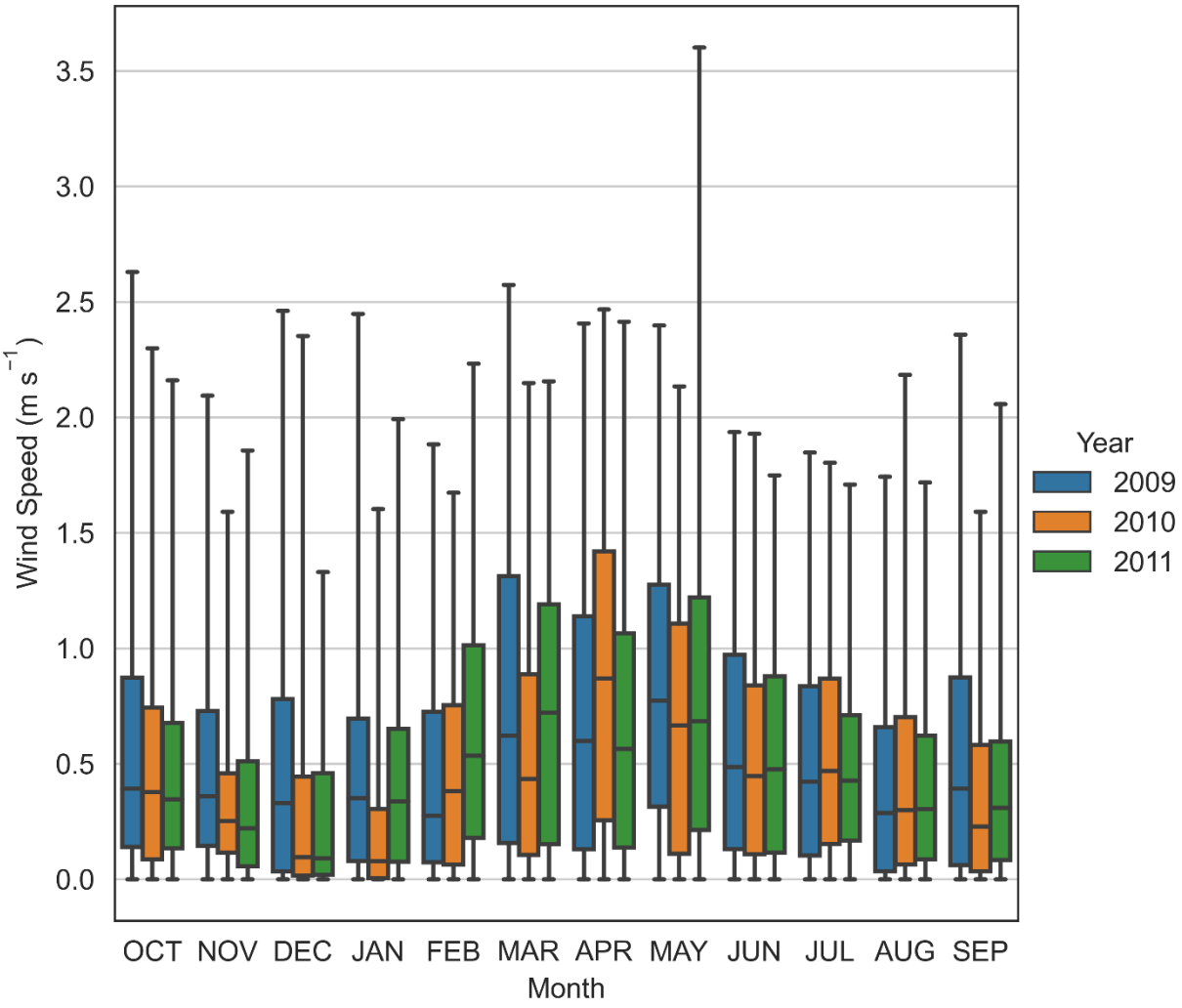

Figure 5-3 Observed Wind Speed from the FORWARD Weather Station within DPA's Watershed used for SHAW Simulations by Simulation Year (Whiskers Maximum/Minimum)

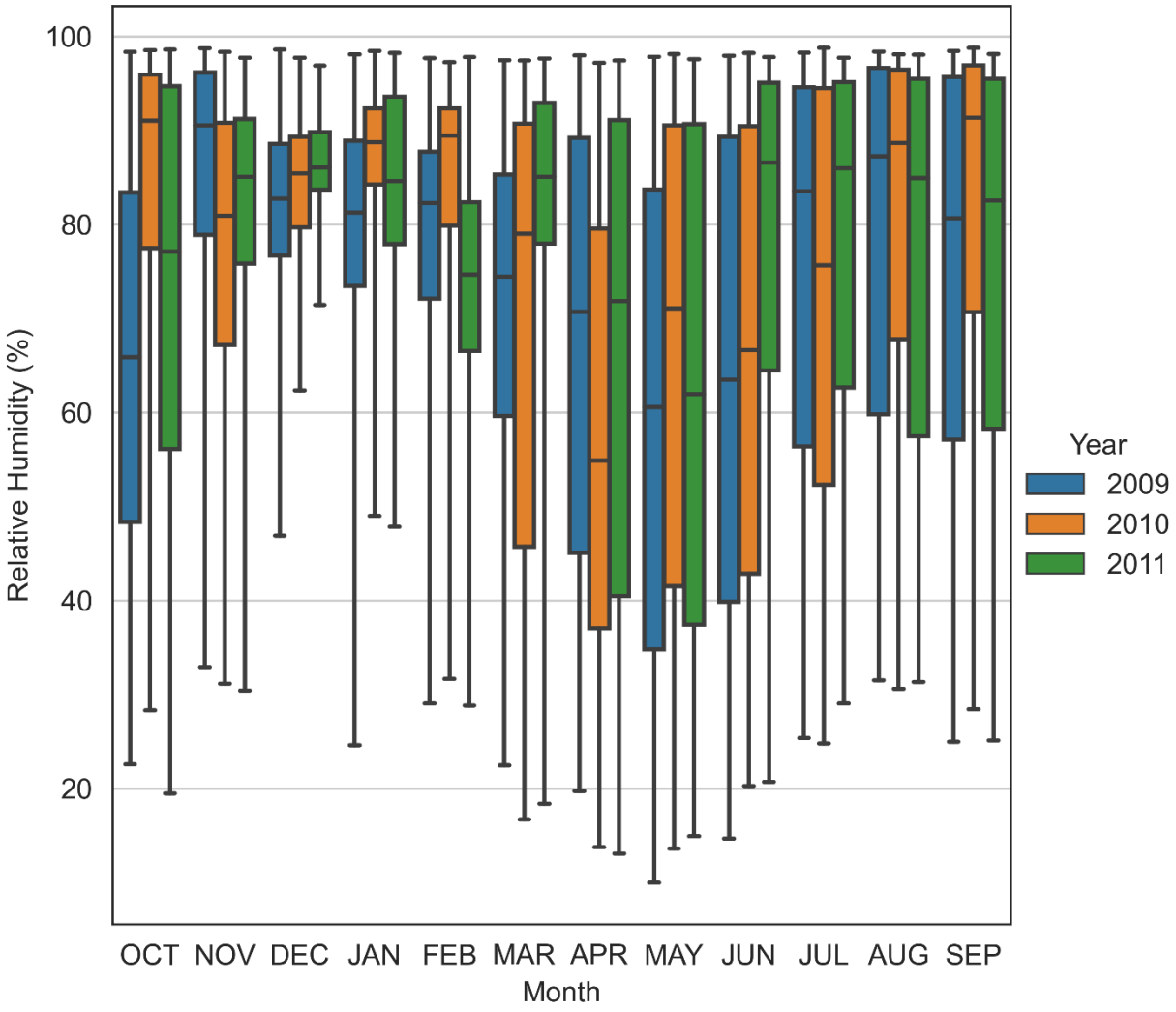

Figure 5-4 Observed Relative Humidity from the FORWARD Weather Station within DPA's Watershed used for SHAW by Simulation Year (Whiskers Maximum/Minimum)

Total precipitation by simulation year ranged from 329 mm in 2009 to 499 mm in 2011, with 425 mm observed in the 2010 simulation year. Precipitation also varied monthly, with June of 2011 being the wettest month with 128.5 mm of recorded rainfall (Figure 5-5). The high amount of rainfall in mid-June 2011, with 15.7 mm on June 19 followed by 24.1 mm on June 23, with 18.3 mm occurring during a two-hour period, resulted in numerical instability during calibration. Due to these issues these observed rainfall events were removed from the SHAW input files and the model simulation was terminated on June 30, 2011, instead of September 30, 2011. The November of the 2010 simulation year was extremely wet with 50 mm compared to 12 and 28 mm in 2009 and 2011 respectively followed by a very dry winter with 23 mm of precipitation for

January, February, and March combined. It was this reason that observed subsurface temperatures, especially at SPB (Figure 3-6, Figure 3-7), was much colder even though observer air temperature were warmer due to the saturated surface conditions with minimal snowpack.

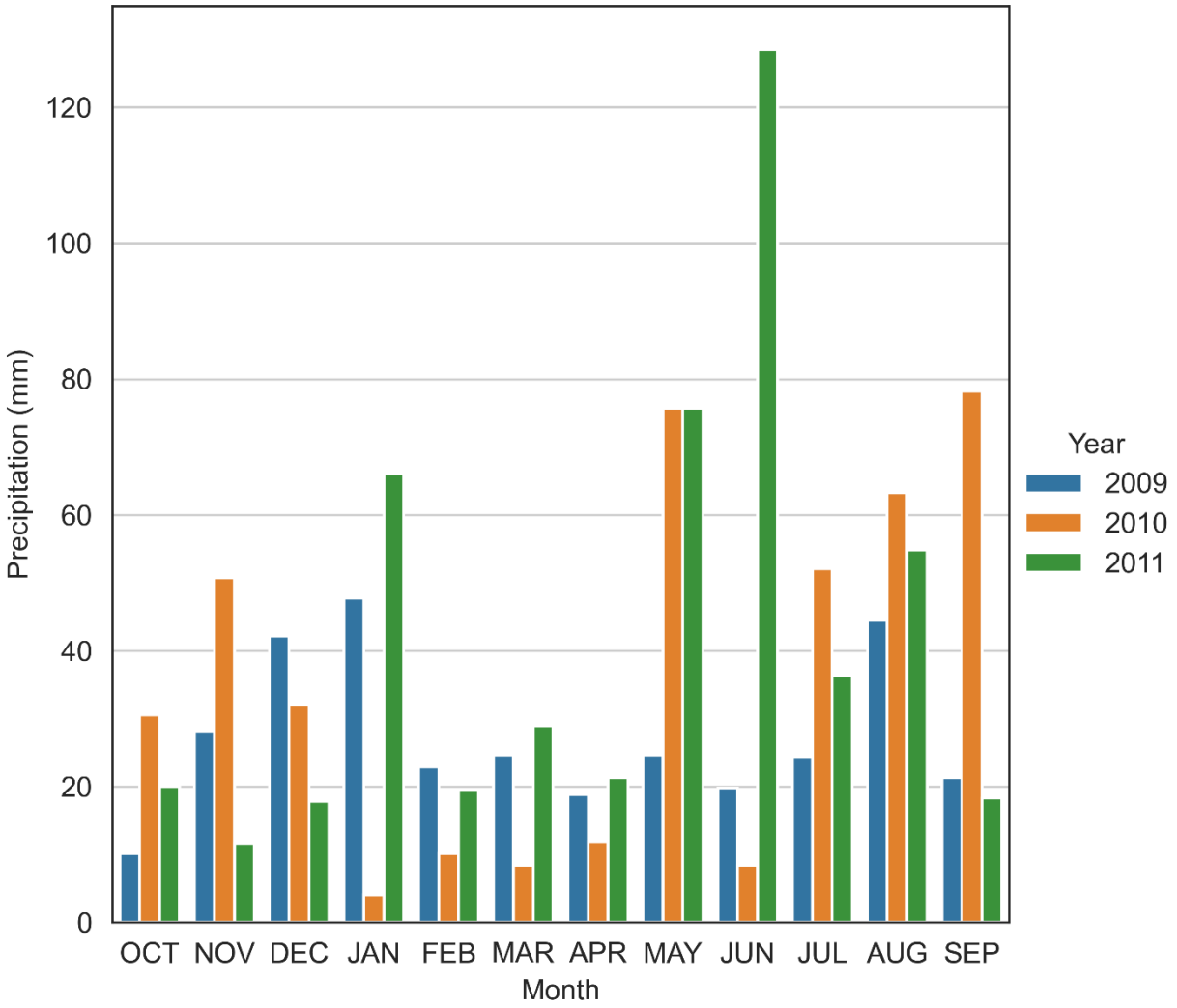

Figure 5-5 Observed Total Monthly Precipitation from the FORWARD Weather Station within DPA's Watershed used for SHAW Simulations

The maximum observed incoming solar radiation was 737 W m^{-2} on July 2, 2009, with 1900 total observed hours during the model simulation with solar radiation greater than 400 W m^{-2}. In comparison the maximum daily solar radiation would barely ever be exceeded 100 W m^{-2} in January and 300 W m^{-2} in February (Figure 5-6). It wasn't until March that there is an appreciable increase in incoming solar radiation with average midday fluxes reaching 400 W m^{-2} in April.

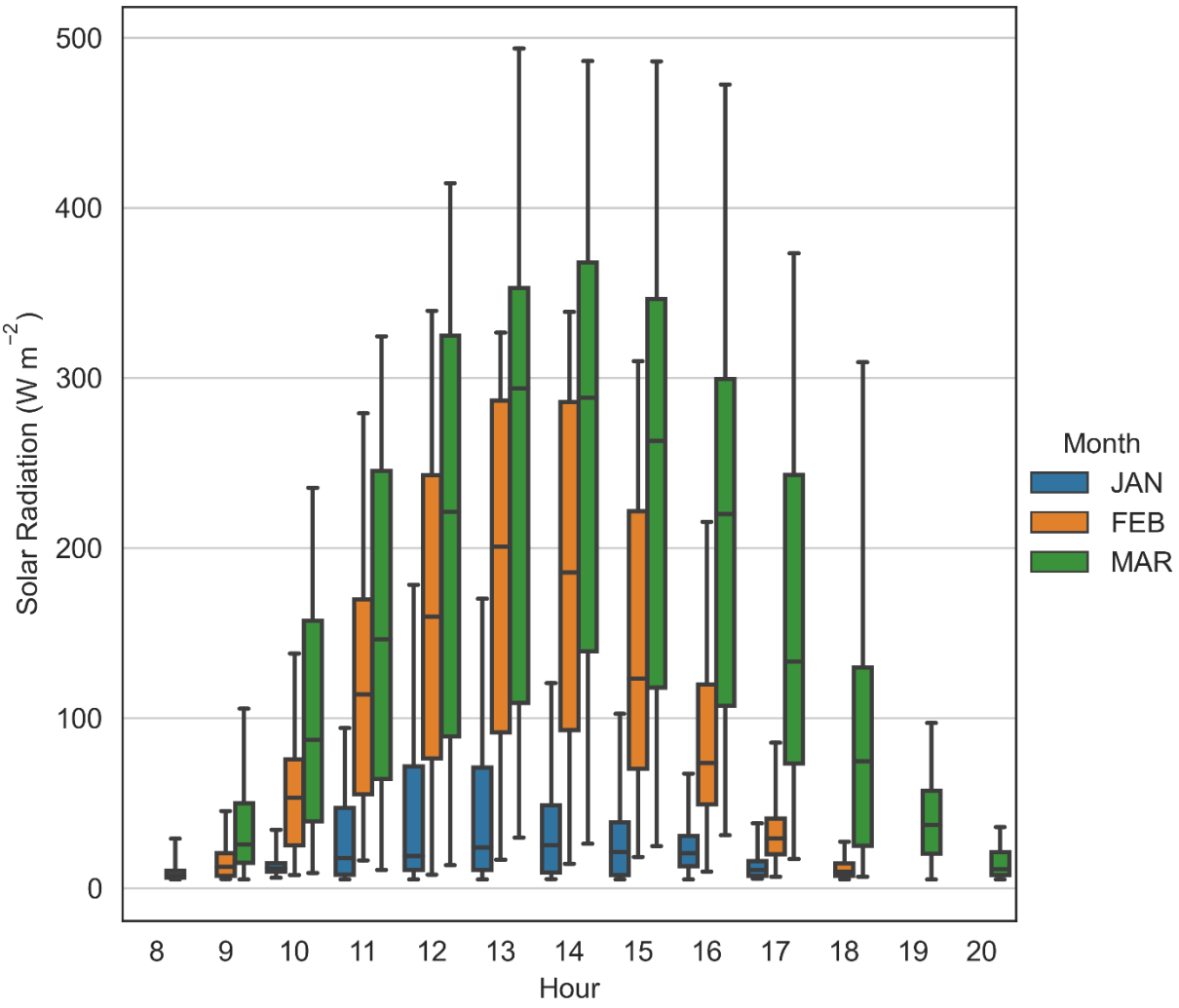

Figure 5-6 Observed Hourly Average Solar Radiation During Winter Months from the FORWARD Weather Station within DPA's Watershed used for SHAW Simulations (Whiskers Maximum/Minimum)

5.2 Numerical Simulation Results

This section presents the calibrated results of the SHAW numerical model for each of the six ecological sites for subsurface temperatures, moisture contents, and estimated parameters.

5.2.1 Subsurface Temperature -10 cm

The SHAW model was able to reasonably simulate average daily temperatures at -10 cm at all the pine sites, which include the upland sites (UPA, UPB) and the shallow peatland site (SPB) for the entire three years of simulations (Figure 5-7). The observed 2010 winter temperatures at SPB were often -5 ºC colder than simulated and was likely due to the surface being flooded in the vicinity of the temperature probe resulting in a higher thermal conductivity from the ice. The SHAW model had difficulty simulating the observed wintertime temperatures at all the black spruce peatlands, but especially at the deep peatland sites (DPA, DPB). Simulated temperatures at the deep peatland sites were often 5 ºC colder than observed temperatures. Therefore, the SHAW model unable to reasonably simulate wintertime temperatures at -10 cm.

5.2.2 Subsurface Temperature -30 cm

The SHAW model was able to reasonably match observed daily average temperatures at -30 cm for all the upland and shallow peatland sites, except for the deep freeze experienced at SPB in 2010 likely due to surface flooding (Figure 5-8). Again, the SHAW model could not simulate winter temperatures at -30 cm at the deep peatland sites, with simulated temperatures often below freezing while the observed were above freezing. However, the SHAW model was able to reasonably simulate observed temperatures throughout the rest of the year at the deep peatland sites.

5.2.3 Subsurface Temperature -50 cm

Like the -30 cm simulations, the SHAW model was able to simulate daily average temperatures at all the upland pine sites and shallow peatland sites comparable to observed temperatures (Figure 5-9). The deep freeze observed at SPB during the 2010 winter was no longer evident at -50 cm likely due to the transition to a mineral soil. The SHAW model still simulated temperatures at -50 cm colder than the observed winter temperatures at the deep peatland sites, with simulated temperatures below 0 ºC at DPA for winter 2011.

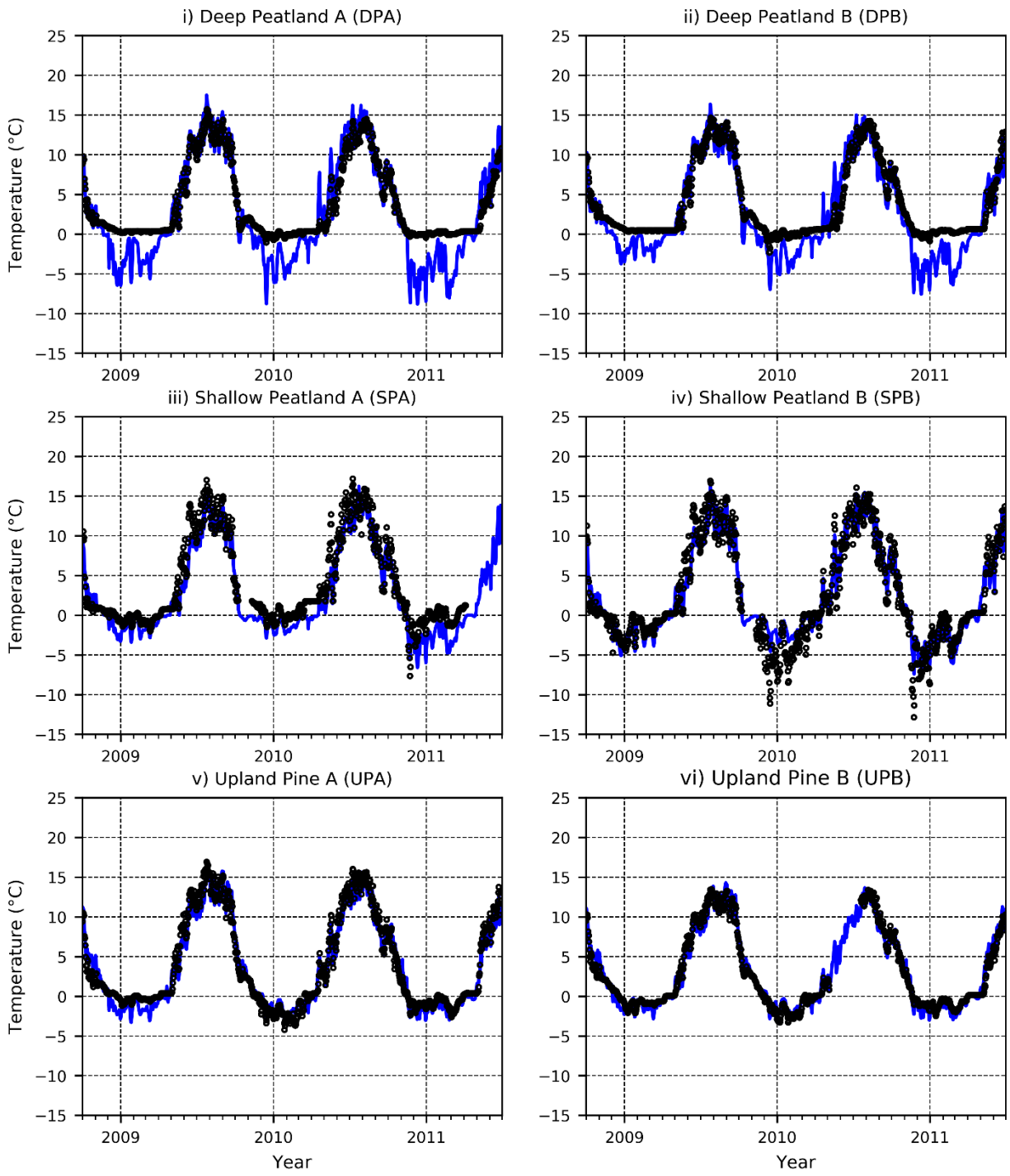

Figure 5-7 Observed (Black Circle) and Simulated (Blue Line) Daily Average Temperatures at -10 cm for each of the Six Ecological Sites

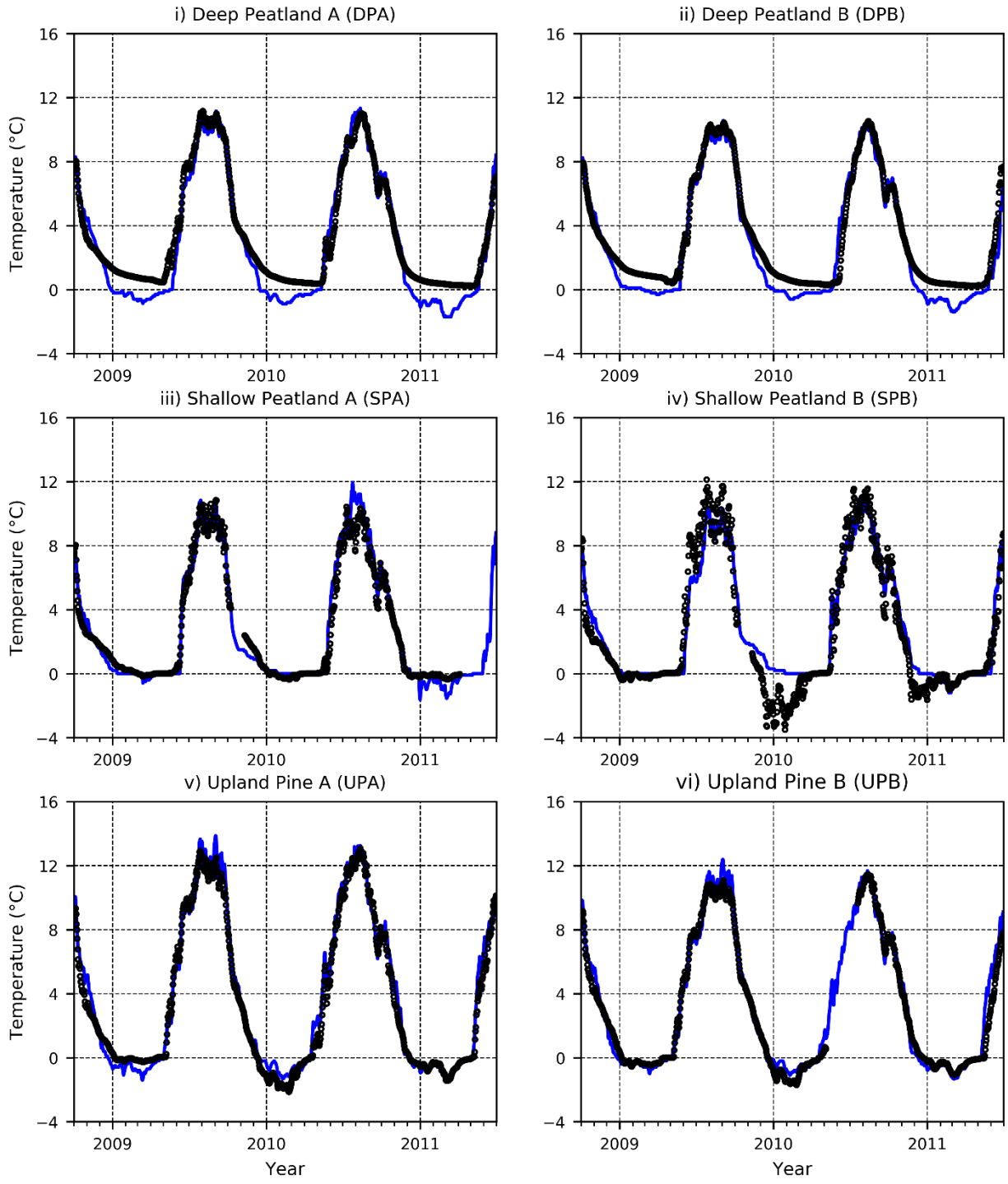

Figure 5-8 Observed (Black Circle) and Simulated (Blue Line) Daily Average Temperatures at -30 cm for each of the Six Ecological Sites

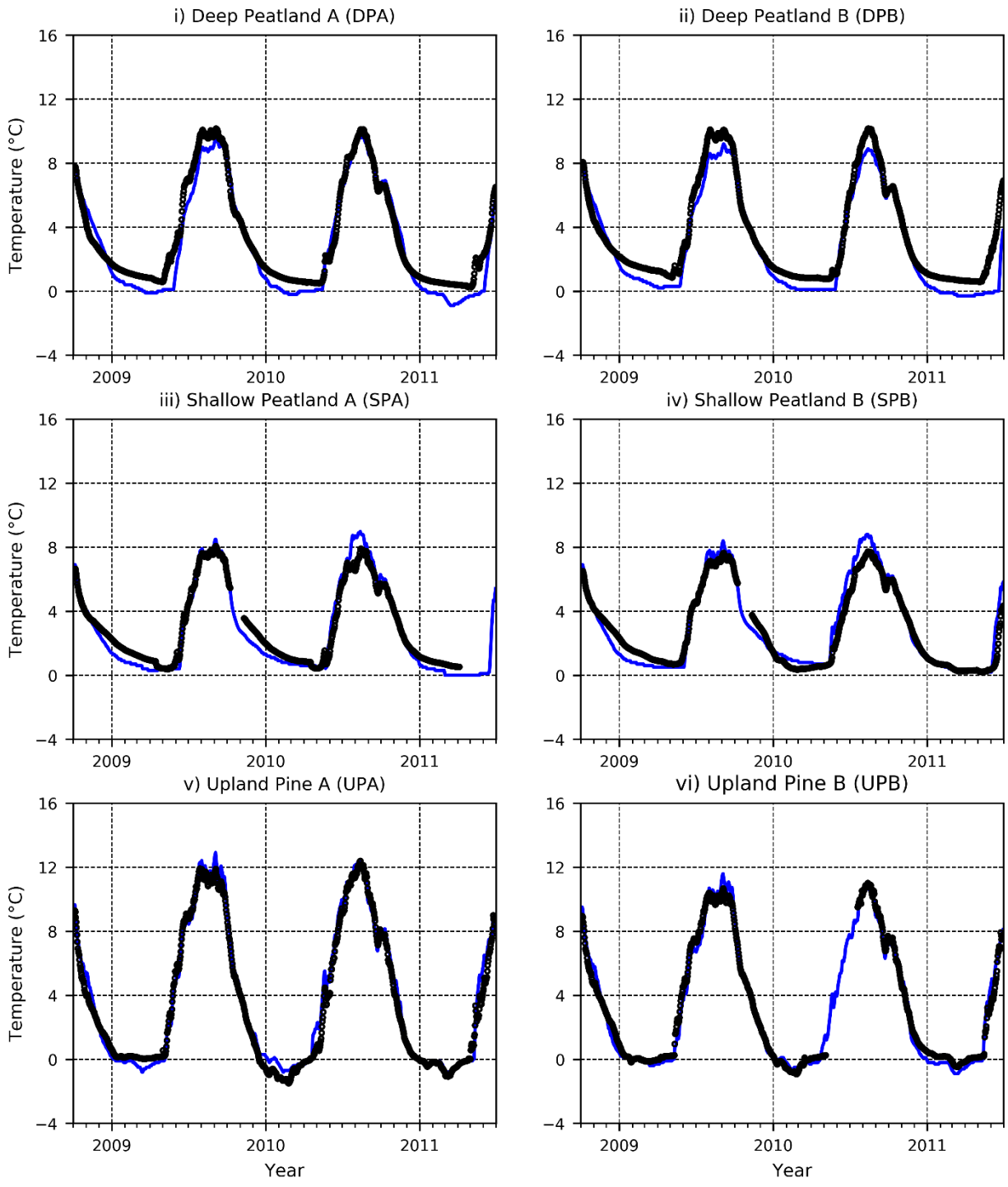

Figure 5-9 Observed (Black Circle) and Simulated (Blue Line) Daily Average Temperatures at -50 cm for each of the Six Ecological Sites

5.2.4 Subsurface Temperature -100 cm

At an elevation of -100 cm, the SHAW model simulated reasonably well weekly average temperatures at all the ecological sites with a few exceptions (Figure 5-10). PEST failed to calibrate to observed temperatures at the deep peatland sites, especially in 2011, with a slightly better result at DPA in 2009. The SHAW model had a poor match to the observed temperatures at SPB in 2010 due to the observed deep freeze as discussed previously. The SHAW model overpredicted the amount of cooling that occurred during this period with temperatures almost 1 ºC cooler than observed. The difference in the amplitude in yearly temperature change between the upland, shallow peatland, and deep peatland sites is related to the thermal capacity and thermal conductivity. The greatest amplitude in temperature was observed at the upland pine sites, with temperatures ranging from approximately 10 ºC to slightly below freezing at 0 ºC. The large amplitude in temperatures observed at the upland sites was expected due to the reduced thermal capacity from lower moisture contents and the increased thermal conduction of mineral soil particles.

In comparison, the annual change in temperatures in the shallow peatlands was approximately 5 ºC, roughly half the amplitude observed at the upland sites. The reduced yearly change in temperatures at the shallow peatlands was a result of the increased thermal capacity from the higher moisture contents and saturated conditions. The deep peatlands had an annual change in temperatures of approximately 7 ºC, a few degrees less than the upland sites but still more than the shallow peatland sites. Even though deep peatland sites had higher moisture contents, with most of the vertical profile completely saturated, the bulk density of the peat is almost an order of magnitude less than the mineral soils resulting in a lower thermal capacity.

5.2.5 Subsurface Temperature -200 cm

The SHAW model simulated reasonably well weekly average temperatures at all the ecological sites at an elevation of -200 cm (Figure 5-11). The simulated results are nearly identical to observed results at both the upland pine sites, and at shallow peatland A. The simulated temperatures at both the deep peatlands begin slightly warmer than observed temperatures, but after the summer of 2009 the simulated winter temperatures were cooler. The annual amplitude of temperature fluctuation was similar between the deep and shallow peatlands of approximately 3 ºC with the deep peatlands now having a slightly larger amplitude. The change in yearly

temperatures at the upland sites were slightly over double the peatland sites, with an amplitude over of 6 ºC.

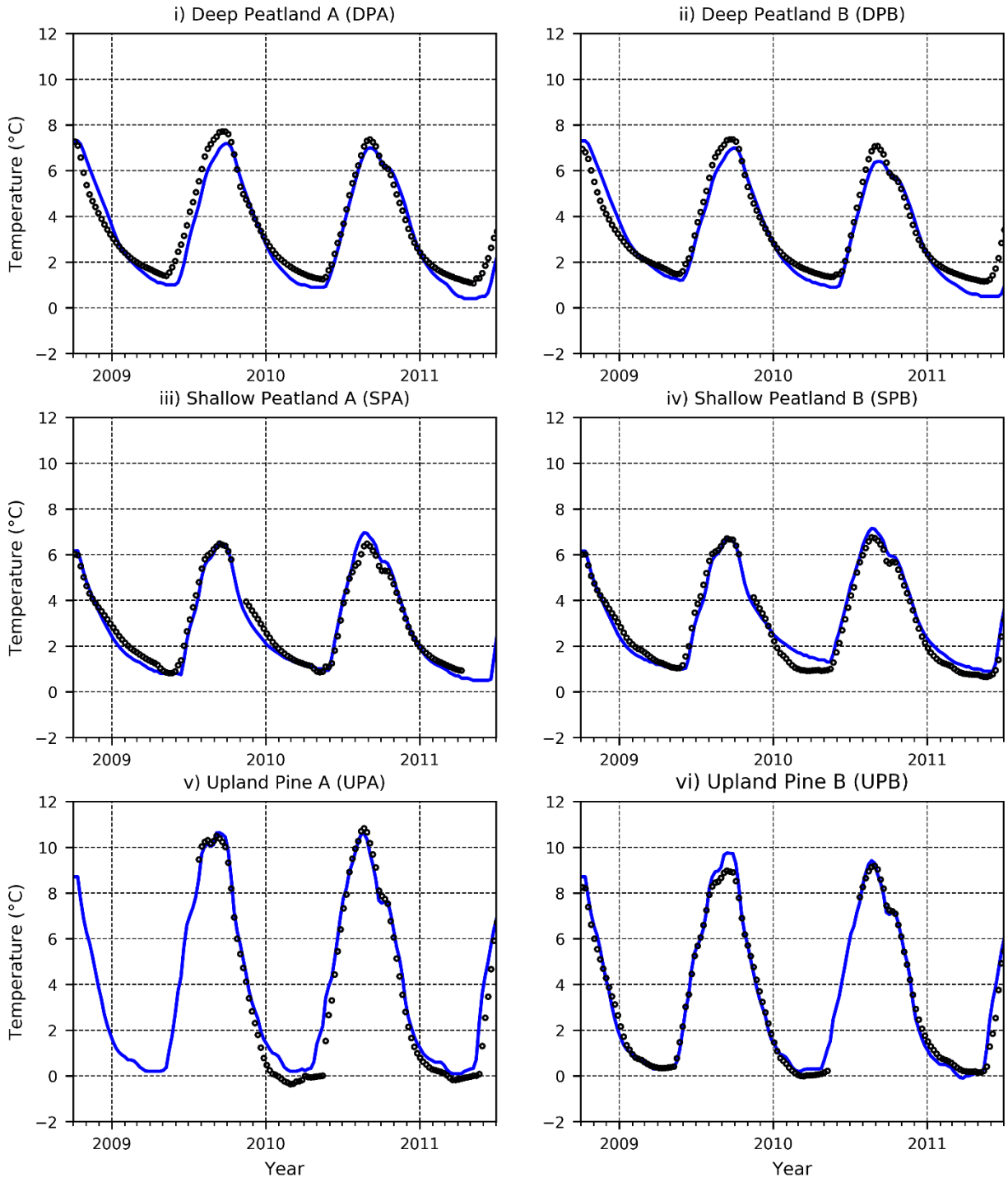

Figure 5-10 Observed (Black Circle) and Simulated (Blue Line) Weekly Average Temperatures at -100 cm for each of the Six Ecological Sites

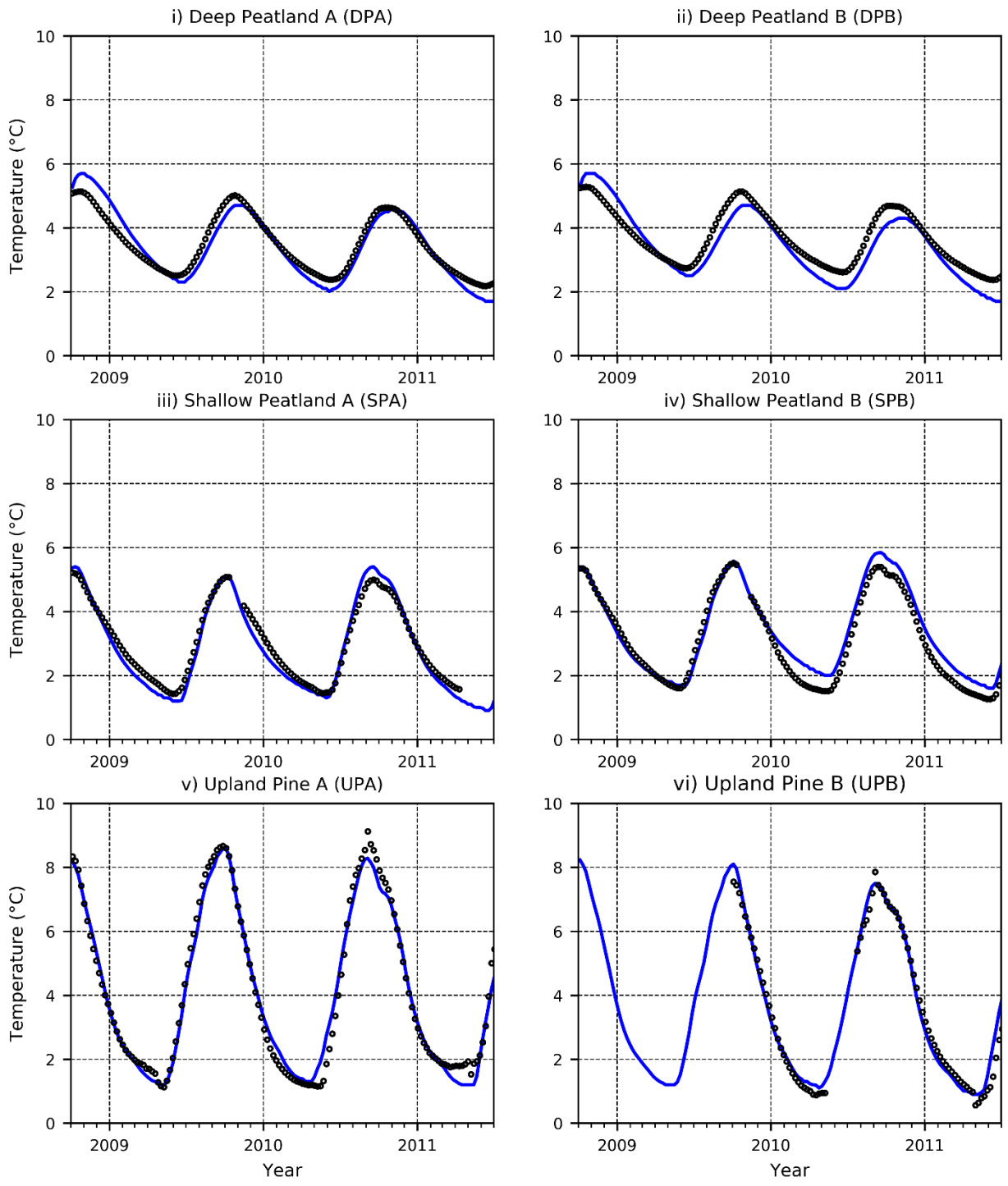

Figure 5-11 Observed (Black Circle) and Simulated (Blue Line) Weekly Average Temperatures at -200 cm for each of the Six Ecological Sites

5.2.6 Subsurface Temperature -300 cm

The calibration to observed weekly average temperatures at -300 cm was slightly worse than at -200 cm, especially at deep peatland B and shallow peatland B (Figure 5-12). The simulated temperatures at DPB begin to underpredict observed temperatures in the late summer to fall in 2010 and 2011, while at SPB observed temperatures were colder than observed starting in 2010. The simulated and observed temperatures at DPA, SPA, UPA, and UPB were reasonably well correlated. At an elevation of -300 cm both the deep peatlands had the smallest annual change in temperature of approximately 1 ºC due to the probes being in mineral soils with a higher bulk density and the large volume of water overlying the sensor. The amplitude of annual temperature change at the shallow peatlands was double that of the deep peatlands of roughly 2 ºC, with the upland site's amplitude being double that of the shallow peatlands at slightly over 4 ºC

5.2.7 Subsurface Moisture Contents -10 cm

PEST had difficulty calibrating to the daily average observed moisture contents at -10 cm, especially the fluctuations due to precipitation events (Figure 5-13). The observed increases in moisture content due to precipitation were negligible at the four peatland sites, with the main change in moisture occurring during the winter due to freeze/thaw. The only exception was at DPA which had an observed flooding event in the spring of 2009, and again in 2011. The reason for the lack of increased moisture contents with rainfall at the peatland sites was likely due to the placement of the probes in elevated hummocks that are disconnected from the water table. Due to the questionable reliability of the data, the moisture content targets for -10 cm were weighted very low with the calibration focused on temperatures in the shallow subsurface. Even at the upland sites, the timing of the observed moisture increases did not correlate well with precipitation events, and again was likely due to surface flooding.

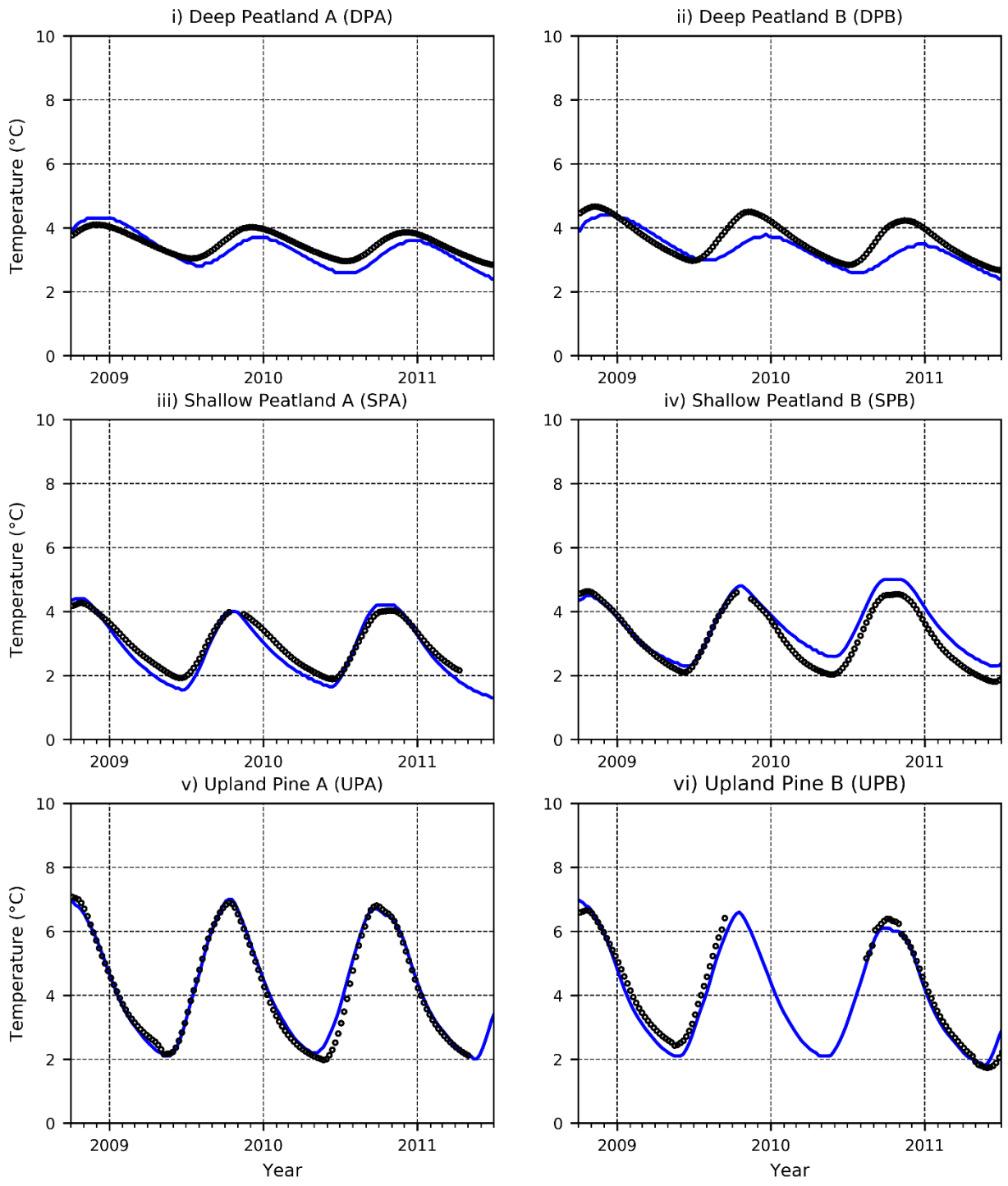

Figure 5-12 Observed (Black Circle) and Simulated (Blue Line) Weekly Average Temperatures at -300 cm for each of the Six Ecological Sites

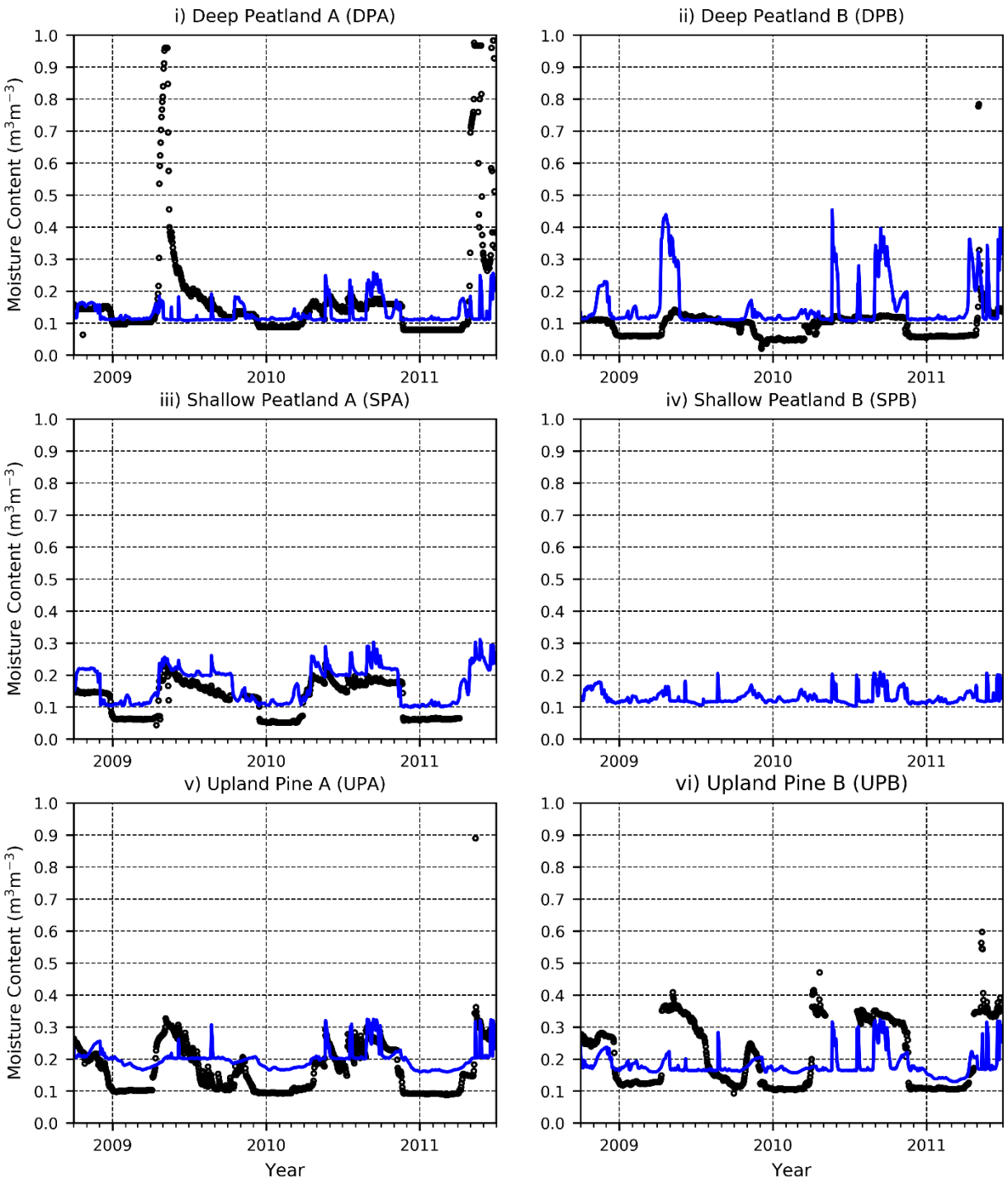

Figure 5-13 Observed (Black Circle) and Simulated (Blue Line) Daily Average Moisture Contents at -10 cm for each of the Six Ecological Sites

5.2.8 Subsurface Moisture Contents -50 cm

PEST again had difficulty simulating the weekly average observed moisture contents at the shallow and deep peatlands with large fluctuations in the simulated moisture contents (Figure 5-14). The observed moisture contents had very little fluctuation due to the probe being very near or below the water table. PEST would estimate hydraulic parameters in the peatlands that would result in a draining of the surface layers to increase insulation during the winter. Even though water has a large thermal capacity, once it freezes the thermal conductivity is over triple that of water, resulting in an increased loss of heat. Thus, PEST estimated hydraulic properties that will result in lower thermal conductivities in the shallow subsurface from lower moisture contents, rather than ones that will result in matching the observed moisture contents.

Some hydraulic properties were estimated outside reasonable bounds, such as the saturated moisture content at both the shallow peatlands with over 50% in mineral soils while the saturated moisture content at SPA was observed to be roughly at 35%. This was allowed as it was more important to simulate the average moisture content to allow for a better estimation of thermal conductivity than ensuring the estimated hydraulic parameters were reasonable. SHAW accurately simulated moisture contents at the two upland sites with reasonable hydraulic properties since there was no issue in matching observed temperatures in the shallow subsurface.

5.2.9 Subsurface Moisture Contents -100 cm

All the moisture content probes at -100 cm in the peatlands and likely in the uplands were below the water table, as illustrated by the weekly averages in Figure 5-15. However, since the SHAW model assumes the water table will be below the simulated depth with gravity driven drainage assigned to the lower boundary condition it was necessary to assign unreasonably high residual moisture contents. This allowed the SHAW model to simulate moisture contents very close to saturation by preventing drainage through the lower boundary condition and is a recommended practice described in the user manual (Flerchinger 2000). Since the main purpose of the numerical simulations is to simulate temperature profiles and better understand thermal properties it is more important that the model simulates accurate moisture contents versus water budgets and fluxes. Due to the fact saturated and residual moisture contents were set slightly above and below the observed values, the SHAW model was able to accurately simulate moisture contents at -100 cm and presumably to the bottom of the model at -450 cm.

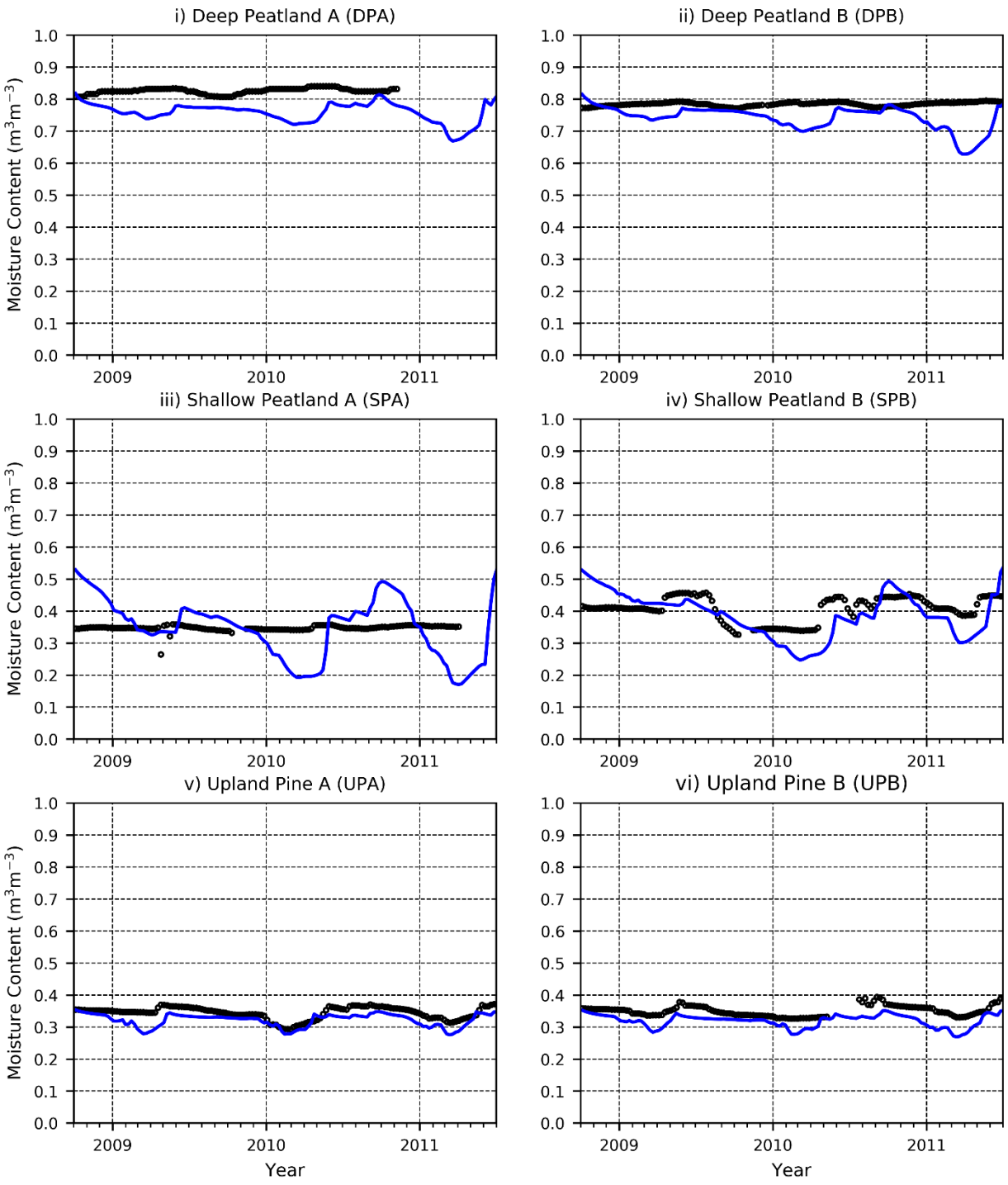

Figure 5-14 Observed (Black Circle) and Simulated (Blue Line) Weekly Average Moisture Contents at -50 cm for each of the Six Ecological Sites

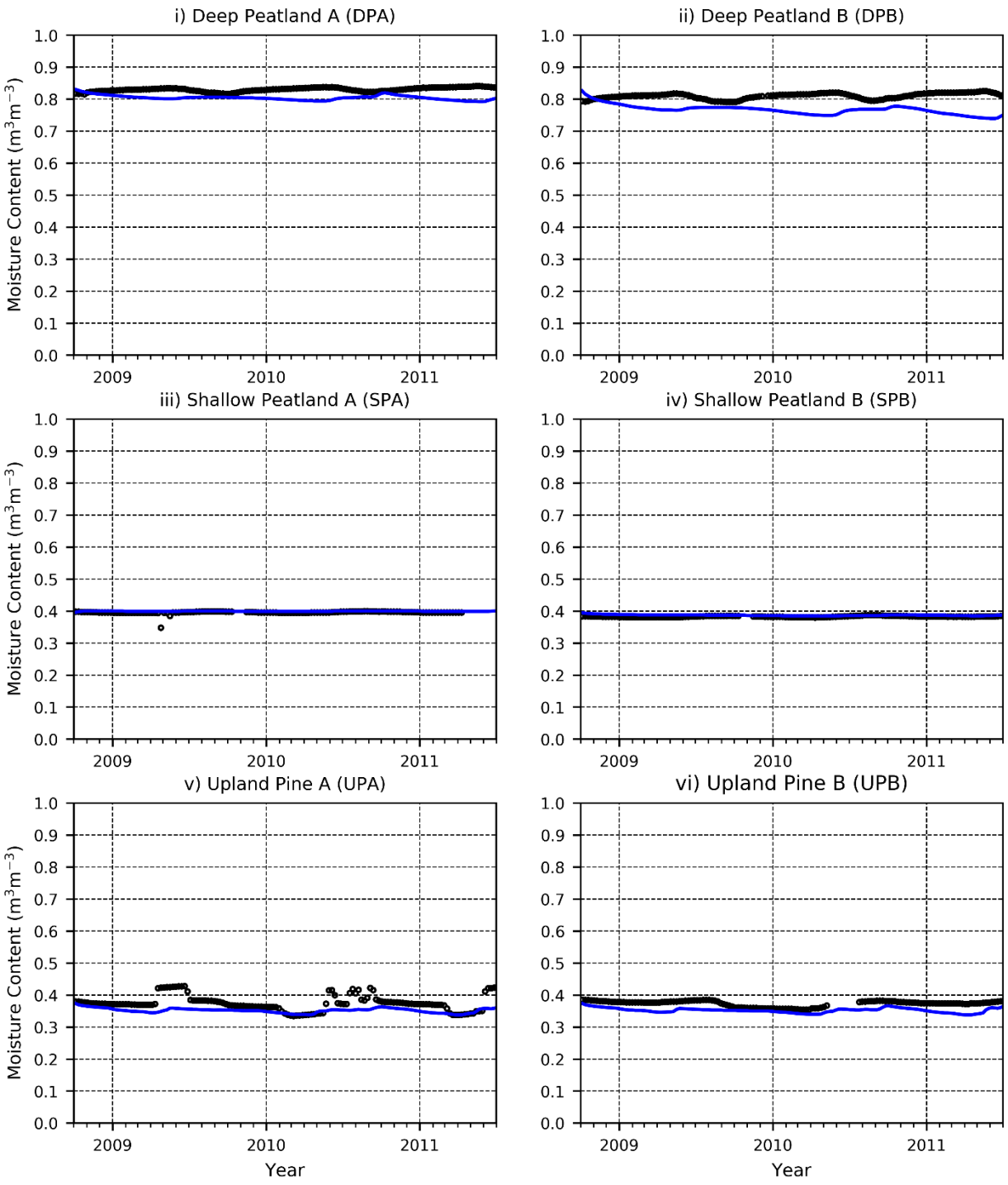

Figure 5-15 Observed (Black Circle) and Simulated (Blue Line) Weekly Average Moisture Contents at -100 cm for each of the Six Ecological Sites

5.2.10 Estimated Parameters

During the calibration process PEST estimated a variety of physical properties at each of the ecological sites by altering parameter values to attempt to reduce residuals. There were three groups of parameters, as discussed previously; 1) the tree crown and surface process parameters that included the average temperature at the damping depth defining the lower boundary of the model, 2) soil properties, and 3) hydraulic properties.

PEST was able to estimate a value for the following tree crown and surface process parameters for each of the ecological sites: dry albedo, the empirical exponent to estimate wet albedo, crown albedo, clumping, crown interception, and damping depth average temperature (Table 5-5). The estimated dry and crown albedos did not vary much between ecological sites with the black spruce sites having a smaller albedo as would be expected. The dry albedo ranged from 0.33 to 0.46, while the crown albedo ranged from 0.05 for black spruce to 0.10 for lodgepole pine. The albedo exponent at the black spruce peatland sites (DPA, DPB, SPA) were estimated to be around 0.5, while the pine sites ranged from 0.7 to 0.9. Crown interception for all the peatlands was estimated to be less than 0.2 mm LAI^{-1}, a third less than the estimated crown interception of 0.65 mm LAI^{-1} for the upland sites. There seemed to be no real correlation in estimated clumping values between tree species. This likely is the result of the distance from the probe to the tree.

Table 5-5 PEST Estimated Tree Crown and Surface Parameters for Each of the Ecological Sites

Parameter	Units	UPA	UPB	SPA	SPB	DPA	DPB
Dry Albedo		0.44	0.80	0.80	0.46	0.34	0.36
Wet Albedo Exponent		0.90	0.90	0.51	0.72	0.52	0.50
Crown Albedo		0.10	0.10	0.09	0.10	0.06	0.06
Crown Interception	mm LAI^{-1}	0.66	0.66	0.21	0.16	0.18	0.19
Clumping		0.98	1.00	0.34	0.46	0.62	0.97
Damping Depth Average Temperature	ºC	4.01	4.20	4.00	4.01	2.50	2.59

Originally the average temperature at the dampening depth was set to the average air temperature over the year of approximately 4 ºC, however it was found to result in a poor calibration at the deep peatlands. PEST was then allowed to estimate the average temperature for the lower boundary condition and found it to be very close to average air temperature of 4 ºC at the

shallow peatlands and the upland pine sites. However, PEST estimated the average temperature to be around 2.5 ºC at the two deep peatland sites approximately 1.5 ºC cooler than the other sites. This may be due to the infiltration of snowmelt which cooled the subsurface to lower than the average air temperature. However it should be noted that a similar adjustment of 1.6 ºC reduction in air temperatures was required for modelling of a black spruce site in Central Saskatchewan using the Forest Hydrology Model (ForHyM)(Jagtar Bhatti et al. 2006).

The only soil property estimated by PEST for each of the six soil zones was the dry bulk density and these are presented in Table 5-6 for each of the ecological sites. Estimated bulk densities near the surface of the organic horizon were all less than 105 kg m^{-3} with both deep peatlands being estimated at the minimum value of 50 kg m^{-3}. The deep peatlands had the lowest estimated bulk densities of approximately 200 kg m^{-3} within the peat layers, Zones 2 thru 5, and roughly 1,200 kg m^{-3} in the mineral soils in Zones 5 and 6. The upland pine sites had the highest bulk densities of roughly 1,600 kg m^{-3} except for UPB in Zone 6 being estimated at 1,330 kg m^{-3}. The estimated shallow peatland bulk densities in Zones 2 and 3 ranged from roughly 200 kg m^{-3} to 450 kg m^{-3} which is expected for peat materials similar in characteristics to the deep peatlands. The estimated shallow peatland bulk densities at depth were more like the upland sites with values of around 1,600 kg m^{-3}. The Zone 6 bulk density at shallow peatland A was estimated at the lower bound of 950 kg m^{-3} for a Cg soil type and is indicative there is likely an issue with the representation of the lower boundary condition or the elevation of the probe.

Table 5-6 PEST Estimated Soil Properties by Soil Zone for each of the Ecological Sites (Peat Zones Shaded)

Soil Zone	Parameter	Units	UPA	UPB	SPA	SPB	DPA	DPB
1	Dry Bulk Density	kg m^{-3}	102	100	67	74	50	50
2	Dry Bulk Density	kg m^{-3}	1688	1678	244	446	187	141
3	Dry Bulk Density	kg m^{-3}	1560	1660	440	292	201	208
4	Dry Bulk Density	kg m^{-3}	1614	1609	1529	1555	186	197
5	Dry Bulk Density	kg m^{-3}	1650	1630	1589	1603	297	1195
6	Dry Bulk Density	kg m^{-3}	1578	1331	1456	950	1216	1242

PEST also estimated the hydraulic properties, which are the variables for the Van Genuchten equation, at each of the ecological sites for the three hydraulic zones (Table 5-7). Van Genuchten n values were generally estimated at a value slightly greater than 1, except for the deep peatlands in Zone A with an estimated n of 1.5 and the shallow peatlands at Zone B with n ranging from 3.5 to 4.5. Van Genuchten α had the greatest variability with depth, with α ranging from 1.2 to 3 m^{-1} in zone A, 0.25 to 0.75 m^{-1} in zone B and 0.5 to 1.5 m^{-1} in zone C.

Table 5-7 PEST Estimated Hydraulic Properties by Hydraulic Zones for each of the Ecological Sites

Hydraulic Zone	Parameter	Units	UPA	UPB	SPA	SPB	DPA	DPB
A	Saturated Moisture Content	$m^3\ m^{-3}$	0.36	0.36	0.24	0.24	0.30	0.59
B			0.37	0.37	0.55	0.55	0.84	0.84
C			0.38	0.38	0.40	0.40	0.84	0.84
A	Residual Moisture Content	$m^3\ m^{-3}$	0.03	0.03	0.08	0.06	0.11	0.11
B			0.14	0.14	0.13	0.13	0.45	0.30
C			0.13	0.13	0.19	0.21	0.56	0.50
A	Saturated Hydraulic Conductivity	cm hr^{-1}	0.43	0.44	0.42	0.41	0.35	0.32
B			0.55	0.54	0.77	0.70	0.21	0.24
C			0.36	0.37	0.22	0.24	0.20	0.19
A	Van Genuchten n		1.09	1.13	1.08	1.16	1.53	1.64
B			1.13	1.14	4.55	3.64	1.13	1.16
C			1.08	1.08	1.08	1.05	1.09	1.18
A	Van Genuchten α	m^{-1}	2.34	2.30	3.15	2.34	1.24	1.60
B			0.60	0.58	0.25	0.30	0.73	0.54
C			0.56	0.56	1.49	1.21	0.76	0.82

The estimated saturated moisture contents at the upland pine sites were consistently around 0.35 $m^3\ m^{-3}$ for all moisture probe elevations and is within the expected range for clay loam. The estimated saturated moisture contents at the shallow peatlands were outside the expected bound in both Zone A at slightly above 0.2 $m^3\ m^{-3}$ and in Zone B with values approaching 0.55 $m^3\ m^{-3}$. It is more likely the saturated moisture contents in Zone A should be closer in value to DPB site estimated 0.58 $m^3\ m^{-3}$, while the Zone B should be closer in values to that of the upland clay loam of 0.35 $m^3\ m^{-3}$. The only suspect saturated moisture content at the deep peatland sites was

at DPA Zone A with a value almost half of that at DPB of 0.3 m^3 m^{-3} and much too low for sphagnum moss/peat.

The estimated saturated hydraulic conductivities were all within an order of magnitude of each other and ranged from 0.19 cm hr^{-1} to 0.77 cm hr^{-1} (Table 5-7). The estimated hydraulic conductivities at the deep peatland sites were always less than the other sites at a given moisture probe depth. The estimated hydraulic conductivity at the shallow peatlands (~0.4 cm hr^{-1}) were closer in value to the upland pine sites in Zone A but had similar values (~0.2 cm hr^{-1}) in Zone C to the deep peatland sites. The saturated hydraulic conductivity in Zone B at the shallow peatland sites was estimated to be larger in magnitude than both the deep peatland and upland sites, and like the larger estimated saturated moisture content was likely a result of PEST trying to manipulate the moisture contents to better match observed temperatures due to how the targets were weighted.

5.3 Updated SHAW Model

PEST was unable to achieve a satisfactory calibration to the observed black spruce peatlands temperature data during the wintertime. The current processes represented within the SHAW model were unable to simulate subsurface temperatures of black spruce peatlands within the Boreal Plains which provides further justification to reject the hypothesis that black spruce peatlands are warmer with a shallower frost depth due to the increased release of latent heat during freezing. Therefore, the SHAW model was modified to include an additional equation for the thermal conductivity of the sphagnum moss, to better represent the thermal properties of the sphagnum moss, and to also allow the user to specify the empirical coefficients used to calculate the thermal conductivity of snow that was previously assumed constant or calculated internally. The hypothesis that the shallower than expected depth of frost at the deep peatlands is due to the insulating effect of the sphagnum moss layer was then tested with the updated SHAW model.

5.3.1 Thermal Conductivity of Sphagnum Moss

The effects of sphagnum moss on thermal conductivities needed to be incorporated into the SHAW model to accurately simulate the thermal profile of black spruce peatland sites. Most of the time, except for the few days after a precipitation event, all of the moisture is contained within specialized hyaline cells (Weber et al. 2017) and unlike mineral soils is not interconnected within the pore spaces. In addition, most of the sphagnum moss organic material and hyaline

cells, which die at maturity but still store water, are on the branches and leaves and separated by air. Mosses are also non-vascular plants, meaning they lack any interconnected system like a xylem, which would greatly increase the thermal conductivity through the plant. However, once the sphagnum moss dies and becomes peat, the organic material becomes compressed and connections form between the branches and leaves resulting in parallel flow of heat, at least through the organic material. Thus, the thermal conductivity was calculated in series, not parallel (Figure 5-16) for the biologically active moss layer (Zone 1), while the conductivities of the underlying peat layers (Zones 2 thru 5) would still be calculated in parallel.

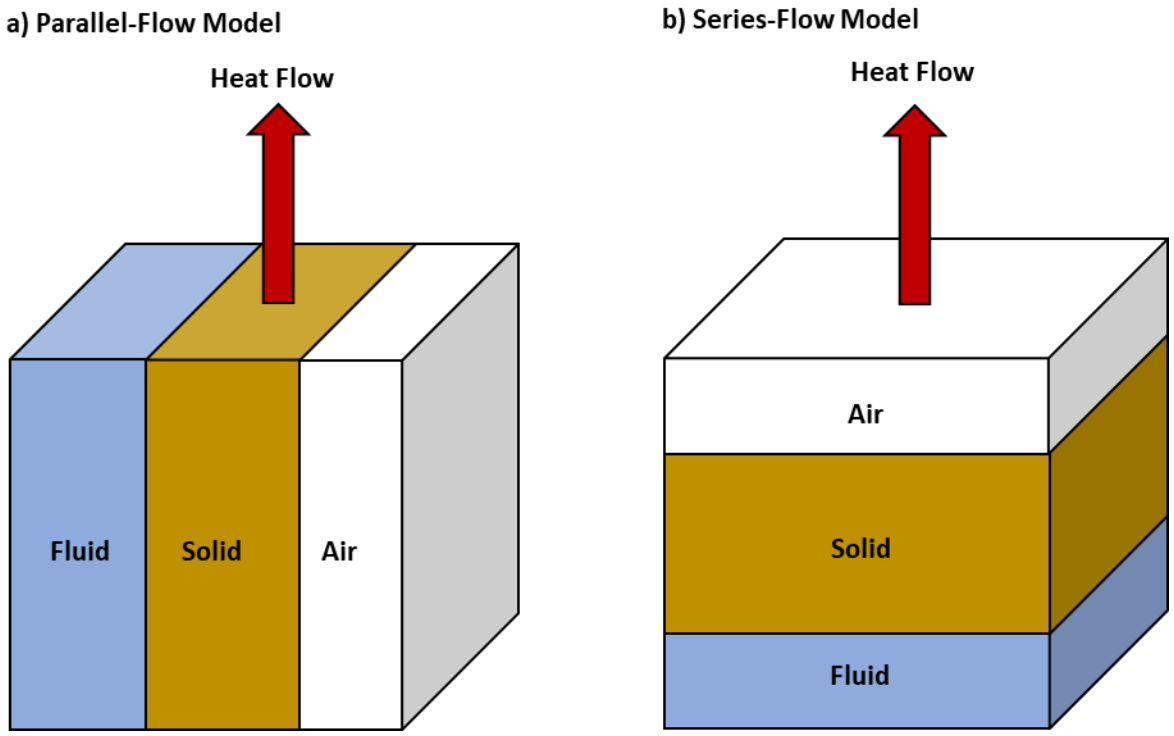

Figure 5-16 Illustration of a) Parallel-flow Model for Soil & Peat b) Series-flow Model for Moss Adapted from: (McGaw 1969)

The thermal conductivities calculated internally for each time step in the SHAW model would be significantly reduced when calculated in series as opposed to parallel. The SHAW model was updated to allow for the thermal conductivities to be estimated by series-flow instead of parallel-flow using Equation 5-5.

Equation 5-5 Soil Thermal Conductivity in Series-Flow (McGaw 1969)

$$1/K = x_s/K_s + x_c/K_c + x_o/K_o + x_w/K_w + x_{i/}K_i + +x_a/K_a \quad \text{……..(5-5)}$$

Where:

K_s is the thermal conductivity of the sand (8.8 W m^{-1} °C^{-1})
K_c is the thermal conductivity of the silt/clay (2.92 W m^{-1} °C^{-1})
K_o is the thermal conductivity of the organic material (0.25 W m^{-1} °C^{-1})
K_w is the thermal conductivity of the liquid water (0.57 W m^{-1} °C^{-1})
K_i is the thermal conductivity of the frozen soil water (ice) (2.2 W m^{-1} °C^{-1})
K_a is the thermal conductivity of the air/vapour (0.025 W m^{-1} °C^{-1})
x is the volumetric fraction of the given media (m^3 m^{-3})

To ensure that the series-flow equation was only implemented for the sphagnum moss layer SHAW was modified to only use the equation when the organic content was equal to 100% and the moisture content was less than 0.60 m^3 m^{-3}. The test condition prevented the use of the series flow equation under wetter conditions. It is expected that as the voids within the moss layer begin to fill with water that the estimation of thermal conductivity would no longer be in series but rather in parallel and was assumed to be 0.60 m^3 m^{-3}, however the exact value of this transition is unknown and would require further investigation. Because the sphagnum moss is 100% organic, Equation 5-5 was simplified by excluding the terms for sand and clay allowing for a simplified calculation for the volumetric factions of the organic material, air, water, and ice from the specified dry bulk density, water, and ice content (Equation 5-6).

Equation 5-6 Thermal Conductivity for Sphagnum Moss Layer in Series

$$1/K = \frac{(\rho_{dry}/\rho_{moss})}{K_o} + \frac{x_w}{K_w} + \frac{x_i}{K_i} + \frac{(1-(\rho_{dry}/\rho_{moss})-(x_w+x_i)}{K_a} \quad \text{……...(5-6)}$$

Where:

K_o is the thermal conductivity of the organic material (0.25 W m^{-1} °C^{-1})
K_w is the thermal conductivity of the liquid water (0.57 W m^{-1} °C^{-1})
K_i is the thermal conductivity of the frozen soil water (ice) (2.2 W m^{-1} °C^{-1})
K_a is the thermal conductivity of the air/vapour (0.025 W m^{-1} °C^{-1})
$X_{w,i}$ is the volumetric fraction for water (w) and ice (i) calculated each time step
ρ_{dry} is the user specified bulk density (kg m^{-3}) for the node
ρ_{moss} is the density (kg m^{-3}) for an organic particle (1300 kg m^{-3})

An example of the sensitivity of bulk dry density (50, 200, 400 kg m^{-3}), total moisture content (0 to 0.65 m^3 m^{-3}), and the percentage of water frozen (0, 50, 100%) on the thermal conductivity of the sphagnum moss layer is illustrated in Figure 5-17 for parallel and in Figure 5-18 for series. When calculated in parallel the thermal conductivity is highly sensitive to the percentage of water, with thermal conductivities tripling at moisture contents greater than 0.25 m^3 m^{-3} when completely frozen.

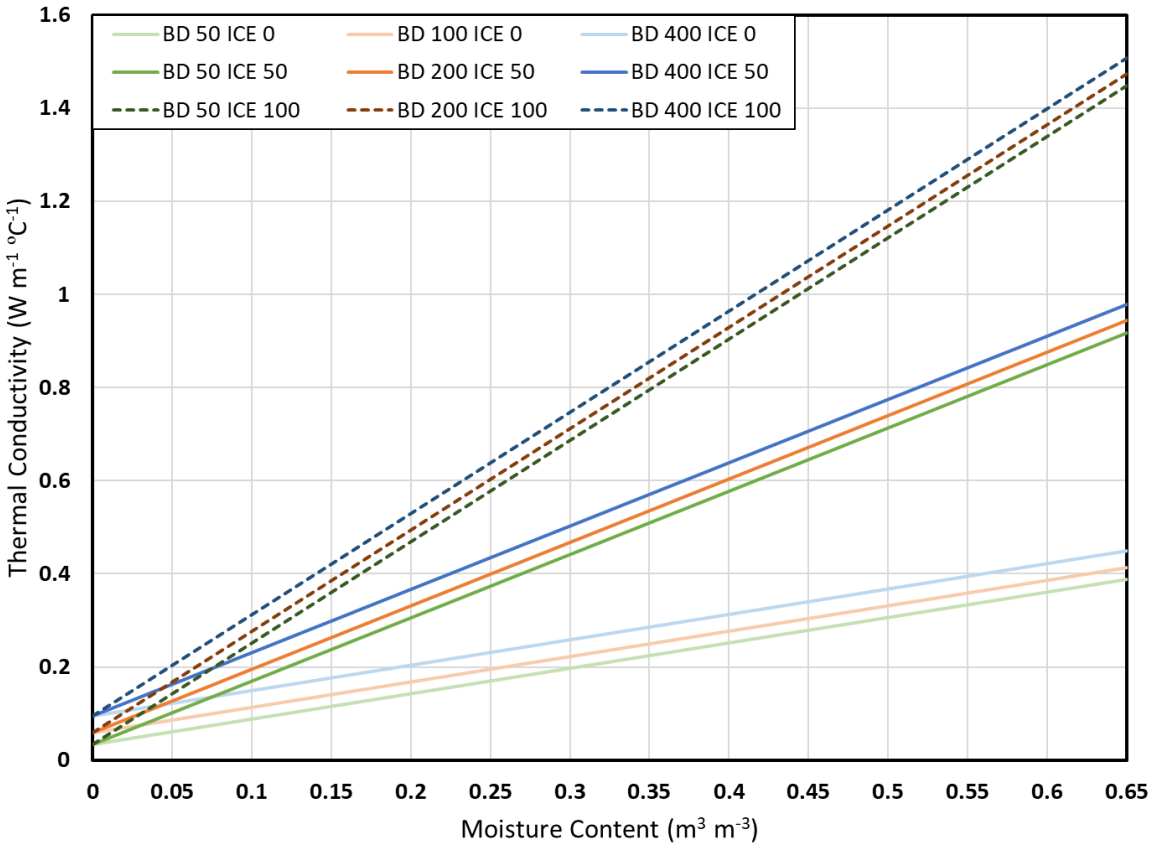

Figure 5-17 Sensitivity of Calculated Thermal Conductivity in Parallel to Dry Bulk Density (BD 50/100/400 kg m^{-3}), Moisture Content (0 to 0.65 m^3 m^{-3}), and Percentage of Water Frozen (ICE 0/50/100%)

In comparison when calculated in series the thermal conductivities are most sensitive to bulk density, which indirectly determines the volume of air (Figure 5-18). With increased bulk density the volume of air is decreased, similarly with the moisture content. The thermal conductivities

are unaffected by the percentage of water frozen except at higher than reasonable bulk densities for sphagnum moss or at moisture contents that are approaching saturation and violating the assumption of disconnected water within pore spaces. During the Phase 2 field study (2015-2016) the moisture content of the sphagnum moss layer was found to be consistently at 0.3 m^3 m^{-3} or less (Figure 4-28), resulting in thermal conductivity of approximately 0.05 W m^{-1} °C^{-1} regardless of the percentage of water frozen or bulk density when calculated in series (Figure 5-18). Under similar conditions the estimated thermal conductivity in parallel would range from 0.2 W m^{-1} °C^{-1} to almost 0.8 W m^{-1} °C^{-1}, 4 to 16 times greater than if calculated in series, under varying percentages of water frozen.

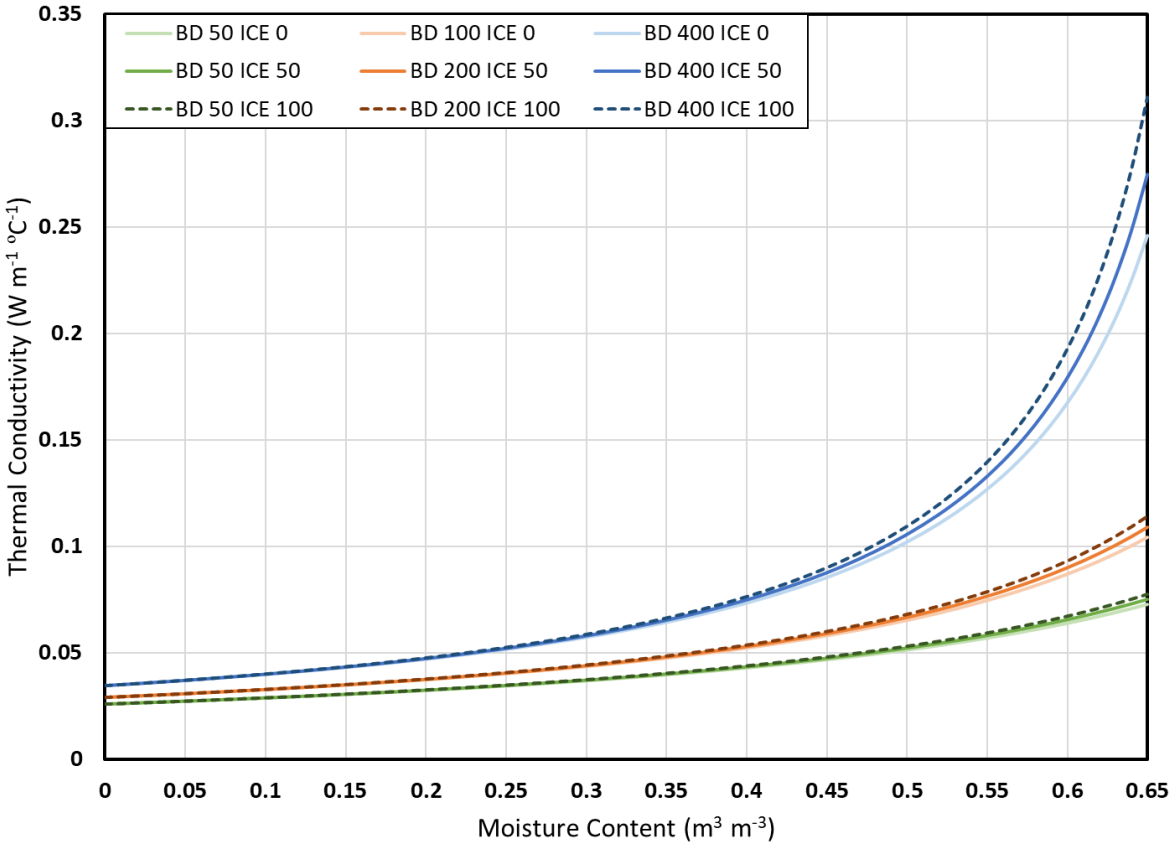

Figure 5-18 Sensitivity of Calculated Thermal Conductivity in Series to Dry Bulk Density (BD 50/100/400 kg m^{-3}), Moisture Content (0 to 0.65 m^3 m^{-3}), and Percentage of Water Frozen (ICE 0/50/100%)

5.3.2 Thermal Conductivity of the Snowpack

The SHAW model was updated to allow for user specification of the empirical coefficients of a_{sp}, b_{sp}, and c_{sp} (Equation 5-4) and these parameters were estimated by PEST. The thermal conductivity of the snowpack is dependent on its density, with increasing thermal conductivity with increased ice density. It is unlikely that two snowpacks of equal densities would have a large variation in thermal conductivities, therefore SHAW does not allow the user to change the empirical coefficients. However, if the snowpack densities are not correctly represented the simulations would result in erroneous thermal conductivities. Therefore, SHAW was modified so the empirical coefficients could be varied to allow for the correct snowpack thermal conductivity to be estimated. Thus, the original SHAW code was altered to read the empirical coefficients of a_{sp}, b_{sp}, and c_{sp} from the site description file instead being defined in code. The empirical constants were set up to be easily defined within the FORTRAN code and recompiled, however this would not allow for PEST to alter the value during calibration.

It would be expected that snowpack density would be far less in black spruce peatlands than the simulated value due to the majority of snowmelt occurring within the black spruce crown and draining through the cavity. But in the SHAW simulations, all the snowmelt refreezes within the snowpack until the snowpack has completely melted resulting in ever increasing densities, and thus thermal conductivities throughout the winter. It was simply easier to allow PEST to estimate new snowpack thermal conductivity empirical coefficients based on the inaccurate simulation of snowpack densities rather than change the code to allow for snowmelt from the crown to be routed to the subsurface rather than the snowpack. Further snowpack empirical coefficients were only estimated at DPA, with the same values being used in DPB as a quasi-verification.

5.4 Updated SHAW Simulation Results

This section presents the calibrated results of the updated SHAW numerical model with the calculation of thermal conductivity in the sphagnum moss layer in series and estimated snowpack thermal conductivity empirical coefficients for deep peatland A (DPA) and deep peatland B (DPB). Results are presented for subsurface temperatures, moisture contents, along with the estimated parameters.

5.4.1 Subsurface Temperature -10 cm

The updated SHAW model greatly improved the calibration of simulated temperatures to observed temperatures (Figure 5-19). During most of the winter period updated simulated temperatures remained above 0 ºC except for a brief period in March 2010 and for two months in December 2010 and January 2011. In comparison the original calibrated SHAW model often estimated winter temperatures below -5 ºC for all three years of simulation. The updated SHAW model was also able to better simulate summer temperatures without lower-than-expected moisture contents. The updated SHAW model still had difficulty matching early spring observed temperatures due to the snowpack melting much earlier than observed outside of the black spruce tree root mat (Figure 4-12). This is likely due to the observed cooling effect living tree trunk bases had in April, resulting in a reduced emission of longwave radiation to the snowpack (Figure 4-25).

The wintertime temperature residuals, observed minus simulated daily average temperature for January, February, and March, were greatly improved and nearly perfect in 2009 (Figure 5-20). In 2010, the updated residuals were slightly better than the upland sites (UPA/UPB) with a smaller range centered around 0, while in 2011 were nearly identical in range and offset from 0.

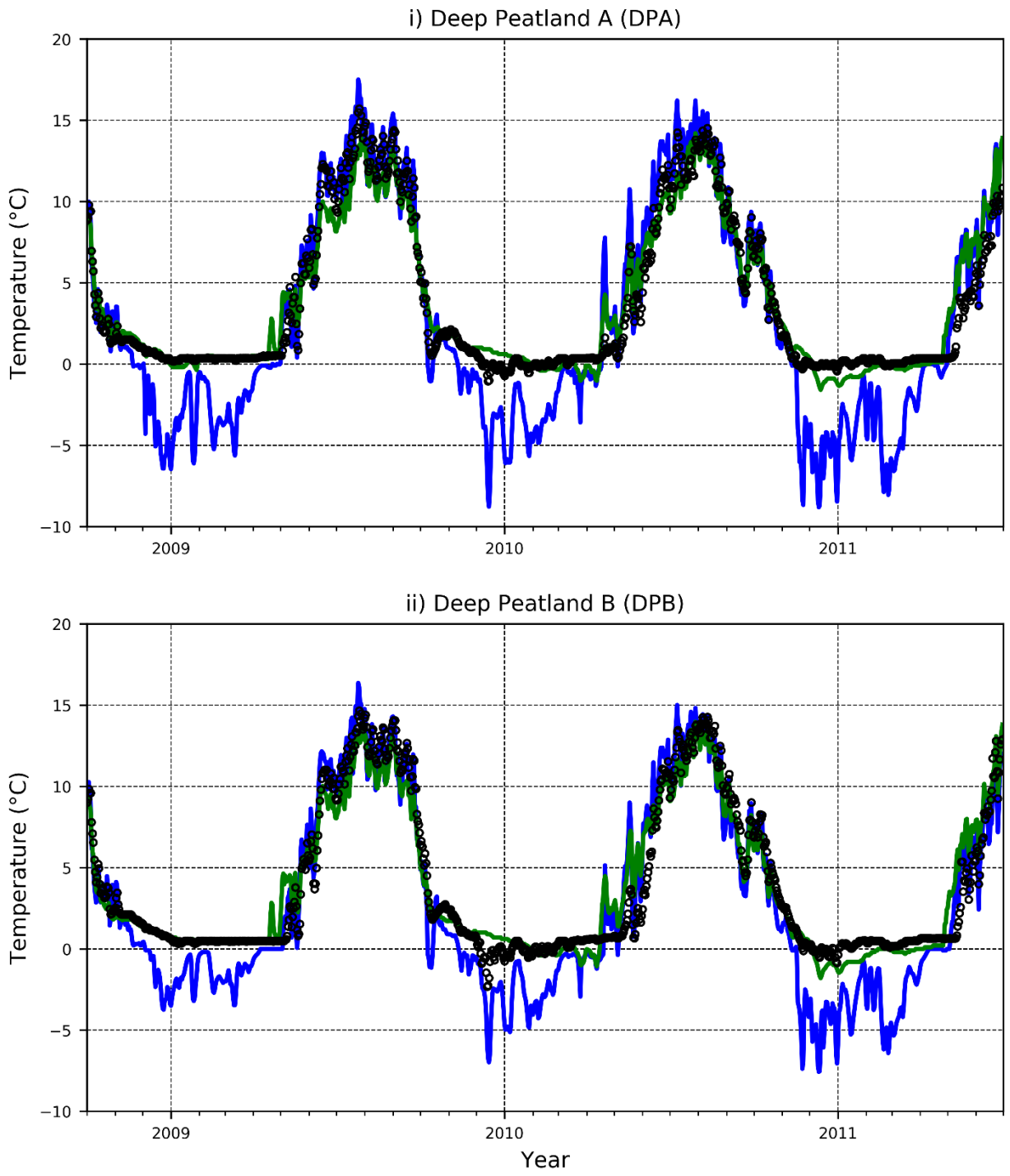

Figure 5-19 Observed (Black) and Simulated (Original-Blue, Updated-Green) Daily Average Temperatures for -10 cm at the Deep Peatland Sites

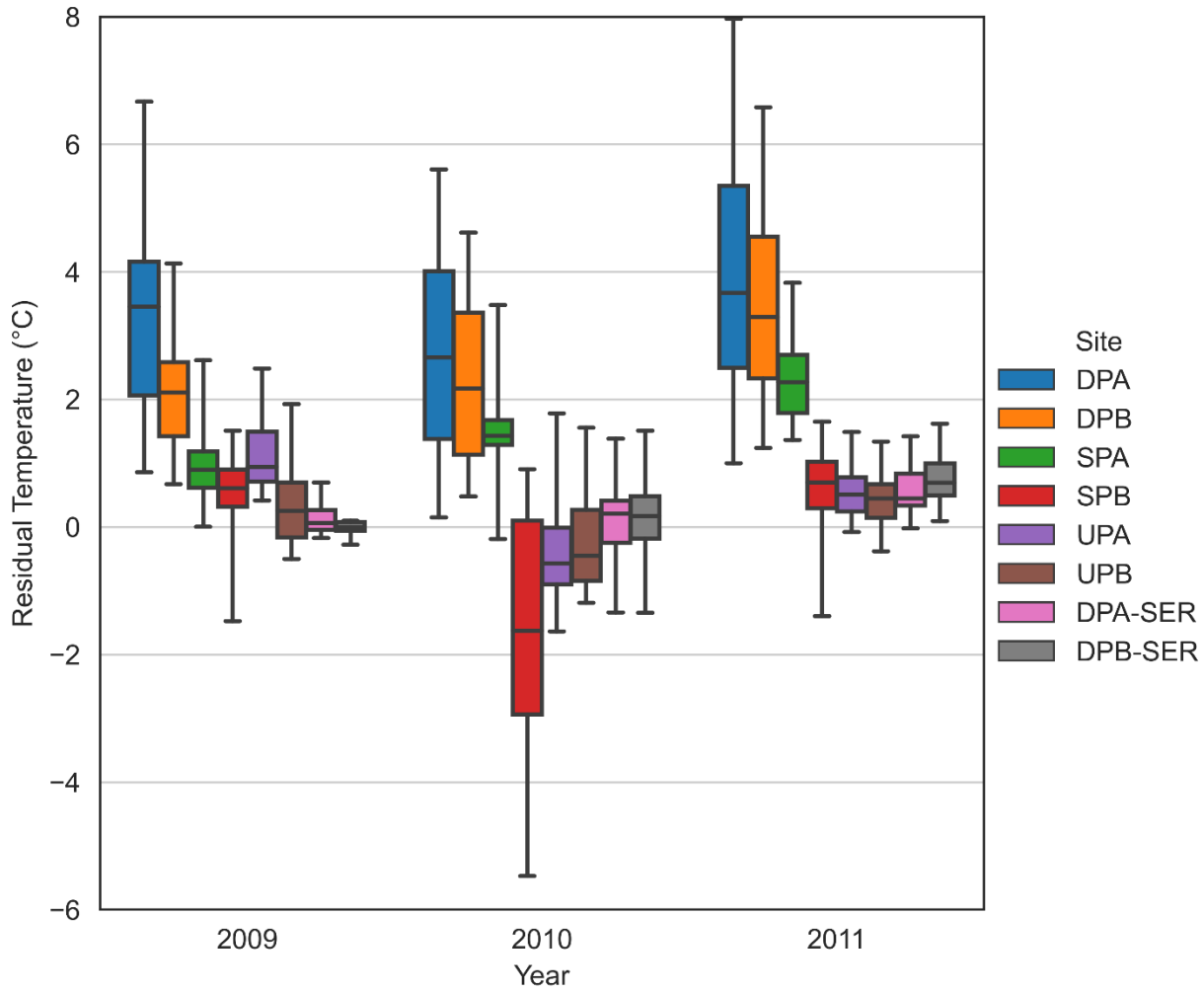

Figure 5-20 Winter Residuals for Daily Averaged Observed Temperatures at -10 cm for Ecological Sites with Original SHAW code and the Deep Peatland Sites using Updated SHAW Series code (SER), Whiskers (Minimum/Max)

5.4.2 Subsurface Temperature -30 cm

Again, the updated SHAW model was able to better match observed wintertime temperatures compared to the original SHAW model (Figure 5-21). While the updated model's simulated temperatures were like the original results and observed temperatures, it often over predicted temperatures in April and early May due to the loss of the snowpack. To improve springtime calibration, the effect of cool black spruce tree trunks on snowmelt will need to be studied and implemented into the model in the future.

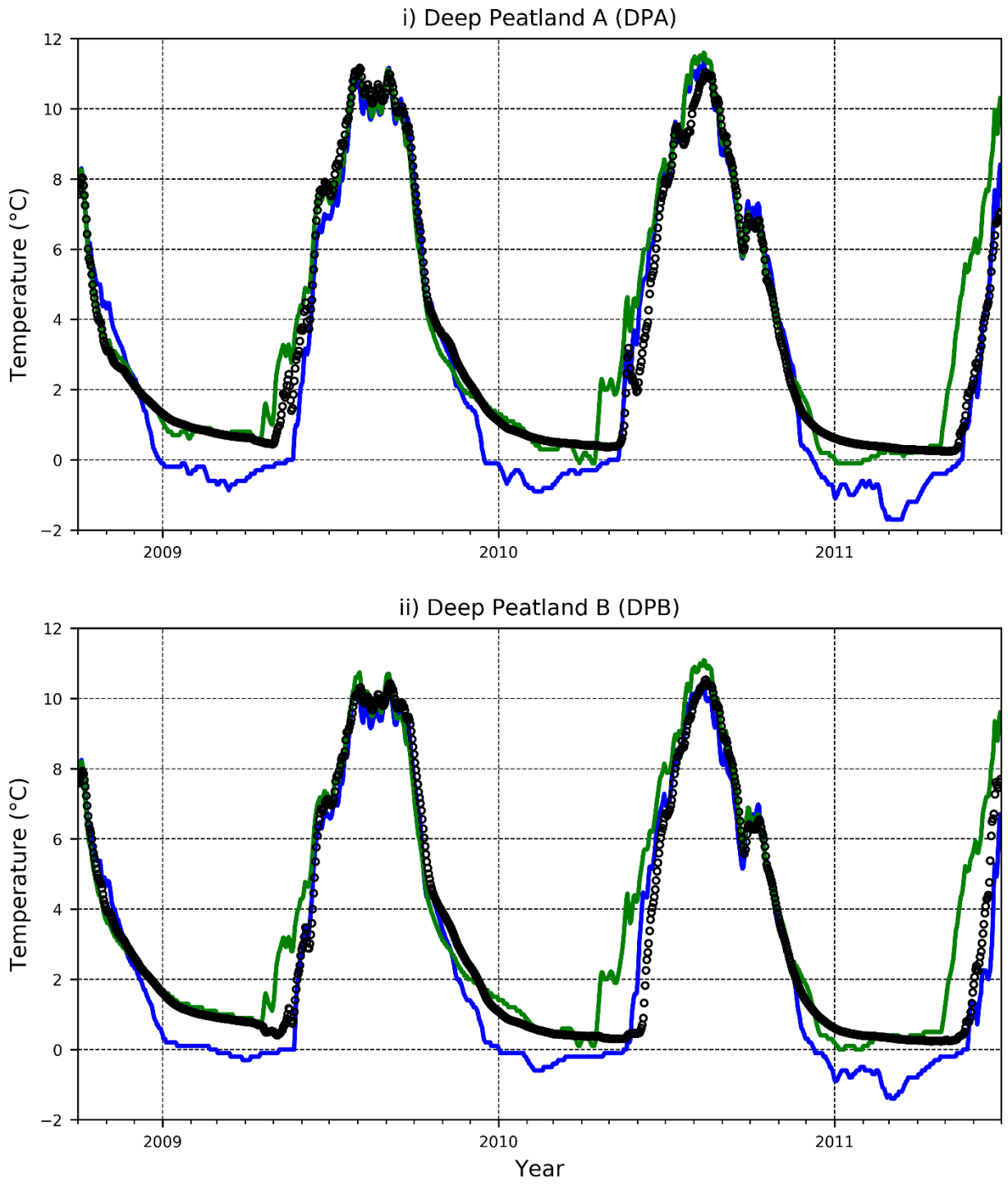

Figure 5-21 Observed (Black) and Simulated (Original-Blue, Updated-Green) Daily Average Temperatures for -30 cm at the Deep Peatland Sites

For most of the wintertime, though, the updated simulated results closely match observed temperatures, except for a few brief periods in 2009 and 2010, and for two months (December, January) in 2011. The updated simulated temperatures also were never lower than a tenth of a degree below freezing (0 ºC), while the original model simulated wintertime temperatures were always below freezing.

The updated wintertime residuals for both the deep peatland sites dropped from over 1 ºC to residuals centered around 0 (Figure 5-22). DPA's 2009 wintertime simulated results were nearly perfect with DPB having very similar residuals to UPB. In 2010 the range in residuals at the deep peatland sites (DPA/DPB) were like the upland sites (UPA/UPB) but were closer to zero by roughly 0.5 ºC. However, in 2011 the deep peatland sites had a greater range in residuals but were nearly just as close to 0 as for the upland sites.

5.4.3 Subsurface Temperature -50 cm

The updated simulated wintertime temperatures at -50 cm were nearly identical or slightly warmer than observed temperatures (Figure 5-23). However, as with the -30 cm simulated temperatures the April and early May, temperatures were much warmer than observed. Beginning in April of 2009, observed temperatures started to decline at an increased rate at the same time simulated temperatures started to rise. This is due to the infiltration of cold snowmelt water through the black spruce cavity bypassing the surface layers, which is why this drop in temperature is only observed at -30 and -50 cm, and not at – 10 cm. There was no observed drop in temperature in 2010 likely due to the minimal snowpack, with a slight decrease detectable in 2011. A 2-D model would be required to allow for the simulation of the tree cavity, and the bypassing of snowmelt through the surface layers.

The updated residuals for the deep peatland sites in 2009 were nearly perfect at DPA while DPB simulated temperatures were slightly warmer (Figure 5-24). Compared to the upland sites (UPA/UPB) the peatland sites simulated in series had a smaller range and was closer to zero in 2009 but had similar residuals to UPB in 2010 and UPA in 2011.

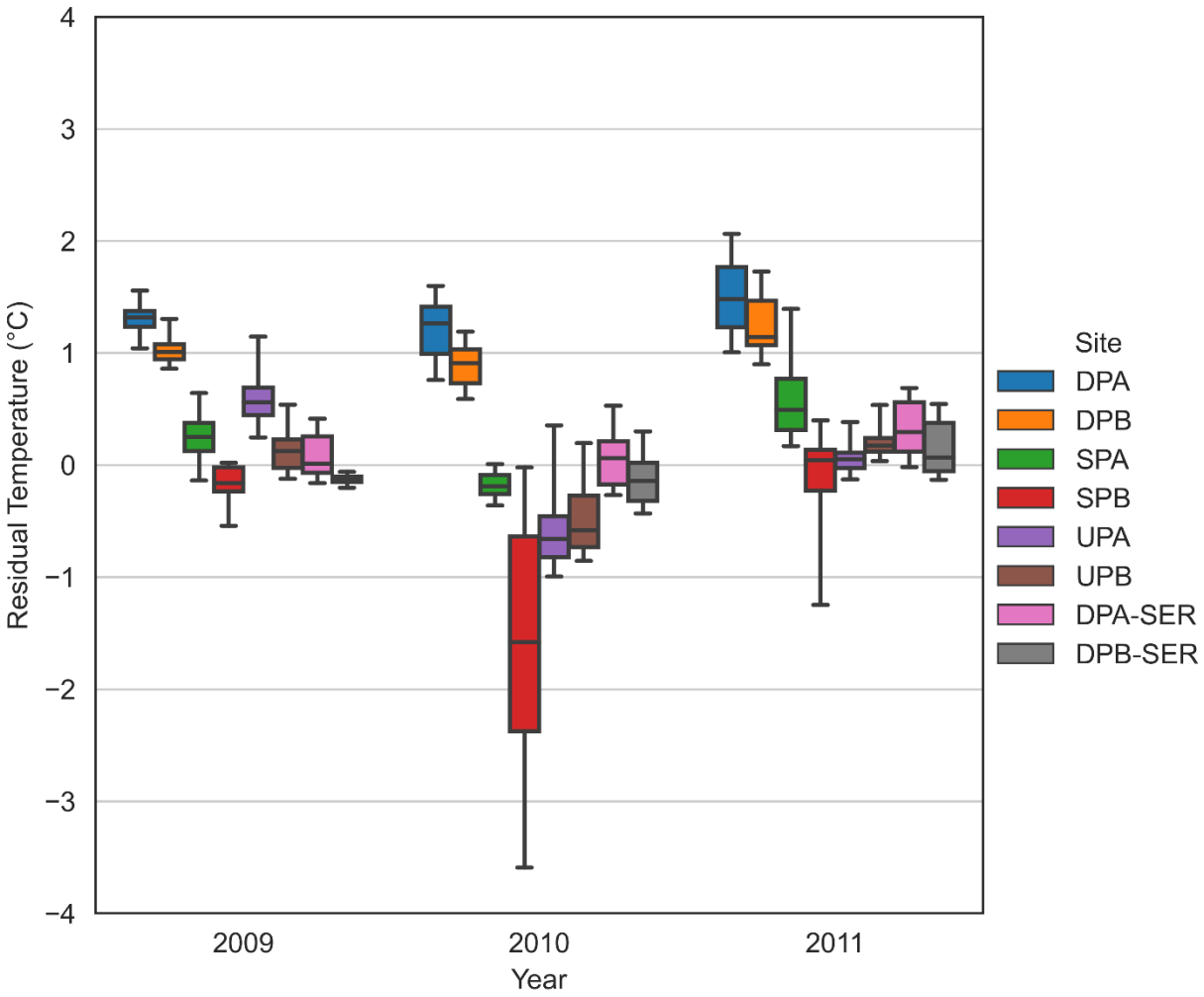

Figure 5-22 Winter Residuals for Daily Averaged Observed Temperatures at -30 cm for Ecological Sites with Original SHAW code and the Deep Peatland Sites using Updated SHAW Series code (SER), Whiskers (Minimum/Max)

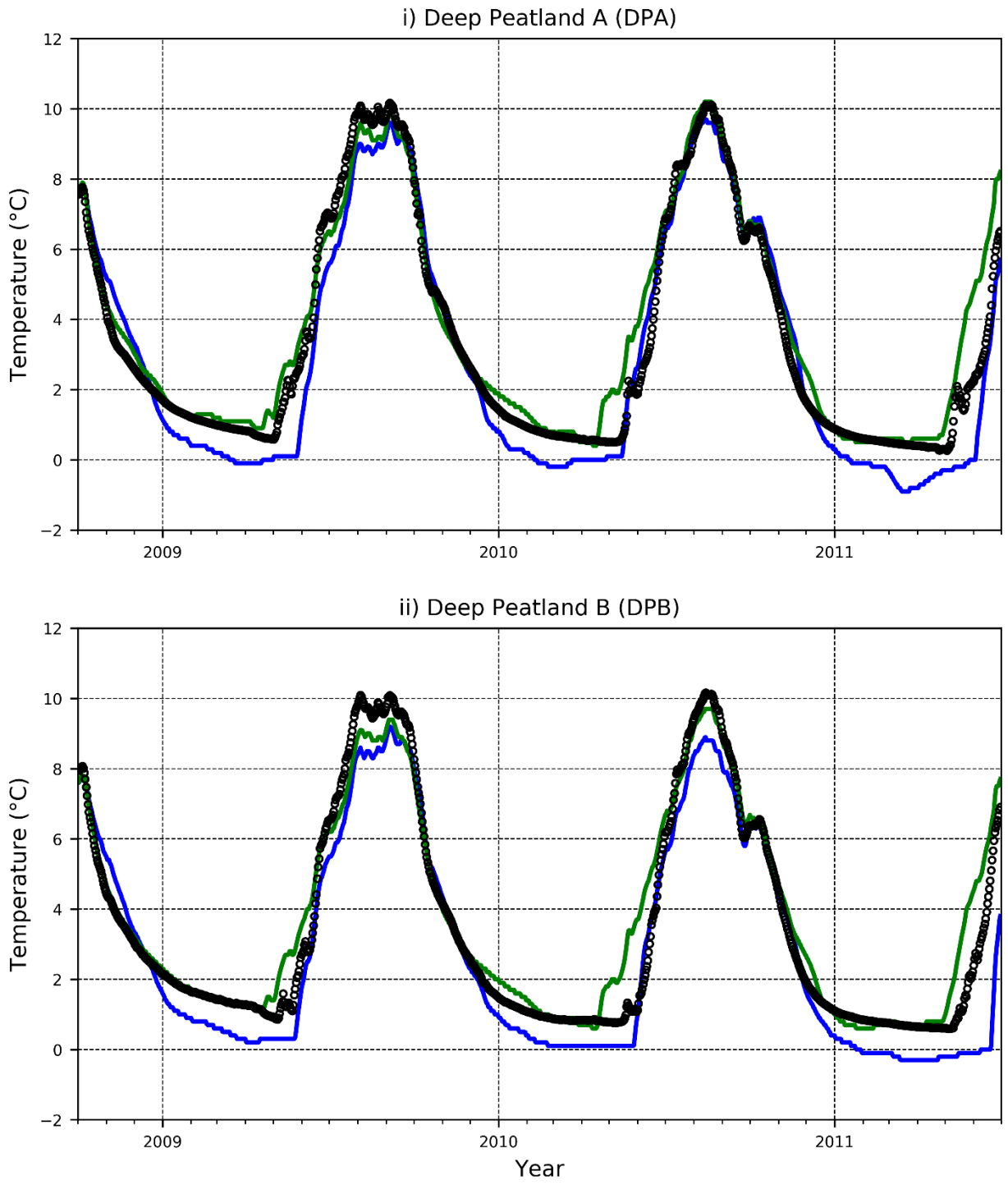

Figure 5-23 Observed (Black) and Simulated (Original-Blue, Updated-Green) Daily Average Temperatures for -50 cm at the Deep Peatland Sites

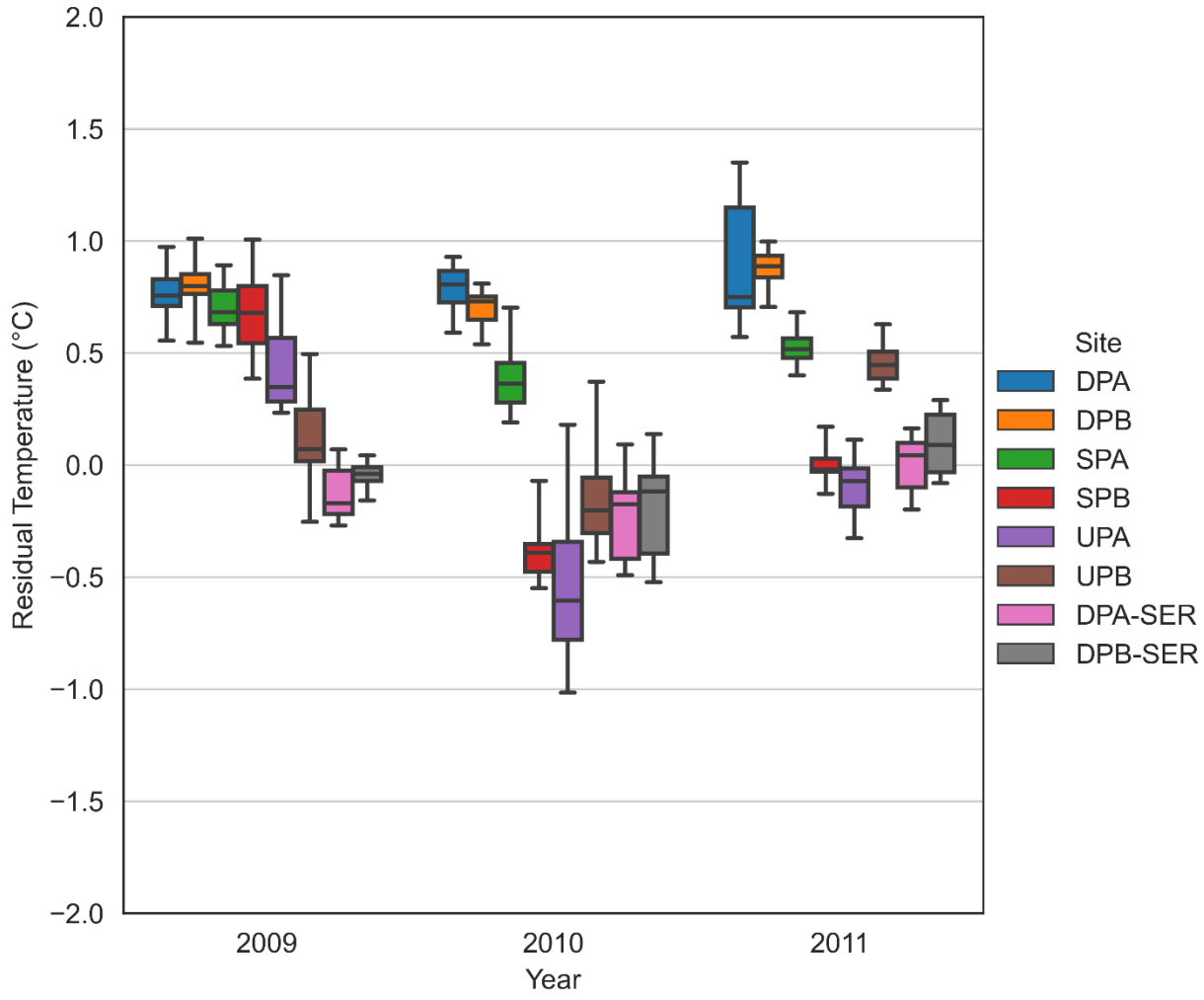

Figure 5-24 Winter Residuals for Daily Averaged Observed Temperatures at -50 cm for Ecological Sites with Original SHAW code and the Deep Peatland Sites using Updated SHAW Series code (SER)

5.4.4 Subsurface Temperature -100

The updated SHAW model was better able to simulate wintertime and summertime temperatures at -100 cm, -200 cm, and -300 cm than the original model. However, the original model often produced better springtime results, especially at DPB at -100 cm in 2009 and 2010 (Figure 5-25). While the range in residuals at deep peatlands sites was significantly reduced the original code was closer to 0 in 2009 (Figure 5-26). In 2010 and 2011 the wintertime residuals were closer to 0 than the original code, but with simulated temperatures being too warm instead of too cold. While the residuals were slightly worse than UPB in 2009, they were comparable in 2010 and better than the upland sites in 2011.

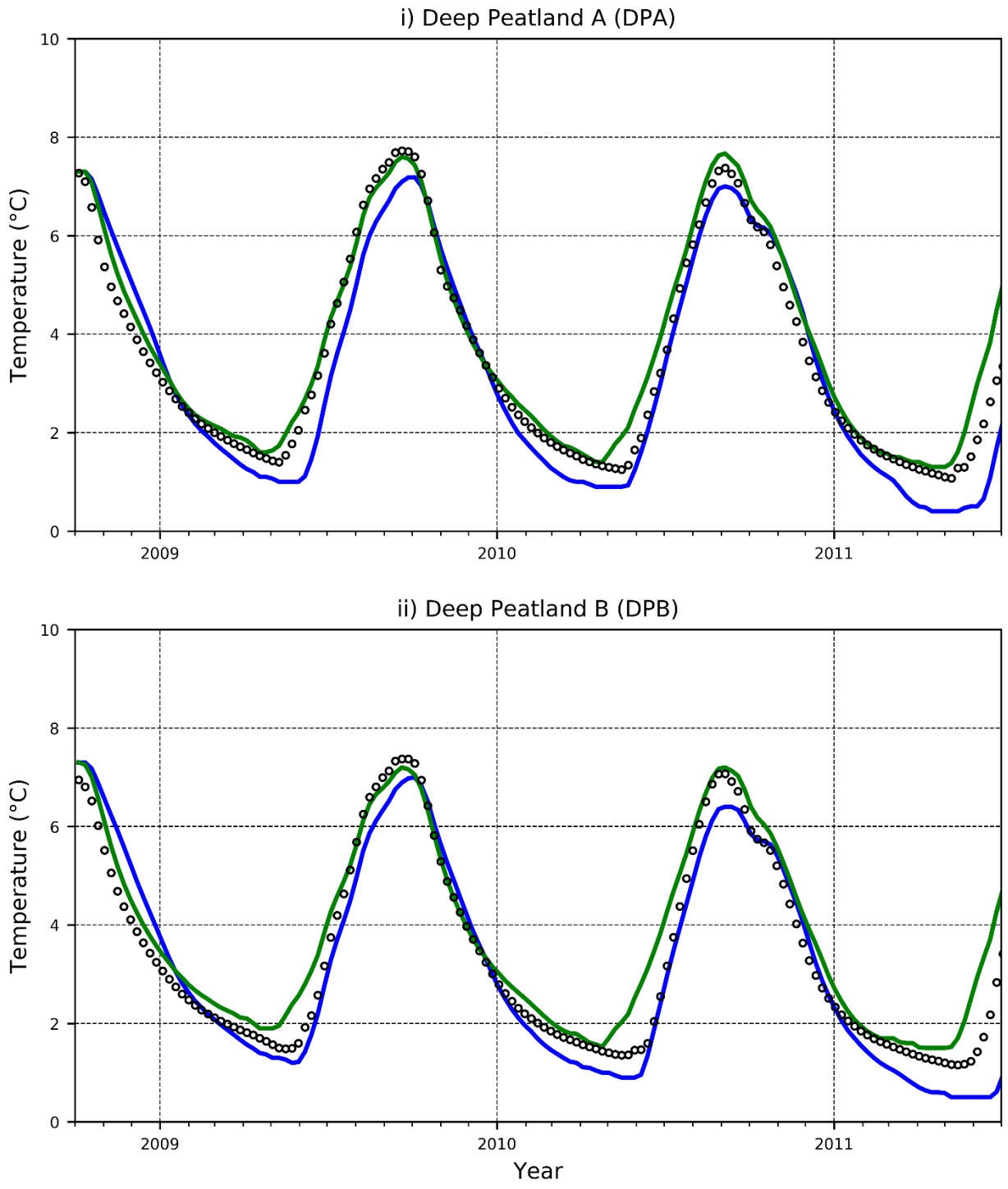

Figure 5-25 Observed (Black) and Simulated (Original-Blue, Updated-Green) Weekly Average Temperatures for -100 cm at the Deep Peatland Sites

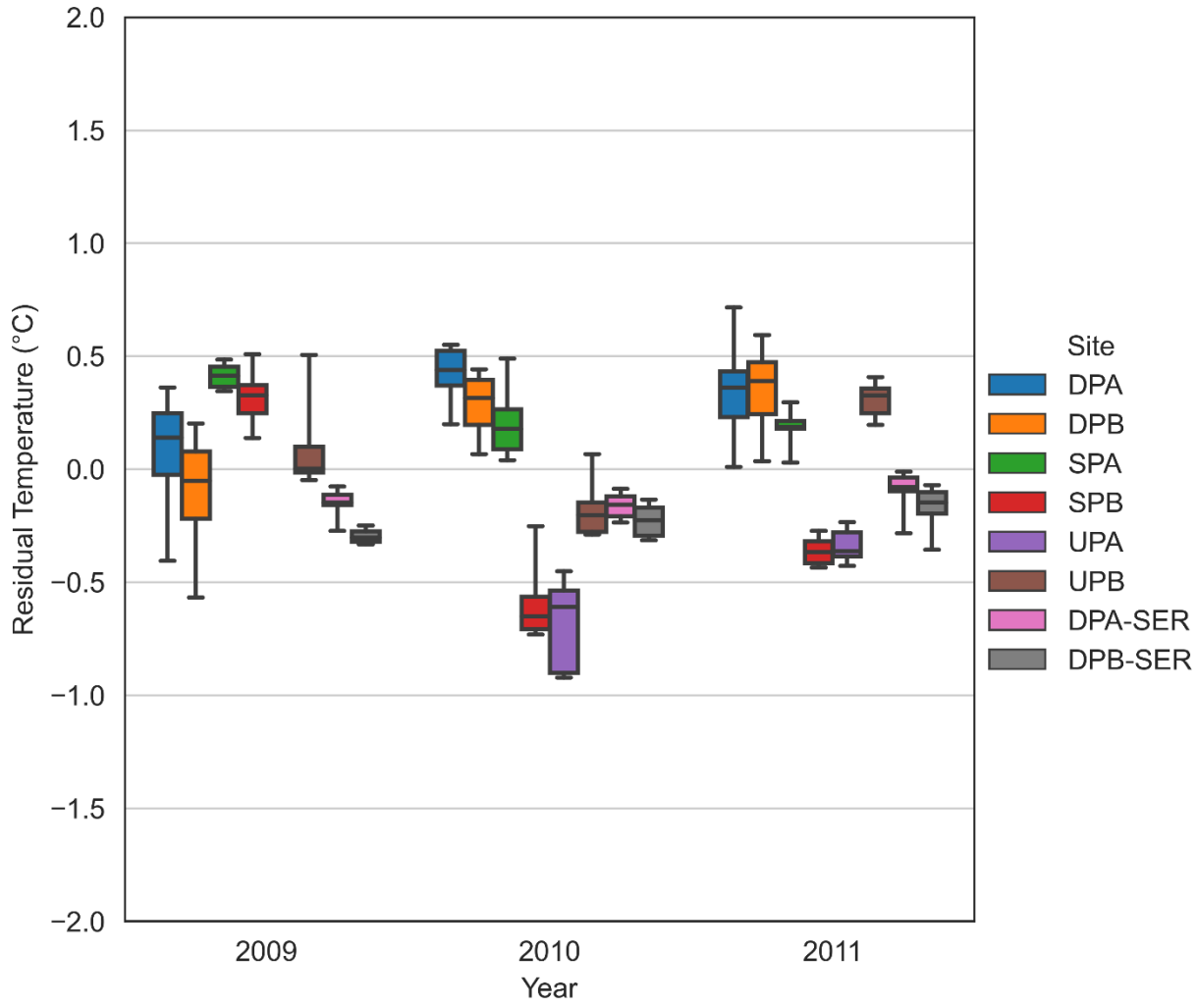

Figure 5-26 Winter Residuals for Weekly Averaged Observed Temperatures at -100 cm for Ecological Sites with Original SHAW code and the Deep Peatland Sites using Updated SHAW Series code (SER)

5.4.5 Subsurface Temperature -200 and -300 cm

Simulated results for -200 and -300 cm were very similar in that the results matched the peak in one or two years, but never all three. At -200 cm the simulated results at DPA matched the peak in 2009 but not at the beginning of the simulation not in 2010, while the opposite was true for DPB (Figure 5-27). It would be expected that the results would be similar at -300 cm, but now DPA was matching the beginning peak and the late 2010 peak along with DPB (Figure 5-28). This is likely due to PEST trying to match the colder wintertime temperatures that are a result of snowmelt infiltration at the sacrifice of peak temperatures in the fall. It would be impossible to

improve the calibration in one year without making it worse in another year without varying the thermal properties of the subsurface year to year.

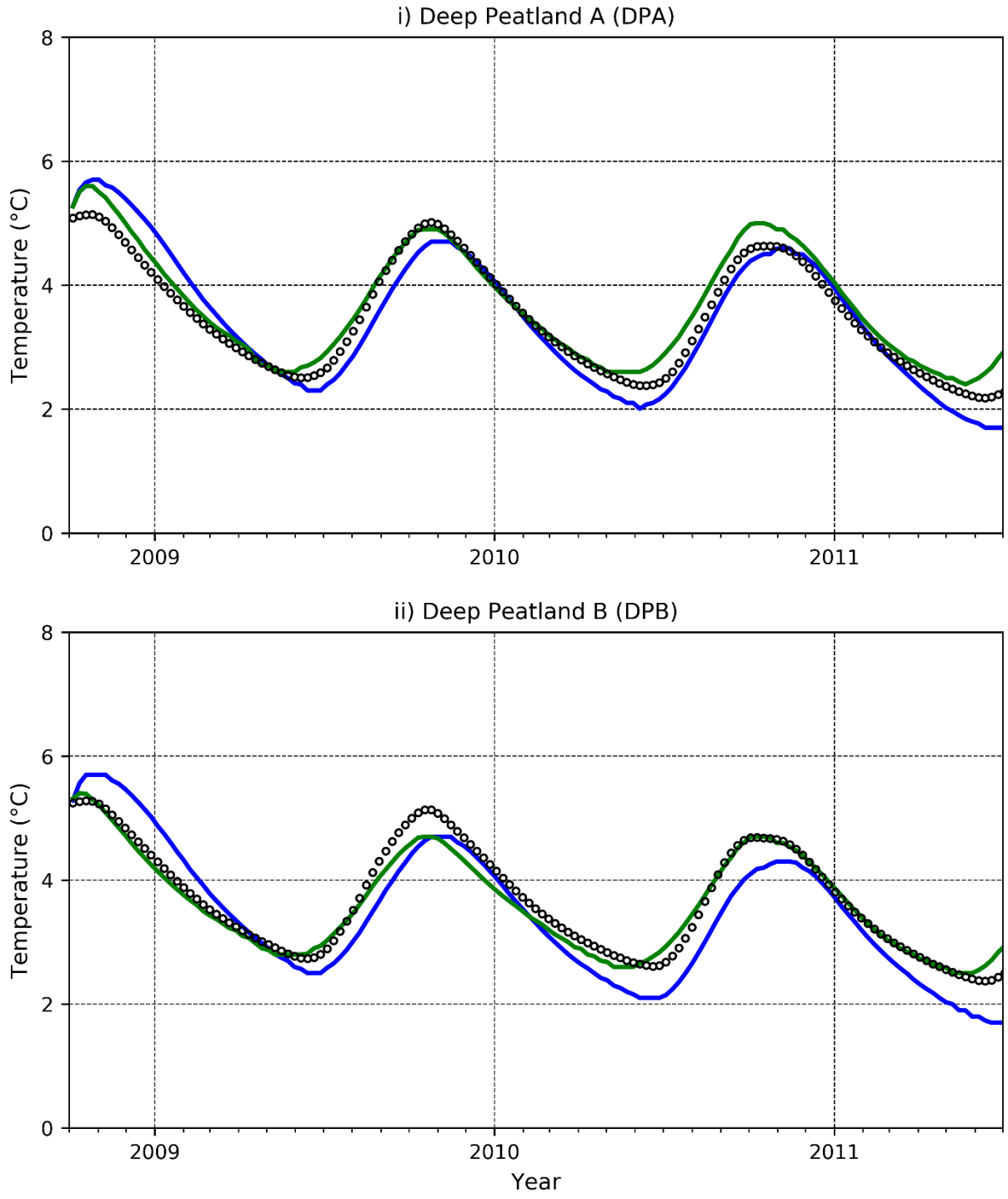

Figure 5-27 Observed (Black) and Simulated (Original-Blue, Updated-Green) Weekly Average Temperatures for -200 cm at the Deep Peatland Sites

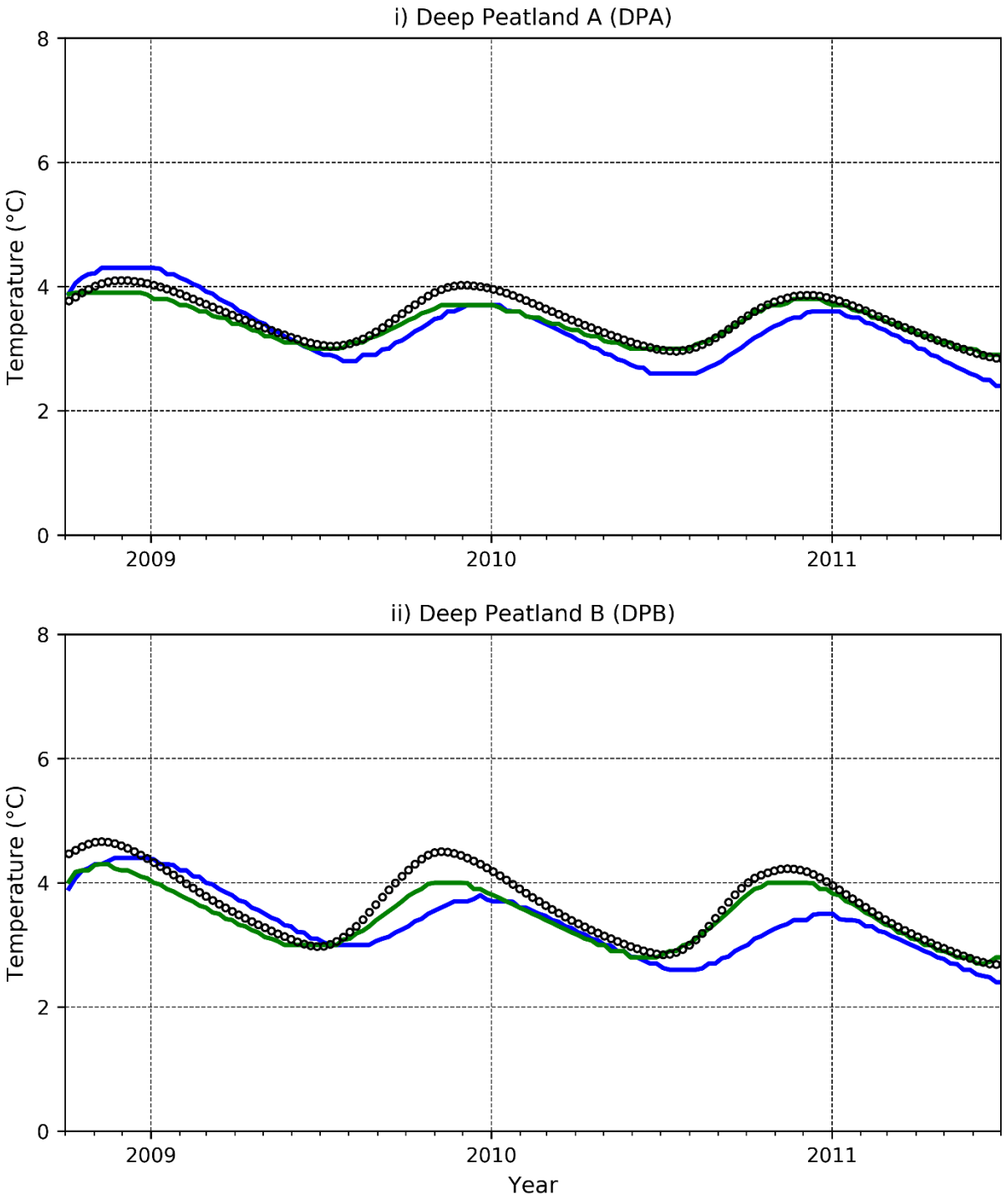

Figure 5-28 Observed (Black) and Simulated (Original-Blue, Updated-Green) Weekly Average Temperatures for -300 cm at the Deep Peatland Sites

The updated residuals at both the deep peatland sites showed a decreased range compared to the original code but were only closer to 0 in 2009 (Figure 5-29). The residuals also tended to be slightly better the upland pine sites; however, it was difficult to identify any trends as most of the residuals had very small ranges of less than 0.25 ºC and were within +/- 0.5 ºC of observed temperatures. There was even less of a difference in residuals between sites with the updated code at -300 cm (Figure 5-30), which is expected since the average temperature at the dampening depth is used to estimate the temperature at the bottom boundary condition. To improve calibration an average temperature that varies by year would be required.

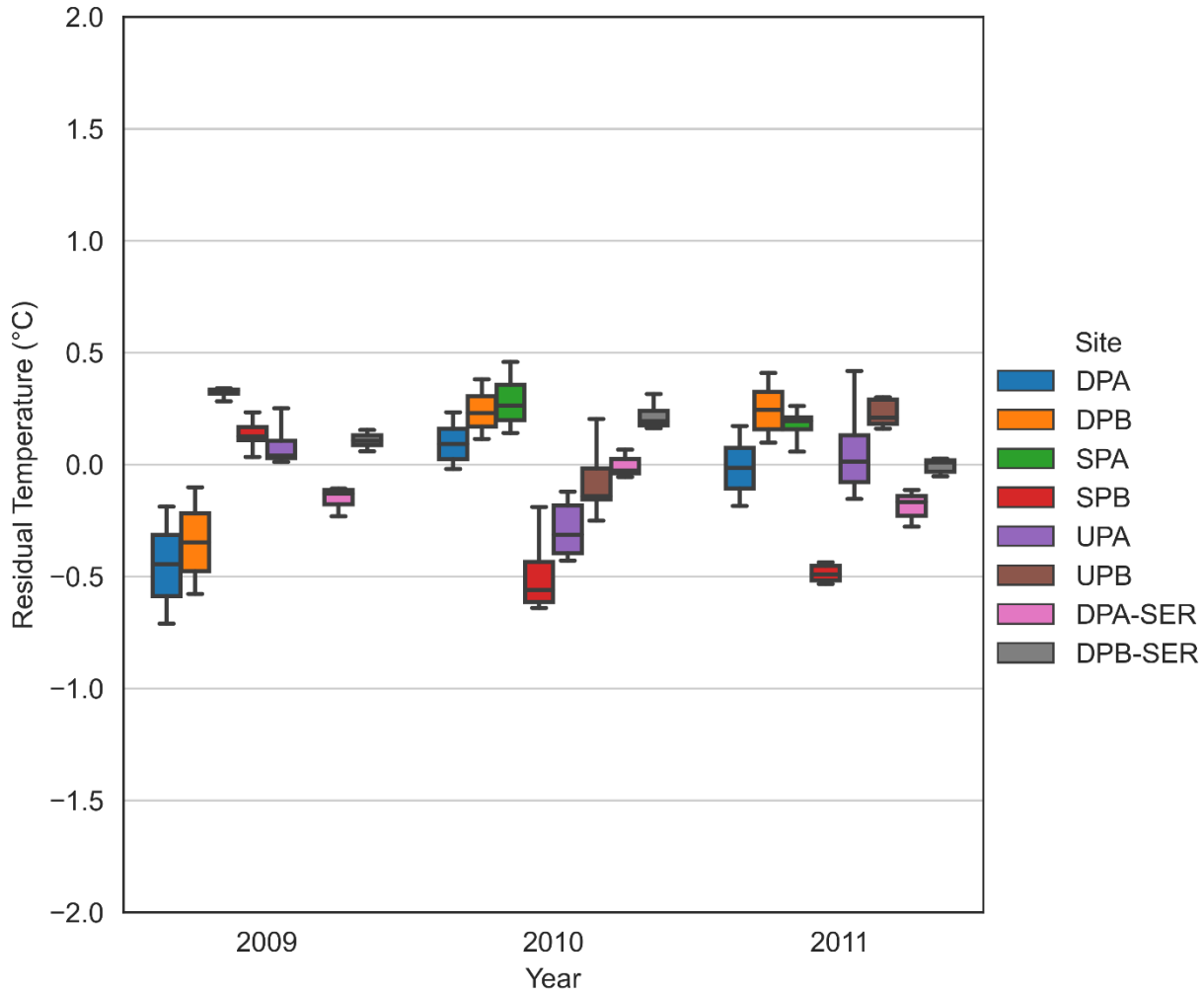

Figure 5-29 Winter Residuals for Weekly Averaged Observed Temperatures at -200 cm for Ecological Sites with Original SHAW code and the Deep Peatland Sites using Updated SHAW Series code (SER)

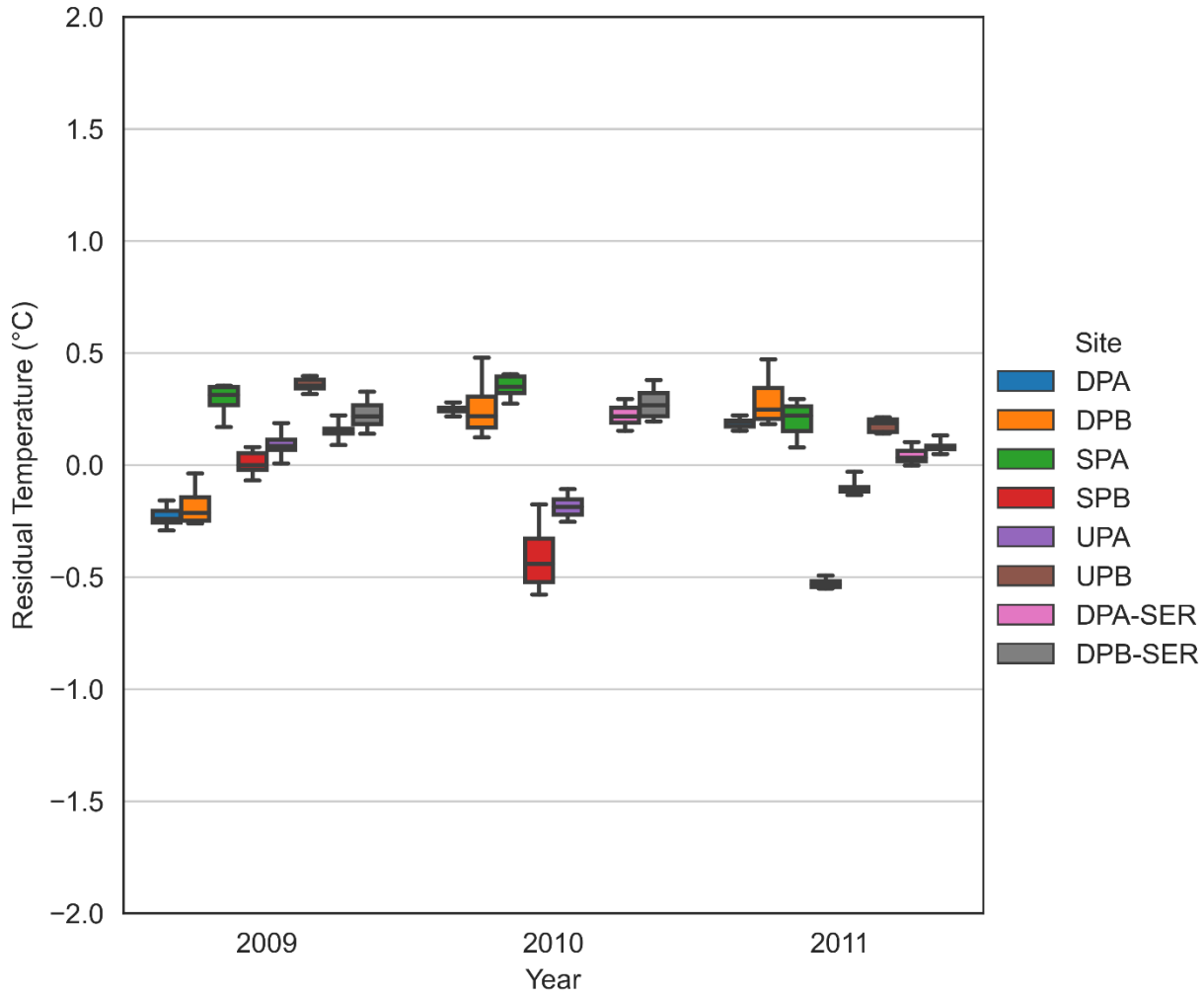

Figure 5-30 Winter Residuals for Weekly Averaged Observed Temperatures at -300 cm for Ecological Sites with Original SHAW code and the Deep Peatland Sites using Updated SHAW Series code (SER)

5.4.6 Moisture Contents

In the updated SHAW simulations, the saturated and residual moisture contents were fixed to prevent PEST from estimating parameters resulting in a drier than expected moisture profile. As discussed previously, the observed moisture contents at -10 cm for both the deep peatland sites were from probes placed in elevated hummocks, resulting in low observed moisture contents. The observed moisture contents during the summer between the two winters of the Phase 2 field survey were always above 0.3 m^3 m^{-3}, so the residual moisture content was set to 0.3 m^3 m^{-3} to ensure the simulated results were always wetter than observed (Figure 5-31). Similarly, the observed saturated and residual moisture contents were set to 0.85 and 0.70 to ensure a simulated

moisture content slightly above 0.8 m^3 m^{-3} at -50 cm (Figure 5-32) and at -100 cm (Figure 5-33). No analysis on residuals was performed as the purpose of the model was to simulate temperatures.

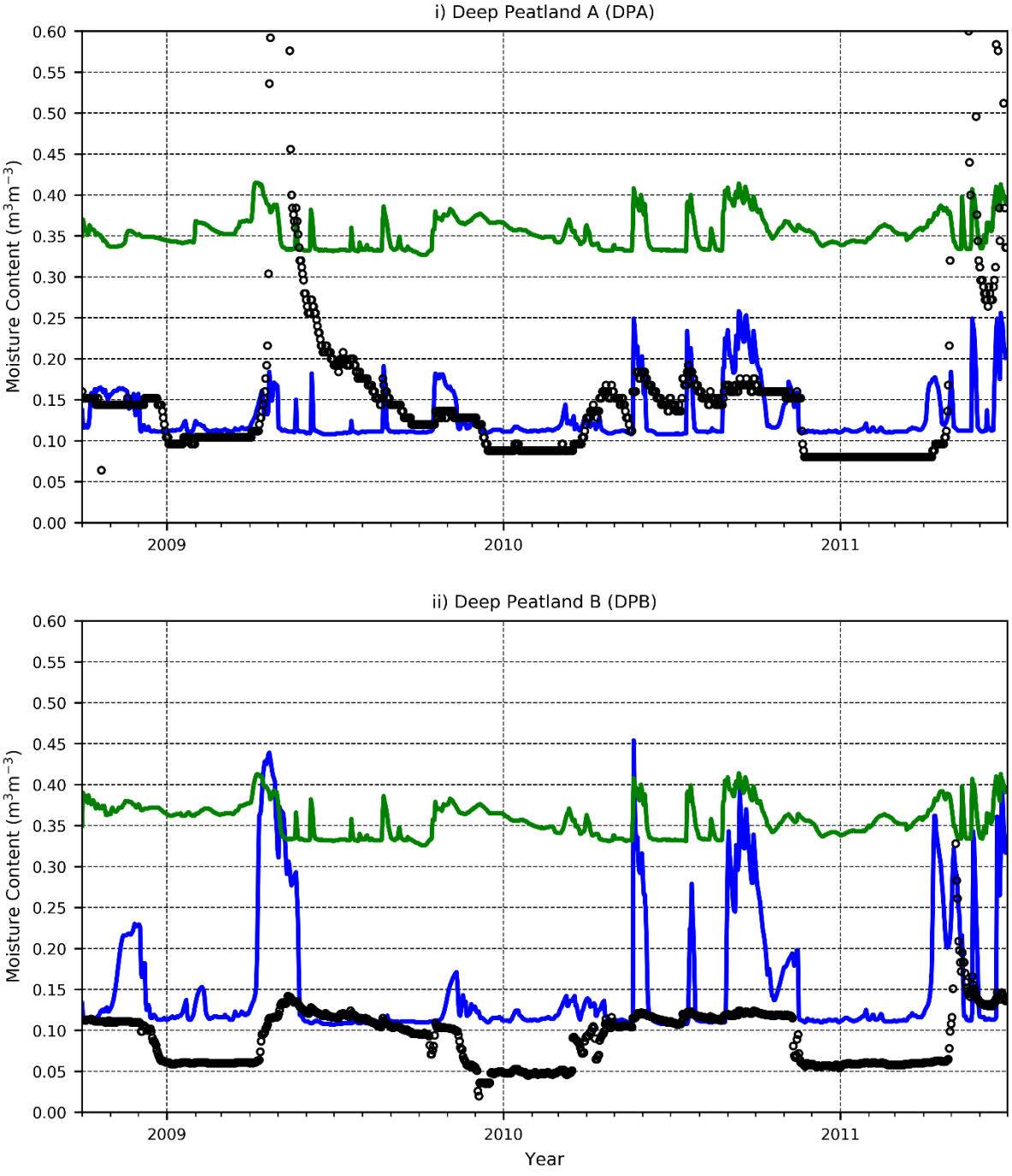

Figure 5-31 Observed (Black) and Simulated (Original-Blue, Updated-Green) Daily Average Moisture Content for -10 cm at the Deep Peatland Sites

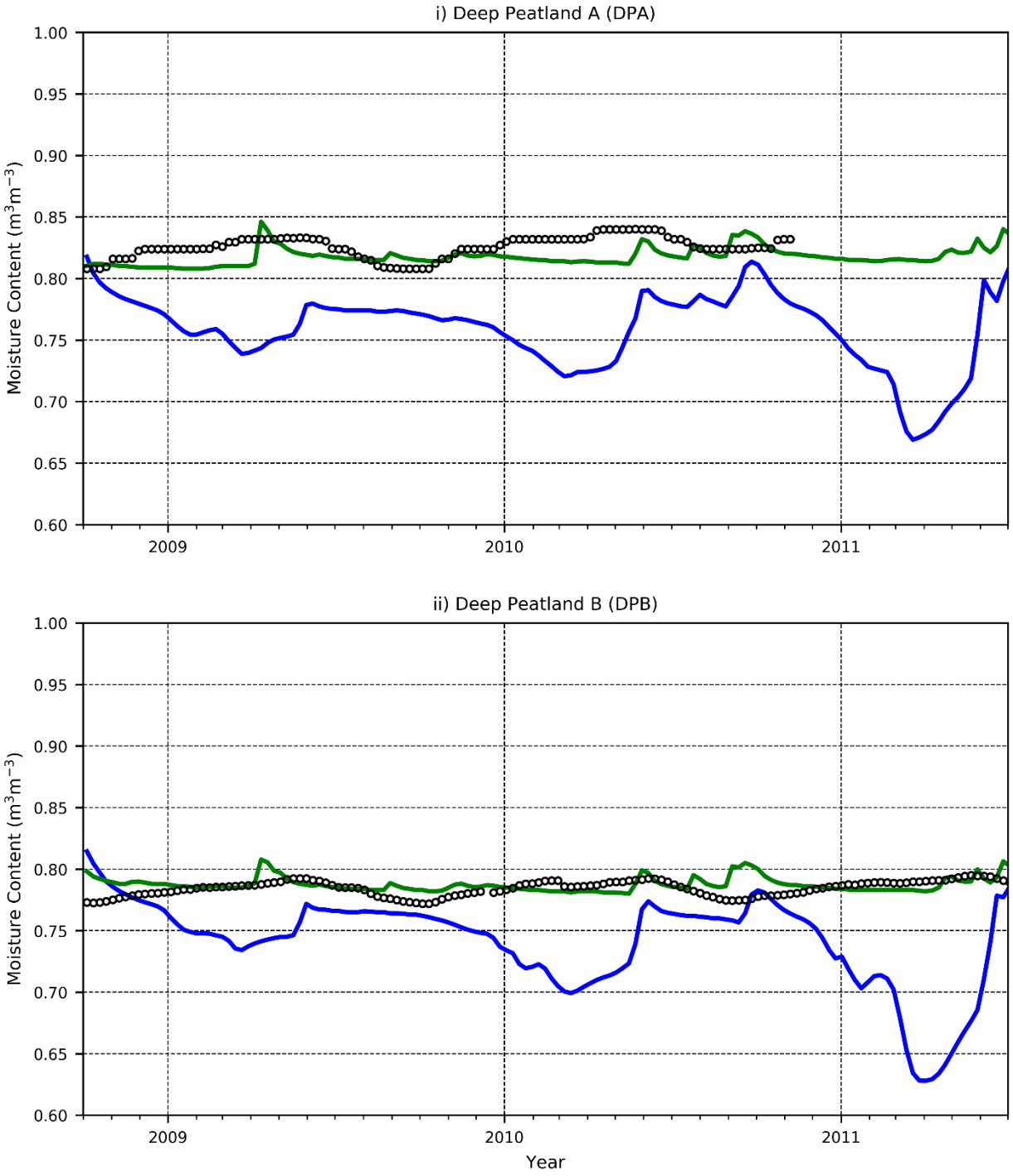

Figure 5-32 Observed (Black) and Simulated (Original-Blue, Updated-Green) Daily Average Moisture Content for -50 cm at the Deep Peatland Sites

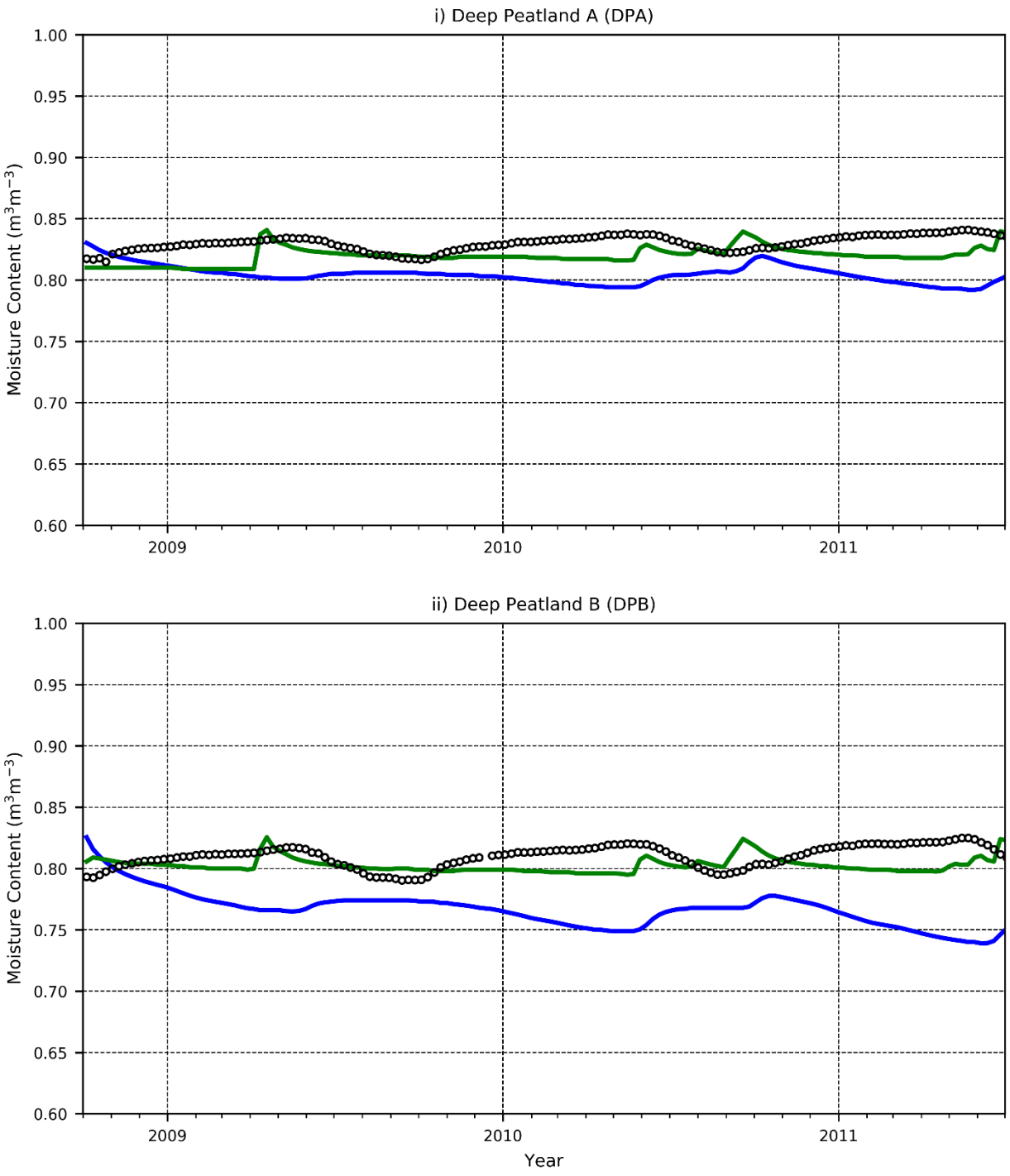

Figure 5-33 Observed (Black) and Simulated (Original-Blue, Updated-Green) Daily Average Moisture Content for -100 cm at the Deep Peatland Sites

5.4.7 Estimated Parameters

PEST estimated parameters for the three snowpack coefficients, dry bulk densities, the average temperature used at the dampening depth, and plant clumping (Table 5-8). The snowpack coefficient a_{sp} (Equation 5-4) was estimated at 0.009 W m^{-1} °C^{-1}, less than half of the SHAW predefined constant of 0.021 W m^{-1} °C^{-1}, while the exponent coefficient b_{sp} was estimated at double the original value at 4.14 compared to 2.00. There was less of a difference between snowpack coefficients b_{sp}, with an estimated value of 2.12, almost 85% of the original value and became insensitive as b_{sp} was increased.

Table 5-8 Estimated Parameters for the Orignal and Updated SHAW Model

		Original SHAW		Updated SHAW	
Parameter	Units	DPA	DPB	DPA	DPB
Snowpack Coefficient a_{sp}	W m^{-1} °C^{-1}	0.021	0.021	0.009	0.009
Snowpack Coefficient b_{sp}	W m^{-1} °C^{-1}	2.51	2.51	2.12	2.12
Snowpack Coefficient c_{sp}	Unitless	2.00	2.00	4.14	4.14
Zone 1 Bulk Density (Moss)	(Dry) kg m^{-3}	50	50	124	157
Zone 2 Bulk Density (Peat)	(Dry) kg m^{-3}	187	141	183	246
Zone 3 Bulk Density (Peat)	(Dry) kg m^{-3}	201	208	143	227
Zone 4 Bulk Density (Peat)	(Dry) kg m^{-3}	186	197	126	129
Zone 5 Bulk Density (Peat/Soil)	(Dry) kg m^{-3}	297	1195	424	1238
Zone 6 Bulk Density (Soil)	(Dry) kg m^{-3}	1216	1242	1411	1345
Average Temperature	°C	2.50	2.59	2.95	2.82
Plant Clumping	Unitless	0.62	0.97	0.12	0.14

Dry bulk densities in the organic layer were very similar to the original model and were within observed range of densities from Alberta's Boreal Plains peatlands, since they were used as bounds in PEST (Hokanson et al. 2016). The only noticeable difference was in the moss layer (-10 cm) with the estimated bulk density always at the lower bound of 50 kg m^{-3}, to reduce the thermal conductivity. The updated SHAW model however estimated the bulk density of the moss layer at 124 and 157 kg m^{-3}, roughly three times greater than the original SHAW model estimates at the lower observed bound in Boreal Plains peatlands. The estimated mineral soil bulk densities of the updated model were also like the original values and ranged from 1,238 to

1,411 kg m^{-3}. DPA's estimated bulk density at -200 cm of 424 kg m^{-3} is slightly on the high end of observed peat densities and is likely beginning to mix with the mineral soils.

The estimated average temperature, which is used to calculate the temperature at the lower boundary of the model, was slightly higher in the updated model at approximately 2.9 ºC. The estimated average temperature was still 1 ºC less than the average temperature estimated at the shallow peatland and upland sites. The lower estimated temperature is likely due to the infiltration of snowmelt in the spring which the model does not simulate.

The biggest difference is estimated parameters between the original and updated SHAW models in the deep peatlands was the clumping factor. The plant clumping factor is used in representing radiation transfer from the plants to the upper most surface layer and can range from 0 to 1, with zero eliminating all radiation interception by plants. While the original SHAW model had a high degree of radiation interception by the plant's crown, the updated SHAW model estimated a much lower clumping factor of 0.12 and 0.14. It is possible that the very low estimated clumping factors was PEST trying to reduce snowmelt in the early spring when simulated temperatures were warmer than observed (Figure 5-19, Figure 5-20). Due to the low albedo of the black spruce trees specified in the model at 0.05, the simulated snowpack begins to melt very quickly in March from the longwave radiation emitted from the crown, which is recorded in the energy balance output files. However, the observed snowpack only melts very quickly underneath the black spruce crown with snow and ice being observed into May outside of the tree wells (Figure 4-12). Thus, it is likely that additional investigations are needed to adequately simulate snowmelt within black spruce peatlands and would require a three-dimensional model.

5.5 Discussion

PEST was able to estimate a reasonable set of parameters for the pine upland sites to accurately simulate the observed subsurface temperatures with the available weather data, The selected parameter set was able to achieve a range of mean wintertime thermal residuals of -0.52 to 0.45 ºC for all depths (Table 5-9, Table 5-10). The pine upland site simulations verified that by altering the thermal resistance and capacity of each of the six thermal zones the observed soil temperatures could be reproduced over a three-year period with a maximum root mean squared error (RMSE) of 0.97 ºC and an average for all depths of 0.41 ºC (Table 5-9, Table 5-10). While PEST was able to estimate a reasonable set of parameters for the shallow peatland sites, it was

not able to achieve as good a match to observed subsurface temperatures for the upland sites. For the shallow peatland sites the maximum RMSE was 1.77 ºC and the average for all depths was 0.67 ºC (Table 5-9 Table 5-10).

Table 5-9 Mean Residual (Observed – Simulated) and Root Mean Squared Error (RMSE) for Daily Simulated Wintertime (Jan-Mar) Subsurface Temperatures (-10, -30, -50 cm) at Each Ecological Site with Original SHAW code in Parallel and in Series (SER) for both Deep Peatland Sites

	Thermal Residual -10 cm		Thermal Residual -30 cm		Residual -50 cm	
	Mean (ºC)	RMSE (ºC)	Mean (ºC)	RMSE (ºC)	Mean (ºC)	RMSE (ºC)
DPA	3.34	3.75	1.33	1.36	0.81	0.83
DPA-SER	0.26	0.53	0.15	0.28	-0.12	0.21
DPB	2.61	2.93	1.05	1.08	0.80	0.81
DPB-SER	0.30	0.59	-0.04	0.22	-0.05	0.19
SPA	1.58	1.77	0.21	0.42	0.53	0.56
SPB	-0.16	1.53	-0.61	1.13	0.09	0.47
UPA	0.45	0.97	0.03	0.53	-0.07	0.45
UPB	0.16	0.64	-0.06	0.38	0.14	0.32

Table 5-10 Mean Residual (Observed – Simulated) and Root Mean Squared Error (RMSE) for Weekly Simulated Wintertime (Jan-Mar) Subsurface Temperatures (-100, -200, -300 cm) at Each Ecological Site with Original SHAW code in Parallel and in Series (SER) for both Deep Peatland Sites

	Thermal Residual -100 cm		Thermal Residual -200 cm		Residual -300 cm	
	Mean (ºC)	RMSE (ºC)	Mean (ºC)	RMSE (ºC)	Mean (ºC)	RMSE (ºC)
DPA	0.29	0.37	-0.12	0.29	0.07	0.23
DPA-SER	-0.13	0.15	-0.11	0.14	0.14	0.16
DPB	0.18	0.32	0.05	0.30	0.12	0.26
DPB-SER	-0.23	0.24	0.11	0.14	0.20	0.22
SPA	0.27	0.30	0.26	0.28	0.29	0.30
SPB	-0.22	0.46	-0.29	0.42	-0.31	0.40
UPA	-0.52	0.56	-0.05	0.22	-0.06	0.14
UPB	0.07	0.24	0.08	0.20	0.27	0.28

Initially PEST was unable to estimate a set of parameters for the deep peatland sites that reproduced the observed subsurface temperatures. The initial maximum mean thermal residual of 3.34 ºC at DPA at -10 cm (Table 5-9) indicated that the simulated wintertime temperatures were on average 3 ºC colder than observed. By estimating the thermal conductivity of the top 10 cm of the subsurface profile, i.e., the living moss layer, in series instead of parallel the maximum RMSE of 3.75 ºC at DPA (-10 cm) was lowered to 0.53 ºC (Table 5-9). The average RMSE for all depths at the deep peatland sites was lowered from 1.04 ºC to 0.26 ºC with the updated code, and was less than the average RMSE of 0.41 ºC that was achieved at the upland sites (Table 5-9 Table 5-10). Therefore, the original SHAW code had to be updated to provide better representation of a living moss layer with a new thermal conductivity algorithm. The new algorithm with the living moss layer represented in series was able to achieve a satisfactory calibration of the deep peatland sites (DPA, DPB) with residuals less than the upland sites (UPA, UPB).

To calibrate the SHAW model to the observed deep peatland temperatures the thermal resistance of the moss layer (Zone 1) had to be calculated in series instead of parallel which drastically reduces the layer's thermal conductivity. Also, revised snowpack thermal conductivity coefficients had to be estimated. The improved calibration obtained with the serial representation of the moss thermal conductivity indicates the hypothesis that it is likely the insulation of the moss layer and not the increased release of latent heat or sap recirculation that causes the shallower than expected depth of frost in the deep peatlands, should be accepted.

While the series formulation was used in the updated SHAW model, the constituents are probably actually in composite, with the organic material of the moss stalk in parallel with the layers of leaves, water, ice, and air which are in series (Equation 5-7, Figure 5-34). However, the volumetric ratios of the moss stalk and leaflets are unknown and could not be estimated due to the non-uniqueness of the equation with respect to dry bulk density already being estimated. For this reason, it is expected that the estimated dry bulk density for the moss would be higher than the observed density to compensate for the thermal connection of the sphagnum stalk.

Equation 5-7 Thermal Conductivity for Sphagnum Moss Layer in Composite

$$K = \frac{K_o}{x_{stalk}} + \left(\frac{K_o}{(x_{leaf})} + \frac{K_w}{x_w} + \frac{K_i}{x_i} + \frac{K_a}{\left(1-(\rho_{dry}/\rho_{moss})-(x_w+x_i)\right)}\right)/(1 - x_{stalk}) \quad \text{.....(5-7)}$$

Where:

K_o is the thermal conductivity of the organic material (0.25 W m^{-1} °C^{-1})
K_w is the thermal conductivity of the liquid water (0.57 W m^{-1} °C^{-1})
K_i is the thermal conductivity of the frozen soil water (ice) (2.2 W m^{-1} °C^{-1})
K_a is the thermal conductivity of the air/vapour (0.025 W m^{-1} °C^{-1})
X is the volumetric fraction for leaf, stalk, water (w) and ice (i)
ρ_{dry} is the user specified bulk density (kg m^{-3}) for the node
ρ_{moss} is the density (kg m^{-3}) for an organic particle (1300 kg m^{-3})

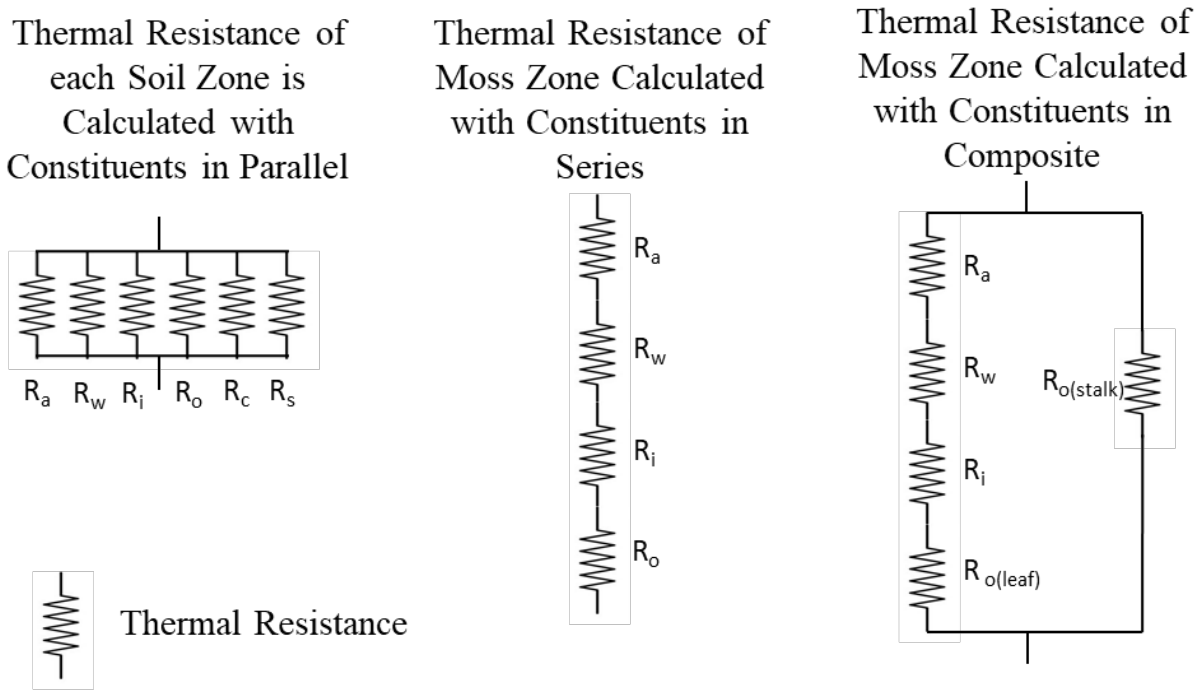

Figure 5-34 Conceptual Schematic of Thermal Resistance in Parallel (Soil), Series (Moss) and Composite (Moss) Comprised of Air (a), Water (w), Ice (i), Organic (o), Clays and Silts (c), and Sand (s) Constituents

Further by simulating the moss layer in series it was demonstrated how it was possible for the black spruce root zone not to freeze during the winter and could allow for snowmelt from the crown to infiltrate to the subsurface from the black spruce cavity. In the original SHAW model, and also predicted by Stefan's equation the entire black spruce tree root zone, which is confined to the unsaturated zone (Lieffers and Rothwell 1987), would be below 0 ºC and inhibit the flow of water. While in the updated SHAW model the simulated maximum depth of frost never fully penetrated the vadose zone.

5.5.1 Maximum Depth of Frost

The original SHAW model estimated the maximum depth of frost to always exceed 30 cm in the deep peatland sites (Table 5-11), the approximate depth of the groundwater table, for extended periods of time (Figure 5-21) with the initial stages of permafrost developing. The presence of ice through the entire unsaturated zone in the early spring would restrict the drainage of liquid water from the black spruce tree cavities, resulting in ponding within the tree well. If water was allowed to pond within the tree well it would eventually refreeze as solid ice drastically increasing the thermal conductivity and encasing the sphagnum moss, which is harmful to the moss colony and could be lethal. Also as demonstrated with Stefan's equation (Equation 3-3) the maximum depth of frost occurs at saturation (Figure 3-16) because the increase in moisture content results in a greater change of thermal conductivity compared to the increase in latent heat.

Table 5-11 Maximum Depth of Frost at Deep Peatland Sites for the Original and Updated SHAW Model

	Observed		Original SHAW		Updated SHAW	
	DPA	DPB	DPA	DPB	DPA	DPB
Year	Maximum Depth of Frost (cm)					
2009	<10	<10	36.7	35	5	5
2010	10-30	10-30	45.1	36.7	17.5	12.5
2011	10-30	10-30	62.7	48.6	22.5	17.5

That was the case with the pine shallow peatland (SPB) which had very deep frost layer with observed temperatures as cold as -4 °C at -10 cm (Figure 5-7). If solid ice were to form at the ground surface, the thermal conductivity would drastically increase to 2.2 W m^{-1} $°C^{-1}$ resulting in extreme losses of heat from the wet peat. Even colder results were observed when peat was used

as a cover at reclaimed sites near Fort McMurray, Alberta with subsurface temperatures dropping to below -20 °C at an elevation of – 5 cm (Zhao and Si 2019). The pine shallow peatland (SPB) did not have a sphagnum moss layer, as the surface was mostly a litter of pine needles which seemed to inhibit sphagnum moss growth. It was also unlikely that there was a moss layer over the peat cover at the reclaimed site near Fort McMurray since it was being used for jack pine and aspen seedlings (Zhao and Si 2019)

The updated SHAW model not only simulated much shallower maximum depths of frost, ranging from 5 to 22.5 cm, but also simulated frozen ground for much shorter periods of time (Table 5-11). Unlike the original SHAW model in which the unsaturated zone was completely frozen until the beginning of May, in the updated model the maximum depth of frost lasted for a week or two in early January. By February the simulated frost from the updated model was only within the moss layer at a depth less than 10 cm, allowing for snowmelt to infiltrate from the tree cavity out radially through the shallow black spruce root zone.

5.5.2 Snowpack Coefficients

The original estimated snowpack coefficients in the updated model resulted in lower than reasonable thermal conductivities for the simulated density. However, the simulated snowpack depths were typically half of the observed snowpack depths often with higher densities (Table 5-12). For the SHAW model to accurately simulate the snowpack yearly adjustments to the precipitation data would be required along with changes to the snowpack melting algorithm, which was not the focus this investigation. Further it is likely that a three-dimensional model would be needed to accurately capture the spatial distribution of the snowpack, especially when considering the black spruce tree wells.

However, by allowing PEST to estimate the snowpack thermal conductivity coefficients (Equation 5-4) the updated SHAW model was able to simulate an equivalent resistance for the snowpack regardless of the depth. Considering that the thermal conductivity of the moss layer could be estimated from the summer temperatures, the estimated snowpack thermal conductivity was what was required to calibrate the model. Thus, if the SHAW model was further updated to improve the simulation of snowpack depths and density, a new set of coefficients would need to be estimated that would result in a similar resistance.

Table 5-12 Observed and Simulated Snowpack Depths, Snow Water Equivalent, and Density for Deep Peatland Sites

	Depth (cm)			Snow Water Equivalent (cm)			Density (kg m^{-3})		
	Observed		Simulated	Observed		Simulated	Observed		Simulated
Date	DPA	DPB		DPA	DPB		DPA	DPB	
1/17/2009	71	74	41	9	9	9	127	124	216
	70	87		7	10		97	119	
	70	71		7	9		94	126	
3/3/2009	77	80	51	19	22	13	247	270	245
	65	73		15	15		237	206	
	71	60		15	13		209	213	
3/1/2010	43	35	30	7	8	10	164	215	326
	40	26		8	7		207	260	
	37	38		5	6		137	163	
2/22/2011	70	76	37	14	17	11	204	225	282
	73	69		14	16		188	226	
	72	69		16	14		226	204	

For example, on January 17, 2009 the simulated snowpack density was 216 kg m^{-3} resulting in an estimated thermal conductivity of 0.138 W m^{-1} °C^{-1} with the original snowpack coefficients, and a thermal conductivity of 0.012 W m^{-1} °C^{-1} with the estimated coefficients. The estimated thermal conductivity is less than air due to the empirical nature of the equation which suggests that there are issues with the simulation of the snowpack thickness and snowmelt processes. While an order of magnitude difference in thermal conductivity is not reasonable, it does not reflect the difference in snowpack depth and density which ultimately affect the total resistivity. However, using the observed snowpack density for the same date, approximately 100 kg m^{-3}, the estimated thermal conductivity with the original coefficients would be 0.046 W m^{-1} °C^{-1}, closer in value to the thermal conductivity estimated with the updated coefficients for the simulated density.

The observed and simulated total resistances for the snowpack can also be estimated for January 17, 2009 by dividing the observed (70 cm) and simulated (41 cm) depths by the thermal conductivity. The observed resistance for the snowpack was calculated to be 15 m^2 °C W^{-1}, half the simulated resistance of 32 m^2 °C W^{-1}. Therefore, while there was an order of magnitude difference in the thermal conductivities estimated with the new snowpack coefficients, it only

resulted in the total resistance being different by a factor of 2, which while reasonable does suggest that there may be additional processes missing from the simulation.

5.5.3 Freezing of Sphagnum Moss

One major assumption of the SHAW model is that sublimation only occurs at the surface of the snowpack and never within the subsurface. However, mosses have the ability to initiate ice nucleation on their leaf surfaces and accumulate water vapour as ice through sublimation (Moffett 2015). If ice were to form in the moss layer from water vapour, as opposed to liquid water, then the latent heat of energy released would be 2,838 kJ kg^{-1} instead of 334 kJ kg^{-1}, almost an order of magnitude greater. The formation of these ice crystals was also observed on the sphagnum moss leaflets during the installation of the moisture content probes, which required the moss layer to be cored and removed. However, it is also possible that the ice crystals formed were due to internal sublimation of the snowpack, depth hoar, and future studies would be required to determine which process is responsible for the crystal formation. It is unlikely though that the conditions for depth hoar would only exist around the black spruce trees, and not within the cutline since air temperature and wind speed are the main factors contributing to depth hoar (Domine et al. 2018).

The Bergeron-Findeisien mechanism (Pruppacher and Klett 2012) could also help explain why the shallow peatlands had a deeper depth of frost compared to the deep peatlands, which typically had similar moisture contents near the ground surface. While the moisture contents were similar at -10 cm it is highly unlikely that the vapour densities were similar, with the deep peatlands having higher vapour densities indicated by the saturation of the -50 cm probes, approximately double the moisture content of the shallow peatlands (Figure 5-14). The higher vapour densities would increase the sublimation rates of ice formation on the moss leaflets, resulting in releases of large amounts of latent heat. For example, 1 gram of liquid water freezing would release the same amount of energy as 0.12 grams of vapour freezing.

The inability for SHAW to simulate changes in latent heat due to the sublimation of ice on the sphagnum moss cells could have also contributed to the low estimation of the thermal conductivity of the snowpack. It is also possible that the large releases of latent heat due to sublimation were the cause of the highly dampened temperature changes observed in the sphagnum moss layer with little or no snowpack (Figure 4-17).

6 SUMMARY, CONCLUSIONS AND RECOMMENDATIONS.

6.1 Summary and Conclusions

Additional field investigations and analysis conducted after initial investigations provided greater insight into the thermodynamics of black spruce treed peatlands. In Chapter 3 the hypothesis that the black spruce deep peatland sites had shallower depths of frost than the pine upland sites due to additional releases of latent heat from the increased moisture of the peat was rejected based upon the application of Stefan's equation (Equation 3-3). While Stefan's equation was found to reasonably predict frost depths at pine upland sites, and to some degree shallow peatland sites, it predicted a frost depth 2 to 3 times deeper than observed for the black spruce deep peatlands (Table 3-6). Further it was demonstrated that while saturation of mineral soils will reduce frost depth, saturation of peat will increase frost depth (Figure 3-16).

It was hypothesised that the black spruce trees conduct sensible heat down their trunks warming the root zone throughout the winter via sap recirculation causing a reduction in the depth of frost. In Chapter 4 additional temperature measurements were obtained from living and dead black spruce tree trunks, the root zone, and the overlying moss layer to test this hypothesis that the recirculation of sap was warming the subsurface throughout the winter. The observed data for the winter months showed this hypothesis to be false, based upon similar observed temperatures in living and dead tree trunks (Figure 4-24,Figure 4-25), but also based upon the lack of correlation between the warming of the root zone and air temperatures (Figure 4-31, Figure 4-32). Considering that the short periods of observed warming, i.e. when the change in the 5-day moving average temperature was positive, often occurred when the maximum daily temperature was below freezing and thus could not be due to the transfer of heat from the atmosphere to the subsurface through sap circulation. The observed periods of warming were also minor and infrequent throughout the winter and was mostly likely due to the release of metabolic heat from either the black spruce roots or the bacteria within the soil and did not appear to be the reason for the shallower than expected frost depth.

However, observations in April provided a strong indication that sap return flow through the phloem was warming the root zone. Throughout April there were significant differences in daytime temperatures between adjacent living and dead trees at the base of their trunks, with the living tree being much cooler than the dead tree on warm days (Figure 4-35). The observed

reduced temperatures at the base of the living trunk were likely due to the flow of sap from the cooler root zone to the branches of the tree crown. During the same periods when the living tree trunk was cooler than the dead tree trunk, the root zone was warming at rate faster than the overlying moss layer and to higher temperatures (Figure 4-36). The observed temperatures in the root zone not only demonstrated a very strong correlation with the trunk temperatures but could not be explained by overlying moss temperatures. It was concluded these observations support the hypothesis that sap recirculation was occurring in April and that it can affect subsurface temperatures.

While warming of the subsurface through sap recirculation was likely occurring in April, it did not seem to be the reason for the shallower than expected frost line. However, during the same wintertime field study mosses were observed to have a very strong insulating effect, with moss temperatures inside a monitored tree well always within 0.5 ºC of the moss temperatures outside of the tree well where there was a much thicker snowpack (Figure 4-18, Figure 4-19). It had been expected that with minimal to no snowpack within the tree well that the observed wintertime temperatures would be much colder than the temperatures obtained from under the snowpack outside the tree well. However, that was not the case. It became apparent that the living moss layer likely had different thermal properties than the underlying peat, and that the thermal conductivity of the peat probably is not representative of that of the sphagnum moss.

Due to the physiological structure of the sphagnum moss, with the single cell layer leaflets and being non-vascular it was hypothesised that the thermal conductivity of the moss should be calculated in series and not in parallel. A series representation and estimation of the thermal conductivity is typically assumed to be the minimum that the thermal conductivity can be for a layer given the volumetric ratios of the constituents. To test this hypothesis an original SHAW numerical model was created for each of the six ecological sites using the same weather station data and calibrated to the observed subsurface temperatures and moisture contents observations at each site using PEST. While the original SHAW code was able to reasonable simulate subsurface temperatures at the upland sites, and to some degree the shallow peatlands, at deep peatland sites it predicted deeper than observed frost depths, similar in depth to what was predicted by Stefan’s equation. The original SHAW model code was then modified to estimate

the thermal conductivity of the moss zone in series instead of parallel and the model recalibrated using PEST.

Although the recalibrated model results for deep peatlands improved with a series representation of the moss zone it became apparent that the snowpack thermal conductivity coefficients also needed to be estimated due to PEST's inability to match both summertime and wintertime temperatures. Thus, PEST was used to estimate a dry bulk density for the moss, which is used to calculate the moss thermal conductivity (Equation 5-6) that best matched the summertime observed temperatures. The moss thermal conductivity was then used with the revised snowpack thermal conductivity estimates providing the additional insulation required to match wintertime temperatures. By simulating the moss in series, and estimating new snowpack coefficients (Equation 5-4) the wintertime temperatures residuals for the deep peatlands were greatly improved, and were comparable or even better than the residuals for the uplands (Figure 5-20, Figure 5-22, Figure 5-24). Further, the updated SHAW model was able to accurately predict the observed depth of frost at the deep peatland sites (Table 5-11). The improved calibration of the deep peatlands with the updated SHAW code and the accurate prediction of the frost depth strongly supports the hypothesis and that a series representation for estimating the thermal conductivity of the moss layer is more representative than a parallel representation.

There are still some unanswered questions and uncertainties regarding the proposed conceptual model for the thermodynamics and temperature modelling of the black spruce peatlands, especially considering the lower than reasonable snowpack thermal conductivity required to obtain representative simulation results. It is unknown if the unreasonable estimation of snowpack thermal conductivity was due to inaccurate representation of the snowpack's physical characteristics, such as depth and density, in the simulation or due to another process not represented in the SHAW model. The SHAW model does not allow for the simulation of heat transfer through sap recirculation or the loss of latent heat due to sublimation in the moss layer. Additionally, it is likely the moss layer is actually a composite configuration, with the moss leaflets in series with the air and water, but in parallel to the moss stalks (Equation 5-7) rather than simply a series configuration as represented in the modified SHAW model.

Considering the above discussion, a schematic diagram of a revised proposed conceptual model of heat flow within a black spruce peatland which includes: 1) the variable resistance of the trunk

due to sap flow; 2) the estimation of the moss layer's thermal conductivity in composite; and 3) the inclusion of sublimination (S) in the release of latent heat from the moss layer is presented in Figure 6-1.

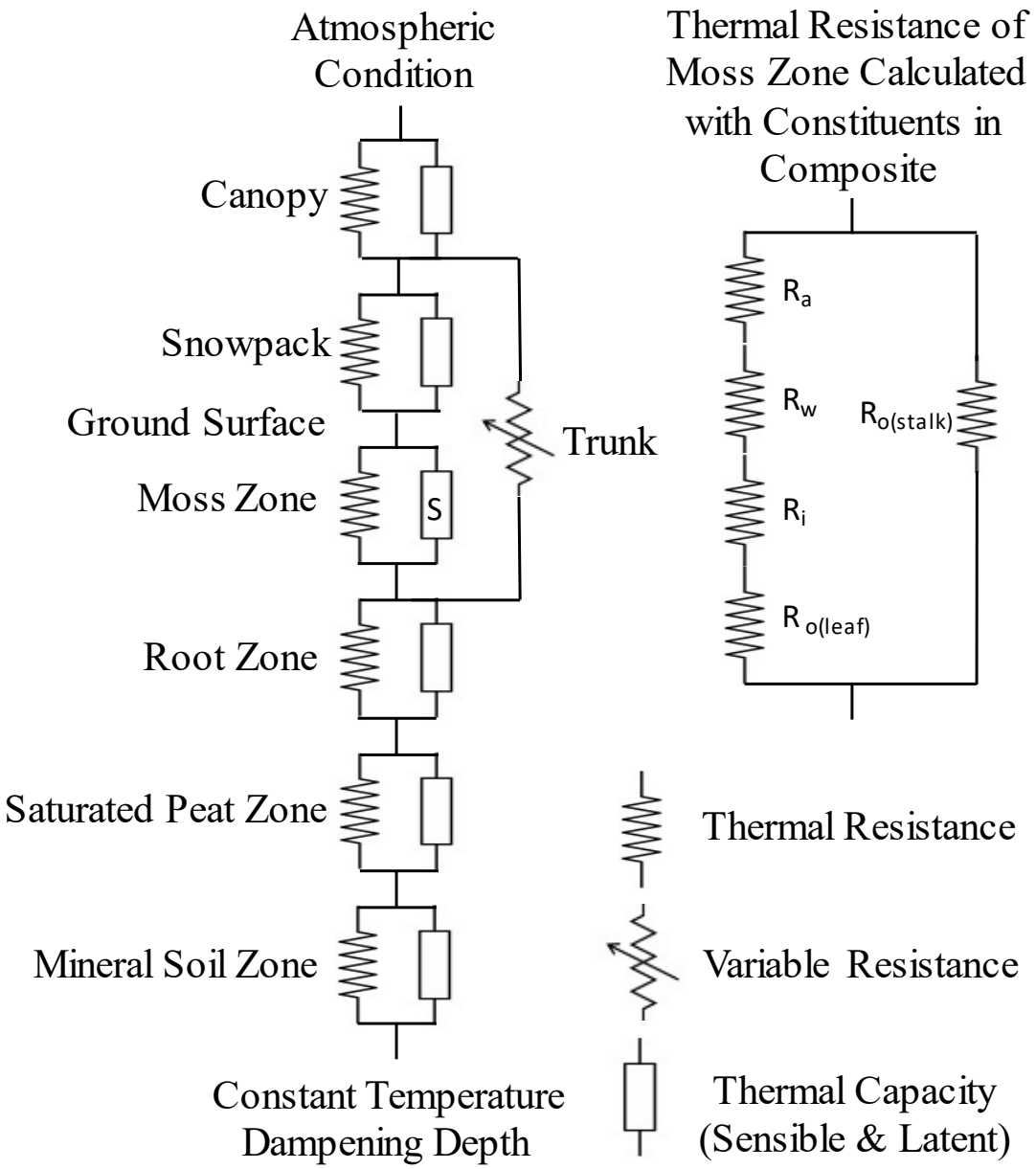

Figure 6-1 Schematic of a Revised Proposed Conceptual Model for Heat Flow in Black Spruce Peatlands with Variable Resistance Due to Sap Flow (Trunk), Latent Heat of Sublimation in the Moss Zone (S), and the Thermal Resistance of the Moss in Composite (Moss) Comprised of Air (a), Water (w), Ice (i), and Organic (o) Constituents

Further, the existence of wintertime infiltration was confirmed to occur at black spruce peatlands through field observations and measurements. Snow captured by the black spruce tree crown would quickly melt during sunny days, especially on the southern exposure, resulting in drip from the tree crown as opposed to throughfall of wet snow (Figure 4-10). The snowmelt drip from the crown was frequently observed and recorded during multiple site visits, but it is unknown if any measurements can be obtained that could differentiate between liquid water dripping from the tree crown from wet snow sliding off the branches, which was only ever observed to occur from the crowns of lodgepole pines. The snowmelt drip from the crown then ran off the frozen surface of the moss layer towards the tree cavity where it likely infiltrated into the subsurface through the thawed root zone.

While the snowmelt drip from the crown was found to result in minor increases in the groundwater table throughout the winter, the unfrozen tree cavity could allow for the capture of upland snowmelt runoff. The crown drip was also the most likely source of water contributing to the minor groundwater increases, a few millimeters per day at most, that occurred after sunny winter days (Figure 4-30). The infiltration of upland snowmelt runoff was likely responsible for the increased groundwater levels over half a meter beginning at the end of March.

It is likely without the presence of black spruce trees on the landscape, the snowmelt would simply pond and eventually runoff the frozen peatland surface, as witnessed within cutlines that became preferential channels for snowmelt (Figure 4-13). The hypothesis that black spruce trees prevent the ponding of snowmelt is further supported by an example of reclaimed peatlands without black spruce trees, in which 80% of the area is covered by ponded snowmelt by mid April and does not infiltrate to the subsurface until sufficient thermal erosion had occurred to create a preferential pathway (Ketcheson and Price 2016). In black spruce peatlands on the natural landscape the black spruce tree cavities can provide the preferential drainage pathway. Further it was demonstrated that the insulation of the moss layer was likely preventing the root zone from freezing, allowing for water captured within the tree cavity to infiltrate laterally to the roots.

The final proposed conceptual model presented for heat flow in black spruce peatlands, along with the observation of wintertime infiltration, suggest a reassessment of the underlying assumptions of hydrological models of Boreal Plains' watersheds is appropriate. While it is not

necessary for the hydrological models to accurately predict subsurface temperatures and the thermal conductivity of moss, it is important to represent preferential pathways for infiltration to occur through black spruce tree cavities while the surface is frozen. This can easily be accomplished by using a very high frozen hydraulic conductivity for peatlands when black spruce trees are present to allow for the infiltration of upslope snowmelt runoff, even when the surface is frozen. It would also become necessary to represent black spruce peatlands as separate hydrological response units, with snowmelt runoff from upland areas being routed through the peatlands.

6.2 Recommendations

The ability for black spruce trees to possibly capture large volumes of upslope snowmelt runoff should be further investigated as a potential important process to consider in tailing ponds closure plans. Current designs for reclaimed wetlands often rely on groundwater fluxes from uplands to maintain groundwater levels, often allowing snowmelt to pond or runoff the frozen peatlands. By planting black spruce trees in reclaimed peatlands, it could be possible to capture the snowmelt runoff from upslope areas, resulting in the peatland becoming a groundwater source instead of a sink. The presence of black spruce trees would also benefit the sphagnum moss by early warming of the subsurface in the spring and creating a moist environment. However, revised reclamation regulations are needed to encourage the planting of black spruce trees, because industry currently favours quick growing species such as aspen and pine in order to meet government criteria for regrowth.

It is recommended that reclamation studies investigate placing more of an emphasis on mimicking the natural landscape as a guide for the design of reclaimed wetlands. To better mimic the natural landscape swales could be dammed, just as beavers would, allowing for water to pond behind the dams. The ponded areas could be backfilled with peat prior to the construction of the dam to an elevation of roughly 50 cm greater than that of the dam (Figure 6-2). The black spruce trees, along with the moss colonies, could then be planted in the flooded back filled peat, allowing for the moss colonies and black spruce tree root zones to be

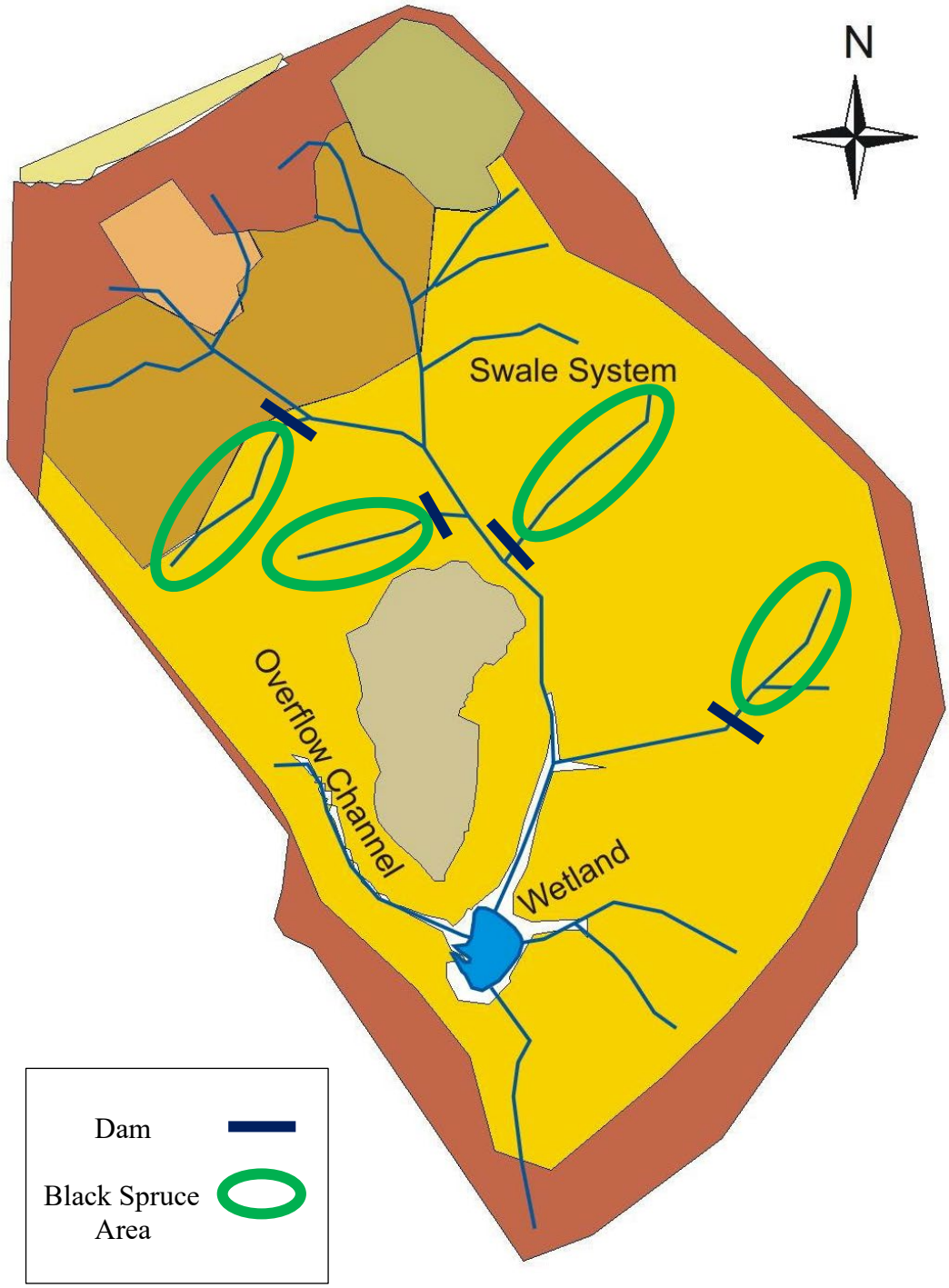

Figure 6-2 Example of Dammed Swales and Black Spruce Plantation Areas for a Reclaimed Site

above the flooded groundwater table. Backfilling the area behind the dams with peat to a slightly higher elevation should prevent the saturation of the black spruce tree root zones and moss layer. By preventing saturation conditions to occur the moss layer should have series thermal conductivity characteristics resulting in better insultation of the subsurface and decreased depth of frost.

Additional investigations are also required to further test the proposed revised schematic for the conceptualization of heat flow within a black spruce peatland which included; 1) the variable resistance of the trunk due to sap flow, 2) the estimation of the moss layer's thermal conductivity in composite, 3) the inclusion of sublimination (S) in the release of latent heat from the moss layer (Figure 6-1).

To further investigate the variable resistance of the trunk and the effect of sap recirculation on subsurface temperatures, future studies should determine if the differences observed in April between living and dead tree trunks (Figure 4-35), continue throughout the summer. To test the hypothesis that sap recirculation is warming the subsurface, temperatures should be observed in all four cardinal directions around the tree from within the root zone and the overlying moss layer. If sap recirculation is warming the subsurface there should be little variation in root zone temperatures between the cardinal directions, with a cooler overlying moss layer. The hypothesis of subsurface warming from circulation of sap is also supported by the concentric nature of the tree wells, suggesting that snow melt is not dependent upon the direction of incoming solar radiation.

If it is found that black spruce trees do warm the root zone through sap recirculation, both in the spring and throughout the summer, it could have a major implication for the simulation of long wave radiation emissions from the black spruce crowns. Currently the very low albedo of black spruce trees results in nearly all the incoming solar radiation being re-emitted as longwave radiation. However, if sap circulation is occurring a portion of the longwave radiation would be directly transferred to the root zone and not re-emitted to the atmosphere and ground surface. It is hypothesised that the transfer of longwave radiation directly to the subsurface via sap recirculation results in the substantial difference in timing between snowmelt overlying black spruce root mats versus in between them. However, further investigations and more detailed

snowpack surveys are required to determine why tree wells are concentric and the reason for the delayed snowmelt in between black spruce tree mats.

In addition to the possible effect sap circulation could have on snowmelt, it could also be of consequence to climate scientists if they are overestimating the longwave radiation emission from black spruce trees. It may be necessary to adjust the albedo of black spruce trees to a higher value in climate models to accurately simulate the actual longwave radiation emitted from the tree crowns. It is still unclear why the presence of black spruce trees result in a cooler ground temperatures, with SHAW simulations in this study requiring an average soil temperature in the deep peatlands of 1.5 ºC less than the uplands, with ForHyM simulations requiring a 1.6 ºC reduction of air temperatures in black spruce stands (Jagtar Bhatti et al. 2006), and with the thawing of permafrost when mean annual air temperatures are above 0 ºC with the removal of black spruce canopies (Mohammed et al. 2017).This effect could be of great importance as climate change scientists often assume increasing the percentage of forest cover would result in a warmer planet due to the decreased albedo (Williams et al. 2021), which may not accurately predict the true emission of longwave radiation from black spruce tree crowns.

Future studies should also investigate the Bergeron-Findeisien mechanism with respect to sublimation rates on sphagnum moss leaflets under varying temperatures and vapour pressures, likely in a laboratory setting, to determine if it is substantial enough to affect the depth of frost. If a larger percentage of the ice is being formed within the moss layer it would drastically reduce the frost depth. If you were to recalculate the depth of frost using Stefan's equation using the estimated thermal conductivity of the moss layer in series, 0.057 W m^{-1} $ºC^{-1}$, and assumed half the ice formation was due to sublimation resulting in an average release of latent heat of 1586 kJ kg^{-1}, the estimated depth of frost would approximate the observed depth of frost of 10 cm in this study.

If laboratory chamber experiments are conducted to quantify sublimation rates it would also be possible to estimate the volumetric ratios of the stalk and leaflets, allowing for the estimation of thermal conductivity in composite (Equation 5-7). The density of the sphagnum moss layer would be known as part of the experiment, along with the observed thermal conductivity obtained from the laboratory results. The density and thermal conductivity measurements would

then allow for the volumetric ratios of the stalk and leaflets to be calculated with a simple rearrangement of the equation.

7 REFERENCES

Alberta Environment. 2006. Land capability classification system for forest ecosystems in the oil sands. *Edited by* Cumulative Environmental Management Association, Fort McMurray, AB.

Alberta Environment. 2008. Guideline for wetland establishment on reclaimed oil sands leases. *Edited by* Cumulative Environmental Management Association, Fort McMurray, AB.

Alberta Environment. 2010. Guidelines for reclamation to forest vegetation in the Athabasca oil sands region, 2nd Edition. *Edited by* Terrestrial Subgroup of the Reclamation Working Group of the Cumulative Environmental Management Association, Fort McMurray, AB.

Alberta Environment. 2014. Guidelines for wetlands establishment on reclaimed oil sands leases. *Edited by* West Hawk Associates for the Reclamation Working Group and the Aquatic Sub-Group and Wildlife Task Group of the Cumulative Environmental Management Association, Fort McMurray, AB.

Alberta Environment and Parks. 2017. Alberta wetland mitigation directive. *Edited by* Water Policy Branch Edmonton, AB.

Alberta Environment and Parks. 2018. Oil Sands Monitoring Program: Annual Report for 2017–2018. *Edited by* Environment and Climate Change Canada, Edmonton, AB.

Andersland, O.B., and Anderson, D.M. 1978. Geotechnical engineering for cold regions. McGraw-Hill, New York.

Andrews, C. 1996. How do plants survive ice? Annals of Botany, **78**(5): 529-536.

Arseneault, D. 2001. Impact of fire behavior on postfire forest development in a homogeneous boreal landscape. Canadian Journal of Forest Research, **31**(8): 1367-1374.

Barr, A.G., Black, T., Hogg, E., Kljun, N., Morgenstern, K., and Nesic, Z. 2004. Inter-annual variability in the leaf area index of a boreal aspen-hazelnut forest in relation to net ecosystem production. Agricultural and Forest Meteorology, **126**(3): 237-255.

Barros, N., Feijóo, S., and Hansen, L.D. 2011. Calorimetric determination of metabolic heat, CO2 rates and the calorespirometric ratio of soil basal metabolism. Geoderma, **160**(3-4): 542-547.

Bedford, B.L., Walbridge, M.R., and Aldous, A. 1999. Patterns in nutrient availability and plant diversity of temperate North American wetlands. Ecology, **80**(7): 2151-2169.

Bélanger, J.A. 2009. Modelling soil temperature on the boreal plain with an emphasis on the rapid cooling period. Masters Thesis in Environmental Engineering, Lakehead University, Thunder Bay, Ont.

Belyea, L.R. 1996. Separating the effects of litter quality and microenvironment on decomposition rates in a patterned peatland. Oikos, **77**(3): 529-539.

Belyea, L.R., and Clymo, R. 2001. Feedback control of the rate of peat formation. Proceedings of the Royal Society of London B: Biological Sciences, **268**(1473): 1315-1321.

Berbigier, P., Bonnefond, J.-M., and Mellmann, P. 2001. CO 2 and water vapour fluxes for 2 years above Euroflux forest site. Agricultural and Forest Meteorology, **108**(3): 183-197.

Black, T.A., Chen, J.-M., Lee, X., and Sagar, R.M. 1991. Characteristics of shortwave and longwave irradiances under a Douglas-fir forest stand. Canadian Journal of Forest Research, **21**(7): 1020-1028.

Bonan, G.B. 1991. A biophysical surface energy budget analysis of soil temperature in the boreal forests of interior Alaska. Water Resources Research, **27**(5): 767-781.

Bonan, G.B., and Shugart, H.H. 1989. Environmental factors and ecological processes in boreal forests. Annual review of ecology and systematics, **20**(1): 1-28.

Bond-Lamberty, B., Wang, C., and Gower, S.T. 2005. Spatiotemporal measurement and modeling of stand-level boreal forest soil temperatures. Agricultural and Forest Meteorology, **131**(1): 27-40.

Boon, S. 2007. Snow accumulation and ablation in a beetle-killed pine stand in Northern Interior British Columbia. Journal of Ecosystems and Management, **8**(3).

Boon, S. 2009. Snow ablation energy balance in a dead forest stand. Hydrological Processes, **23**(18): 2600-2610.

Borkenhagen, A.K., and Cooper, D.J. 2019. Establishing vegetation on a constructed fen in a post-mined landscape in Alberta's oil sands region: a four-year evaluation after species introduction. Ecological Engineering, **130**: 11-22.

Boyce, R.L., Friedland, A.J., Webb, E.T., and Herrick, G.T. 1991. Modeling the effect of winter climate on high-elevation red spruce shoot water contents. Forest science, **37**(6): 1567-1580.

Breshears, D.D., McDowell, N.G., Goddard, K.L., Dayem, K.E., Martens, S.N., Meyer, C.W., and Brown, K.M. 2008. Foliar absorption of intercepted rainfall improves woody plant water status most during drought. Ecology, **89**(1): 41.

Buchner, O., and Neuner, G. 2010. Freezing cytorrhysis and critical temperature thresholds for photosystem II in the peat moss Sphagnum capillifolium. Protoplasma, **243**(1-4): 63-71.

Burgess, S.S.O., and Dawson, T.E. 2004. The contribution of fog to the water relations of Sequoia sempervirens (D. Don): foliar uptake and prevention of dehydration. Plant, Cell & Environment, **27**(8): 1023.

Campbell, D.I., Laybourne, C.E., and Blair, I.J. 2002. Measuring peat moisture content using the dual-probe heat pulse technique. Soil Research, **40**(1): 177-190.

Canada Agriculture, Canadian Agricultural Services Coordinating Committee. Soil Classification Working Group, National Research Council Canada, and Agri-Food Canada. Research Branch. 1998. The Canadian system of soil classification. No. 93. NRC Research Press.

Carey, S.K., and Pomeroy, J.W. 2009. Progress in Canadian snow and frozen ground hydrology, 2003-2007. Canadian Water Resources Journal, **34**(2): 127.

Carrera-Hernández, J.J., Mendoza, C.A., Devito, K.J., Petrone, R.M., and Smerdon, B.D. 2012. Reclamation for aspen revegetation in the Athabasca oil sands: Understanding soil water dynamics through unsaturated flow modelling. Canadian Journal of Soil Science, **92**(1): 103.

Chakrawal, A., Herrmann, A.M., and Manzoni, S. 2021. Leveraging energy flows to quantify microbial traits in soils. Soil Biology and Biochemistry, **155**: 108169.

Chanasyk, D., Whitson, I., Mapfumo, E., Burke, J., and Prepas, E. 2003. The impacts of forest harvest and wildfire on soils and hydrology in temperate forests: A baseline to develop hypotheses for the Boreal Plain. Journal of Environmental Engineering and Science, **2**(S1): S51-S62.

Chasmer, L., Quinton, W., Hopkinson, C., Petrone, R., and Whittington, P. 2011. Vegetation canopy and radiation controls on permafrost plateau evolution within the discontinuous permafrost zone, Northwest Territories, Canada. Permafrost and Periglacial Processes, **22**(3): 199-213.

Chee, W.-L., and Vitt, D.H. 1989. The vegatation, surface water chemistry and peat chemistry of moderate-rich fens in central Alberta, Canada. Wetlands, **9**(2): 227-261.

Clymo, R. 1984. The limits to peat bog growth. Philosophical Transactions of the Royal Society of London B: Biological Sciences, **303**(1117): 605-654.

Clymo, R. 1992. Productivity and decomposition of peatland ecosystems. *In* Peatland Ecosystems and Man: An Impact Assessment. *Edited by* O.M. Bragg and P.D. Hulme and H.A.P. Ingram and R.A. Robertson. Department of Biological Sciences, Dundee, U.K. pp. 3-16.

Cobbaert, D., Rochefort, L., and Price, J. 2004. Experimental restoration of a fen plant community after peat mining. Applied Vegetation Science, **7**(2): 209-220.

Cobos, D. 2015. Measurement volume of Decagon volumetric water content sensors. Application Note Decagon Devices; Decagon Devices Inc.: Pullman, WA, USA: 1-4.

Coleman, M.D., Hinckley, T.M., McNaughton, G., and Smit, B.A. 1992. Root cold hardiness and native distribution of subalpine conifers. Canadian Journal of Forest Research, **22**(7): 932-938.

Cooke, J., and Johnson, M. 2002. Ecological restoration of land with particular reference to the mining of metals and industrial minerals: A review of theory and practice. Environmental Reviews, **10**(1): 41-71.

Cooper, D.J., and MacDonald, L.H. 2000. Restoring the vegetation of mined peatlands in the southern Rocky Mountains of Colorado, USA. Restoration Ecology, **8**(2): 103-111.

Côté, J., and Konrad, J.-M. 2005. A generalized thermal conductivity model for soils and construction materials. Canadian Geotechnical Journal, **42**(2): 443-458.

Couling, K., Prepas, E.E., and Smith, D.W. 2007. Improved estimation of wetland cover in the western Canadian boreal forest. Lake and Reservoir Management, **23**(3): 245-254.

Cowling, J.E., and Kedrowski, R.A. 1980. Winter water relations of native and introduced evergreens in interior Alaska. Canadian Journal of Botany, **58**(1): 94-99.

Crowe, J.H., Carpenter, J.F., Crowe, L.M., and Anchordoguy, T.J. 1990. Are freezing and dehydration similar stress vectors? A comparison of modes of interaction of stabilizing solutes with biomolecules. Cryobiology, **27**(3): 219-231.

De Schepper, V., and Steppe, K. 2010. Development and verification of a water and sugar transport model using measured stem diameter variations. Journal of experimental botany, **61**(8): 2083-2099.

De Vries, D.A. 1963. Thermal properties of soils. *In* Physics of plant environment. *Edited by* W.R. van Wijk, North Holland, Amsterdam. pp. 210-235.

Deng, J., Li, C., and Frolking, S. 2015. Modeling impacts of changes in temperature and water table on C gas fluxes in an Alaskan peatland. Journal of Geophysical Research: Biogeosciences, **120**(7): 1279-1295.

Devito, K., and Hill, A. 1997. Sulphate dynamics in relation to groundwater–surface water interactions in headwater wetlands of the southern Canadian Shield. Hydrological Processes, **11**(5): 485-500.

Devito, K., Waddington, J., and Branfireun, B. 1997. Flow reversals in peatlands influenced by local groundwater systems. Hydrological Processes, **11**(1): 103-110.

Devito, K., Creed, I., Gan, T., Mendoza, C., Petrone, R., Silins, U., and Smerdon, B. 2005. A framework for broad-scale classification of hydrologic response units on the Boreal Plain: is topography the last thing to consider? Hydrological Processes: An International Journal, **19**(8): 1705-1714.

Doherty, J. 2016. PEST user manual part I and II. Watermark Numerical Computing, Brisbane, Australia.

Domine, F., Belke-Brea, M., Sarrazin, D., Arnaud, L., Barrere, M., and Poirier, M. 2018. Soil moisture, wind speed and depth hoar formation in the Arctic snowpack. Journal of Glaciology, **64**(248): 990-1002.

Dyrness, C. 1982. Control of depth to permafrost and soil temperature by the forest floor in black spruce/feathermoss communities. *Edited by* US Department of Agriculture and US Forest Service. Pacific Northwest Research Note PNW-396, Fairbanks, Alaska.

Ecological Stratification Working Group. 1996. A National Ecological Framework for Canada. Centre for Land and Biological Resources Research, Research Branch, Agriculture and Agri-Food Canada, and State of the Environment Directorate. Food Canada, Ottawa, Ont.

Eller, C.B., Lima, A.L., and Oliveira, R.S. 2013. Foliar uptake of fog water and transport belowground alleviates drought effects in the cloud forest tree species, Drimys brasiliensis (Winteraceae). New Phytologist, **199**(1): 151.

Ellis, C.R., and Pomeroy, J.W. 2007. Estimating sub-canopy shortwave irradiance to melting snow on forested slopes. Hydrological Processes, **21**(19): 2581-2593.

Ellis, C.R., Pomeroy, J.W., Brown, T., and MacDonald, J. 2010. Simulation of snow accumulation and melt in needleleaf forest environments. Hydrology and Earth System Sciences Discussions, **7**(1): 1033.

Ellis, C.R., Pomeroy, J.W., Essery, R.L.H., and Link, T.E. 2011. Effects of needleleaf forest cover on radiation and snowmelt dynamics in the Canadian Rocky Mountains. Canadian Journal of Forest Research, **41**(3): 608.

Ensminger, I., Sveshnikov, D., Campbell, D.A., Funk, C., Jansson, S., Lloyd, J., Shibistova, O., and Öquist, G. 2004. Intermittent low temperatures constrain spring recovery of photosynthesis in boreal Scots pine forests. Global Change Biology, **10**(6): 995-1008.

Environment Canada. 2015. Digital archive of Canadian climatological data (surface). *Edited by* Atmospheric Environment Service. Canadian Climate Centre, Downsview, ON.

Essery, R., and Etchevers, P. 2004. Parameter sensitivity in simulations of snowmelt. Journal of Geophysical Research: Atmospheres (1984–2012), **109**(D20).

Essery, R., Pomeroy, J., Ellis, C., and Link, T. 2008. Modelling longwave radiation to snow beneath forest canopies using hemispherical photography or linear regression. Hydrological Processes, **22**(15): 2788-2800.

Ewers, F.W. 1985. Xylem'Structure and Water Conduction in Conifer Trees, Dicot Trees, and Llanas. IAWA Journal, **6**(4): 309-317.

Farouki, O.T. 1981. Thermal properties of soils. *Edited by* Cold Regions Research and Engineering Lab Monograph 81-1. U.S. Army Corps of Engineers, Hanover, NH.

Ferone, J.M., and Devito, K.J. 2004. Shallow groundwater–surface water interactions in pond–peatland complexes along a Boreal Plains topographic gradient. Journal of Hydrology, **292**(1): 75.

Finkelstein, M. 1990. National parks system plan. *Edited by* Park Services. Environnement Canada, Ottawa, ON.

Flerchinger, G., and Saxton, K. 1989. Simultaneous heat and water model of a freezing snow-residue-soil system I. Theory and development. Trans. ASAE, **32**(2): 565-571.

Flerchinger, G., and Hanson, C. 1989. Modeling soil freezing and thawing on a rangeland watershed. Transactions of the ASAE, **32**(5): 1551-1554.

Flerchinger, G., and Pierson, F. 1991. Modeling plant canopy effects on variability of soil temperature and water. Agricultural and Forest Meteorology, **56**(3-4): 227-246.

Flerchinger, G., and Pierson, F. 1997. Modelling plant canopy effects on variability of soil temperature and water: Model calibration and validation. Journal of Arid Environments, **35**(4): 641-653.

Flerchinger, G.N. 2000. The simultaneous heat and water (SHAW) model: user's manual. *In* Technical Rep. NWRC 2000-10. *Edited by* Northwest Watershed Research Center. USDA Agriculture Research Service, Boise, ID.

Foster, D., and Wright Jr, H. 1990. Role of ecosystem development and climate change in bog formation in central Sweden. Ecology: 450-463.

Fowler, W.B., and Helvey, J. 1981. Soil and air temperature and biomass after residue treatment. *Edited by* Forst Service Pacific Northwest Forest and Range Experiment Station PNW-383. USDA, Portland, OR.

Fraser, C., Roulet, N., and Lafleur, M. 2001. Groundwater flow patterns in a large peatland. Journal of Hydrology, **246**(1): 142-154.

Frolking, S., Roulet, N.T., Moore, T.R., Richard, P.J.H., Lavoie, M., and Muller, S.D. 2001. Modeling northern peatland decomposition and peat accumulation. Ecosystems, **4**(5): 479.

Frolking, S., Bubier, J., Moore, T., Ball, T., Bellisario, L., Bhardwaj, A., Carroll, P., Crill, P., Lafleur, P., and McCaughey, J. 1998. Relationship between ecosystem productivity and photosynthetically active radiation for northern peatlands. Global Biogeochemical Cycles, **12**(1): 115-126.

Gelfan, A.N., Pomeroy, J.W., and Kuchment, L.S. 2004. Modeling forest cover influences on snow accumulation, sublimation, and melt. Journal of Hydrometeorology, **5**(5).

Ghanbarian-Alavijeh, B., Liaghat, A., Huang, G.-H., and Van Genuchten, M.T. 2010. Estimation of the van Genuchten soil water retention properties from soil textural data. Pedosphere, **20**(4): 456-465.

Goldsmith, G.R. 2013. Changing directions: the atmosphere–plant–soil continuum. New Phytologist, **199**(1): 4.

Gorham, E. 1995. The biogeochemistry of northern peatlands and its possible response to global warming. Biotic Feedback in the Global Climatic System, GM Woodwell and FT Mackenzie (eds.), Oxford University Press, New York: 169-187.

Hacker, J., and Neuner, G. 2007. Ice propagation in plants visualized at the tissue level by infrared differential thermal analysis (IDTA). Tree physiology, **27**(12): 1661-1670.

Hansen, J., Vogg, G., and Beck, E. 1996. Assimilation, allocation and utilization of carbon by 3-year-old Scots pine (Pinus sylvestris L.) trees during winter and early spring. Trees, **11**(2): 83-90.

Hayashi, M., van der Kamp, G., and Schmidt, R. 2003. Focused infiltration of snowmelt water in partially frozen soil under small depressions. Journal of Hydrology, **270**(3): 214-229.

Hayashi, M., Goeller, N., Quinton, W.L., and Wright, N. 2007. A simple heat-conduction method for simulating the frost-table depth in hydrological models. Hydrological Processes: An International Journal, **21**(19): 2610-2622.

Hayhoe, H. 1994. Field testing of simulated soil freezing and thawing by the SHAW model. Canadian Agricultural Engineering, **36**(4): 279.

Hedstrom, N., and Pomeroy, J. 1998. Measurements and modelling of snow interception in the boreal forest. Hydrological Processes, **12**(1011): 1611-1625.

Hendrick, R.L., Filgate, B.D., and Adams, W.M. 1971. Application of environmental analysis to watershed snowmelt. Journal of Applied Meteorology, **10**(3): 418-429.

Hendry, M.J. 1982. Hydraulic Conductivity of a Glacial Till in Albertaa. Groundwater, **20**(2): 162-169.

Hilbert, D.W., Roulet, N., and Moore, T. 2000. Modelling and analysis of peatlands as dynamical systems. Journal of Ecology, **88**(2): 230.

Hirota, T., Pomeroy, J.W., Granger, R.J., and Maule, C.P. 2002. An extension of the force-restore method to estimating soil temperature at depth and evaluation for frozen soils under snow. Journal of Geophysical Research: Atmospheres, **107**(D24): ACL 11-11-ACL 11-10.

Hock, R. 2003. Temperature index melt modelling in mountain areas. Journal of Hydrology, **282**(1): 104-115.

Hogg, E.H. 1993. Decay potential of hummock and hollow Sphagnum peats at different depths in a Swedish raised bog. Oikos, **66**(2): 269-278.

Hokanson, K., Peterson, E., Devito, K., and Mendoza, C. 2020. Forestland-peatland hydrologic connectivity in water-limited environments: hydraulic gradients often oppose topography. Environmental Research Letters, **15**(3): 034021.

Hokanson, K., Lukenbach, M., Devito, K., Kettridge, N., Petrone, R., and Waddington, J. 2016. Groundwater connectivity controls peat burn severity in the boreal plains. Ecohydrology, **9**(4): 574-584.

Ippisch, O., Vogel, H.-J., and Bastian, P. 2006. Validity limits for the van Genuchten–Mualem model and implications for parameter estimation and numerical simulation. Advances in Water Resources, **29**(12): 1780-1789.

Ireson, A., Barr, A., Johnstone, J., Mamet, S., Van der Kamp, G., Whitfield, C., Michel, N., North, R., Westbrook, C., and DeBeer, C. 2015. The changing water cycle: the Boreal Plains ecozone of Western Canada. Wiley Interdisciplinary Reviews: Water, **2**(5): 505-521.

Jagtar Bhatti, V.B., Mark Castonguay, R.E., and Arp, P.A. 2006. Modeling snowpack and soil temperature and moisture conditions in a jack pine, black spruce and aspen forest stand in central Saskatchewan (BOREAS SSA). Canadian Journal of Soil Science, **86**(Special Issue): 203-217.

Jarvis, P., and Linder, S. 2000. Botany: constraints to growth of boreal forests. Nature, **405**(6789): 904-905.

Johansen, O. 1977. Thermal conductivity of soils. Cold Regions Research and Engineering Lab, Ph.D. Thesis University of Trondheim, Hanover, NH.

Johnson, L., and Damman, A. 1993. Decay and its regulation in Sphagnum peatlands. Advances in bryology, **5**: 249-296.

Jost, G., Weiler, M., Gluns, D.R., and Alila, Y. 2007. The influence of forest and topography on snow accumulation and melt at the watershed-scale. Journal of Hydrology, **347**(1): 101-115.

Katz, C., Oren, R., Schulze, E.-D., and Milburn, J. 1989. Uptake of water and solutes through twigs of Picea abies (L.) Karst. Trees, **3**(1): 33-37.

Kersten, M.S. 1949. Thermal properties of soils. Bull. No. 28. University of Minnesota Inst. of Technol. Eng. Exp. Station, Minneapolis, MN.

Keshta, N., Elshorbagy, A., and Barbour, L. 2010. Comparative probabilistic assessment of the hydrological performance of reconstructed and natural watersheds. Hydrological Processes, **24**(10): 1333-1342.

Ketcheson, S.J., and Price, J.S. 2016. Comparison of the hydrological role of two reclaimed slopes of different ages in the Athabasca oil sands region, Alberta, Canada. Canadian Geotechnical Journal, **53**(9): 1533-1546.

Klassen, R.W. 1989. Quaternary geology of the southern Canadian Interior Plains. *In* Quaternary geology of Canada and Greenland. *Edited by* R.J. Fulton. Geological Survey of Canada, Ottawa, ON. pp. 138-174.

Knoblauch, M., Knoblauch, J., Mullendore, D.L., Savage, J.A., Babst, B.A., Beecher, S.D., Dodgen, A.C., Jensen, K.H., and Holbrook, N.M. 2016. Testing the Münch hypothesis of long distance phloem transport in plants. Elife, **5**: e15341.

Kuhry, P., Nicholson, B.J., Gignac, L.D., Vitt, D.H., and Bayley, S.E. 1993. Development of Sphagnum-dominated peatlands in boreal continental Canada. Canadian Journal of Botany, **71**(1): 10.

Kujala, K., Seppälä, M., and Holappa, T. 2008. Physical properties of peat and palsa formation. Cold Regions Science and Technology, **52**(3): 408-414.

Kuz'min, P.P. 1963. Snow Cover and Snow Reserves: Translated from Russian. Israel Program for Scientific Translations. U.S. National Science Foundation, Washington, D.C.

Langford, J.E., Schincariol, R.A., Nagare, R.M., Quinton, W.L., and Mohammed, A.A. 2020. Transient and transition factors in modeling permafrost thaw and groundwater flow. Groundwater, **58**(2): 258-268.

LaRose, S., Price, J., and Rochefort, L. 1997. Rewetting of a cutover peatland: hydrologic assessment. Wetlands, **17**(3): 416-423.

Laur, J., and Hacke, U.G. 2014. Exploring Picea glauca aquaporins in the context of needle water uptake and xylem refilling. New Phytologist, **203**(2): 388-400.

Lawrence, D.M., and Slater, A.G. 2008. Incorporating organic soil into a global climate model. Climate Dynamics, **30**(2-3): 145-160.

Leonard, R., Kettridge, N., Krause, S., Devito, K.J., Granath, G., Petrone, R., Mendoza, C., and Waddington, J. 2017. Peatland bryophyte responses to increased light from black spruce removal. Ecohydrology, **10**(1): e1804.

Leonard, R., Moore, P., Krause, S., Devito, K., Petrone, G., Mendoza, C., Waddington, J., and Kettridge, N. 2021. The influence of system heterogeneity on peat-surface temperature dynamics. Environmental Research Letters, **16**(2): 024002.

Li, C., Flannigan, M., and Corns, I.G. 2000. Influence of potential climate change on forest landscape dynamics of west-central Alberta. Canadian Journal of Forest Research, **30**(12): 1905-1912.

Lieffers, V., and Rothwell, R. 1987. Rooting of peatland black spruce and tamarack in relation to depth of water table. Canadian Journal of Botany, **65**(5): 817-821.

Liesche, J., Martens, H.J., and Schulz, A. 2011. Symplasmic transport and phloem loading in gymnosperm leaves. Protoplasma, **248**(1): 181-190.

Limm, E.B., Simonin, K.A., Bothman, A.G., and Dawson, T.E. 2009. Foliar water uptake: a common water acquisition strategy for plants of the redwood forest. Oecologia, **161**(3): 449.

Link, T.E., and Marks, D. 1999. Point simulation of seasonal snow cover dynamics beneath boreal forest canopies. Journal of Geophysical Research: Atmospheres (1984–2012), **104**(D22): 27841-27857.

Little-Devito, M., Mendoza, C., Chasmer, L., Kettridge, N., and Devito, K. 2019. Opportunistic wetland formation on reconstructed landforms in a sub-humid climate: influence of site and landscape-scale factors. Wetlands Ecology and Management, **27**(5): 587-608.

Lu, S., Ren, T., Gong, Y., and Horton, R. 2007. An improved model for predicting soil thermal conductivity from water content at room temperature. Soil science society of America journal, **71**(1): 8-14.

Lundmark, T., Hedén, J., and Hällgren, J.-E. 1988. Recovery from winter depression of photosynthesis in pine and spruce. Trees, **2**(2): 110-114.

Mäkelä, A., Hari, P., Berninger, F., Hänninen, H., and Nikinmaa, E. 2004. Acclimation of photosynthetic capacity in Scots pine to the annual cycle of temperature. Tree physiology, **24**(4): 369-376.

Manies, K.L., Harden, J.W., Silva, S.R., Briggs, P.H., and Schmid, B.M. 2004. Soil data from Picea mariana stands near Delta Junction, Alaska of different ages and soil drainage type. US Department of the Interior, US Geological Survey, Open-File Report 2004-1271. p. 19.

Maseyk, K., Green, T., and Klinac, D. 1999. Photosynthetic responses of New Zealand sphagnum species. New Zealand Journal of Botany, **37**(1): 155-165.

Mayr, S., Schmid, P., Laur, J., Rosner, S., Charra-Vaskou, K., Dämon, B., and Hacke, U.G. 2014. Uptake of water via branches helps timberline conifers refill embolized xylem in late winter. Plant Physiology, **164**(4): 1731-1740.

McEachern, P., Prepas, E., and Chanasyk, D. 2006. Landscape control of water chemistry in northern boreal streams of Alberta. Journal of Hydrology, **323**(1): 303-324.

McGaw, R. 1969. Heat conduction in saturated granular materials. *In* Effects of Temperature and Heat on Engineering Behavior of Soils Special Report 103. *Edited by* E.W. Jackson. Highway Research Board, Washington, D.C. pp. 114-131.

Moffett, B.F. 2015. Ice nucleation in mosses and liverworts. Lindbergia, **38**(1): 14-16.

Mohammed, A.A., Schincariol, R.A., Quinton, W.L., Nagare, R.M., and Flerchinger, G.N. 2017. On the use of mulching to mitigate permafrost thaw due to linear disturbances in sub-arctic peatlands. Ecological Engineering, **102**: 207-223.

Moore, P.D. 1989. The ecology of peat-forming processes: a review. International Journal of Coal Geology, **12**(1): 89-103.

Munch, E. 1930. Stoffbewegungen in der Pflanze. Verlag Gustav Fischer, Jena, Germany.

Nadezhdina, N., David, T.S., David, J.S., Ferreira, M.I., Dohnal, M., Tesař, M., Gartner, K., Leitgeb, E., Nadezhdin, V., and Cermak, J. 2010. Trees never rest: the multiple facets of hydraulic redistribution. Ecohydrology, **3**(4): 431-444.

National Wetlands Working Group. 1988. Wetlands of Canada. Ecological land classification series, **24**: 452.

Nicolsky, D., Romanovsky, V., and Panteleev, G. 2009. Estimation of soil thermal properties using in-situ temperature measurements in the active layer and permafrost. Cold Regions Science and Technology, **55**(1): 120-129.

O'Donnell, J.A., Romanovsky, V.E., Harden, J.W., and McGuire, A.D. 2009. The effect of moisture content on the thermal conductivity of moss and organic soil horizons from black spruce ecosystems in interior Alaska. Soil Science, **174**(12): 646-651.

Ollinger, S.V., Aber, J.D., Reich, P.B., and Freuder, R.J. 2002. Interactive effects of nitrogen deposition, tropospheric ozone, elevated CO2 and land use history on the carbon dynamics of northern hardwood forests. Global Change Biology, **8**(6): 545-562.

Oogathoo, S., Houle, D., Duchesne, L., and Kneeshaw, D. 2020. Vapour pressure deficit and solar radiation are the major drivers of transpiration of balsam fir and black spruce tree species in humid boreal regions, even during a short-term drought. Agricultural and Forest Meteorology, **291**: 108063.

Öquist, G., and Huner, N.P. 2003. Photosynthesis of overwintering evergreen plants. Annual Review of Plant Biology, **54**(1): 329-355.

Ottander, C., and Öquist, G. 1991. Recovery of photosynthesis in winter-stressed Scots pine. Plant, Cell & Environment, **14**(3): 345-349.

Owston, P.W., Smith, J.L., and Halverson, H.G. 1972. Seasonal water movement in tree stems. Forest science, **18**(4): 266-272.

Parker, J. 1963. Cold resistance in woody plants. The Botanical Review, **29**(2): 123-201.

Patankar, R., Quinton, W.L., Hayashi, M., and Baltzer, J.L. 2015. Sap flow responses to seasonal thaw and permafrost degradation in a subarctic boreal peatland. Trees, **29**(1): 129-142.

Petrone, R., Devito, K., Silins, U., Mendoza, C., Brown, S., Kaufman, S., and Price, J. 2008. Transient peat properties in two pond-peatland complexes in the sub-humid Western Boreal Plain, Canada. Mires Peat, **3**(5): 1-13.

Pollard, J., McKenna, G., Fair, J., Daly, C., Wytrykush, C., and Clark, J. 2012. Design aspects of two fen wetlands constructed for reclamation research in the Athabasca oil sands. *In* Proceedings of the Seventh International Conference on Mine Closure. Australian Centre for Geomechanics. pp. 815-829.

Pomeroy, J., Gray, D., Hedstrom, N., and Janowicz, J. 2002. Prediction of seasonal snow accumulation in cold climate forests. Hydrological Processes, **16**(18): 3543-3558.

Pomeroy, J., Granger, R., Hedstrom, N., Gray, D., Elliott, J., Pietroniro, A., and Janowicz, J. 2005. The process hydrology approach to improving prediction of ungauged basins in Canada. Prediction in Ungauged Basins, approaches for Canada's cold regions. Cambridge: Cambridge University Press/Canadian Water Resources Association: 67-95.

Pomeroy, J.W., Parviainen, J., Hedstrom, N., and Gray, D.M. 1998. Coupled modelling of forest snow interception and sublimation. Hydrological Processes, **12**(15): 2317.

Porada, P., Ekici, A., and Beer, C. 2016. Effects of bryophyte and lichen cover on permafrost soil temperature at large scale. The Cryosphere, **10**(5): 2291-2315.

Pouliot, R., Rochefort, L., and Graf, M.D. 2012. Initiatives in oil sand reclamation Considerations for building a fen peatland in a post-mined oil sands landscape. Restoration and reclamation of boreal ecosystems: attaining sustainable development: 179.

Prepas, E.E., Putz, G., Smith, D.W., Burke, J.M., and MacDonald, J.D. 2008. The FORWARD Project: objectives, framework and initial integration into a Detailed Forest Management Plan in Alberta. The Forestry Chronicle, **84**(3): 330-337.

Prepas, E.E., Planas, D., Gibson, J.J., Vitt, D.H., Prowse, T.D., Dinsmore, W.P., Halsey, L.A., McEachern, P.M., Paquet, S., and Scrimgeour, G.J. 2001. Landscape variables influencing nutrients and phytoplankton communities in Boreal Plain lakes of northern Alberta: a comparison of wetland- and upland-dominated catchments. Canadian Journal of Fisheries and Aquatic Sciences, **58**(7): 1286.

Price, J.S., and Whitehead, G.S. 2001. Developing hydrologic thresholds for Sphagnum recolonization on an abandoned cutover bog. Wetlands, **21**(1): 32-40.

Price, J.S., McLaren, R.G., and Rudolph, D.L. 2010. Landscape restoration after oil sands mining: conceptual design and hydrological modelling for fen reconstruction. International Journal of Mining, Reclamation and Environment, **24**(2): 109.

Pruppacher, H.R., and Klett, J.D. 2012. Microphysics of Clouds and Precipitation: Reprinted 1980. Springer Science & Business Media.

Puranen, R., Mäkilä, M., and Säävuori, H. 1999. Electric conductivity and temperature variations within a raised bog in Finland: implications for bog development. The Holocene, **9**(1): 13-24.

Redding, T., and Devito, K. 2011. Aspect and soil textural controls on snowmelt runoff on forested Boreal Plain hillslopes. Hydrology Research, **42**(4): 250-267.

Reddy, K., Kadlec, R., Flaig, E., and Gale, P. 1999. Phosphorus retention in streams and wetlands: a review. Critical reviews in environmental science and technology, **29**(1): 83-146.

Reifsnyder, W.E., and Lull, H.W. 1965. Radiant energy in relation to forests. No. 1344. US Department of Agriculture, Forest Service.

Riddell, J.T.F. 2008. Assessment of Surface Water Groundwater Interaction at Perched Boreal Wetlands, North-central Alberta. University of Alberta.

Romanovsky, V., and Osterkamp, T. 1997. Thawing of the active layer on the coastal plain of the Alaskan Arctic. Permafrost and Periglacial Processes, **8**(1): 1-22.

Romanovsky, V.E., and Osterkamp, T. 2000. Effects of unfrozen water on heat and mass transport processes in the active layer and permafrost. Permafrost and Periglacial Processes, **11**(3): 219-239.

Rooney, R.C., Bayley, S.E., and Schindler, D.W. 2012. Oil sands mining and reclamation cause massive loss of peatland and stored carbon. Proceedings of the National Academy of Sciences of the United States of America, **109**(13): 4933. doi:10.1073/pnas.1117693108; 10.1073/pnas.1117693108.

Roy, M.-C., Foote, L., and Ciborowski, J.J. 2016. Vegetation community composition in wetlands created following oil sand mining in Alberta, Canada. Journal of environmental management, **172**: 18-28.

Sakai, A., and Larcher, W. 1987. Frost survival of plants. Responses and adaptation to freezing stress. Springer-Verlag.

Schaberg, P., Wilkinson, R., Shane, J., Donnelly, J., and Cali, P. 1995. Winter photosynthesis of red spruce from three Vermont seed sources. Tree physiology, **15**(5): 345-350.

Scheidegger, A.E. 1965. The algebra of stream-order numbers. Washington, DC: US Geological Survey, Professional Paper B, **525**.

Schulze, E., Mooney, H., and Dunn, E. 1967. Wintertime photosynthesis of bristlecone pine (Pinus aristata) in the White Mountains of California. Ecology: 1044-1047.

Schwarz, P.A., Fahey, T.J., and Dawson, T.E. 1997. Seasonal air and soil temperature effects on photosynthesis in red spruce (Picea rubens) saplings. Tree physiology, **17**(3): 187-194.

Schwärzel, K., Šimůnek, J., Stoffregen, H., Wessolek, G., and Van Genuchten, M.T. 2006. Estimation of the unsaturated hydraulic conductivity of peat soils: Laboratory versus field data. Vadose Zone Journal, **5**(2): 628-640.

Sevanto, S., Suni, T., Pumpanen, J., Gronholm, T., Kolari, P., Nikinmaa, E., Hari, P., and Vesala, T. 2006. Wintertime photosynthesis and water uptake in a boreal forest. Tree physiology, **26**(6): 749.

Sharratt, B. 1997. Thermal conductivity and water retention of a black spruce forest floor. Soil Science, **162**(8): 576-582.

Shurpali, N., Verma, S., Kim, J., and Arkebauer, T. 1995. Carbon dioxide exchange in a peatland ecosystem. Journal of Geophysical Research: Atmospheres (1984–2012), **100**(D7): 14319-14326.

Sicart, J.E., Essery, R.L., Pomeroy, J.W., Hardy, J., Link, T., and Marks, D. 2004. A sensitivity study of daytime net radiation during snowmelt to forest canopy and atmospheric conditions. Journal of Hydrometeorology, **5**(5): 774-784.

Siegel, D.I., and Glaser, P.H. 1987. Groundwater flow in a bog-fen complex, Lost River Peatland, northern Minnesota. The Journal of Ecology, **75**(3): 743-754.

Siltanen, R., Apps, M., Zoltai, S., Mair, R., and Strong, W. 1997. A soil profile and organic carbon data base for Canadian forest and tundra mineral soils. *Edited by* Natural Resources Canada and Northern Forestry Centre. Canadian Forest Service, Edmonton, AB. p. 50.

Silvola, J., Alm, J., Ahlholm, U., Nykanen, H., and Martikainen, P.J. 1996. CO2 fluxes from peat in boreal mires under varying temperature and moisture conditions. Journal of Ecology, **84**(2): 219-228.

Smerdon, B., Devito, K., and Mendoza, C. 2005. Interaction of groundwater and shallow lakes on outwash sediments in the sub-humid Boreal Plains of Canada. Journal of Hydrology, **314**(1): 246-262.

Smerdon, B., Mendoza, C., and Devito, K. 2008. Influence of subhumid climate and water table depth on groundwater recharge in shallow outwash aquifers. Water Resources Research, **44**(8).

Smith, C., Webb, K., Kenney, E., Anderson, A., and Kroetsch, D. 2011. Brunisolic soils of Canada: Genesis, distribution, and classification. Canadian Journal of Soil Science, **91**(5): 695-717.

Smith, D.W., Prepas, E.E., Putz, G., Burke, J.M., Meyer, W.L., and Whitson, I. 2003. The Forest Watershed and Riparian Disturbance study: a multi-discipline initiative to evaluate and manage watershed disturbance on the Boreal Plain of Canada. Journal of Environmental Engineering and Science, **2**(S1): S1.

Sparks, J.P., and Black, R.A. 2000. Winter hydraulic conductivity and xylem cavitation in coniferous trees from upper and lower treeline. Arctic, Antarctic, and Alpine Research, **32**(4): 397-403.

Sparks, J.P., Campbell, G.S., and Black, A.R. 2001. Water content, hydraulic conductivity, and ice formation in winter stems of Pinus contorta: a TDR case study. Oecologia, **127**(4): 468.

Sperry, J. 1993. Winter xylem embolism and spring recovery in Betula cordifolia, Fagus grandifolia, Abies balsamea, and Picea rubens. Water transport in plants under climatic stress. Cambridge University Press, Cambridge, UK: 86-98.

Sperry, J.S., and Sullivan, J.E. 1992. Xylem embolism in response to freeze-thaw cycles and water stress in ring-porous, diffuse-porous, and conifer species. Plant Physiology, **100**(2): 605-613.

Sperry, J.S., Nichols, K.L., Sullivan, J.E., and Eastlack, S.E. 1994. Xylem embolism in ring-porous, diffuse-porous, and coniferous trees of northern Utah and interior Alaska. Ecology, **75**(6): 1736-1752.

Stocks, B.J., Fosberg, M., Lynham, T., Mearns, L., Wotton, B., Yang, Q., Jin, J., Lawrence, K., Hartley, G., and Mason, J. 1998. Climate change and forest fire potential in Russian and Canadian boreal forests. Climatic change, **38**(1): 1-13.

Stone, E.C. 1963. The ecological importance of dew. Quarterly Review of Biology, **38**(4): 328-341.

Strahler, A.N. 1957. Quantitative analysis of watershed geomorphology. Eos, Transactions American Geophysical Union, **38**(6): 913-920.

Sturm, M., Perovich, D.K., and Holmgren, J. 2002. Thermal conductivity and heat transfer through the snow on the ice of the Beaufort Sea. Journal of Geophysical Research: Oceans, **107**(C10): SHE 19-11-SHE 19-17.

Suni, T., Rinne, J., Reissell, A., Altimir, N., Keronen, P., Rannik, U., Maso, M., Kulmala, M., and Vesala, T. 2003. Long-term measurements of surface fluxes above a Scots pine forest in Hyytiala, southern Finland, 1996-2001. Boreal Environment Research, **8**(4): 287-302.

Tanner, W., and Beevers, H. 2001. Transpiration, a prerequisite for long-distance transport of minerals in plants? Proceedings of the National Academy of Sciences, **98**(16): 9443-9447.

Tarnawski, V.R., and Leong, W.H. 2012. A series-parallel model for estimating the thermal conductivity of unsaturated soils. International Journal of Thermophysics, **33**(7): 1191-1218.

Teskey, R.O., and Hinckley, T.M. 1981. Influence of temperature and water potential on root growth of white oak. Physiologia plantarum, **52**(3): 363-369.

Teti, P.A. 2008. Effects of overstory mortality on snow accumulation and ablation. *Edited by* Natural Resources Canada and Pacific Forestry Centre. Canadian Forest Service, Victoria, BC.

Thormann, M.N., and Bayley, S.E. 1997. Aboveground plant production and nutrient content of the vegetation in six peatlands in Alberta, Canada. Plant Ecology, **131**(1): 1-16.

Tixier, A., Sperling, O., Orozco, J., Lampinen, B., Roxas, A.A., Saa, S., Earles, J.M., and Zwieniecki, M.A. 2017. Spring bud growth depends on sugar delivery by xylem and water recirculation by phloem Münch flow in Juglans regia. Planta, **246**(3): 495-508.

Tolonen, K., and Turunen, J. 1996. Accumulation rates of carbon in mires in Finland and implications for climate change. The Holocene, **6**(2): 171-178.

US Army, and US Air Force. 1988. Calculation methods for determination of depths of freeze and thaw in soils. *In* Technical Manual: TM5-852-6/AFR 88-19.

Van Genuchten, M.T. 1980. A closed-form equation for predicting the hydraulic conductivity of unsaturated soils. Soil science society of America journal, **44**(5): 892-898.

Varhola, A., Coops, N.C., Weiler, M., and Moore, R.D. 2010. Forest canopy effects on snow accumulation and ablation: An integrative review of empirical results. Journal of Hydrology, **392**(3): 219.

Vitt, D.H., and Chee, W.-L. 1990. The relationships of vegetation to surface water chemistry and peat chemistry in fens of Alberta, Canada. Vegetatio, **89**(2): 87-106.

Vitt, D.H., Bayley, S.E., and Jin, T.-L. 1995. Seasonal variation in water chemistry over a bog-rich fen gradient in continental western Canada. Canadian Journal of Fisheries and Aquatic Sciences, **52**(3): 587-606.

Vitt, D.H., House, M., and Hartsock, J.A. 2016. Sandhill Fen, an initial trial for wetland species assembly on in-pit substrates: lessons after three years. Botany, **94**(11): 1015-1025.

Volik, O., Elmes, M., Petrone, R., Kessel, E., Green, A., Cobbaert, D., and Price, J. 2020. Wetlands in the Athabasca Oil Sands Region: the nexus between wetland hydrological function and resource extraction. Environmental Reviews, **28**(3): 246-261.

Waddington, J., and Roulet, N. 1996. Atmosphere-wetland carbon exchanges: Scale dependency of CO2 and CH4 exchange on the developmental topography of a peatland. Global Biogeochemical Cycles, **10**(2): 233-245.

Walter, M.T., Brooks, E.S., McCool, D.K., King, L.G., Molnau, M., and Boll, J. 2005. Process-based snowmelt modeling: does it require more input data than temperature-index modeling? Journal of Hydrology, **300**(1): 65-75.

Watson, B.M., and Putz, G. 2014. Comparison of temperature-index snowmelt models for use within an operational water quality model. Journal of environmental quality, **43**(1): 199-207.

Weber, T.K., Iden, S.C., and Durner, W. 2017. Unsaturated hydraulic properties of Sphagnum moss and peat reveal trimodal pore-size distributions. Water Resources Research, **53**(1): 415-434.

Williams, C.A., Gu, H., and Jiao, T. 2021. Climate impacts of US forest loss span net warming to net cooling. Science Advances, **7**(7): eaax8859.

Windt, C.W., Vergeldt, F.J., De Jager, P.A., and Van As, H. 2006. MRI of long-distance water transport: a comparison of the phloem and xylem flow characteristics and dynamics in poplar, castor bean, tomato and tobacco. Plant, Cell & Environment, **29**(9): 1715-1729.

Winkler, R., Spittlehouse, D., and Golding, D. 2005. Measured differences in snow accumulation and melt among clearcut, juvenile, and mature forests in southern British Columbia. Hydrological Processes, **19**(1): 51-62.

Winter, T.C., and Woo, M.-K. 1990. Hydrology of lakes and wetlands. IN: Surface Water Hydrology. Geological Society of America, Boulder, Colorado. 1990. p 159-187, 20 fig, 91 ref.

Winter, T.C., and Rosenberry, D.O. 1995. The interaction of ground water with prairie pothole wetlands in the Cottonwood Lake area, east-central North Dakota, 1979–1990. Wetlands, **15**(3): 193-211.

Winter, T.C., and LaBaugh, J.W. 2003. Hydrologic considerations in defining isolated wetlands. Wetlands, **23**(3): 532-540.

Winter, T.C., Rosenberry, D.O., Buso, D.C., and Merk, D.A. 2001. Water source to four US wetlands: implications for wetland management. Wetlands, **21**(4): 462-473.

Woynillowicz, D., Severson-Baker, C., and Raynolds, M. 2005. Oil sands fever: The environmental implications of Canada's oil sands rush. Pembina Institute Edmonton.

Wright, N., Quinton, W.L., and Hayashi, M. 2008. Hillslope runoff from an ice-cored peat plateau in a discontinuous permafrost basin, Northwest Territories, Canada. Hydrological Processes: An International Journal, **22**(15): 2816-2828.

Yi, S., Manies, K., Harden, J., and McGuire, A.D. 2009. Characteristics of organic soil in black spruce forests: Implications for the application of land surface and ecosystem models in cold regions. Geophysical Research Letters, **36**(5).

Yoshikawa, K., and Hinzman, L.D. 2003. Shrinking thermokarst ponds and groundwater dynamics in discontinuous permafrost near Council, Alaska. Permafrost and Periglacial Processes, **14**(2): 151-160.

Yoshikawa, K., Bolton, W.R., Romanovsky, V.E., Fukuda, M., and Hinzman, L.D. 2002. Impacts of wildfire on the permafrost in the boreal forests of Interior Alaska. Journal of Geophysical Research: Atmospheres, **107**(D1): FFR 4-1-FFR 4-14.

Zhao, Y., and Si, B. 2019. Thermal properties of sandy and peat soils under unfrozen and frozen conditions. Soil and Tillage Research, **189**: 64-72.

Zhuang, Q., Romanovsky, V., and McGuire, A. 2001. Incorporation of a permafrost model into a large-scale ecosystem model: Evaluation of temporal and spatial scaling issues in simulating soil thermal dynamics. Journal of Geophysical Research: Atmospheres, **106**(D24): 33649-33670.

Zoltai, S., Morrissey, L., Livingston, G., and de Groot, W. 1998. Effects of fires on carbon cycling in North American boreal peatlands. Environmental Reviews, **6**(1): 13-24.